Deconvolution of *Mycobacterium tuberculosis* drug targets using high throughput screening approaches

By

Panchali Kanvatirth

A thesis submitted to the

University of Birmingham

for the degree of

DOCTOR OF PHILOSOPHY

Institute of Microbiology and Infection

School of Biosciences

College of Life and Environmental Sciences

University of Birmingham

September 2017

ABSTRACT

Tuberculosis (TB) is an infectious bacterial disease mainly infecting the pulmonary system of the human body. It affects around 1.5 million people every year, most of whom live in developing countries. The incidence of TB has increased in line with the rise in incidences of Human Immunodeficiency Virus (HIV) infections and Acquired immune deficiency syndrome (AIDS). Due to the pressing concerns of TB, the World Health Organisation (WHO) came up with the Direct Observed Treatment (DOTS) programme. Unfortunately, the development of several resistant strains against first-line drugs and consequently second and third-line drugs have developed. As the current TB drug regimen is inadequate, a good screening strategy, discovery of newer drugs and identification of the mode of action would help in developing better treatment routines and determining bacterial pathways more clearly. Drug discovery follows two major routes, one leading from the drug to the target and the other from target to the drug. Both methods have been applied in this work in order to identify new drugs effective against mycobacteria. Screens performed against a drug library approved by the Food and Drug Administration (FDA) have resulted in some promising hits. Functional characterisation of a putative enoyl CoA hydratase EchA12, which was targeted by florfenicol, revealed a novel lipid chaperone functionality associated with cell wall lipid biosynthesis. Furthermore, a target based phenotypic drug screen of the GSK177 box set against *Mtb*-PrsA provided further evidence that this enzyme as a viable drug target (Ballell *et. al.*, 2013).

DECLARATION

The work presented in this thesis was carried out in the School of Biosciences at the University of Birmingham, U.K., B15 2TT during the period September 2013 to September 2016. The work in this thesis is original, except where acknowledged by references.

No part of the work is being, or has been, submitted for a degree, diploma or any other qualification at any other University.

ACKNOWLEDGEMENTS

I would like to take this opportunity to express my gratitude towards the people who have made the production of this thesis possible. Firstly, I would like to thank my supervisors Dr. Luke Alderwick and Prof. Gurdyal Besra for giving me the opportunity to conduct this research project as a part of my PhD in an excellent laboratory. I am thankful for the guidance, support and patience of Dr. Luke Alderwick, who also supervised me during my master's degree and inspired me to continue my journey to a postdoctoral degree. I would like to acknowledge Dr. Apoorva Bhatt for his regular input and helpful observations during my progress meetings.

I would like to thank Dr. Rian Griffiths for her help with the LESA-MS analysis. I would also like to thank the masters and undergraduate students Clare, Charlotte and Tom who contributed to some of the work undertaken during my PhD. I am immensely grateful for the support of the entire TB lab cohort at Birmingham: Cristian, Monika, Natacha, Padraic, Asma, James, Pat, Kat, Jon, Nabiela, Perla, Rebeca, Hayleigh, Stephen and Chris for their continuous help in the lab and a fabulously cohesive environment in the office. In addition to his company in the office and the lab, I would like to extend special thanks to Albel Singh for providing me with excellent images of my results.

I would also like to say thank you to Ben for being there as my best friend and confidante during all my years in Birmingham. I would like to thank Vinay for his support and care during my masters and PhD.

A special thank you to Kymon, Nikki and Christos for their constant encouragement and being my family away from home. I am grateful for the love and support of my family without which none of this would have been possible.

This thesis is dedicated to my family.

LIST OF FIGURES

LIST OF TABLES

LIST OF ABBREVIATIONS

[^{14}C] radioactive carbon 14

° degrees

°C degrees centigrade

Acp Acyl carrier protein

ADP Adenosine diphosphate

AG Arabinogalactan

AIDS Acquired immune deficiency syndrome

AMP Adenosine monophosphate

Ara*f* Arabinofuranose

Asp Aspartate

ATP Adenosine triphosphate

BCG Bacille Calmette-Guérin

BCIP 5-Bromo-4-chloro-3-indolyl phosphate

BSL Biosafety Level

BTZ Benzothiazinones

$CaCl_2$ Calcium chloride

Cys Cysteine

DMSO Dimethyl sulfoxide

DNA Deoxyribonucleic acid

dNTP Deoxynucleotide triphosphate

DOTS Directly Observed Therapy Shortcourse

DPA β-D-arbinofuranosyl-1-monophosphoryldecaprenol

DPPR Decaprenylphosphoryl-5-β-D-phosphoribose

DPR Decaprenylphosphoryl-5-β-D-ribose

DPX Decaprenylphosphoryl-2-keto-β-D-*erythro*-pentofuranose

DTT Dithiothreitol

EDTA Ethylenediaminetetraacetic acid

EMB Ethambutol

ES-MS Electrospray Mass Spectrometry

FAMES Fatty Acid Methyl Esters

FAS Fatty acid synthase

FDA Food and Drug Administration (US)

g gram

Gal*f* Galactofuranose

GalN Galactosamine

GalNAc *N*-acetylgalactosamine

Gal*p* Galactopyranose

GFP Green fluorescent protein

GlcNAc *N*-acetylglucosamine

GlfT Galactofuranosyl transferase

Gly Glycine

GSK GlaxoSmithKline

HCl Hydrochloric acid

His/H Histidine

HIV Human Immunodeficiency Virus

Hyg Hygromycin

I-TASSER Iterative Threading ASSEmbly Refinement

IC_{50} Half maximal inhibitory concentration

Ile Isoleucine

INH Isoniazid

IPTG Isopropyl β-D-1-thiogalactopyranoside

K_2HPO_4 Dipotassium hydrogen phosphate

ka kiloannus

KAc Potassium acetate

Kan Kanamycin

kb kilobase pairs

kDa kilodaltons

KH_2PO_4 Potassium dihydrogen phosphate

L litre

L-ala L-alanine

LAM Lipoarabinomannan

LB Luria-Bertani

LCP LytR-CpsA-Psr

Lcp1 Peptidoglycan-arabinogalactan Ligase Leu/L Leucine

Leu Leucine

LM Lipomannan

LU Linker Unit

Lys Lysine

M Molar

m-DAP *meso*-diaminopimelate

m/z mass/charge

mA milliamp

MA Mycolic Acids

mAGP Mycolyl-arabinogalactan-peptidoglycan

MAMES Mycolic Acid Methyl Esters

mCi/mmol millicurie per millimole

MDR Multi-drug resistant

Met/M Methionine

mg Magnesium

mg milligram

MIC Minimum inhibitory concentration

min minute

mL millilitre

mM millimolar

Mtb Mycobacterium tuberculosis

MurNAc *N*-acetylmuramic acid

MurNGlyc *N*-glycolylmuramic acid

NaCl Sodium chloride

NADH Reduced nicotinamide adenine dinucleotide

NADPH Reduced nicotinamide adenine dinucleotide phosphate

NaOH Sodium Hydroxide

ng nanogram

nm nanometre

NRP Non-replicating

PAGE Polyacrylamide gel electrophoresis

PAINs Pan assay interference compounds

PAT Pentaacyl trehalose

PCR Polymerase chain reaction

PDIM Phthiocerol dimycocerosate

PEP Phosphoenol pyruvate

PG Peptidoglycan

pH “Power of Hydrogen”

Pi Inorganic phosphate

PI Phosphatidyl-myo-inositol

PIM Phosphatidyl-myo-inositol mannoside

PKLDH Pyruvate kinase/Lactate dehydrogenase

PMA Phosphomolybdicacid

PPD Purified protein derivative

pRpp 5-phosphoribosyl-1-pyrophosphate R_f retention factor

PYZ Pyrazinamide

R-5-P Ribose-5-phosphate

$RbCl_2$ Rubidium chloride

Rha Rhamnose

RIF Rifampicin

RNA Ribonucleic acid

RNAP Ribonucleic acid polymerase

RNAse Ribonuclease

rpm revolutions per minute

SDS Sodium dodecyl sulfate

Ser Serine

SGL Sulfoglycolipid

SUMO Small ubiquitin-like modifier

TB Tuberculosis

TBS Tris-buffered saline

TDM Trehalose dimycolate

TDR Totally drug resistant

TFB Transformation buffer

TLC Thin Layer Chromatography

TLR Toll like receptor

TMM Trehalose monomycolate

TSA Tryptic soy agar

TSB Tryptic soy broth

Tyr Tyrosine

UDP Uridine diphosphate

Und-P Undecaprenyl phosphate

V Volt

v/v volume/volume

Val Valine

w/v weight/volume

WHO World Health Organisation

WT Wild-type

XDR Extensively drug resistant

µg/mL microgram per millilitre

μL microliter

μm micrometre

μM micromolar

TABLE OF CONTENTS

Chapter 1

Introduction

1.Introduction

1.1 The etiology of Tuberculosis

Tuberculosis (TB) is a severe bacterial infection that predominantly affects the lungs leading to its most prevalent form of infection that is pulmonary tuberculosis. It has been known to affect around 1.5 million people every year most of whom are affected in developing countries (Fleischman and Greenberg, 1998). The incidences of tuberculosis have increased in line with the rise of HIV infections and AIDS, which compromise the hosts immunity, making it easier for the disease to develop. Statistically TB affects around 19-43% of populations infected with HIV (Fleischman and Greenberg, 1998; Flynn and Chan, 2001)

Tuberculosis has afflicted humans for several thousand years, the oldest case was reported in Hungary 7000 years ago (Knechel, 2009). The causal organism of this disease is *Mycobacterium tuberculosis* (*Mtb*) which was reported by Robert Koch on March 24, 1882. In 1881, based on the lesions Koch observed in the lungs of infected animals, he named the bacteria the tubercle bacillus (Koch, 1982; Rook and Bloom, 1994). The lesions had been also described as “pthisis” which were initially thought to be hereditary and not infectious (Pease, 1940). After developing a new staining method and the ability to culture these bacilli, Koch named the bacillus *M. tuberculosis* in 1882 (Cambau and Drancourt, 2014). It has been posited that mycobacteria have existed for approximately 150 million years (Hayman, 1984) and *Mtb* has been isolated from mummies during the Egyptian pre-dynastic era (Cave and Demonstrator, 1939; Morse *et. al.*, 1964). The oldest isolates of *Mtb* were found in the 9000 kiloannus (ka) old skeletal remains of a woman and child from a settlement in Israel and from the remains of an extinct bison (17,000 ka) found in the Natural Trap Caves in Wyoming. The *Mtb* from these isolates were confirmed by analysing the samples and identifying lipid biomarkers unique to

this species (Lee *et. al.*, 2015).

Once *Mtb* invades the lungs and establishes an infection it causes symptoms such as persistent coughing, tiredness, exhaustion, night sweats and clubbing of fingers (possibly due to low oxygenation of the extremities). Prolonged infection can result in secondary symptoms such as sputum production (sometimes with blood) when coughing, pain in the chest and joints, shortness of breath and leucocytosis (immune cell migration towards the site of infection) (Cambau and Drancourt, 2014).

TB is spread through aerosolised bacilli through droplet nuclei approximately 1-5μm in diameter. These droplets are spread through coughing, sneezing, spitting and singing by an actively infected host. These aerosolised bacilli tend to be airborne for a longer period of time, although that does not necessarily entail infection in people coming in contact with the aerosol. There are 4 main factors which govern potential infection in a healthy individual: 1) The number of organisms expelled in the aerosol, 2) The concentration of the bacilli within the column of air and ventilation in that area, 3) Length of exposure to the aerosol, 4) Immune status of the exposed individual (Glickman and Jacobs, 2001). Once a person inhales the droplet nuclei, the bacilli enter the bronchioles and alveolus through the pharynx and bronchial tree. The infection may or may not be established depending on the immune response generated in the individual's body against the bacilli. *Mtb* does not have any known endo- or exo-toxins therefore it does not elicit an immediate immune response in the host when the bacterial load is low. The bacteria reside within the alveolus and multiply over a period of time, which is approximately a few weeks, to get to a count of 10^3-10^4; this amount of bacterial load then triggers an immune response (Glickman and Jacobs, 2001; Gupta *et. al.*, 2012). The primary immune response against the bacteria is via the recruitment of alveolar macrophages, although the bacillus has a special mechanism of avoiding destruction by the macrophages by obtaining

entry into the macrophage with the help of cell surface receptors; it then proceeds to modify the maturation of the phagosome to increase its survival possibility (Glickman and Jacobs, 2001). Once the bacilli have been phagocytosed into the macrophage, an inflammatory response is generated by recruitment of mononuclear cells leading to the formation of a granuloma. A granuloma is the main centre of infection, where foamy giant cells and other lymphocytes surround the infected macrophages in order to contain the infection. Within the macrophage, the bacilli create an environment to help its survival by not allowing the fusion of the phagosome with the lysosome, acidifying the phagosome and resisting the oxygenated metabolites (Basu, 2004).

The continued clash between the immune cells and the bacteria causes the formation of a caseating tubercle which leads to the leaking of the bacilli into the extracellular milieu of cellular debris. This further leads to a caseating necrosis, whereby the T-cells and activated macrophages surround the tubercle. In immunocompromised patients, due to the weakened immune system, new macrophages are low in supply and this leads to non-specific destruction of lung tissue, as opposed to patients with a good immune system where activated macrophages and cytotoxic T-cells continue fighting the infection. Once the infection causes necrosis, the bacilli might disperse through the lung tissue causing an active infection which can be transmitted to other people. In some cases, if the bacilli leak into the blood vessels they can travel to various parts of the body causing extrapulmonary tuberculosis (Clark-Curtiss and Haydel, 2003). Approximately 913,000 people developed extrapulmonary tuberculosis in 2015 according to the World Health Organisation (WHO, 2016).

Statistically, 10% of the infections are likely to become symptomatic while 90% of infected individuals develop a latent infection. A latent infection involves a delayed hypersensitivity to the purified protein derivative (PPD) that delivers a positive tuberculin test without presenting

any symptoms of the disease. 5-10% of the latent infections are said to develop into active infections when hosts are immunocompromised due to chemotherapeutic influence or age (Clark-Curtiss and Haydel, 2003; Tufariello *et. al.*, 2003).

1.2 Taxonomy of *M. tuberculosis*

Mycobacterium tuberculosis, the causative agent of tuberculosis in humans, belongs to the phylum and class Actinobacteria (which is found mostly in the soil) and order Actinomycetales based on the high guanine and cytosine residue content in its DNA and the complex cell wall of the bacteria. The bacteria belong to the suborder Corynebacterium and is a member of the Mycobacteriaceae family. It is genetically similar to other mycobacterial species and some species of the Corynebacterium sub order such as *Corynebacterium glutamicum*. *Mtb* belongs to a group of closely related mycobacterial species which belong to what is known as the mycobacterial complex. The complex includes other mycobacterial species such as *M. africanum*, *M. microti, M. canetti* and *M. bovis.*

M. africanum is phenotypically very similar to *Mtb* and *M. bovis*. *Mycobacterium microtii* was isolated for voles in the UK in the 1930s and was causing tuberculosis in rodents (Lapage, 1947; Cavanagh *et. al.*, 2002).

Mycobacterium bovis is a strain of mycobacteria that predominantly causes tuberculosis in animals. Earlier it was assumed that the *Mtb* developed only from *M. bovis*, a species of *Mycobacterium* which has been known to infect animals and humans. The latest genomic experiments have proved this theory to be false, instead it was proved that the *Mtb* species developed from a variety of species in the *Mycobacterium* complex such as *M. microti, M. canetti and M. bovis* (Smith, 2003).

The vaccine strain *M. bovis* BCG (Bacillus Calmett-Guérin) against tuberculosis was developed from *M. bovis*. *M. bovis* BCG is an attenuated strain of *M. bovis* with three of the major virulent regions known as the region of difference (RD) deleted from the genome. There are primarily three regions of difference RD1, RD2 and RD3 which are found both in *Mtb* and *M. bovis*. Overall, there are 16 regions of differences throughout the mycobacterium complex involving genes which have regulatory roles and secret proteins involved in virulence and survival of the bacterium. *M. africanum* has RD3 and RD9 missing compared to *Mtb*, while the closely associated strain *M. bovis* has RD4 to RD10 and RD12 to RD13 missing in its genome (Magdalena *et. al.*, 1998).

M. cannetti is a strain from the complex that causes tuberculosis, although is different from *Mtb* in its colony morphology given that it produces smooth colonies as opposed to the rough crenulated colonies of *Mtb*. In addition, *Mtb* also has a longer generation time (around 24 h) than *M. cannetti* (James *et. al.*, 2000; Koeck *et. al.*, 2011; Van Soolingen *et. al.*, 1997). There are other mycobacterial species which are considered to be in the complex such as *M. caprae* (can cause TB), *M. pinnipedii* (causes TB in seals) (Cousins, 2003), *M. suricattae* and *M. mungi* (Huard *et. al.*, 2006).

Due to their infectious nature, *Mtb* and *M. bovis* are classified as biosafety level 3 organisms and while in use within laboratories they have to be handled as per such guidelines. The vaccinated strain of *M. bovis* BCG along with the saprophytic mycobacterial strain *M. smegmatis* have been designated to a biosafety level 2, as they possess a lower threat to humans in terms of infectivity (Mahairas *et. al.*, 1996)

1.3 Epidemiology

In 2015, 10.4 million new cases of TB were reported globally. Of these, 5.9 million cases (56%) were men, 3.5 million cases (34%) were women and 1 million (10%) were children. Approximately 1.2 million cases were amongst patients with the human immunodeficiency virus HIV, constituting 11% of the global cases reported. The largest number of cases reported were from Asia (61%) and Africa (26%), these continents accounting for 87% of all cases. India, Indonesia, China, Nigeria, Pakistan and South Africa were the countries with the highest burden, combining to represent 60% of the global incidences reported in 2015. The cases reported from the Eastern Mediterranean region (7%), European region (3%) and the Americas (3%) form a smaller percentage of the cases reported (figure 1.1) (WHO, 2016).

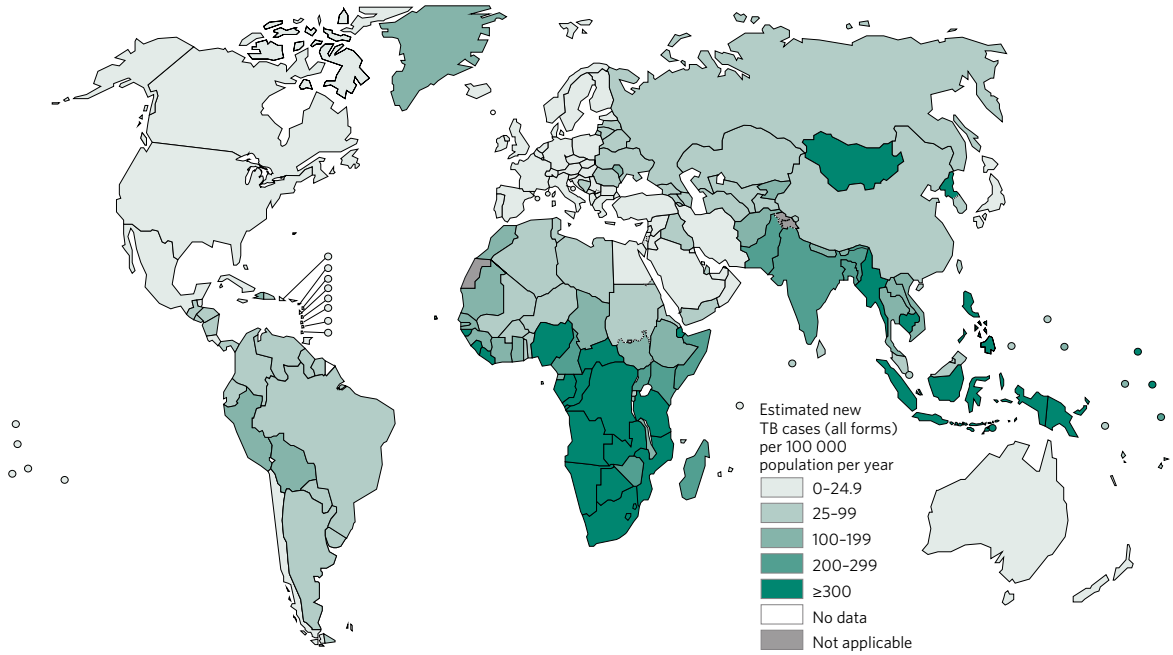

Figure 1.1: The global map depicting the new cases of TB in 2015. The map illustrates that most cases were reported in south east Asia and Africa and the least number of incidences were reported in the Mediterranean region, Europe and America.

Although the TB mortality rate has shown a decrease of 34% from 2000 to 2015, there were an estimated 1.4 million deaths among HIV negative people. 85% of deaths were in African regions and Southeast Asia (figure 1.2). India and Nigeria comprised 48% of the total deaths caused amongst HIV negative patients infected with TB. Despite this statistic, the TB treatment programme averted the deaths of 39 million patients (HIV negative) and with the additional use of anti-retroviral treatment, 9.6 million HIV positive patients (WHO, 2016).

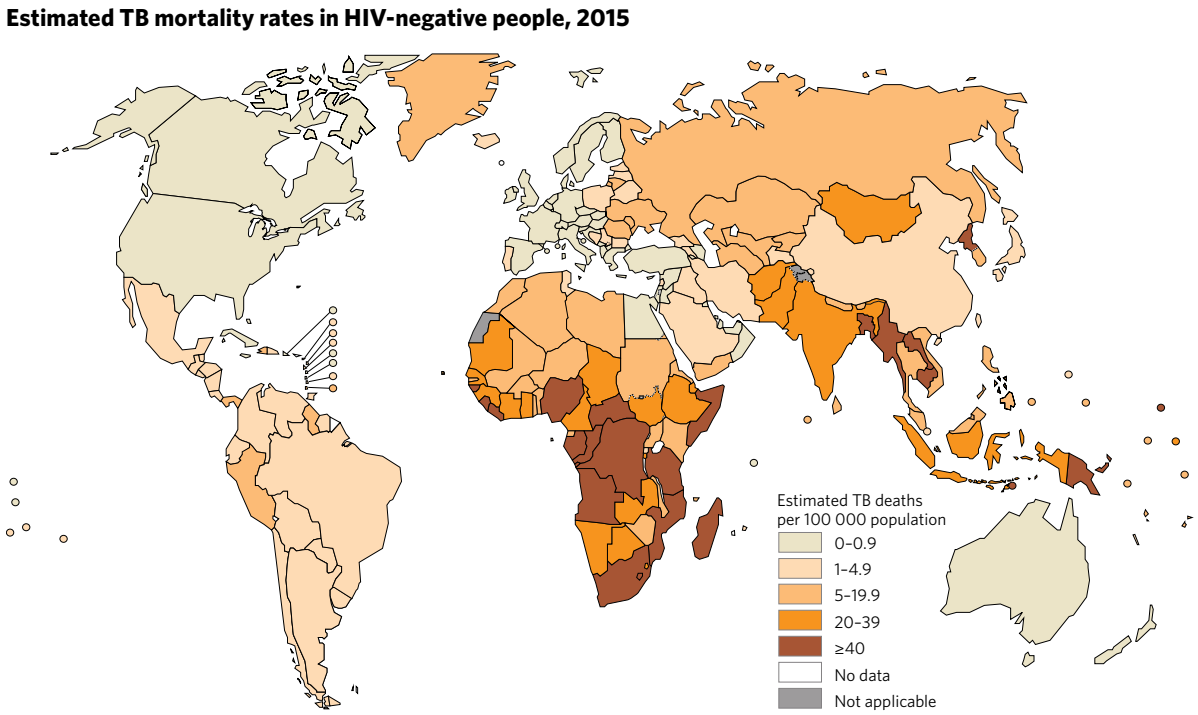

Figure 1.2: The global map of morbidity caused by TB infections in HIV negative patients in 2015. The map highlights that most deaths occurred in Africa and Southeast Asia.

With the launch of the drug resistance surveillance in 1994, the WHO took the necessary steps to monitor the development of drug resistance globally. In 2015, 3.9% new and 21% of previously treated cases reported multidrug resistant tuberculosis (MDR-TB) and rifampicin resistant tuberculosis (RR-TB). Out of the 580,000 resistant cases reported, MDR-TB comprised 83% of the total. China, India and the Russian Federation form the majority of the

resistance cases reported globally (figure 1.3). There were 250,000 deaths reported for patients infected with resistant tuberculosis (WHO, 2016).

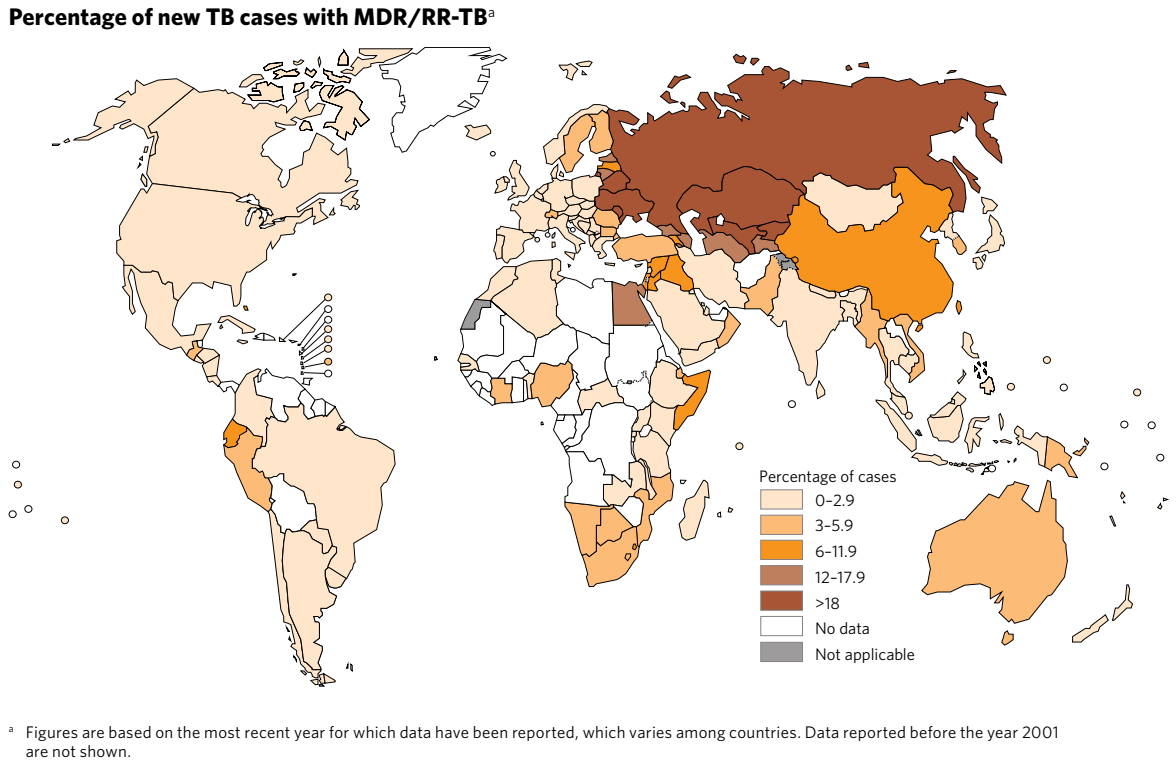

Figure 1.3: The global map of multidrug resistant TB incidences reported in 2015.

The map depicts that most cases were reported from the Russian Federation, followed by China and India.

117 of the WHO member states reported the occurrence of extensively drug resistant tuberculosis (XDR-TB) although the average proportion of the XDR-TB cases within the MDR-TB cases remains similar to the previous years at approximately 9.5% in 2015.

There is an expected proportional increase in the MDR-TB cases, with the increasing global burden of TB highlighting the importance of the need for new drugs and a better understanding about the resistance mechanism of *Mtb*.

1.4 The cell wall

The cell wall of mycobacteria is a special feature of the bacillus which acts as a barrier for penetration of drugs and creates a protective layer against host immune cells. The cell wall essentially is comprised of two major components which are the mycolyl arabinogalactan peptidoglycan (mAGP) complex and lipoarabinomannan (LAM) (Tam and Lowary, 2009). The mycobacterial cell wall is known for its low permeability and an unusually high amount of unique lipid molecules in the cell wall which constitute approximately 60% of the wall and are responsible for its waxy nature of the cell wall (Kolattukudy *et. al.*, 1997). The core of the cell wall is essentially made up of the mAGP complex, with lipids and carbohydrates covalently attached to the core (figure 1.4) (Brennan, 2003). The free lipids, lipoglycans and phosphatidyl-*myo*-isnositols (PIMs) are components that make up the outer leaflet of the cell wall. These molecules, along with other important molecules such as lipoarabinomanan (LAM) and lipomanan (LM), have a key role in host immune evasion (Wolfe *et. al.*, 2010). The suborder Corynebacterianeae which includes organisms such as *Mtb*, *M. smegmatis* and *C. glutamicum* have various liposaccharides in their cell wall. The LAM and other related glycoconjugates vary minutely within these organisms (Tam and Lowary, 2009). The lipids in the cell wall involved in virulence are trehalosemonomycolate (TMM), trehalosedimycolate (TDM), sulpholipids (SL) and phthiocerol dimycocerosate (PDIM). The cell wall associated proteins such as LpqH (19kDa), PstS1 (38kDa) and Toll-like receptor-2 (TLR-2) agonists play a more regulatory role. They are mainly involved in regulating the activity of macrophages and dendritic cells. On the other hand, the secreted proteins act as antigens and genes involved in the production of these proteins are considered important drug targets and the proteins themselves act as biomarkers (Wolfe *et. al.*, 2010).

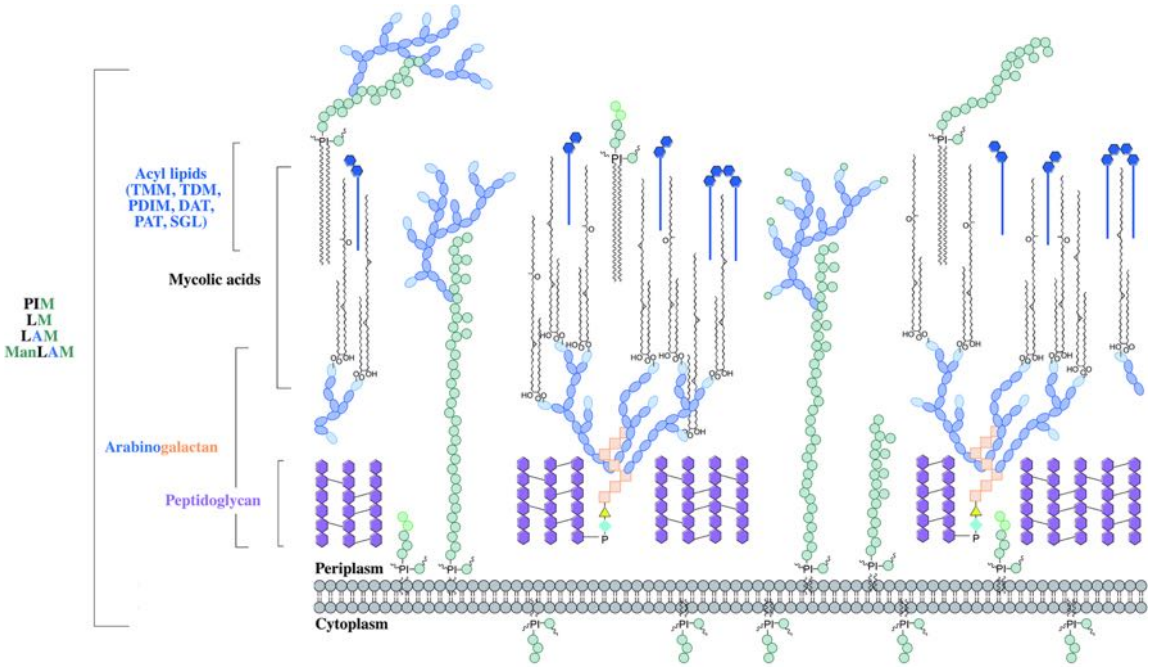

Figure 1.4: The mycobacterial cell wall. The cell wall structure of *Mycobacterium tuberculosis* depicting the major components such as peptidoglycan, arabinogalactan, phthiocerol dimycocerosate (PDIM), phosphatidyl-*myo*-inositol mannosides (PIMs), lipomannan (LM), lipoarabinomannan (LAM), mannosylated lipoarabinomannan (ManLAM) and mycolic acids. Other molecules that are interspersed into the mycolate layer such as trehalose monomycolate (TMM), trehalose dimycolate (TDM), diacyltrehalose (DAT), polyacyltrehalose (PAT) and sulfoglycolipid (SGL) (Abrahams and Besra, 2016).

The biosynthesis of the cell wall involves a series of interconnected cycles and enzymes (Acharya and Goldman, 1970). The synthesis of the mAGP complex mainly involves the synthesis of its key component, arabinogalactan (AG), which is sandwiched between the peptidoglycan (PG) layer and mycolic acid (MA) layer (figure 1.4).

The biosynthesis of peptidoglycan begins with the formation of Uridine diphosphate N- acetyl glucosamine (UDP-GlcNAc) which is synthesised by the addition of N- acetyl glucosamine (GlcNAc) to enoylpyruvate derived from phosphoenoylpyruvate (PEP) (Young *et. al.*, 1999). The UDP-GlcNAc is then converted to Uridine Diphosphate N- acetyl muramic acid (UDP-MurNAc) in two consecutive reactions catalysed by two enzymes, MurA (Rv1315) and MurB (Rv0482) (figure 1.5). MurA catalyses the addition of the enoylpyruvate residues onto the

GlcNAc which is then reduced by MurB to form UDP-MurNAc (Mahapatra *et. al.*, 2000; Raymond *et. al.*, 2005).

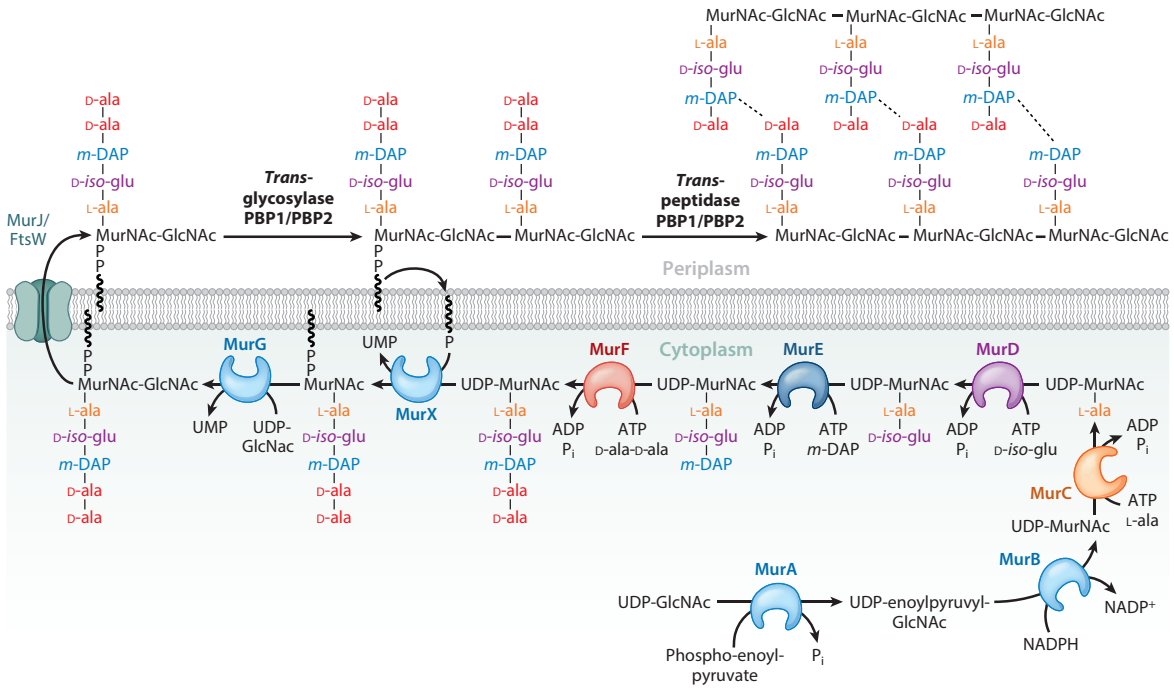

Figure 1.5: The biosynthesis of peptidoglycan. The figure depicts the stepwise conversion of initial peptidoglycan substrates into the peptidoglycan polymer (Jankute *et. al.*, 2015).

The synthesis cycle then continues with a sequential addition of molecules, beginning with the attachment of the L-alanine (L-ala) moiety to the UDP-MurNAc by the MurC (Rv2152c) enzyme to form UDP-Muramyl-L-ala (Mahapatra *et. al.*, 2000; Raymond *et. al.*, 2005). The UDP-Muramyl-L-ala is then transformed into UDP-Muramyl-L-ala-D-glutamic acid by the addition of D-glutamate by MurD (Rv2155c). MurE (Rv2158c) then adds the *m*-diaminopimelic acid (DAP) onto the UDP-Muramyl-L-ala-D-glutamic acid to form UDP-Muramyl-L-ala-D-glutamate-*m*-DAP (Morayya *et. al.*, 2015; Munshi *et. al.*, 2013). The final step in the formation of "Park's nucleotide", UDP-Muramyl-L-ala-D-glutamate-*m*-DAP-D-ala-D-ala is the addition of the D-alanyl-D-alanine (D-ala-D-ala) residue by MurF (Rv2157c) to

form the UDP-MurNAc pentapeptide (Feng and Barletta, 2003; Kurosu *et. al.*, 2007). This pentapeptide molecule is transferred over to the cell membrane beginning with the initial attachment of the molecule with an undecaprenyl phosphate (Und-P) and a membrane bound enzyme called MurX/MraY (Rv2156c) to form Lipid I. GlcNAc is then added to this Lipid I molecule by MurG (Rv2153c) to form Lipid II, a β 1-4 linked GlcNAc-Muramyl-pentapeptide (Kurosu *et. al.*, 2007). Lipid II is the monomer of the peptidoglycan polymer and is flipped over by a transmembrane protein MurJ or FtsW (Rv2154c) which has been proven to have flippase activity *in vitro* (Meeske *et. al.*, 2015). The monomer is added to other monomers to form a polymer by sequential transglycosylation and transpeptidation reactions catalysed by enzymes PonA1/PBP1 (Rv0050) and PonA2/PBP2 (Rv3682). PonA1/PonA2 (PBP1/PBP2) is a bifunctional enzyme which attaches the muramyl molecule to the PG chain and then crosslinks the *m*-DAP to the neighbouring D-ala moiety through a 3→4 linkage by cleaving the terminal D-ala (Hett *et. al.*, 2010; Chang *et. al.*, 1990; Ghuysen, 1991) (figure 1.5).

The peptidoglycan is then covalently attached to the arabinogalactan via a linker unit. This unique structure of the linker unit found in mycobacteria and Actinomycetes has a diglycosylphosphoryl bridge, α-L-*Rha*p-(1→3)-α-D-GlcNAc-(1→P) (Daffe *et. al.*, 1990). The linker unit links the galactan chain at the C-6 position of the N-glycocylmuramic acid (MurNGly) (McNeil *et. al.*, 1987; 1990). This linker unit is synthesised by the addition of a UDP-GlcNAc residue onto a lipid carrier by a GlcNAc transferase WecA (Rv1302) which is homologous to gram negative bacteria such as *E. coli* (Jin *et. al.*, 2010). This UDP-GlcNAc moiety attached to the lipid carrier is then converted to the linker unit by the addition of a Rhamnosyl residue (Rha) by a rhamnosyltransferase WbbL (Rv3265c) (Mikušová *et. al.*, 1996). The WbbL enzyme is essential in mycobacteria for the formation of the linker unit (C50-P-P-GlcNAc-Rha) (Mills *et. al.*, 2004). The linker unit acts as an acceptor for the formation of the

galactan chain which has 30 units of galactofuranose (Gal*f*) with alternating β (1→5) and β(1→6) residues (McNeil *et. al.*, 1987; 1990; Kremer *et. al.*, 2001). This addition of the residues is performed by two bifunctional enzymes Gal*f*T1 and Gal*f*T2. The Gal*f*T1 recognises the linker unit and adds the initial 2 Gal*f* residues at the C-4 position of the Rha in the linker unit while Gal*f*T2 adds the rest of the residues to the chain (Belanova *et. al.*, 2008; Kremer *et. al.*, 2001). This linear galactan chain is then connected to a highly-branched structure containing three arabinan chains at position 8, 10 and 12 (Alderwick *et. al.*, 2006). The α-D-arabinofuranosyl (Ara*f*) residues are added onto the linker unit containing the 30 Gal*f* residues (C50-P-P-GlcNAc-*Rha*-Gal*f*30). These residues are supplied by the only known contributor in mycobacteria, decapreylmonophosphoryl-D-arabinose (DPA) (Wolucka, 2008). The Ara*f* residues are generally added in a linear chain with α-5 linkages with branching at C-3 introducing an α-3,5 DPA, which is synthesised through a multienzyme cycle. This begins with the conversion of 5-phosphoribosyl-1-pyrophosphate (pRpp) into decaprenylphosphoryl-5-phosphoribose (DPPR) by an enzyme UbiA (Rv3806c) (Alderwick *et. al.*, 2005; 2011) which has also been predicted to be a target for an antimycobacterial drug ethambutol (Safi *et. al.*, 2013). Prpp is synthesised by an essential enzyme PrsA (phosphoribosyl synthetase, Rv1017c) utilising ribose-5-phosphate (R-5-P) acquired from the pentose phosphate pathway. Prpp can also be redirected to be used for the biosynthesis of amino acid, purines and pyrimidines in the cell cytoplasm (Alderwick *et. al.*, 2011). The gene responsible for the conversion of pRpp to DPPR (*ubiA*) when disrupted in *C. glutamicum* leads to the loss of cell wall arabinan and a mutant that has a truncated or variant version of LAM indicating a different pathway for LAM synthesis (Tatituri *et. al.*, 2007). The DPPR is then flipped over to the extracellular space and dephosphorylated to form decaprenol-1-monophosphoribose (DPR) by a phospholipid phosphatase (Rv3807c) (Jiang *et. al.*, 2011). The DPR is then oxidised to form decaprenol-1-

phosphoryl-2-keto-β-D-erythropentofuranose (DPX) which is then consequently reduced to form decaprenol-1-monophosphoarabinose (DPA).

There are two key enzymes involved in these two steps, decaprenylphosphoryl-β-D-ribose oxidase, DprE1 (Rv3790) and decaprenylphosphoryl-β-D-ribose-2-epimerase, DprE2 (Rv3791) which are present as heterodimers. Deletion studies in *C. glutamicum* and conditional knock-out studies in mycobacteria revealed that out of the two enzymes, DprE1 is essential and has recently proven to be targeted by a class of new drugs called benzothiazinones (Meniche *et. al.*, 2008; Batt *et. al.*, 2012; Crellin *et. al.*, 2011).

The arabinose residue is then transferred from the DPA molecule by an arabinofuranosyltransferase (ArafT) forming decaprenol-1-monophosphate onto the galactan chain at positions 8, 10 and 12 by the enzyme AftA (Rv3792) (Alderwick *et. al.*, 2006). This ultimately primes the galactan chain for the addition of further arabinose molecules and the extension of the polymeric chain. The AftA enzyme is essential for the cell viability and has also been recognised as a target for ethambutol (Safi *et. al.*, 2013; Shi *et. al.*, 2008). The extension of the arabinan chain by polymerisation and the formation of the terminal hexa-arabinofuranosyl unit is then taken over by a heterodimeric set of enzymes EmbA (Rv3794) and EmbB (Rv3795) from the *emb* locus having transferase activity. The *M. smegmatis* and *C. glutamicum* homolog of these enzymes produce viable mutants with truncated or decreased amounts of arabinan (Escuyer *et. al.*, 2001; Shi *et. al.*, 2008). The other ArafT enzymes such as AftC (Rv2673) are involved in the internal domain of the arabinan to form α-1,3 branches along with the AftD (Rv0236c) (which is the largest mycobacterial glysoyl transferase) and together they most likely act as a large scaffold for the arabinosylation of the cell wall. The final addition of the Ara*f* residues at the β (1→3) position is performed by AftB (Rv3805c), bringing the synthesis of arabinogalactan to completion (Birch *et. al.*, 2010; 2008).

The attachment of the arabinogalactan layer to the peptidoglycan layer is achieved by the mycobacterial enzyme Lcp1 (Rv3267) belonging to the LytR-CysA-Psr (LCP) family, which ligates the AG to the PG layer through the α-L-rhamnopyranose–(1→3)-α-D-GlcNAc-(1→P) linker unit. The finished arabinogalactan polymer is transferred over to the Lcp1 enzyme which attaches the polymer to the 6′-OH of the muramyl residue of the peptidoglycan via a phosphodiester bond, consequently releasing a decaprenol-1-monophosphate (Harrison *et. al.*, 2016). Two essential enzymes belonging to the LCP family, CpsA1(Rv3267) and CpsA2 (Rv3484), have also been discovered to have the same activity and are known to be involved in the ligation of the AG to the PG (Grzegorzewicz *et. al.*, 2016).

The non-reducing part of the arabinogalactan structure is attached to the mycolic acid (MA) via the branched arabinan to form the mAG complex (Kaur *et. al.*, 2009). The mycolic acid is attached to the hexa-arabinofuranosyl structure at the 5th position of both the terminal β-D Ara*f* and 2-α-D Ara*f*. The mycolyl units are attached to the hexa-arabinofuranosyl structure in groups of four, of which only 2 of the hexa-arabinofuranosyl residues are mycolated in physiological conditions. There are other molecules that are interspersed and attached covalently to the arabinogalactan unit in slow growing mycobacterial species (McNeil *et. al.*, 1990; 1991).

There are non-acylated galactosamines (D-GalN) which attach to the arabinogalactan at the C-2 position of the inner 3,5-α-D-Ara*f* units. It was found that succinyl esters were attached to the arabinogalactan and non mycolated chains. In non-mycolated chains, succinyl esters were considered to control mycolation through negative regulation. Together, the galactosamine and succinyl esters enhance the rigidity and tightness of the arabinogalactan component of the cell wall (Draper *et. al.*, 1997; Bhamidi *et. al.*, 2008).

There are a number of non-covalently bound glycophospholipids present in the outer leaflet of the cell wall such a PIMs, LM and LAM. PIMs are the precursors to the synthesis of LM and

LAM, which are important molecules for recognition by macrophages (Wolfe *et. al.*, 2010). PIMs are glycolipids which are synthesised from the starting molecule phosphatidyl-*myo*-inositol (PI) which is mannosylated twice sequentially by PimA (Rv2610c) and PimB (Rv2188c) to form phosphatidyl-*myo*-inositol mannoside (PIM_1) and then phosphatidyl-*myo*-inositol dimannoside (PIM_2) respectively (Ballou *et. al.*, 1963). The PIM_2 is then acylated to form monoacyl-phosphatidyl-*myo*-inositol dimannoside (Ac_1PIM_2) which acts as a base for other PIMs molecules and can be further acylated to form diacyl-phosphatidyl-*myo*-inositol dimannoside (Ac_2PIM_2) (Kordulakova *et. al.*, 2002; 2003). PimC then further adds another α-mannopyranosyl (Man*p*) residue to Ac_1/Ac_2PIM_2 to form Ac_1/Ac_2PIM_3. PimE then adds two mannose residues consecutively to form Ac_1/Ac_2PIM_4 and Ac_1/Ac_2PIM_6 (figure 1.6). The Ac_1/Ac_2PIM_4 are also redirected towards synthesis of lipomannan (LM) and lipoarabinomanan (LAM) by glycosyltransferases belonging to the GT-C superfamily (Lea-Smith *et. al.*, 2008; Mishra *et. al.*, 2008).

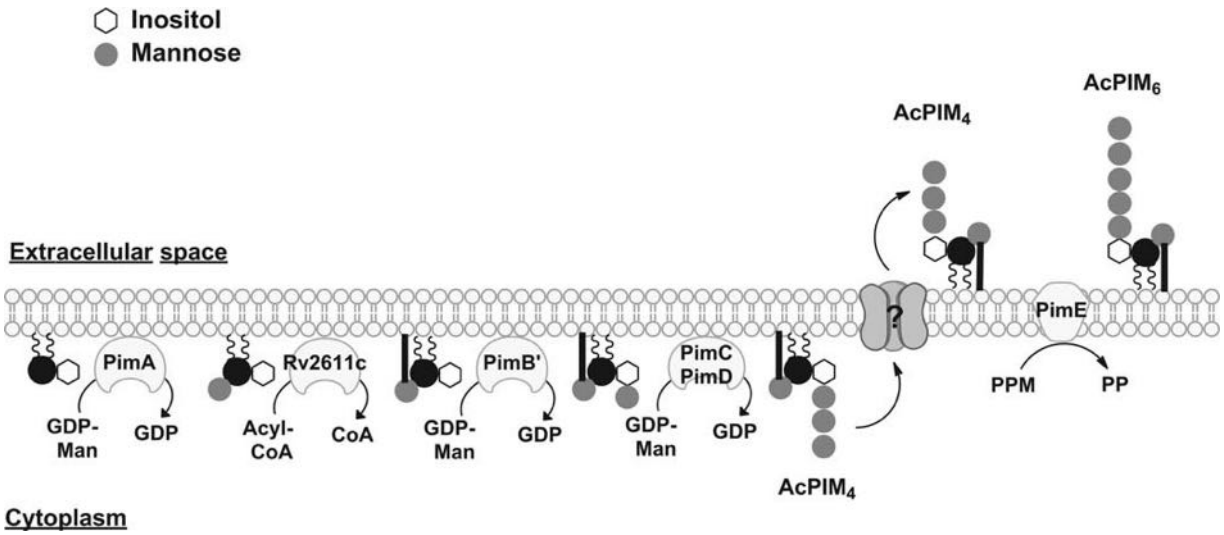

Figure 1.6: Biosynthesis of Phosphatidyl-myo-inositol mannoside. The figure is a pictorial depiction of the sequential biosynthesis of PIMs involving the various enzymes (PimA, PimB, PimC, PimD and PimE) (Jankute *et. al.*, 2014).

Mycolic acids are long chain α-alkyl β-hydroxy fatty acids and are a characteristic of *Mtb* contributing to their high hydrophobicity (Takayama *et. al.*, 2005). Bioinformatic study and the knowledge of the *M. leprae* genome unravelled the genes which play a vital role in the survival and virulence of mycobacteria. This is due to the fact that *M. leprae* has undergone reductive evolution and therefore potentially only retained essential genes required for survival (Bhatt *et. al.*, 2005). Most genes involved in the mycolic acid biosynthesis are essential for the survival and virulence of the bacteria. Understanding the importance of the genes in the mycolic acid biosynthesis pathway came through conditional mutants in *M. smegmatis* which gave the functional importance of essential genes and the ability of *C. glutamicum* to survive in the absence of mycolic acids when these essential genes are knocked out of the organism (Gande *et. al.*, 2004).

Mycobacterial mycolic acids are made of merochains which are of three different types: α-mycolates, methoxy-meromycolates and keto-mycolates. The α-mycolates also known as the *cis*-dicyclopropyl fatty acids are the most abundant type in the bacterial cell wall (~70%) and is a *cis* only mycolate (Takayama *et. al.*, 2005). It has two variations in its structure based on the length of the alkyl groups at the terminal ends and the number of methylene groups between the cyclopropane rings and the carboxyl group. The methoxy- and keto-mycolates on the other hand form only a minor proportion of the mycolates and consist of both *cis*- and *trans*-cyclopropane rings (Glickman *et. al.*, 2000; 2001; Dubnau *et. al.*, 2002).

In 1970, Bloch discovered that mycobacteria have two fatty acid synthase cycles (FAS). The Fatty Acid Synthase-I (FAS-I) is similar to the synthase cycle in eukaryotes and evolved prokaryotes and Fatty Acid Synthase-II (FAS-II) is found in plants and bacteria (Bloch, 2006). The bimodal FAS-I utilizes an acetyl CoA molecule to produce an acyl CoA after addition of 2 carbon units per cycle, forming an elongated chain of C_{16}-C_{18} carbon units and then feeding

it into the FAS-II system. The FAS-II system utilizes a malonyl CoA which is synthesised from the acetyl CoA by an acetyl CoA carboxylase (AccD6, Rv2247) and is further converted into a malonyl-ACP (acyl carrier protein) by FabD, a ketoacyl synthase (Rv2243) (Bhatt *et. al.*, 2007b). From this point forward there are a few key enzymes involved in FAS-II which are the β-ketoacyl ACP synthase, β-ketoacyl ACP reductase, β-hydroxyacyl-ACP hydratase and enoyl ACP reductase (Bhatt *et. al.*, 2007b).

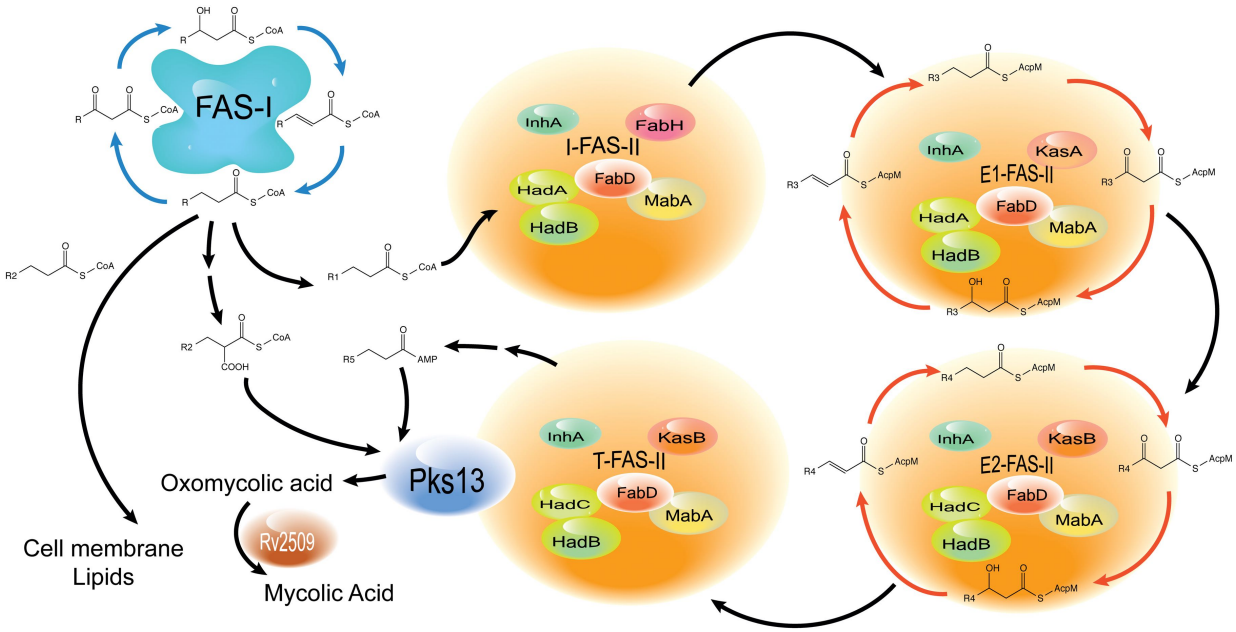

Figure 1.7: Synthesis of Mycolic acids. A pictorial depiction of the biosynthesis of mycolic acids through the two major fatty acid synthase cycles (FAS-I and FAS-II) highlighting the presence of more than one FAS-II cycle (Nataraj *et. al.*, 2015).

The malonyl-ACP chain is extended by the addition of the acyl CoA from FAS-I into β-ketoacyl-ACP by the β-ketoacyl ACP synthases, KasA (Rv2245) and KasB (Rv2246). Out of the two synthases it was demonstrated that KasA is essential while KasB is not, although the *kasB* mutant produced shorter mycolic acid chains (Bhatt *et. al.*, 2005; 2007a). The ketoacyl-ACP then follows a chain of reduction by the β-ketoacyl ACP reductase (MabA, Rv1483)

followed by dehydration by the β-hydroxyacyl-ACP dehydratase forming a *trans*-2-enoyl-ACP (Labesse *et. al.*, 2002).

There are three functional dehydratase enzymes involved in the FAS-II cycle: HadA (Rv0635), HadB (Rv0636) and HadC (Rv0637) which form heterodimers in different combinations with each other based on the type of mycolic acid being synthesised (Cantaloube *et. al.*, 2011) (figure 1.7). The *trans*-2-enoyl-ACP is then reduced by the enoyl ACP reductase (InhA, Rv1484), which is the site of action for isoniazid, forming the acyl-ACP with C_{16}-C_{32}. The acyl-ACP formed is then condensed with the acyl CoA from the FAS-I by Pks13 (Rv3800c) to form an oxomycolic acid intermediate and then reduced by a mycolyl reductase (Rv2509) into the mature mycolic acid (Portevin *et. al.*, 2004; Gande *et. al.*, 2004; Bhatt *et. al.*, 2008).

It has been recently suggested that there might be more than one FAS-II cycle. The new model posites a chain of individual FAS-II cycles that feed the product sequentially to each other and culminate in the condensation of the merochains and formation of a mature mycolate at the end. In this model, there are five arrays of an assembly chain which lead to the final condensation by Pks13 involving a variable combination of FAS-II, FAS-IIA, FAS-IIB and enzymes involved in mycolic acid modifications to synthesise α-mycolic acids, *cis*-methoxy mycolates, trans-methoxy mycolates, cis-keto mycolates and trans-keto mycolates (Nataraj *et. al.*, 2015).

The first array is the FAS-II complex, which links the FAS-I to FAS-II and contains the core (MabA, InhA, FabD) and FabH. The FAS-II then interacts with two elongation complexes E1-FAS-II and E2-FAS-II. The E1-FAS-II is the initial elongation complex consisting of the core, KasA and a HadA-HadB heterodimer while the E2-FAS-II is responsible for further elongating mycolic acid chains from the E1 complex utilizing the core, KasB and HadB-HadC heterodimer (Bhatt *et. al.*, 2007b; Cantaloube *et. al.*, 2011) (figure 1.7). The meromycolate chain is then passed onto the termination FAS-II (T-FAS-II) which involves Pks13 condensing the

meromycolate chain with the C_{26} fatty acid molecule from FAS-I to an oxomycolic acid. This is then reduced by a mycolyl reductase (Rv2509) to form concluding mature mycolate. This "mycolic acid biosynthesis interactome" was deciphered using protein-protein interaction studies with two- and three-hybrid systems. The modifying enzymes involved in these cycles, which introduce modifications such as methylations, isomerisation etc., show a specific preference towards a certain type of Had heterodimer which therefore govern the kind of modification the meromycolate chain undergoes (Nataraj *et. al.*, 2015).

Once the mycolates have been synthesised they are utilised for the synthesise of mycolate containing cell wall components such as TMMs and TDMs. The antigen 85 complex has three proteins which possess mycolyl transferase activity. The proteins FbpA (Rv3804c), FbpB (Rv2886c) and FbpC (Rv0129c) are involved in the transfer of mycolates onto the trehalose components which form TMMs which are then further converted to TDMs (Belisle *et. al.*, 1997).

Cell wall mycolic acids are main components for the growth and survival for the bacilli both *in vivo* and *in vitro*. As depicted in Figure 1.4, the mycolic acids are bound to the mAG complex and are involved in the inflammatory response involving activation of macrophages and dendritic cells through the TLR-2 and TLR-4 receptors. Free mycolates in the outer periphery of the cell wall are responsible for maintaining the structure of granulomas (Verschoor *et. al.*, 2012). In the host system, it has been observed that mycolic acids stimulate production of antibodies which could be important for diagnostic and therapeutic purposes (Tam and Lowary, 2009).

Many of the genes involved in the biosynthetic cycles of cell wall components and related enzymes involved in these pathways have been deemed essential for the survival of the mycobacterial cell. Due to the essentiality of the genes, understanding these cycles and the roles

the enzymes play within them is important in order to develop new inhibitors and unearth new drug targets (Mishra *et. al.*, 2011).

1.5 Tuberculosis treatment

Due to the pressing concerns of the increasing instances of tuberculosis the WHO came up with the Direct Observed Treatment Short-course (DOTS) programme. The DOTS programme was developed with five major elements: 1) Political commitments to TB affected areas in various countries, 2) Detection of the infection by analysing the sputum of patients, 3) Short course chemotherapy (SCC) administered to the people with a positive infection as per the sputum analysis, 4) Proper case management by DOTS, 5) Regular recording and reporting of every case. With the application of this programme, there was an increased control of tuberculosis with proper drug administration for a period of time (Gupta *et. al.*, 2001). Unfortunately, resistance to first line drugs started to develop after a few years which led to a new strain of TB called Multidrug resistant tuberculosis (MDR-TB). The strain of *Mtb* causing this infection was resistant to isoniazid and rifampicin, the key first line drugs (FLDs) administered in the DOTS programme (Blanchard, 2003). Resistance is thought to have been caused through lack of knowledge, improper prescription of the drugs, a non-standardised regimen and poor patient adherence to the antibiotics prescribed. In order to deal with the MDR-TB problems, a Green Light Committee was formed to monitor the proper use of second line drugs (SLDs) to combat this resistant strain (Shah *et. al.*, 2007). Under this programme, 4 or more SLDs were administered in different combinations to those people diagnosed with MDR-TB. Unfortunately, cases of resistance against the SLDs developed shortly after, forming yet another strain of TB called extensively drug resistant (XDR-TB). XDR-TB is defined as the strain of

TB resistant to isoniazid, rifampicin, any of the flouroquinolones and at least one injectable SLD (Shah *et. al.*, 2007; Munro *et. al.*, 2007). A more recent strain of resistant tuberculosis known as extremely drug resistant tuberculosis (XXDR-TB) or totally drug resistant tuberculosis (TDR-TB) resistant to both first and second line drugs has taken us back into the era without any antibiotic resources to treat it (Farnia *et. al.*, 2010). The recent resistant strain has been seen to show morphological changes affecting 15-20% of the cell population of the bacillus by changing its shape into an oval or round shape while 5-7% of the cell population show extremely thick walls (21-26nm) similar to non-replicating bacilli (NRP) or anaerobic dormant bacilli (Farnia *et. al.*, 2010).

It has still not been conclusively defined how the bacteria acquire resistance to the antibiotics. It is thought to be because of chromosomal alterations (Cole, 1994) due to sequential mutations (mutations that would develop for one drug at a time) (Fenner *et. al.*, 2012; Motiwala *et. al.*, 2010). The bacilli seem to use efflux pumps to resist dying in the presence of the antibiotics and this attribute could play an important role in developing long term resistance. It is thought that horizontal gene transfer of genetic elements such as plasmids, integrons and transposons could also be responsible for the development of resistance, but this has not been clearly proven (Srivastava *et. al.*, 2010).

The standard drug regimen for DOTS involves these first line antimycobacterial antibiotics:

1.5.1 Isoniazid

Isoniazid or isonicotinylhydrazide is an antibiotic containing a pyridine ring with a hydrazide group, both of which are essential to its activity (figure 1.8). Its complex mode of action is via interference with the mycolic acid synthesis process (Middlebrook and Cohn, 1953). It does so by inhibiting the NADH dependant enoyl ACP reductase that is encoded by the gene *inhA*

(Rawat *et. al.*, 2003) which is involved in the final step in the FAS-II cycle of the mycolic acid biosynthesis process (Marrakchi *et. al.*, 2000; Kremer *et. al.*, 2003).

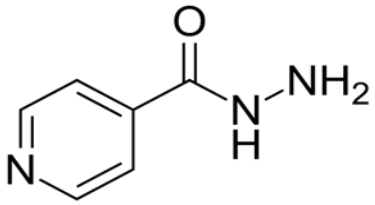

Figure 1.8: Structure of Isoniazid.

Isoniazid enters the cells through passive diffusion and needs to be activated by a catalase enzyme KatG in the presence of manganese dichloride ($MnCl_2$) (Zabinski and Blanchard, 1997) to form an anion which then covalently attaches to NADH to form the adduct that inhibits the InhA protein (Marrakchi *et. al.*, 2000). Strains of *Mtb* which developed resistance against isoniazid showed mutations in two genes *inhA* and *katG* (Silva *et. al.*, 2003; Ramaswamy *et. al.*, 2003). In 40% of the strains resistant to isoniazid a mutation in the *katG* gene was identified, which causes the amino acid substitution of a serine to a threonine at the 315 position (Somoskovi *et. al.*, 2001). The study of three genes *ihhA*, *katG* and *kasA* revealed that the drug targeted only KatG and subsequently InhA without any activity against KasA, a ketoacyl ACP (Kremer *et. al.*, 2003). The most prominent mutation observed in the *inhA* gene was a point mutation causing a substitution of Ser94Ala which causes a decrease in the affinity of the Isoniazid-NAD adduct to the active site of the InhA protein. The loss of serine in the mutated InhA protein causes the disruption of hydrogen bonding due to movement in an ordered water molecule which in turn reduces the binding capability of the drug NAD complex (Vilchèze *et. al.*, 2000). *katG* mutations are seen to be more in case of MDR strains as opposed to monoresistant strains (Hazbón *et. al.*, 2006).

1.5.2 Rifampicin

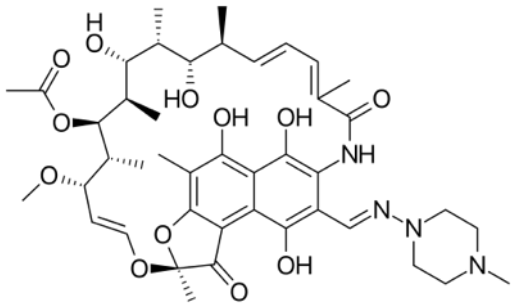

Figure 1.9: Structure of Rifampicin.

Rifampicin is a lipophyllic ansamycin drug with a heterocyclic structure and a napthoquinone core depicting an antimicrobial action (Rattan *et. al.*, 1998) (figure 1.9). Its mode of action involves the molecule binding to the β-subunit of the RNA polymerase enzyme, by inhibiting the binding of the first triphosphate to the polymerase and consequently inhibiting the elongation process of mRNA (McClure and Cech, 1978; Blanchard, 2003). The drug is active against both replicating and non-replicating bacteria. The resistance to rifampicin is seen due to mutations in the *rpo* gene in the region of 507-533 codons now known as the rifampicin resistance-determining region (RRDR) (Ramaswamy and Musser, 1998). Analysis of 29 rifampicin resistant strains from Hungary revealed an 81-bp region and a N-terminal region in the *rpo* gene where most mutations occurred. The most common substitutions observed were Asp516Val, Ser531Leu, His526Tyr and His526Asp (Bártfai *et. al.*, 2001). Of these common mutations, the Ser531Leu and His526Asp depicted the highest amount of resistance to the drug by disrupting the hydrogen bonds, increasing repulsion and therefore decreasing the affinity of the drug to the polymerase protein (Pang *et. al.*, 2013; Bártfai *et. al.*, 2001). These substitutions increased the minimum inhibitory concentration (MIC) values against the drug to more than 32μg/mL (Somoskovi *et. al.*, 2001). Resistance to rifampicin has shown co-resistance to other

drugs, primarily isoniazid (Traore *et. al.*, 2000).

1.5.3 Ethambutol

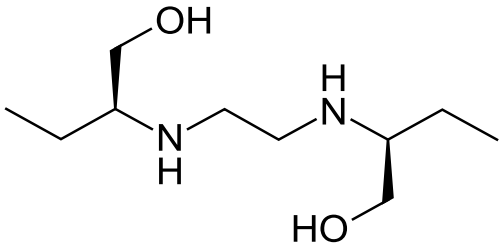

Figure 1.10: Structure of Ethambutol.

Ethambutol is a linear alcoholic molecule ((2S)-2-[2-[[(2S)-1-hydroxybutan-2-yl]amino]ethylamino]butan-1-ol) (figure 1.10) which was first used as a first line drug in combination with isoniazid, rifampicin and pyrazinamide (Sreevatsan *et. al.*, 1997). The mode of inhibition of this drug is by the interference with the biosynthesis of cell wall arabinogalactan (Takayama *et. al.*, 1979). Ethambutol blocks the polymerisation step in the arabinan synthesis causing the accumulation of the precursor β-D-arabinofuranosyl-P-decaprenol (C_{50}-P-D-Ara*f*). The drug partially blocks the synthesis of LAM leading to the production of truncated LAM which has a knock-on effect on the mycolic acids. Due to the absence of LAM moieties the mycolic acids cannot be attached to them which therefore causes redirection of these molecules towards non-arabinan pathways and accumulation of trehalose dimycolates (Mikusova *et. al.*, 1995a). The gene producing arabinosyl transferase is *embC, embA* and *embB* (Sreevatsan *et. al.*, 1997). EmbA and EmbB form heterodimers to synthesise the hexa-arabinoside structures and disruptions of genes encoding these enzymes produce a growth defective mutant. Although *embA* and *embB* are co-transcribed, it was proven that the *embA* is essential for the survival of the cell (Amin *et. al.*, 2008). Mutation in the 306th codon of the *embB* gene was seen in 50% of

the resistant strains. Amino acid substitution in *embB* was observed in 69% of the resistant isolates (Telenti *et. al.*, 1997). The Met306Leu and Met306Val mutations cause an increase in the MIC from 5μg/mL to ~40μg/mL while the Met306Ile caused the MIC to increase to only 20μg/mL. The mutation in the *embC* gene causing the substitution Val981Leu increased the MIC to 15μg/mL(Sreevatsan *et. al.*, 1997; Rinder *et. al.*, 2001). It has been mentioned that although the majority of mutations occur in the *embB* gene, this does not present resistance to the drug but only makes the bacteria susceptible to acquiring more mutations (Srivastava *et. al.*, 2009).

The *aftA* gene, essential for the bacteria and encoding the enzyme which catalyses the addition of the first arabinofuranosyl residue to galactan, has been indicated to confer resistance to ethambutol, increasing the MIC value to 8μg/mL (Alderwick *et. al.*, 2006). A mutation in another gene called *ubiA* (Rv3806c) not only leads to increased resistance with an MIC value of 16-32μg/mL, but also mutations in *embB* and increase in DPA synthesis (Safi *et. al.*, 2013).

1.5.4 Pyrazinamide

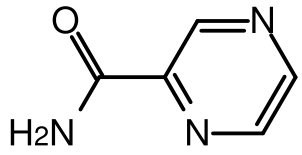

Figure 1.11: Structure of Pyrazinamide.

Pyrazinamide is a pyrazinoic acid amide analogous to nicotinamide (figure 1.11). It is a prodrug, which needs activation through an enzyme pyrazinamidase (Pzase), which converts it into pyrazonoic acid (Konno and Feldmann, 1967). The enzyme is encoded by the gene *pncA* (Scorpio and Zhang, 1996). The active drug component destroys the bacterial membrane

energetics and inhibits membrane transport. The antibiotic is known for its activity against semi-dormant bacilli surviving within an acidic environment and it kills the bacteria by changing the membrane potential of the cell (Zhang *et. al.*, 2003; Mitchison, 1985). Another mechanism of action is thought to be via inhibition of the fatty acid synthase type-I in the replicating bacteria (Zimhony *et. al.*, 2007). Resistance develops when mutations are observed in the promoter region of the *pncA* gene (Scorpio *et. al.*, 1997; Jureen *et. al.*, 2008). Mutation in the *pncA* gene causes an amino acid substitution of Cys169Gly, which does not allow the drug to be activated and produces a 3-fold resistance to the drug (Shi *et. al.*, 2011).

1.6 New antitubercular drugs in the pipeline

An estimated 0.6 million cases were diagnosed with MDR-TB in 2015 (WHO, 2016) and with almost 11 million people co-infected with HIV, the TB drug regimen is failing against upcoming challenges (Sala and Hartkoorn, 2011). To make matters worse, the recent developments of lifestyle diseases like diabetes mellitus is affecting treatment of TB (Sala and Hartkoorn, 2011) and necessitates the development and discovery of new drugs. The current TB pipeline has not produced many new drugs since the mid-1980s (figure 1.12), although recent developments have led to newer drugs undergoing trials to be used as combinatorial therapy for tuberculosis including non-resistant, latent and resistant strains (Lalloo and Ambaram, 2010).

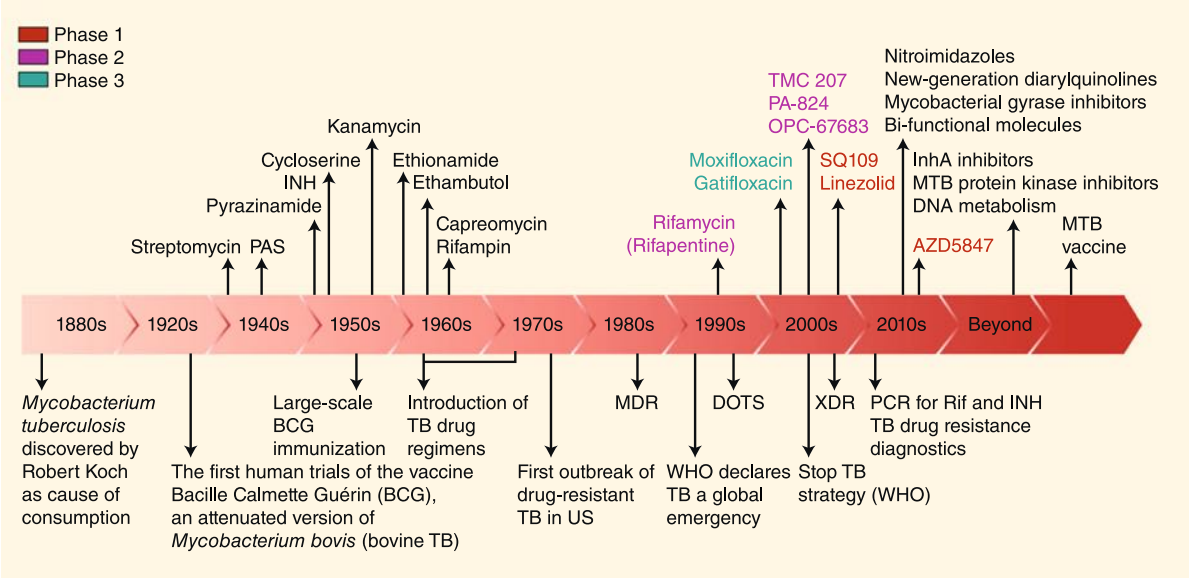

Figure 1.12: The TB drug discovery timeline. The figure represents the drugs discovered over the years from the identification of the bacteria to the recent development of resistant strains of *M. tuberculosis* (Lalloo and Ambaram, 2010)

Several new drugs as illustrated in figure 1.13 detailed as follows:

1.6.1 Diarylquinolones TMC-207

Bedaquiline (also known and TMC-207 or R207910) was discovered after screening 70,000 compounds against *M. smegmatis* (Lounis *et. al.*, 2006; Huitric *et. al.*, 2007). The drug is effective against mono and multi-resistant strains of tuberculosis. The drug target was identified as the c subunit of the ATP synthase enzyme by mutations caused in the *atpE* gene in resistant mutants of *Mycobacterium* (figure 1.14). The drug also binds to the epsilon subunit (Koul *et. al.*, 2006; Ji *et. al.*,2006).

The drug seems to have other targets or mechanism of resistance, which is drug efflux. Although the FDA recently approved the use of bedaquiline as a combinatorial therapy for resistant tuberculosis it does have serious side effects such as induction of arrhythmia, tissue

accumulation, elevated transaminase levels and high mortality rates (Lounis *et. al.*,2006; Arjona *et. al.*, 2008).

1.6.2 Nitroimidazoles

A specific characteristic of nitroimidazoles is that they are active against both replicating and non-replicating *Mycobacterium*. Currently two major drugs under this class are under clinical trials (Sala and Hartkoorn, 2011).

The first drug PA-824, is a potent drug showing cidal activity against MDR-TB. It is a prodrug, which is activated by the enzyme deazaflavin dependant nitroreductase (Ddn) by forming three different metabolites (Singh *et. al.*, 2008; Dogra *et. al.*,2010). The target of the drug, although unclear, is thought to affect cell wall biosynthesis and cause respiratory poisoning (figure 1.13) (Manjunathan *et. al.*, 2009; Jawed Ahsan *et. al.*, 2015). The response to the drug was seen by activation of various genes involved in cell wall synthesis such as FAS-I and FAS-II operon genes. Several genes involved in respiration were also activated such as *nyd* (Manjunathan *et. al.*,2009).

The other drug, OPC-67683, is also a prodrug requiring activation potentially by Ddn. The drug inhibits the mycolic acid synthesis. It shows activity against drug sensitive TB and MDR TB (Matsumoto *et. al.*, 2006; Dogra *et. al.*,2010). It is unaffected by liver microsomal enzymes which gives it an advantage to be used in combination with antiretroviral therapies. Both the drugs have now entered the second phase of clinical trials (Matsumoto *et. al.*, 2006).

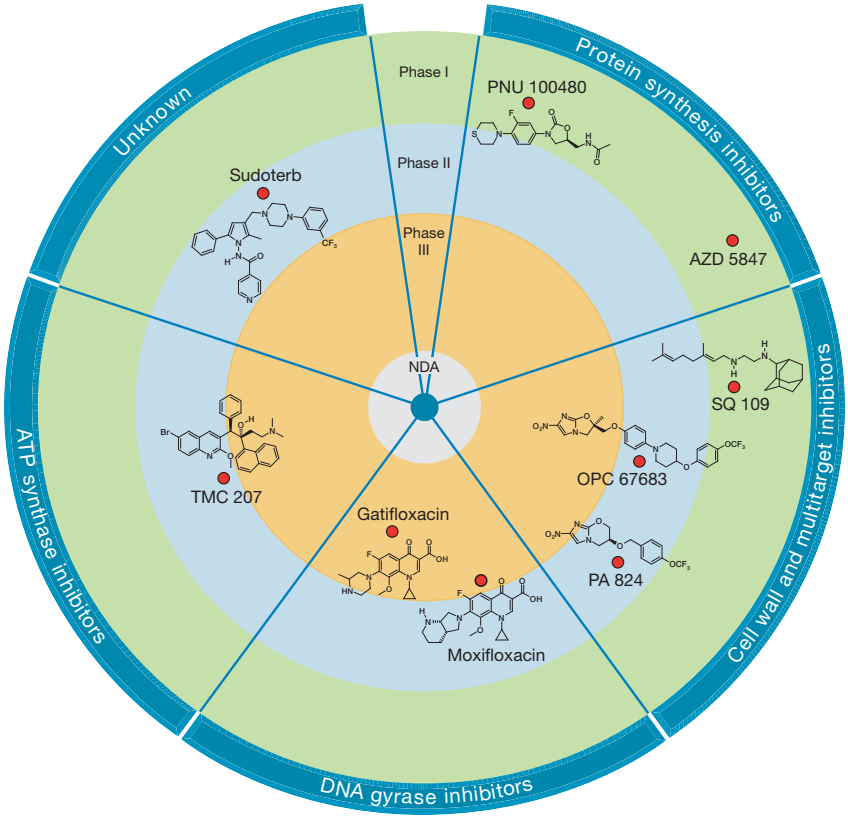

Figure 1.13: Potential new antimycobacterial drugs in clinical trials. The figure illustrates the current TB pipeline with various drugs in every phase of clinical trials (Koul *et. al.*, 2011).

1.6.3 Diamines

Drugs based on the structure of 1,2- ethylenediamine in ethambutol have led to a potential new drug, SQ109 (Boshoff *et. al.*, 2004) (figure 1.13). SQ109 is an ethambutol analogue identified by screening 60,000 compounds from a library (Reddy *et. al.*, 2010). The target of the drug is a trehalose meromycolate (TMM) transporter, Mmpl3. The drug therefore affects mycolic acid synthesis principally the cord factor (figure 1.14) (Boshoff *et. al.*, 2004). Used with bedaquiline it seems to have a synergistic effect and therefore is a more effective combinatorial therapy. The drug is under phase II clinical trials (Cole and Riccardi, 2011).

1.6.4 Oxazolidinones

Oxazolidinones are one of the novel classes of antibacterial drugs which target the protein synthesis. They bind to 23S rRNA of the 50S ribosomal subunit of the bacteria (Arias *et. al.*,2008) (figure 1.14). There are three drugs in this category which have been approved by the FDA: linezolid, Sutezolid (PNU-100480) and AZD5847. Linezolid was approved by the FDA in 2000 and although it is very effective against MDR-TB and XDR-TB, it has a lot of side effects and toxicity (Sbardella *et. al.*,2004; Lee *et. al.*, 2012).

A safer drug, Sutezolid (PNU-100480), shows higher efficacy when used in combination either with SQ-109 or in combination with moxifloxacin and pyrazinamide is very effective against the MDR strain (Williams *et. al.*, 2009; Reddy *et. al.*, 2012) (figure 1.13). AZD5847 also has a strong bactericidal activity and also targets the 50S ribosomal RNA. Both these drugs are under phase II trial (Shaw and Barbachyn *et. al.*, 2011).

1.6.5 Benzothiazinones

Benzothiazinones are a new class of drugs, highly potent against MDR and XDR-TB. The drug affects an essential enzyme decaprenyl phosphoryl-β-D-ribose 2′ epimerase encoded of *dprE1* gene. The enzyme is a major player in the synthesis of arabinogalactan. Inhibition of this essential enzyme causes cell lysis and cell wall damage (Makarov *et. al.*, 2009; Lechartier *et. al.*, 2012).

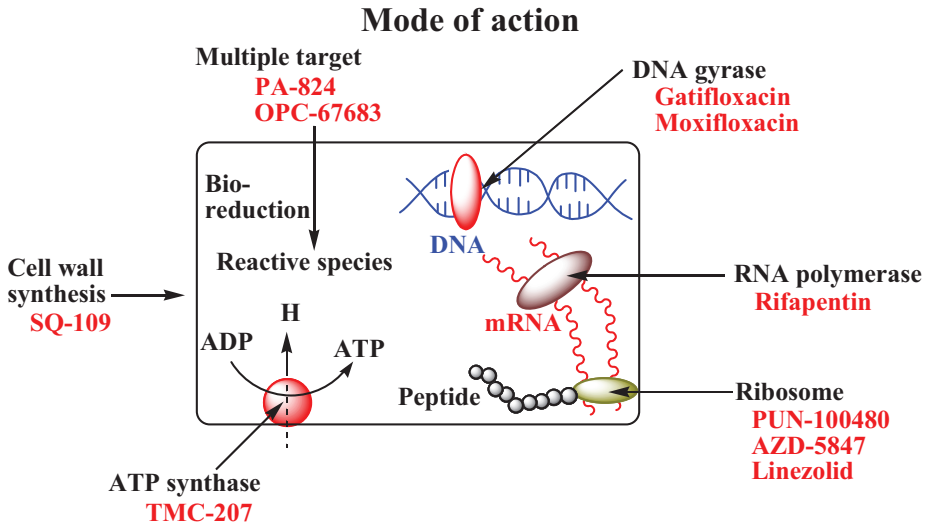

Figure 1.14: Modes of action of the potential new antitubercular drugs. The figure elucidates the various modes of actions of drugs currently in phase 2 and 3 of clinical trials (Jawed Ahsan *et. al.*, 2015)

1.6.6 Flouroquinolones

A new class of flouroquinolones are currently in phase III clinical trials (Ma *et. al.*, 2010). Gatifloxacin and moxifloxacin are being studied to be used as a combinatorial therapy with first line drugs in the TB regimen (Ahmad *et. al.*, 2011; Engohang-Ndong, 2012) (figure 1.13). Their basic mode of action is through inhibition of the protein synthesis machinery chiefly by interacting with DNA gyrase (Jawed Ahsan *et. al.*, 2015) (figure 1.14). Although these drugs reached phase III clinical trials neither seem to be particularly potent in converting sputum, reducing bacterial load or preventing morbidity when compared to exisiting mycobacterial drugs (Ruan *et. al.*, 2016; Anthony T Podany, 2016).

1.7 High throughput screening (HTS) strategies for tuberculosis drug discovery

The development of MDR and subsequent rapid succession to both XDR and XXDR/TDR strains of *Mtb* has rendered the current drug regimen ineffectual. A good screening strategy, discovery of newer drugs and identification of the mode of action would help in developing better treatment regimens and determining bacterial pathways more clearly.

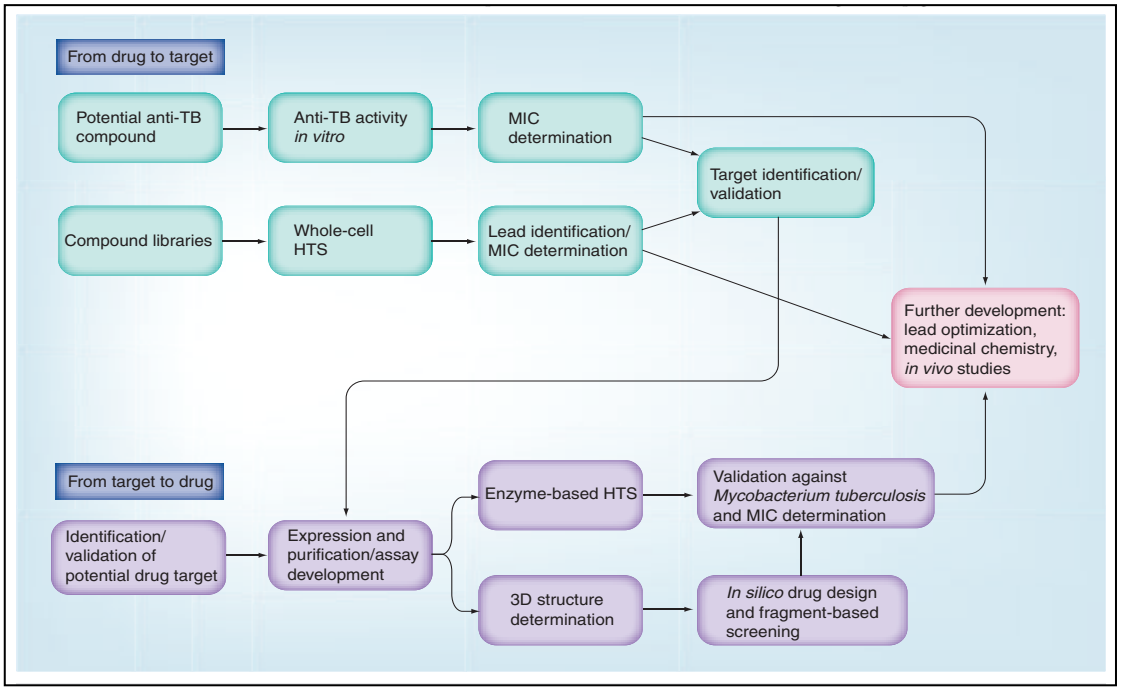

Figure 1.15: A flowchart representing drug discovery strategies describing the drug development from drug to target and from target to drug. The two strategies overlap at a level for *in vivo* studies. HTS – High throughput screening (Sala and Hartkoorn, 2011).

There are predominantly two strategies undertaken for performing drug screens in the drug discovery process: one type of assay is target specific while the other is a whole cell screening assay. Both are implemented against compound or inhibitor libraries and performing mode of action studies with the latter leads to the discovery of the target (Sala and Hartkoorn, 2011) (figure 1.15). Phenotyping screening strategies have improved and branched out to utilise indicators to scale up screens to make them high throughput. Although they provided kinetic

data in a high biocontainment level, BACTEC based radiometric assays proved to be more expensive and less adaptable to high throughput strategies than alamar blue susceptibility tests (MABA) (Collins and Franzblau, 1997). Luminescence based assays have been proactively used and have now been adapted to screen antimicrobials against non-replicating (NRP) bacteria either under the influence of a selectable promoter such as acetamidase (Cho *et. al.*, 2007) or a constitutive promoter such as for heat shock proteins (Cooksey *et. al.*, 1993). Phenotypic screens are also improvised to mimic physiological challenges that bacteria experience such as nutrient starvation, hypoxia and non-replicating states which cause the bacteria to be tolerant to the antimicrobials and prolong treatment duration accordingly. Assays adopted for hypoxia involve the application of the Wayne model of hypoxia and dormancy (Wayne and Hayes, 1996) and can be combined with indicators of cell physiology such as ATP depletion (Mak *et. al.*, 2012) or luciferase activity under the influence of an anhydrotetracycline inducible promoter (Grant *et. al.*, 2013) to screen antimicrobials or chemical compounds against the bacteria. Models for starvation were designed to mimic the *in vivo* conditions the bacteria encounter during infection and involve reducing the available nutrients in growth media, typically containing a minimal salt media without additional supplements like Middlebrook OADC/ADC. The Middlebrook 7H9 medium is used with a detergent to reduce clumping of the bacteria, one such approach used tylaxopol in combination with the media to screen compounds and read the assays using luciferase or the expression of green fluorescent protein (Pethe *et. al.*, 2010; Grant *et. al.*, 2013). Cell based kinetic assays have been designed to be combined with high content screening to understand infection *in vivo* and effectiveness of antimicrobials on infected mammalian cells. A real time electronic sensing (RT-CES) was designed with E-plates that contained gold microelectrodes at the bottom of the wells in assay plates which generated an electric field in the presence of media. This electric field is disrupted

with the growth of cells and the kinetic curves vary depending on cell type, morphology and adherence characteristics to give a time dependent cell response profile (TDCRPs) (Abassi *et. al.*, 2009). Another assay was designed using macrophage cell lines (RAW264.7) infected with green fluorescence protein expressing *Mtb* and automated high content microscopy to screen compounds that are active against intracellular bacteria (Christophe *et. al.*, 2009).

Target based screening assays generally involve screening drugs against validated drug targets which are mainly essential enzymes involved in cell wall biosynthesis, shikimate pathway, folate pathways and other physiologically important processes. The issue with target-based discovery is the validation of targets and the understanding of the role of the target *in vivo* versus *in vitro*. Assays designed to screen validated targets involve biochemical assays often using enzyme couples, for example some assays used an enzyme couple to screen dihyrdrofolate reductase (DHFR) inhibitors comprised of NADH, which in the presence of an active enzyme and substrate (dihydrofolate) produced trihydrofolate (THF) and a $NADP^+$ molecule (Kumar *et. al.*, 2012). The presence of an active DHFR enzyme can be measured by the $NADP^+$ accumulation at absorbance at 340nm and when the enzyme is inhibited in the presence of antimicrobials the addition of resazurin leads to the formation of resorfin (emission at 590nm) due to the excess NADPH in the assay mix (Kumar *et. al.*, 2012). New target based assays have been designed utilizing chromatographic principles to understand ligand-enzyme interactions. Ultrafitration-liquid chromatography/mass spectrometry (UF-LC/MS) has been used to allow interaction of the ligand and enzyme through LC and then the complex is analysed by MS while the UF element helps with the separation of the complex and unused ligand. This process has been tested to screen inhibitors against shikimate kinase an enzyme involve in the shikimate biosynthesis process (Mulabagal and Calderón, 2010). For targets that are difficult to approach, fragment based approaches have been undertaken to identify inhibitors based on

target substrates. The targets are screened spectroscopically for activity against analogues of substrates and then the most potent substrate molecules are modified with pharmacophores to get a custom designed inhibitor (Matthew B Soellner *et. al.*, 2007).

Due to the success of phenotypic screening for tuberculosis drug discovery over target based screening, the recent advances have combined these two approaches. Target based whole cell screening approaches have been implemented to screen targets in a whole cell by generating mutant strains for these targets involving either underexpressing or overexpressing the target in a whole cell in the presence of an inducible promoter. The strains underexpressing the targets are hypersensitive to the inhibitors which inhibit the target gene while overexpressing strains are resistant to the inhibitors (Abrahams *et. al.*, 2012). Along with these two major approaches, virtual screening of inhibitors directed towards specific targets is another way of looking for potential drugs. *In silico* screening for drugs against targets involve software which can perform structural matching, docking of the inhibitor molecule on target structures and deciphering affinity of the binding between the inhibitor and the target molecule (Segura-Cabrera and Rodríguez-Pérez, 2008; Jadaun *et. al.*, 2015).

Although drug screening and discovery efforts are being made for tuberculosis treatment and overcoming the treatment failure issues due to resistance, it is important to be aware of the failures of drug discovery and the reasons for it. It is imperative that there is an awareness among researchers involved in drug discovery regarding the false positive inhibitors which are misleadingly highlighted as potential drugs due to their ability to interfere with assay signalling, formation of aggregates and reactivity towards protein molecules (Baell and Holloway, 2010). Identifying Pan Assay Interference compounds (PAINs), which comprise 5-12% of a compound library in academia and are found repeatedly in different assay settings, is vital. These compounds form artefacts which may mislead researchers towards considering the

inhibitors as positives due to their molecular properties such as the fluorescent nature of the compound, its ability to coat proteins and sequester the metal ions in an assay. A lot of these compounds also act as chemical moieties releasing hydrogen peroxide which kill the cells and can seem to be a potent inhibitor (Baell and Walters, 2014). It is therefore useful to have a counteractive methodology by understanding the common structures depicted by the PAINs molecules. Approximately 400 structural classes form these molecules and using tools and filters to understand the structural basis of the inhibitors and diversity metric of the molecules can help to identify the inhibitors that seem like prospective drugs (Ekins *et. al.*, 2014; Baell and Walters, 2014). Another key aspect to bear in mind when screening for drug like compounds is using Lipinski's rule of five which defines the criteria to consider which compounds or chemical molecules lead to a high possibility of good inhibitors. These mainly involve the physiochemical properties of the compound wherein the molecules with a molecular weight of less than 500, log P (partition coefficient to measure solubility) value of less than 5, less than 5 donor hydrogen bonds and less than 10 acceptor hydrogen bonds have a high possibility of making a good drug. However, this list of physiochemical characteristics does not guarantee a strong drug like compound it increases the likelihood of a successful positive outcome (Lipinski, 2004). Awareness of the pitfalls of the current drug discovery strategies and a keen eye for false positive results can reduce the high iteration rate in the tuberculosis drug discovery process which is has been leading to the failure of potential compounds reaching the market.

Aims and Objectives

There is an imminent requirement to develop and discover new drugs to treat tuberculosis due to the development of resistance against the current antitubercular drugs.

This thesis can be divided into three major objectives:

1. Using a high throughput screening platform, the screening of the Prestwick FDA library will be implemented against both slow and fast-growing strains of mycobacteria, *M. bovis BCG and M. smegmatis* respectively. Compounds will be evaluated for potency by minimum inhibitory concentration (MIC) determination. Preliminary mode of action studies will be undertaken by the generation of spontaneous resistant mutants with subsequent whole genome sequencing.
2. A comprehensive mode of action decovolution study of florfenicol (a hit emerging from aim 1) will be undertaken. This will involve both genetic and biochemical investigation of the function of the target within the mycobacteria and its essentiality will be tested.
3. To perform a target based phenotypic screening of the GSK177 box set (Ballell *et. al.*, 2013) against *Mtb*-PrsA, a well validated target. The inhibitors will be screened using a whole cell overexpression assay and validated through a biochemical screen.

Chapter 2

Screening the FDA approved library against mycobacteria

2. Screening the FDA approved library against mycobacteria

2.1 Introduction

All the front line drugs used to treat tuberculosis were discovered through a drug to target based approach using phenotypic screening of drugs against mycobacteria, where the study of the inhibitory activity of the drug was followed by target deconvolution (Konno *et. al.*, 1967; Mitchison, 1979; Crofton and Mitchison, 1948; Bernstein *et. al.*, 1952; Ramaswamy and Musser, 1998*;* Maiga *et. al.*, 2012). Phenotypic assays are more beneficial over target based assays as they are helpful in identifying compounds which show activity against whole cells bypassing permeability issues and generating lead compounds for further optimisation simultaneously giving us tools for finding newer drug targets (Ballell *et. al.*, 2013; Brown, 2007). This method has proved more useful in terms of generating lead compounds, which are currently under clinical trials or have been approved for use by the FDA such as bedaquiline, benzothiazinone (BTZ), nitroimidazole such as PA-824 and OPC-67683 (also known as Delaminid), diamine SQ-109 (Stover *et. al.*, 2000; Protopopova *et. al.*, 2005; Matsumoto *et. al.*, 2006; Makarov *et. al.*, 2009). Delaminid and nitroimidazole PA-824 also known as Pretomanid are prodrugs that inhibit mycobacterial F-420 dependant nitroreductase mediated activation releasing nitric oxide which causes a pleiotropic effect, killing the bacterium (Evangelopoulos *et. al.*, 2015; Manjunatha *et. al.*, 2009).

Bedaquiline or TMC 207 was another important drug discovered through a screen against *M. smegmatis* using a corporate collection screen at Tibotec. The compound then underwent further medicinal chemistry iterations (Andries *et. al.*, 2005). It has been recently approved by

the FDA after 16 years of going through the drug pipeline to be used for MDR-TB treatment only due to the toxicity issues with the drug (Mikušová and Ekins, 2017; Cooper, 2013; Mdluli *et. al.*, 2014; Lechartier *et. al.*, 2014). BTZ was detected from a phenotypic screen through the NM4TB programme while 2- aminothiazole-4-carboxylases also known as ATC were identified from the TBD-UK consortium (Al-Balas *et. al.*, 2009). BTZs are a class of sulphur containing heterocyclic drugs which inhibit mycobacteria by targeting the DprE1 protein which is involved in the cell wall synthesis (Mikušová and Ekins, 2017). The disadvantages of whole cell screening is mainly issues with target identification of 'active' compounds which creates a bottleneck with taking the compound forward as a 'lead' for clinical trials (Mdluli *et. al.*, 2014).

2.1.2 Drug repurposing

In recent years, even though we have antibiotics available to treat most infections, there are diseases which are causing substantial levels of morbidity and mortality due to factors including resistance, socio-economic factors etc. Although we need to develop new antibiotics against a plethora of organisms, the cost estimated to bring a new drug to market is approximately 800 million euros. This includes approximately 10 years of research and development and clinical trials. There have been very few drugs which have come into the market since the mid-1980s especially ones with a unique mechanism of action (Vicente *et. al.*, 2006). For example, Bedaquiline is the first drug in 40 years to have been approved after the approval of Rifampicin in 1967 (Mikušová and Ekins, 2017). Most drugs from the 1980s were screened from natural products and have been improvised on structurally ever since (Vicente *et. al.*, 2006). There is now a need for alternate strategies for discovering and developing new drugs (Vicente *et. al.*, 2006). There are several new ways in which new antimicrobials for bacteria can be discovered and developed, these include finding new targets and processes, blocking multidrug efflux

channels and using alternative methods such as bacteriophages. Repurposing existing drugs is an expedient option because in theory these drugs do not require toxicity profiling, hit to lead optimisations and *in vivo* metabolic studies. In addition to that, it has been known that drugs used to treat one specific condition or disease interact with other targets which can be an assortment of enzymes, transport channels or myriad cellular components causing secondary biological consequences (Maitra *et. al.*, 2015). Sildenafil by Pfizer is one of the best examples of repurposing, as the drug was initially designed for hypertension but had a secondary effect of inhibiting the phosphodiesterases in humans. The result being that the drug is now used for patients with erectile dysfunction (Moreland *et. al.*, 1998). Based on the results from the mouse model studies it has recently been advocated to be used as an adjuvant host directed therapy in order to shorten treatment time in patients with TB. Another example of repurposing is Thalidomide, which is prescribed for leprosy and meningitis albeit judiciously due to its teratogenic effects on unborn babies. The drug is currently being progressed to treat meningitis symptoms in children caused due to tuberculosis (Maiga *et. al.*, 2012).

It has been suggested that certain classes of drugs already approved by the FDA have antimicrobial properties. Certain classes of anti-cancer drugs and gallium containing compounds have been proven to have anti-microbial properties, possibly due to the similarities between certain cancer cells and bacterial cells (Rangel-Vega *et. al.*, 2015). Gallium compounds are known to have anti-mycobacterial properties as well as being toxic to certain other classes of bacteria. 5-fluorouracil is another drug, which has antibacterial, anti-biofilm properties and acts as a virulence inhibitor to many gram-negative bacilli. It inhibits ribosome and protein synthesis in the bacteria which are mainly deprived of magnesium ions (Rangel-Vega *et. al.*, 2015). The above examples prove that repurposing drugs could be an alternative to screening against compound libraries using a reliable screening assay.

2.1.2 Phenotypic drug screening strategy

Earlier screening of antibiotics was carried out using whole cell-based assays, which were performed manually and therefore had to be optimised individually (Singh *et. al.*, 2011). The process of drug screening has become more efficient and less time consuming due to the development of assay/ micro well plates with 96, 348 and 1536 wells in terms of the number of antibiotics/ compounds screened at a time. The advent of automated liquid handling systems helped by improving the speed and accuracy of screening assays by reducing any discrepancies caused by manual handling (Singh *et. al.*, 2011). Assays designed to screen out compounds were mainly based on cell density using optical density (O.D) of cell cultures as a parameter to decide the effectiveness of a compound/ antibiotic. But O.D based assays had their own drawbacks primarily variability in cell number and growth rate of cells. In order to get a more reliable assay the use of redox dyes such as alamar blue or tetrazolium were employed which used molecular conversion in ATP, FAD and NADH to determine cell activity level (Singh *et. al.*, 2011, Collins *et. al.*, 1998). Unfortunately, use of redox dyes (even though much reliable than optical density based assays) could cause possible physiological changes in the cell when mixed in and incubated (Singh *et. al.*, 2011) and is not very useful to perform kinetic assays or real time monitoring (Collins *et. al.*, 1998). Colony forming unit (cfu) based assays are challenging for mycobacterial screening due to slow cell growth (Singh *et. al.*,2013) and it is difficult to handle *Mtb* for screening as it requires a BSL-3 facility. But in order to overcome that, most primary screens use model organisms from the mycobacterial species such as *Mycobacterium bovis, Mycobacterium smegmatis* and the weakened vaccine strain *Mycobacterium bovis* BCG. Nowadays, fluorescence assays utilising either green fluorescence protein (GFP) (Christophe *et. al.*2009) or resazurin dyes (Kumar *et. al.*, 2012) are frequently used to do kinetic and end point assays respectively. Around 20,000 molecules were screened

in the Broad institute against inhibitors targeting DprE1 (enzyme involved in cell wall synthesis) and Mmpl3 (a mycobacterial cell membrane protein large 3) using GFP fluorescence as a reporter in the assay (Stanley *et. al.*, 2012). Therefore, an optimised and validated assay utilizing fluorescent proteins produced by the bacillus could give real time results of antitubercular activity as well as decreasing the risk of interaction with other dyes and reagents at the same time, which would not influence the physiology of the bacillus.

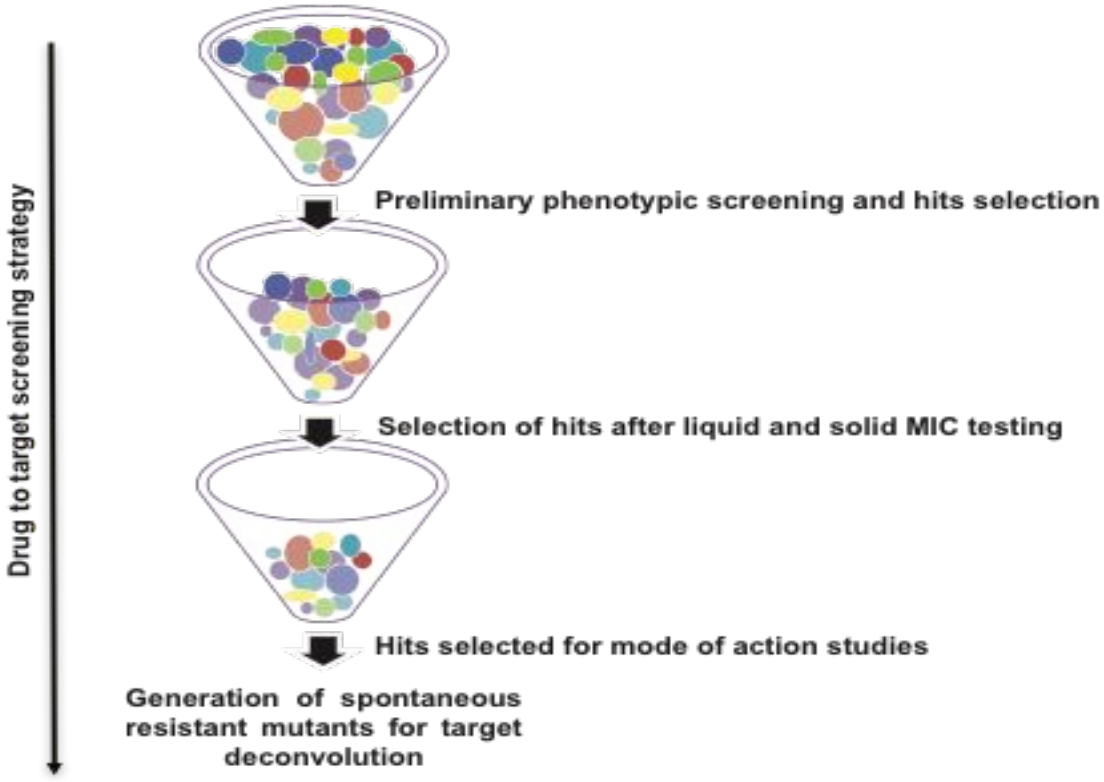

Figure 2.1: A flowchart depicting the whole cell screening strategy employed in this chapter. The top funnel represents the preliminary screen of the Prestwick library, the subsequent funnels represent the filtering of the hits through a shortlisting procedure and then MIC studies moving towards target deconvolution through generation of spontaneous resistant mutants.

In this study, we have performed a drug screen using a library of FDA approved drugs against GFP expressing strains of fast and slow growing mycobacteria based on the drug to target approach of drug discovery. The strategy involved preliminary screening of the drugs against

both the mycobacterial strains and then filtering down the hits based on various criteria in order to deconvolute the mode of actions of the drugs (figure 2.1).

2.2 Results

2.2.1 Primary screening of the Prestwick library against *M. smegmatis*_pSMT3_eGFP and *M. bovis* BCG_pSMT3_eGFP

The 1200 FDA approved drugs in the Prestwick library were screened against the GFP expressing strain of *M. smegmatis* and *M. bovis* BCG (Section 6.11.1). The data generated from these screens were then normalised against the positive and negative controls to produce a scatter graph of the survival percentages for every drug on each plate for both the mycobacterial species (figure 2.2).

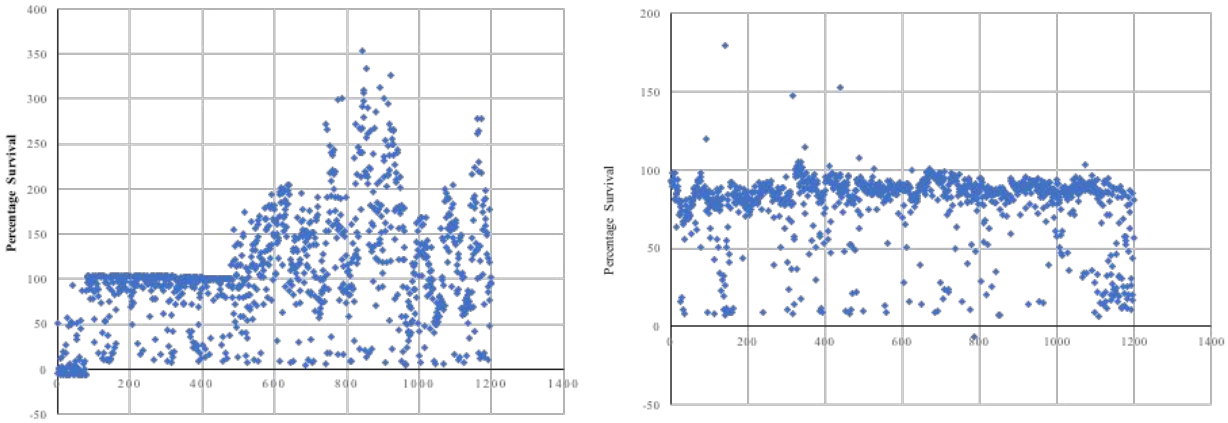

Figure 2.2: The cumulative percentage survival values observed during the whole cell screening of the Prestwick library. The graph represents the scatter graph of average percentage survivals from a duplicate data set for *M. smegmatis*_pSMT3_eGFP (A) and *M. bovis* BCG_pSMT3_eGFP (B) when screened against the Prestwick library.

The initial screen against *M. smegmatis* generated 133 hits which inhibited the survival of this fast-growing species of mycobacterium below 50% (appendix 3). As observed in the scatter

graphs (figure 2.2) representing the cumulative survival percentages of each strain for all the drugs in the library, there were some drugs specially the ones screened against *M. smegmatis* that depict very high survival percentages. (appendix 1). This was potentially caused due to the growth rate of this fast-growing mycobacterial strain and some artefacts observed in the controls during plate incubation and cross contamination due to condensation of some of the wells. The drugs showing such high survival percentages were discounted as the cut off window was set to 50% survival.

The screen against the GFP producing slow growing mycobacterial strain *M. bovis* BCG revealed 138 hits (appendix 3) which inhibited the growth of the bacteria below 50% (figure 2.2).

2.2.2 Analysis of correlation

The preliminary screens performed for both the fast and slow growing mycobacterial strains were performed in duplicates (Section 2.2.1). screen a correlation analysis was performed in order to determine the coefficient of correlation for individual plates for both strains.

It was observed that the coefficient of correlation values ranged from 0.53 to 0.86 (appendix 4) representing a positive correlation between both sets of the screen against *M. smegmatis*. When the data was plotted as a cumulative the overall correlation observed was 0.64 as an average which relates to 60% positive correlation of the data from the preliminary screen against *M. smegmatis* (figure 2.3).

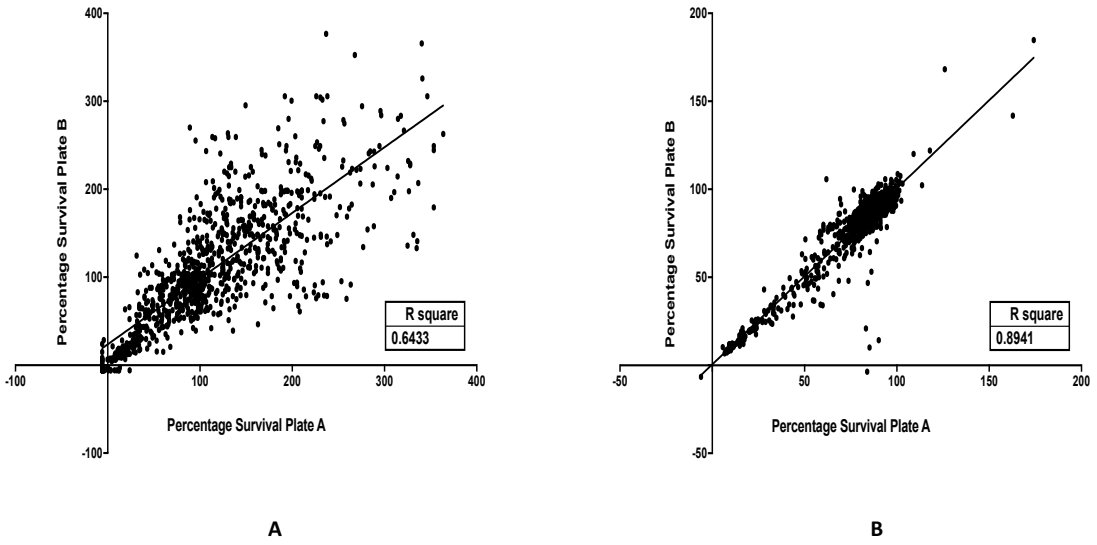

Figure 2.3: A correlation analysis of the whole cell screen against the Prestwick library. Scatter graphs representing correlation analysis of the cumulative data of the average percentage survivals between plate A and B (duplicates) during the preliminary screen of the Prestwick library against *M. smegmatis pSMT3*_eGFP (A) and *M. bovis* BCG_pSMT3_eGFP (B).

In order to understand the variability in the data and significance of the hits retrieved from the

The coefficient of correlation values ranged from 0.54 to 0.98 (appendix 5) for the screen performed against *M. bovis* BCG leading to a very high positive correlation between the screens. The cumulative correlation for *M. bovis* BCG was 0.89 leading to 89% positive correlation of the replicate data sets (figure 2.3).

A significant correlation between each replicate was therefore observed for both screens performed, which verified the validity and reproducibility of the screens against both strains.

2.2.3 Comparative analysis of the hit frequency based on the preliminary hits between *M. smegmatis* and *M. bovis* BCG

In order to understand the variation between the two strains of mycobacteria and the frequency of hits between them a comparative analysis was performed (figure 2.4). It was seen that the majority of the drugs had a survival percentage of 100%, which is valid as there were a high number of drugs that did not inhibit the growth of mycobacteria during the preliminary screen. It was also noted that there were some drugs with frequency ranging from 1 to 25 that had survival percentages higher than 100%. This was observed during the initial analysis of the preliminary screening data as mentioned in section 2.2.1. The frequency data verifies that the

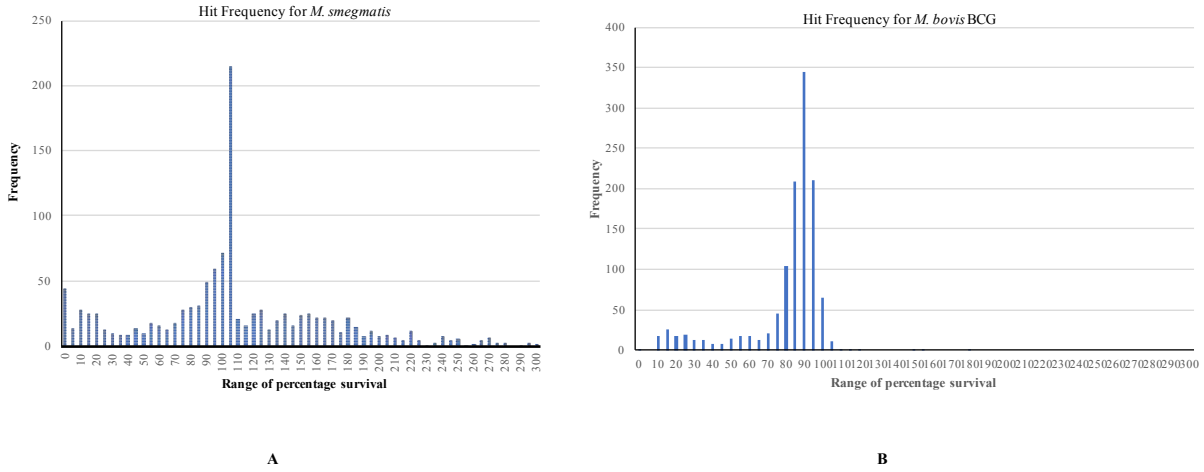

Figure 2.4: Hit frequency distribution of the whole cell screening against the Prestwick library. The bar graph represents the frequency distribution of the hits observed during the preliminary screen of *M. smegmatis*_pSMT3_eGFP (A) and *M. bovis* BCG_pSMT3_eGFP (B) against the Prestwick library.

outliers were in low numbers and were caused due to experimental conditions but not to the extent to discount the overall results obtained from the screens.

The cut off survival percentage for a drug to be considered as a "hit" was set to a percentage survival of 50%. It was observed that in case of the fast-growing strain of mycobacteria, *M. smegmatis* had a higher frequency of hits that had survival percentages ranging from 0-20% while in case of the slow growing strain *M. bovis* BCG the hits were mainly clustered in the survival percentage range of 10-30% (figure 2.4).

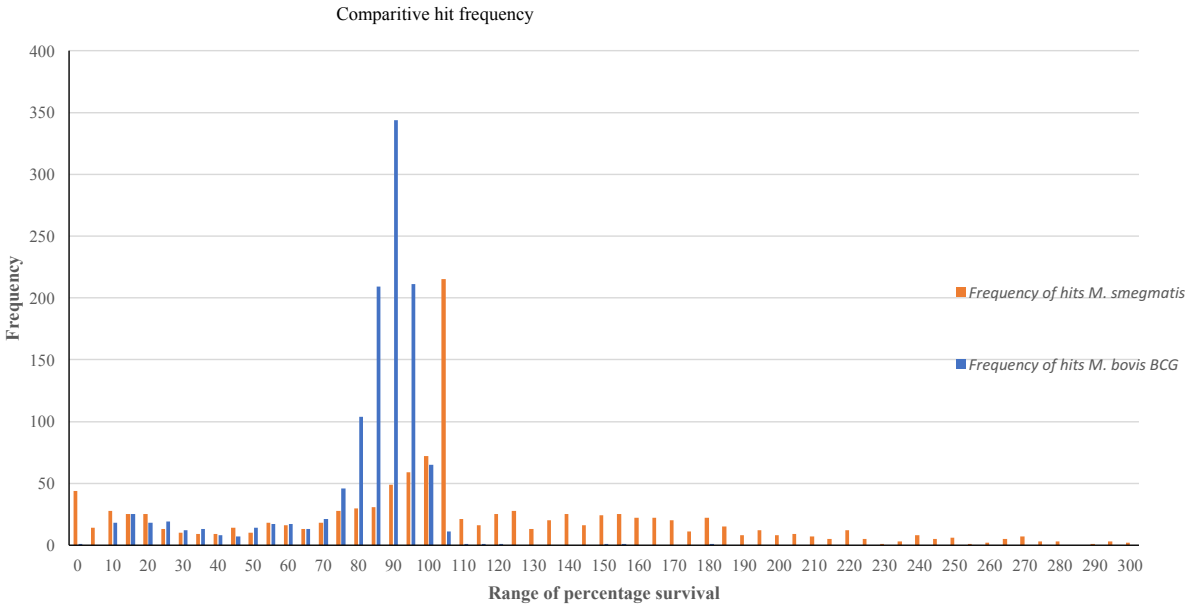

Figure 2.5: A comparative frequency distribution of the hit frequency distribution observed from the whole cell screen against the Prestwick library. The bar graph represents the comparative frequency distribution of the hits observed during the preliminary screen of *M. smegmatis*_pSMT3_eGFP (A) and *M. bovis* BCG_pSMT3_eGFP (B) against the Prestwick library.

It was also observed that in the survival percentage ranges of 10-14% and 30-34% the frequency of hits for both these strains was identical (figure 2.5).

The comparative analysis of the hits gave a general idea as to what category of drugs inhibits each strain and to what extent. A detailed analysis based on chemical properties of the drugs and literature based evidence for antimycobacterial activity was then performed for all the hits in order to shortlist a set of potentially useful drugs perform mode of action studies.

2.2.4 Z` analysis of the whole cell screen against the Prestwick library

As mentioned in Section 6.11.4, Z` factor analysis of the screen has been described and it indicates the quality of the screen. The Z` factor values for the primary screen against *M.*

smegmatis vary between different plates to a greater extent within the drug set (figure 2.6). The plates qualify for a robust screen as most of them have a value greater than 0.5. Those with the lower Z factor values were caused due to artefacts created in the plates during incubation and cross contamination due to condensation. This probably explains some of the variation observed. In case of the primary screen for *M. bovis* BCG, the Z` factor values are consistent and very robust, all of them being above 0.5 with some close to the ideal value of 1. The Z` factor was improved due to change in incubation strategy and plate handling during that period (figure 2.6).

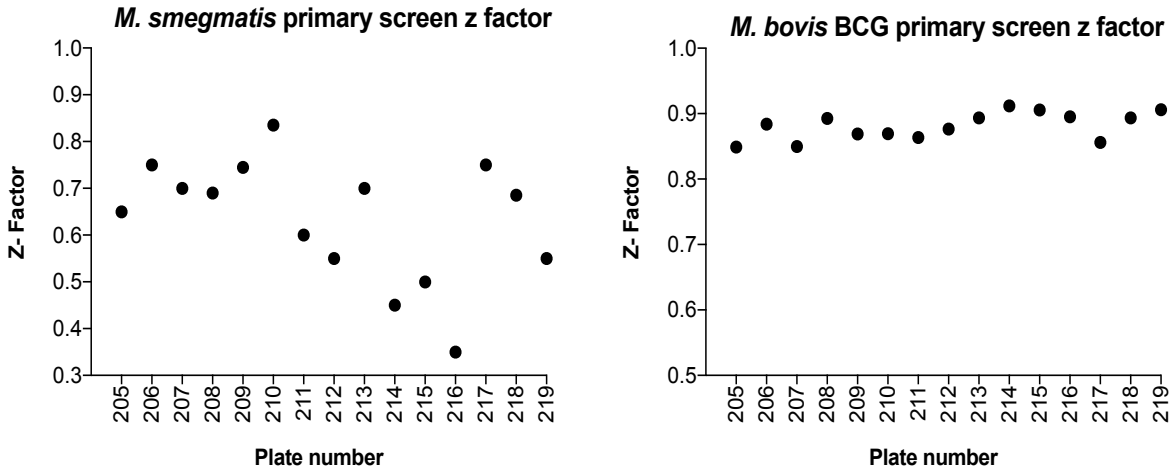

Figure 2.6: *Z`***analysis of the whole cell screen against the Prestwick library.** A scatter graph representing the Z`-factor values for each plate in the Prestwick library screened against both *M. smegmatis*_pSMT3_eGFP and *M. bovis* BCG_pSMT3_eGFP.

Overall, based on the previous correlation analysis (section 2.2.2) and the Z` factor values observed for each the plate, the screens have produced reliable outcomes which were further investigated and will be discussed further in this chapter.

2.2.5 Distribution of the preliminary hits

While classifying the hits observed during the preliminary drug screen against both the fast and slow growing strains of mycobacteria, a clear majority of hits were antimicrobials. These were then further sub divided into various classes to give a deeper understanding of the types of antimicrobials inhibiting the two strains.

Amongst the 28 hits observed within the 10-14% survival percentage range for both strains in section 2.2.3, there were eight drugs which were common between the strains, while in the 30-34% range they only have one drug in common. The common drugs were chlortetracycline, clarithromycin, rifapentine, rifamixin, vancomycin, pentamidine, tylosin, moxifloxacin and carbadox. All of these drugs are antibiotics of which some have known antitubercular activity. Chlortetracycline is a tetracycline derivative used as broad spectrum antibiotic in veterinary medicine (Lewis, 2013). Although it hasn't been reported to be effective against a mycobacterial infection as it shares its chemical structure with tetracycline, which is an antimycobacterial drug, it would therefore be expected to have some inhibitory activity against mycobacteria. Rifapentine is a known antimycobacterial drug used to treat pulmonary tuberculosis (Munsiff *et. al.*, 2006). It has also been used in conjunction with isoniazid to treat latent tuberculosis and HIV positive patients having tuberculosis (Sterling *et. al.*, 2011; 2016). Rifamixin is an antibiotic based on rifamycin and is known to inhibit both gram negative and gram positive bacteria. It also kills mycobacteria *in vitro* but due to the low absorption properties of the drug, it is ineffective *in vivo* (Soro *et. al.*, 1997). Another antibiotic which inhibits both the strains is clarithromycin, it is an antibiotic commonly used to treat pneumonia and throat infections. It was initially reported to have a synergistic effect on rifampicin during inhibition of *Mtb* (Luna-Herrera *et. al.*, 1995) but was later discovered to have a bacteriostatic effect and not provide any additional inhibitory effects to rifampicin (Almeida *et. al.*, 2011).

Moxifloxacin on the other hand, which is a fluoroquinolone antibiotic, has been proven to clear mycobacterial infections and help in culture conversion (Gillespie, 2016) and has been enrolled to be considered for a TB Alliance phase III clinical trial after successfully treating human patients with pulmonary tuberculosis (Maitra *et. al.*, 2015). Vancomycin is a well-known antibiotic used for treating symptoms caused by methicillin resistant *Staphylococcus aureus* infections (Griffith, 1981) but has not been reported to have any antimycobacterial activity. Two other drugs mentioned earlier have no known antimycobacterial activity. These are, tylosin which is a veterinary antibiotic used as a bacteriostat in animal feed (Books, LLCGeneral Books LLC, 2010) and carbadox, which is used to treat swine dysentery (Carbadox, 2014) and has been known to cause phage mediated gene transfer in *Salmonella,* Shiga toxin production in Shiga toxin-producing *Escherichia coli* and antibiotic resistant gene transfer in *Brachyspira hyodysenteriae* (Bearson *et. al.*, 2014). Among the aforementioned drugs the one that was of interest based on the literature search was Pentamidine, an antimicrobial used in the treatment of parasitic infections (Dorlo and Kager, 2008) Its mechanism of action is not completely understood but it involves the inhibition of topoisomerase II causing damage to the organism (Singh and Dey, 2007).

There was an indication of some of the classes affecting one type of strain more than the other. It was noticed that the aminoglycosides and antifungal drugs were prominently inhibiting *M. smegmatis* than *M. bovis* BCG (figure 2.7 A and B). Antifungal drugs mostly comprising of azoles are known to inhibit mycobacteria by interacting with the cytochrome P450; this has been specifically proven in *M. smegmatis* (Jackson *et. al.*, 2000a; Warrilow *et. al.*, 2009) while the susceptibility of *M. smegmatis* to aminoglycosides has been dependant on the presence of the aminoglycoside transferase gene. This gene has been shown to be present in all mycobacterial species and is responsible for resistance against aminoglycosides although the

sequence identity is variable among different species (Aínsa *et. al.*, 1997) which might be the cause of the variation in inhibition observed between the two species. A higher number of aminoglycosides seem to inhibit the *M. smegmatis* strain, this might be due to the higher efflux pump activity in *M. bovis* BCG (Li *et. al.*, 2004) in addition to the sequence variation in the aminoglycoside transferase gene mentioned earlier.

It was also observed that a higher number of drugs from the beta-lactam category inhibited *M. bovis* BCG as opposed to *M. smegmatis (*figure 2.7B). *Mtb* is known to be intrinsically resistant to beta-lactam due to its ability to produce the beta-lactamase enzyme BlaC (Chambers *et. al.*, 1995; Flores, 2005). Although, imipenem a beta-lactam antibiotic has been used to treat patients with MDR-TB successfully and meropenem, another antibiotic belonging to this class, has been known to have synergistic antitubercular effects (Chambers *et. al.*, 2005; Diacon *et. al.*, 2016). Meropenem-clavulanic acid has been proven to reduce the bacterial load *in vivo*. Amoxicillin-clavulanic acid has been listed as a third line treatment without known efficiency by the WHO (Diacon *et. al.*, 2016). The drugs mentioned here have shown activity against *M. bovis* BCG and some against *M. smegmatis.* This proves that the drugs within this class have activity against mycobacteria, not all of which have been explored in detail.

Cephalosporins is another class of drugs which inhibit *M. bovis* BCG more than *M. smegmatis* (figure 22B). In a recent screen against 600 commercially available drugs from the Sweet library, it was shown that cephalospoins had a high synergy with rifampicin although that was not particularly the case when tested with rifapentine and rifabutin. Cephalosporins also show synergies with the recently approved anti-TB drugs bedaquiline and delaminid (Ramón-García *et. al.*, 2016). These orally bioavailable drugs have activity against non-replicating *Mtb* without causing any lethal effects to the mammalian cells or macrophages (Gold *et. al.*, 2016; Ramón-García *et. al.*, 2016). Carbapenems, which are members of the beta lactam family, and

cephalosporins work by deactivating the L,D-transpeptidase responsible for the 3,3 crosslinking in the peptidoglycan and therefore affects the cell wall of the bacterium (Dubée *et. al.*, 2012).

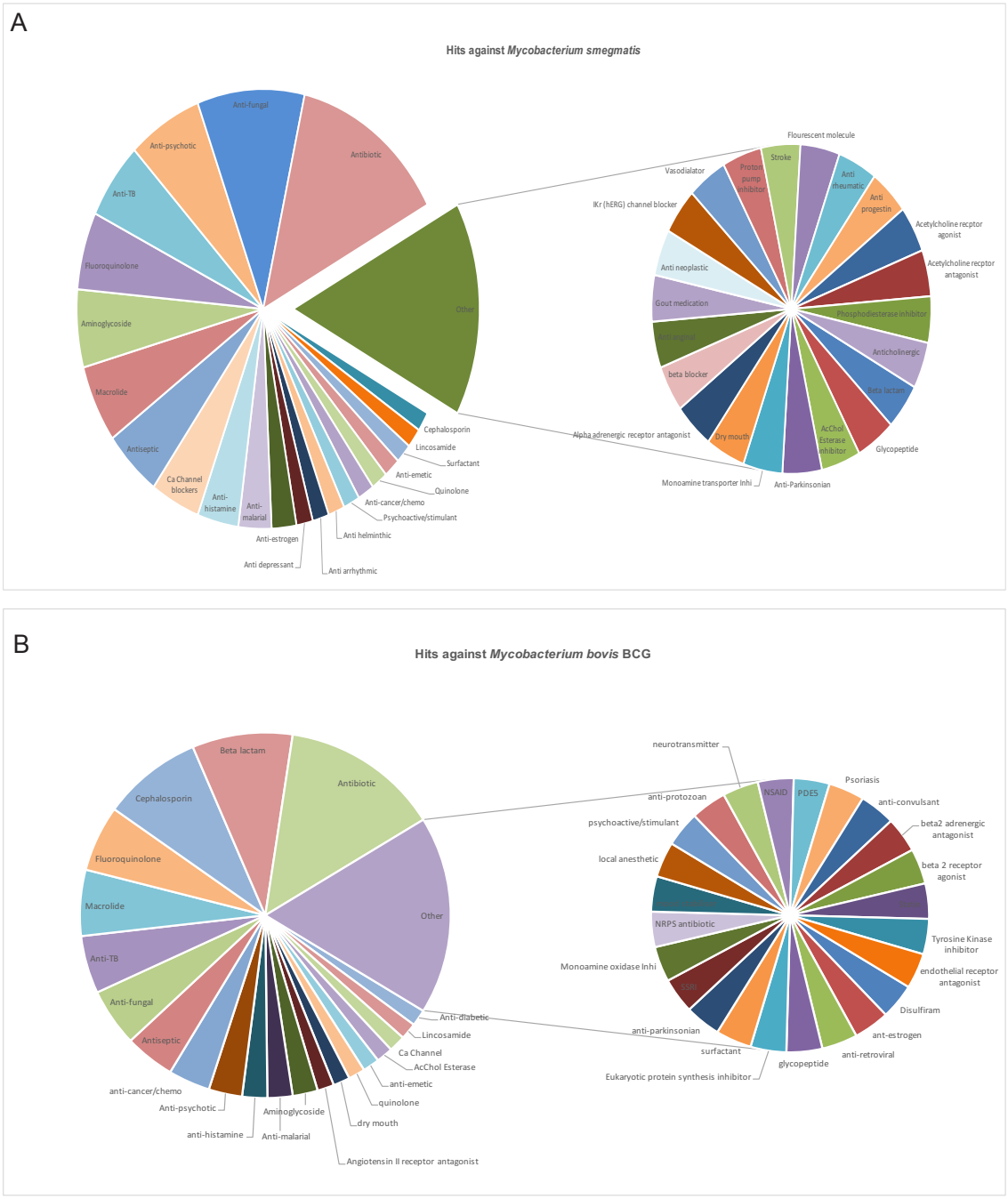

Figure 2.7: A distribution and classification of the hits from the whole cell screen against the Prestwick library. A. Represents the different classes of drugs that inhibited the growth of *M. smegmatis.B.* Represents the different classes of drugs that inhibited the growth of *M. bovis* BCG

There were other interesting classes of drugs which inhibited the growth of mycobacteria in this *in vitro* screen such as antihistamines, calcium channel blockers, oestrogen modulators, anti-cancer drugs. The drugs from the preliminary screen were carefully evaluated and compared to compile a list of hits for further studies.

2.2.6 Rationale for selection of hits

The primary hits were shortlisted based on several factors such as physiochemical properties of the drug and the evidence of anti-mycobacterial activity of the drugs. Drugs which were formulated for use as topical creams or eye drops were not taken to the next stage of secondary studies in order to avoid bioavailability and solubility issues. Drugs which are currently being used for anti-TB treatment such as isoniazid, rifampicin, ethambutol, chloramphenicol, tetracycline, streptomycin and modified structural analogues of these drugs were not considered for further study.

Drugs belonging to the antiseptic and disinfectant category, which are known to affect the bacterial membranes in various ways such oxidation of thiol groups by generation of free radicals, protein damage on the membranes, membrane leakage and disturbance of the cell homeostasis (McDonnell and Russell, 1999), were disregarded to avoid the study of dirty drugs which might not have a selective mode of action and may just be causing general damage to the cells leading to cell death.

An extensive literature search was performed in order to find out if some of the hits already had known activity against mycobacteria and were then omitted from the shortlist. Antifungal drugs have been known to have inhibitory effects against mycobacteria as mentioned earlier and therefore were carefully researched and selected based on absence of any mode of action

evidence and known functionality. Some compounds containing heavy metals such as mercury (Thimerosol) were not studied due to possible implication of presence of heavy metal use in drugs. Other drugs that were taken off from further investigation were those with known activity in pulmonary or respiratory infections and steroidal hormones which had side effects.

2.2.7 Determination of the minimum inhibitory concentration (MIC) in a liquid broth

The liquid MIC concentrations were determined against *M. smegmatis*_pSMT3_eGFP and *M. bovis* BCG_pSMT3_eGFP as mentioned in section 6.11.2. In order to determine the MIC values a dose response curve was plotted on graph representing percentage survival against the long concentrations of the respective drug being tested (appendix 6).

Among the drugs tested for *M. smegmatis*_pSMT3_eGFP the most potent drug was meclocycline sulfosalicylate with a liquid MIC of 0.1μM (table 2.1) and is a known broad spectrum antibacterial (Fritzler and Zhu, 2012). Other drugs tested for MIC determination were alexidine and chlorhexidine which both had low MIC values, 6.15μM and 1.98μM and are used as antimicrobials in dentistry (McDonnell and Russell, 1999). Estrogen receptor modulating drugs clomiphene citrate, raloxifen, toremifene, and tamoxifen citrate (Boostanfar *et. al.*, 2001; Khovidhunkit and Shoback, 1999) had MIC values ranging from 9.03μM to 26.64μM (table 2.1). GBR12909, a dopamine transport inhibitor (Andersen, 1989) has a liquid MIC of 26.48μM (table 1). Other drugs which were tested had very high liquid MIC values ranging from 77μM to greater than $8x10^6$μM (table 2.1). Two of the drugs which were tested against *M. smegmatis*_pSMT3_eGFP; auranofin and ebselen had MIC values of 0.27μM and 18.5μM respectively. Both of these drugs were partially pursued further and will be discussed in detail.

Dose response studies against *M. bovis* BCG revealed thonzonium bromide as the drug with the lowest MIC value of 0.16μM (table 2.1). Thonzonium bromide is a quaternary ammonium compound which is used as a surface active agent (Chafetz *et. al.*, 1986) and has been known to disrupt ATP dependant proton transport in vacuolar membranes along with alexidine dihydrochloride, which are responsible for pH regulation in yeast and *Candida albicans* causing growth defects (Chan *et. al.*, 2012). It is also used to treat osteolytic diseases as it deters the formation of osteoclasts and has a protective effect in mice models (Zhu *et. al.*, 2016).

Florfenicol, a fluorinated analog of thiamphenicol with known broad spectrum activity against gram negative bacteria and strains which were resistant to chloramphenicol and thiamphenicol (Syriopoulou *et. al.*, 1981), exhibited a MIC values of 0.67μM against *M. bovis* BCG (table 2.1). The drug influences the microbiota of the intestine reducing the amount of uncultured bacterial species similar to *Corynebacterium* and *Mycobacterium* (He *et. al.*, 2010). It shows *in vitro* potency against *Actinobacillus pleuropneumoniae* and *Pasteurella multocida* from pig isolates with higher potency in sample media containing animal serum (Dorey *et. al.*, 2016). Another antibiotic called josamycin, which is a 16-membered macrolide with inhibitory activity against gram negative and positive bacteria (Arsic *et. al.*, 2017), had a dose dependant activity against *M. bovis* BCG with a MIC of 0.1μM (appendix 2).

Antihistamines were another class of drugs that had inhibitory activity against *Mycobacterium bovis* BCG during the preliminary screen, of which a few were selected to study further. Three antihistamines, namely astemizole, tripelennamine and olopatadine which, are H1 receptor antagonists used for allergies, asthma and rhinitis; and allergic conjunctivitis and rhinitis respectively (Tardioli *et. al.*, 2012; Mah *et. al.*, 2008; Pipkorn *et. al.*, 2008), were examined for MIC values. Astemizole had the lowest MIC value of 17.8μM within the group followed by

tripelennamine with 41.9μM and olopatadine with the highest MIC value of 202.3μM in the group (appendix 2).

Table 2.1: Liquid minimum inhibitory concentration of hits from the whole cell screen against the Prestwick library. The table lists the drugs selected for further study which were seen to have activity against *M. smegmatis* and *M. bovis* BCG based on the preliminary screen and their minimum inhibitory concentrations (MIC) in liquid media

Shortlisted Drugs (*M. smegmatis*)	**Liquid MIC (μM)**	**Shortlisted Drugs (*M. bovis* BCG)**	**Liquid MIC (μM)**
Meclocyline sulfosalicylate	0.1013	Thonzonium	0.1586
Auranofin	0.2681	Florfenciol	0.6746
Chlorhexidine	1.948	Pentamidine	3.223
Alexidine	6.147	Astemizole	17.78
Clomiphene citrate	9.03	Pinaverium	28.29
Ebselen	18.51	Josamycin	0.1011
Raloxifene	22.1	Tripelennamine	41.87
Toremifene	23.76	Rosiglitazone	43.15
Tamoxifen citrate	26.48	Glipizide	~ 191.1
GBR 12909	26.64	Olopatadine	~ 202.3
Fendiline hydrochloride	77.57	Granisteron	~ 210.6
Sulocitidil	87.22	Phenteramine	~ 37530
Apomorphine	241.7		
Nisoldipine	396.2		
Sertraline	526.7		
Fluspirilene	8275000		

Antidiabetic drugs was another class of drugs that was analysed against *M. bovis* BCG. Among the class, glipizide and rosiglitazone were two drugs that showed an MIC value of 191.1μM and 43.15μM (table 2.1). Glipizide is a second-generation sulfonylurea drug that is prescribed for hypoglycaemia in type II diabetes. It is known to act by stimulating insulin production and correcting cellular lesions which occur during diabetes mellitus (McCaleb *et. al.*, 1984; Pontiroli *et. al.*, 1984; Riddle, 1999). Rosiglitazone, on the other hand, functions by activating peroxisome proliferator activated receptors in adipocytes and sensitising them to insulin

(Hwang *et. al.*, 2011). Pinaverium, that inhibits L-type calcium channels stopping influx of the ions (Christen, 1990), had an MIC of 28.3μM.

Two other drugs which depicted high MIC values were granisetron and phentermine. Granisetron an antiemetic drug which is an agonist to the 5-hydroxytryptamine-3 receptor which stimulates the vagus nerve responsible for reflex motility response (Navari *et. al.*, 1994; Grundy *et. al.*, 1994), had an MIC value of 210.6μM. Phentermine, which has been prescribed as an appetite suppressant to control obesity and acts as an agonist to the human TAAR1 (trace amine associate receptor 1), displayed a MIC of 37.5mM and was not tested further due to the high inhibitory concentrations.

These drugs were then further tested for inhibitory concentrations on solid media to determine accurate concentrations for mode of action studies.

2.2.8 Determination of the solid minimum inhibitory concentration (MIC)

Inhibitory concentrations of selected drugs were tested in solid media as mentioned in section 6.11.3. Drugs tested against *M. smegmatis*_pSMT3_eGFP presented a MIC ranging from 0.2μM to 625μM (table 2.2).

Some drugs were not tested in solid media, these were alexidine dihydrochloride, ebselen and fluspirilene. Fluspirelene had a high liquid MIC as mentioned in section 2.2.7 therefore it was not considered feasible to study it further. Alexidine dihydrochloride was discounted for further study due to its structural and functional similarity to chlorhexidine. Among the two drugs, alexidine had a higher liquid MIC and therefore was deemed to be less potent than chlorhexidine which had a solid MIC of 15.6μM (table 2.2).

Ebselen studies were ceased due to the mode of action deconvolution that was discovered by Favrot *et. al.*, 2013. Ebselen is an organoselenium compound approved by the FDA with a well-known pharmacological profile and is being currently tested for use in case of bipolar disorders and strokes. It was shown that the drug has antimycobacterial properties and is also effective against multidrug resistant *Staphylococcus aureus* (MRSA) (Thangamani *et. al.*, 2015). In *Mtb*, the drug acts on the bacillus by covalently binding to a cysteine residue near the active site of antigen 85. Antigen 85 is a complex of secreted proteins which play an important role in the synthesis of trehalose dimycolates (TDM) and mycolylarabinogalactan (mAG) (Favrot *et. al.*, 2013).

Inhibitory concentrations in solid media were very high for apomorphine and sulocitidil at 0.625mM, while for sertraline and nisoldipine it was 0.09mM and 0.1mM with the drugs precipitating out into the media at higher concentrations. Apomorphine also seemed to produce a colorimetric reaction while in the solid media (table 2.2); it was unclear if that impeded the drug's capability to inhibit the strain. Meclocycline sulfosalicyalte had a low solid MIC value of 0.2μM which was very close to its liquid MIC value (0.1μM) and can be visibly seen in appendix 8. Auranofin also depicted a fairly low solid MIC of 6.25μM although not very close to its liquid MIC values (0.27μM).

The estrogen modulating drugs tamoxifen citrate, toremifene and clomiphene had MIC values in a close range from 31μM to 62.5μM, to which raloxifen was an exception with a MIC value of 312.5μM (table 2.2). All MIC values were tested with a positive and negative control to be sure that there was no contamination of the media and that the inoculum contained actively growing cells (appendix 8 and 9). After performing the solid MIC testing for *M. bovis* BCG as mentioned in section 6.11.3, it was observed that the general MIC trend was that the drugs inhibited the strain in solid media at 5 to 100-fold higher concentrations. For some of the drugs

this was attributed to low solubility in the solid media and precipitation during the cooling process of the agar medium.

Table 2.2: Solid minimum inhibitory concentration of the shortlisted hits from the whole cell screen against the Prestwick library. The table lists the MIC values in solid media for drugs active against *M. smegmatis* (column 1&2) and *M. bovis* BCG (column 3&4). N/T, not tested.

Shortlisted Drugs (*M. smegmatis*)	**Solid MIC (µM)**	**Shortlisted Drugs (*M. bovis* BCG)**	**Solid MIC (µM)**
Meclocyline sulfosalicyla	0.1953125	Thonzonium	≥ 5.5556
Auranofin	6.25	Florfenciol	5.56
Chlorhexidine	15.625	Pentamidine	~ 50
Alexidine	N/T	Astemizole	~ 50
Clomiphene citrate	37.5	Pinaverium	~ 50
Ebselen	N/T	Josamycin	~ 100
Raloxifene	312.5	Tripelennamine	~ 500
Toremifene	62.5	Rosiglitazone	~ 1500
Tamoxifen citrate	31.25	Glipizide	≥ 500
GBR 12909	62.5	Olopatadine	≥ 500
Fendiline hydrochloride	15.625	Granisteron	≥ 500
Sulocitidil	625	Phenteramine	N/T
Apomorphine	625		
Nisoldipine	100		
Sertraline	90		
Fluspirilene	N/T		

As mentioned in section 2.2.7, phentermine was not tested for solid MIC studies. Glipizide, olopatadine and granisetron had solid MIC values greater than 0.5mM, the drugs precipitated out at concentrations that were higher than that and did not seem to inhibit *M. bovis* BCG (appendix 9). Rosiglitazone had the highest MIC value at approximately 1.5mM without any inhibition. Thonzonium and florfenicol had a 5-fold increase in their solid MIC values but were still around 5µM and effectively inhibited the growth of the *M. bovis* BCG.

Pentamidine, astemizole and pinaverium had solid MIC values of around 0.05mM while there was a 10-fold increase in the MIC value for tripelennamine with an MIC of 0.5mM (table 2.2).

2.2.9 Generation of spontaneous resistant mutants to determine mode of action of selected drugs

Mutants were generated for meclocyline sulfosalicylate, tamoxifen citrate and GBR12909 in *M. smegmatis* and for florfenicol, pentamidine and tripelennamine in *M. bovis* BCG as mentioned in section 6.12.

The whole genome sequencing revealed mutations in genes for each drug indicating towards the mode of actions (table 2.3). Meclocyline sulfosalicylate mutants revealed mutations in the gene Rv1856c, a probable oxidoreductase deemed non-essential by the Himar-I based transposon mutagenesis (Sassetti *et. al.*, 2003). A point mutation was observed in the gene *glyA* which is a serine hydroxymethyltransferase (table 2.3) responsible for interconversion of glycine and serine in the presence of a single carbon carrier. It plays an important role in providing single carbon groups required in purine, thymidylate and methionine biosynthesis. It has also been identified as one of the proteins which undergoes PUPylation (Ubquitinylation by prokaryotic ubiquitin protein) (Watrous *et. al.*, 2010).

The tamoxifen citrate mutant exhibited a frame shift mutation in the gene *espR* (Rv3849) (table 2.3) which produces a protein involved in transcriptional regulation of the three genes Rv3136c-Rv3614c required for the ESX-1 system. The protein binds to the DNA and regulates ESX-1 therefore controlling the virulence of mycobacteria (Raghavan *et. al.*, 2008). The crystal structure of the protein shows that it is a dimer in its physiological form with each monomer having the N-terminal helix-turn-helix which is the DNA binding domain and the C-terminal

domain which is where the protein dimerises (Gangwar *et. al.*, 2014). Spontaneous resistant mutants raised against GBR12909 in *M. smegmatis* produced consistent multiple mutations in Rv2538c (table 2.3) an essential gene for *Mtb* (Sassetti *et. al.*, 2003) which encodes for 3-dehyoquinote synthase which is one of the enzymes participating in the shikimate pathway (Garbe *et. al.*, 1991). This homomeric enzyme encoded by the gene *aroB* is the second enzyme in the pathway and is present in various bacterial strains such as *Corynebacterium glutamicum*, *Escherichia coli*, *Bacillus subtilis* and other fungi, plant and apicomplexan parasites (de Mendonça *et. al.*, 2007; Zhang *et. al.*, 2015; Lee *et. al.*, 2017). It makes for an important target due to its essentiality in *Mtb* and absence of the pathway in mammals (de Mendonça *et. al.*, 2007).

Table 2.3: Mode of action determination through spontaneous resistant mutants for drugs inhibiting *M. smegmatis*. The table represents the single nucleotide polymorphisms obtained through whole genome sequencing of the spontaneous resistant mutants raised against selected drugs in drug sensitive *M. smegmatis.*

Drug Name (*M. smegmatis* hits)	Mutated Genes	Rv Number	Positions	Amino acid substitutions	Probable function
Meclocycline	MSMEG_3619	Rv1856c	A/G		Short chain dehydrogenase/ oxidoreductase
Meclocycline	MSMEI_5111		Ccg/Tcg	P122S	Serine hydroxymethyltransferase
Tamoxifen	MSMEG_6431	Rv3849	ttc/ (Frame shift)	F24	Conserved hypothetical protein
GBR12909	aroB	Rv2538c	Ggg/Agg	G282R	Involved at the second step in the biosynthesis of chorismate within the biosynthesis of aromatic amino acids (the shikimate pathway) [catalytic activity: 7-phospho-3-deoxy-arabino-heptulosonate = 3-dehydroquinate + orthophosphate].
GBR12909	aroB	Rv2538c	gGc/gAc	G284D	
GBR12909	aroB	Rv2538c	Tgc.GTtgc (Frame shift)	C356V	
GBR12909	aroB	Rv2538c	cTa/cCa	L363P	

Auranofin, a gold atom containing FDA approved drug used in the treatment of rheumatoid arthritis, was found to be active against *M. smegmatis* as mentioned previously in section 2.2.7.

It was recently proved to have activity against *Mtb* amongst other gram positive bacteria including MRSA. It inhibits the thioredoxin reductase enzyme in the bacterial cell, which is

Table 2.4: Mode of action determination through spontaneous resistant mutants for drugs inhibiting *M. bovis* BCG. The table represents the single nucleotide polymorphisms obtained through whole genome sequencing of the spontaneous resistant mutants raised against selected drugs in drug sensitive *M. bovis* BCG.

Drug Name (*M. bovis* BCG hits)	Mutated Genes	Rv Number	Positions	Amino acid substitutions	Probable function
Florfenicol	EchA12	Rv1472	Gga/Aga	G239R	Possible enoyl-CoA hydratase echA12 [*Mycobacterium bovis* BCG str. Pasteur 1173P2]
Florfenicol	PPE50	Rv3135	gGc/gAc	G251D	PPE family protein
Florfenicol	rpsI	Rv3442c	Ccc/Gcc	P17A	Probable 30S ribosomal protein S9 RPSI
Florfenicol	glpK	Rv3696c	gTc/gCc	V271A	Probable glycerol kinase GlpK (ATP glycerol 3-phosphotransferase)
Pentamidine	BCG_0763	Rv0713	aTt/aCt	I274T	Probable conserved transmembrane protein [*Mycobacterium bovis* BCG str. Pasteur 1173P2]
	BCG_0763	Rv0713	gCg/gTg	A281V	Probable conserved transmembrane protein [*Mycobacterium bovis* BCG str. Pasteur 1173P2]
Pentamidine	mmpL6	Rv1557	Gcc/Acc	A31T	Probable conserved transmembrane protein
Pentamidine	glpK	Rv3696c	gTc/gCc	V271A	Probable glycerol kinase GlpK (ATP glycerol 3-phosphotransferase)
Trippelennamine	promoter region of gene BCG3090 (Rv 3065)	Location: -8	Upstream gene BCG 3089c (Rv 1904)	Gene Rv 3065 mmr gene (efflux pump)	
	glpK	Rv3696c	gTc/gCc	V271A	Probable glycerol kinase GlpK (ATP glycerol 3-phosphotransferase)

responsible for helping the cell to cope with reactive oxidative stress and is also involved in DNA synthesis and protein repair. The impairment of the enzyme leads the cell to become susceptible to a variety of oxidative stresses in the body while also compromising its replicating machinery (Harbut *et. al.*, 2015).

Due to the target deconvolution study presented by Harbut *et. al.* in 2015, further studies were ceased for this drug and no spontaneous resistant mutants were raised against it. Spontaneous resistant mutants were generated for florfenicol in *M. bovis* BCG, showing a point mutation in *echA12* gene which produces an enoyl CoA hydratase (table 2.4). The protein is located in the membrane fraction (Mawuenyega *et. al.*, 2005) but the gene was not found to be essential through the Himar-I based transposon mutagenesis (Sassetti *et. al.*, 2003). The protein has been known to be involved in the lipid membrane metabolism and is found to co-localise with thioredoxine A (Mawuenyega *et. al.*, 2005) and CtpD which is an ATPase involved with the metalation of the proteins secreted during redox stress (Raimunda *et. al.*, 2014). There were two other point mutations observed in the florfenicol mutant, one was in the gene Rv3135 which produces a protein belonging to the PPE family and the other was in the gene *rpsI* producing a probable 30S ribosomal protein (table 2.4). Florfenicol is a fluorinated form of thiamphenicol which belongs to the chloramphenicol family, whose mode of action is through binding to the 23S rRNA of the 50S ribosomal unit (Schifano *et. al.*, 2013). Therefore, it is fair to expect that the mode of action of florfenicol might be similar to that of chloramphenicol.

The mode of action suggested through the spontaneous resistant mutants for pentamidine was through *mmpl6* (table 2.4). Mycobacterial membrane protein large (Mmpl) are membrane proteins involved in shuttling lipid components across the cell membrane and have been known to play an important role in membrane physiology and virulence of the bacterium (Viljoen *et. al.*, 2017).

Tripelennamine mutants had a point mutation in the promoter region of the *mmr* gene (table 2.4) which is a known efflux pump involved in drug resistance with high susceptibility to quaternary compounds (Rodrigues *et. al.*, 2013). This might indicate a regulatory action of the drug affecting the production of the Mmr proteins which might therefore cause a change in the ability of the bacterium to pump out drugs.

It was observed that there was a point mutation in the *glpK* gene in each of the *M. bovis* BCG mutants (table 2.4). This gene encodes for a glycerokinase which catalyses the rate limiting step in glycerol metabolism of converting glycerol to glycerol-3-phosphate (Domenech *et. al.*, 2014; Keating *et. al.*, 2005). The protein is essential for glycerol metabolism and the knockout mutant of the gene struggles to grow in the presence of glycerol therefore reducing its ability to grow (Sassetti *et. al.*, 2003; Keating *et. al.*, 2005).

The single nucleotide polymorphisms revealed through whole genome sequencing indicate towards the mode of actions of these drugs and are a key component in understanding the feasibility of the drugs to be used in antimycobacterial treatment.

2.3 Discussion

Screening the Prestwick library of 1200 FDA approved drugs against a fast growing and slow growing strain of mycobacteria revealed an array of active inhibitors against both these strains. A higher number of drugs inhibited the slow growing vaccine strain *M. bovis* BCG versus the fast-growing *M. smegmatis*. There were categories of drugs which affected each of these mycobacterial strains individually which indicates variation in the physiology and genetics of each of them.

For screening compounds, *M. smegmatis* has an obvious advantage over the slow growing *M.*

bovis BCG strain, as it has a shorter generation time therefore boosting the high throughput nature of screening and is lower risk bacteria to work with. However, it is less efficient in availing antitubercular compounds than *M. bovis.* It was observed during a screen of the LOPAC library against *M. tuberculosis, M. smegmatis* and *M. bovis* BCG*;* 50% of the drugs that inhibited *Mtb* were not identified in *M. smegmatis* while it was only 21% of the drugs that were not identified in *M. bovis* BCG. It was observed that 30% of proteins in *Mtb* do not have conserved orthologs in *M. smegmatis* (Altaf *et. al.*, 2010). Despite this fact, bedaquiline, the most recent drug approved for the treatment of tuberculosis, was discovered through a whole cell screen assay against *M. smegmatis* (Cooper, 2013) which makes the case for the use of the strain as a model for drug screening. A comparative DNA analysis of different strains from the mycobacterial complex such as *Mtb*, *M. bovis, M. bovis* BCG, *M. microti* and *M. africanum* was performed to reveal that 90% of the DNA amongst the strains matched. 85-89% of similarity was observed between the *M. bovis*, *M. bovis* BCG and *M. africanum* with *M. microti.* The analysis was performed through the restriction enzyme cleavage analysis which works on the premise that the enzyme sites are located in specific locations on the chromosome and do not change a lot when the species are related (Imaeda, 1986).

Although genetically similar, there are obvious physiological variations between *Mtb* and *M. bovis* which have been attributed to differential gene expression of around 6% of genes in the genome. The main class of genes which are upregulated in *Mtb* were the PE/PPE genes which are involved in some of the cell wall proteins while in case of *M. bovis* it was the genes encoding for transcriptional regulators. Major variations were observed for genes involved in cell wall processes, intermediary metabolism and respiration and hypothetical proteins (Rehren *et. al.*, 2007). The variations in the strains of mycobacteria explain why there are different classes of drugs that inhibit each strain individually (figure 14). The genetic and physiological similarities

explain the overlapping drugs and drug categories (appendix 3) that inhibited the fast and slow growing mycobacteria. Apart from a few categories of drugs which inhibited the strains individually, the majority of the drugs that inhibited both the strains belonged to a similar class of drugs such as antibiotics, antifungal, calcium channel blockers, antihistamines, estrogen modulators and of course the antitubercular drugs.

Target deconvolution through whole cell screening has long been the bottleneck of this drug discovery strategy. There is an apparent trend observed for inhibitors obtained through whole cell screening against mycobacteria. A high number of targets are membrane based albeit susceptible and in a lot of cases essential to the survival of the bacterium. Some examples of these targets include *dprE1*, a gene encoding the arabinose precursor for the synthesis of cell wall components mainly arabinogalactan and lipoarbinomanan; MmpL3 which is a membrane protein involved in translocation of trehalose monomycolate across the periplasm, this is the target protein for SQ109. QcrB, another regular target observed during whole cell screening which encodes for the b subunit of the cytochrome bc1 oxidase that plays an important role in the electron transport in the cell and the inhibition of which leads to ATP depletion. *Pks13* is another gene which comes up as a frequent target in whole cell screens, this gene encodes for a protein with a thioesterase activity releasing mycolates. This high probability of membrane proteins as targets for the bacterium could be due to the high hydrophobicity of the inhibitors screened against the cell (Cole, 2016). The drugs from the Prestwick library have an average log P value of 5.7, which is the partition coefficient and is used to measure the lipophilicity of a molecule (Goldman, 2013). This therefore affects the ability of the drug to move across the cell membrane. Hydrophobic drugs have a tendency to enter into the lipid bilayer and then move laterally through the membrane due to their inability to cross the lipid bilayer into the cytoplasm easily. While traversing the bilayer they interact with membrane proteins and thus

there is a high probability of the drugs inhibiting membrane proteins thereby producing membrane protein related mutations in spontaneously generated mutants during mode of action studies (figure 2.8) (Goldman, 2013).

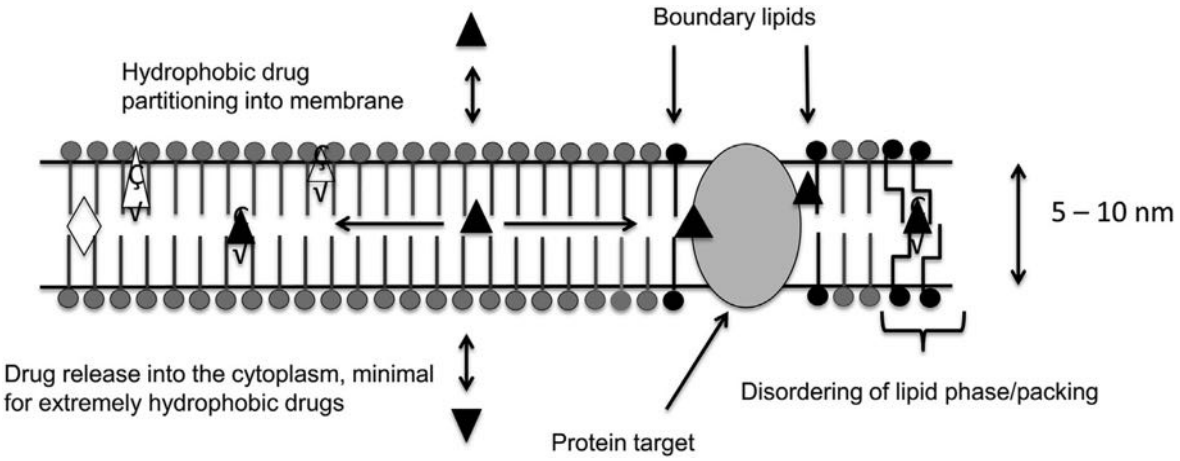

Figure 2.8: A model describing the movement of drug molecules across and through the cell membrane. The drugs partition through the membrane based on their hydrophobicity. The drug entering the bilayer then generally moves through the membrane laterally interacting with various protein in the bilayer and some on the surface or boundary. It is quite rare for very hydrophobic drugs (Goldman, 2013).

Membrane proteins are also selected if the inhibitor is an uncoupling agent causing disruption of the proton motive force and therefore affecting synthesis of ATP (Goldman, 2013). Alexidine dihydrochloride and thonzonium bromide were amongst the hits that have uncoupling properties and would have possibly generated a membrane protein mutation. Another factor that might cause most inhibitors to target membranes is the location of these proteins which are mostly localised at the cell pole where the cell wall synthesis takes place; *murG* and *wag31* involved in peptidoglycan production, *glfT2* responsible for arabinogalactan production and *mmpL3*, *pks13* in mycolic acid translocation (Cole, 2016).

Some resistant mutants depict a mutation in the *glpK* (table 2.4) for the drugs, which encodes for an enzyme involved in glycerol uptake and metabolism. This mode of action is due to *in vitro* growth conditions where the inhibitor causes a disturbance in the glycerol metabolism leading to accumulation of toxic metabolites in the cell inhibiting the growth of the organism

(Goldman, 2013). This explains the mutations observed in the spontaneous mutants generated in *M. bovis* BCG against the shortlisted drugs.

The screening of the Prestwick library, generates inhibitors such as calcium channel blockers, antihistamines, antifungal azoles and anti-infectives. The calcium channel inhibitors are generally small and hydrophobic molecules which have the ability to enter the phospholipid bilayer and can diffuse through the membrane inhibiting metabolic functions due to interactions with proteins and boundary lipids. Antifungal azoles which have known activity against mycobacteria act by targeting the CYP121 and CYP130. The antihistamine mefloquine, which disrupts membrane transport and the regulators involved in cellular replication, gives an idea about possible mode of actions for this class (Goldman, 2013). Tripelennamine, which is an antihistamine, had a mutation in the promoter of the *mmr* gene which is an efflux pump (table 2.4), this is an example of a combination of regulation and efflux pump mediated inhibition of the drug (Goldman, 2013).There were anti-infective drugs which had inhibitory activity against both the strains but were not pursued due to the possibility of their pleiotropic activity. Anti-infectives have been recently approved to be used as a systemic treatment for infection. They act by disrupting the membrane integrity and in some cases inhibit processes like transpeptidation this suggests that it is still unclear whether or not they have specific targets (Goldman, 2013).

The screening of the Prestwick library and generation of a high number of hits which had antimycobacterial activity proves that repurposing is a feasible and efficient way of mining for new drugs against TB. The drugs shortlisted and studied here have given us an idea of the potential drug targets to pursue and a possibility for designing drug scaffolds based on the antimycobacterial activity of the current FDA approved drugs in the scenario where there is low feasibility of using them against TB directly. Florfenicol although being a potentially active

drug against *M. bovis* BCG might not be considered for administration in humans as it is currently a veterinary drug. Although the protein that is targeted by it that is *echA12* belongs to a family of non-catalytic enoyl coenzyme A hydratases whose function is not clearly understood. Therefore, this target was further explored and has been discussed in Chapter 3.

Chapter 3

Genetic and biochemical characterisation of the florfenicol target *echA12*

3. Genetic and biochemical characterisation of the florfenicol target *echA12*

3.1 Introduction

The cell wall plays a major role in the survival and virulence of this organism due to its high lipid content and low permeability, making it very difficult for antibiotics to enter the cell (Brennan and Nikaido, 1995; Jarlier and Nikaido, 1994). The cell wall contains peptidoglycan which is covalently bound to the mycolylarabinogalactan (mAG) complex via phosphodiester bonds, this forms the core of the cell wall. The mycolic acids in this core complex are attached to the arabinan molecules in groups of four through ester bonds to a terminal hexa-arbinofuranosyl unit (Brennan and Besra, 1997). The arabinan units are linked linearly through glycosidic bonds to D-galactan. The mycolic acid chains run perpendicular to both the arabinogalactan and other cell wall associated glycolipids, which intersperse into the mycolic acid layer (Chatterjee, 1997). Mycolic acids are α-alkyl β-hydroxy very long chain fatty acids, the longest chains are around C_{70}-C_{90} with the largest α-branch with C_{20}-C_{25}. The synthesis of these fatty acids occurs through two fatty acid synthase cycles called FAS-I and FAS-II. The FAS-I cycle is a multifunctional cycle which produces *de novo* fatty acyl-CoA with two types of chain lengths (C_{16}-C_{18} and C_{24}-C_{26}). These products are then distributed through a bimodal system based on the presence of methylglucose or methylmannose containing polysaccharides. The FAS-I system has a limited capacity to generate long chains and cannot extend fatty acid chains. This function is performed by the acyl carrier protein (ACP) utilizing FAS-II system (Brennan and Besra, 1997; Kolattukudy *et. al.*, 1997). While the cell wall is anchored to the

inner membrane with PI, PIMs, LAM and LM molecules (Hunter and Brennan, 1990) it is also covered in a capsule mainly made up of polysaccharides and lipid-glycans which play an important role in virulence and infection (Minnikin, 1982; Daffé and Lanéelle, 2001).

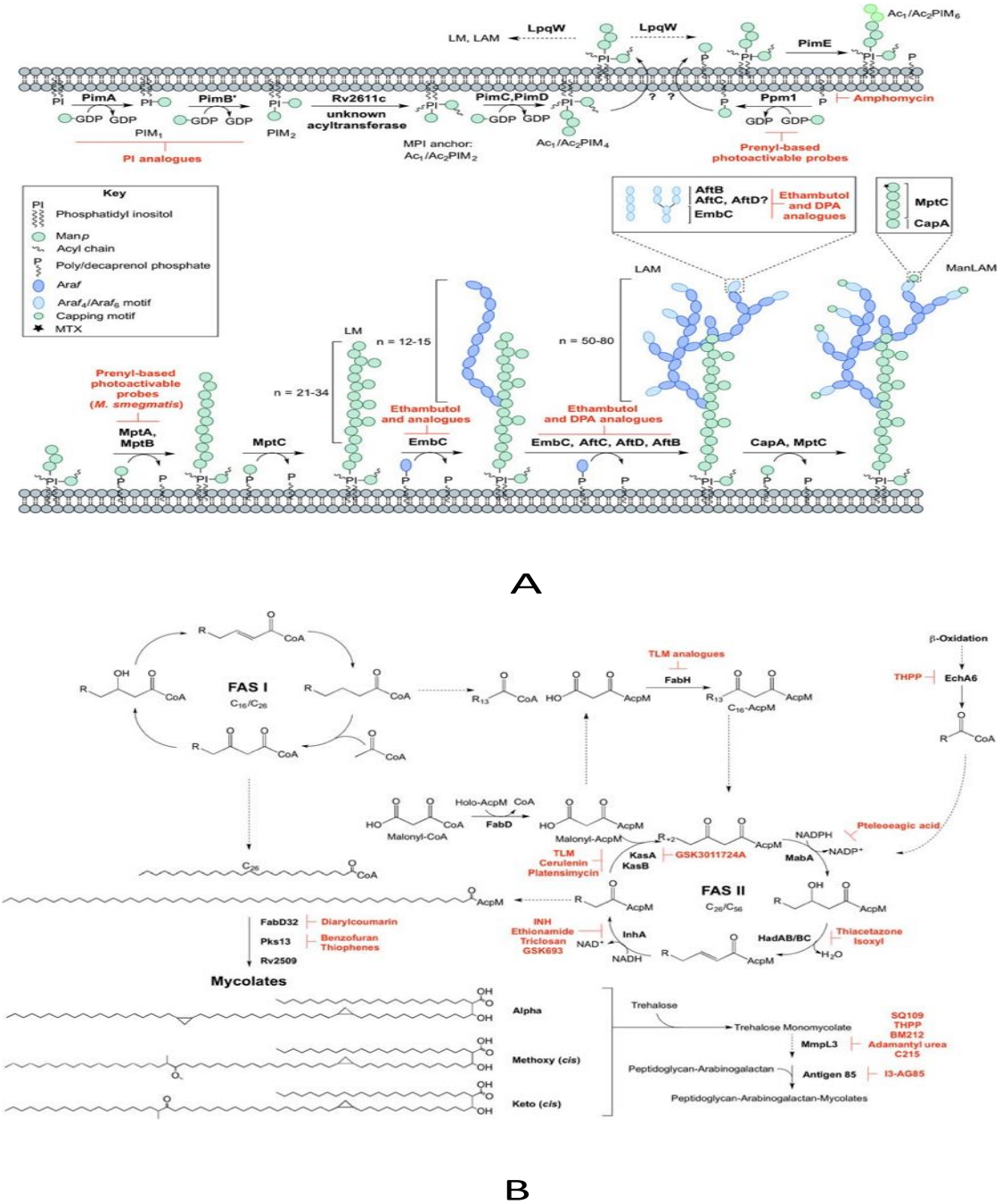

Figure 3.1: A pictorial depiction of the drugs targeting various enzymes in the biosynthesis of essential cell wall components in mycobacteria. A. Represents inhibitors targeting the biosynthesis of phosphatidylinositol mannosides (PDIM), lipomannan (LM) and lipoarabinomannan (LAM) including ethambutol. B. Presents the drugs that inhibit the enzymes in mycolic acids biosynthesis (Abrahams and Besra, 2016).

Given that the cell wall is important for the bacteria to survive in the host and establish an infection, its components and the enzymes involved in the biosynthesis of the cell wall have been attractive drug targets. A host of antibiotics that are used to treat tuberculosis or considered to be potential antitubercular drugs target components of the cell wall. Prominent examples amongst the front-line drugs which target cell wall biosynthetic components are isoniazid and ethambutol (Freiberg and Brötz-Oesterhelt, 2005; Abrahams and Besra, 2016) (figure 3.1). Isoniazid inhibits the mycolic acid synthesis when activated by the catalase-peroxidase KatG, this therefore affects the integrity of the cell wall causing the bacterium to become vulnerable to the immune system (Hu *et. al.*, 2017; Winder and Collins, 1970; Vilchèze *et. al.*, 2000). On the other hand, ethambutol disrupts the synthesis of arabinogalactan causing an accumulation of the precursors involved in the formation of this macromolecule, chiefly β-D arbinofuranosyl-1-monophosphoryldecaprenol (DPA) (Wolucka *et. al.*, 1994; Mikusova *et. al.*, 1995b). Given the fact that the current drug regimen is failing due to the rise in resistant strains, there is a need to understand unexplored biosynthetic components of the cell wall as these could be potential drug targets. In recent drug discovery attempts, it has been highlighted that drugs shortlisted through whole cell drug screens target cell wall components or enzymes involved in the synthesis of the cell wall.

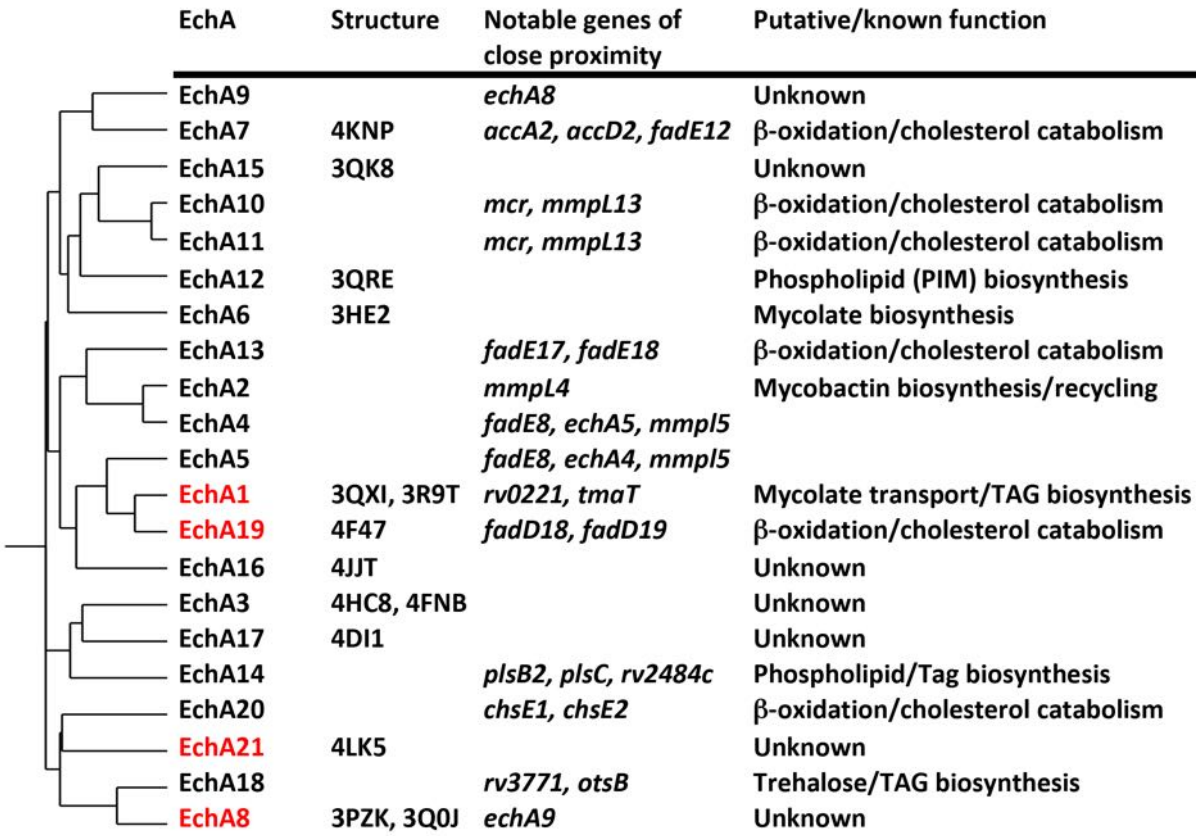

EchA	Structure	Notable genes of close proximity	Putative/known function
EchA9		*echA8*	Unknown
EchA7	4KNP	*accA2, accD2, fadE12*	β-oxidation/cholesterol catabolism
EchA15	3QK8		Unknown
EchA10		*mcr, mmpL13*	β-oxidation/cholesterol catabolism
EchA11		*mcr, mmpL13*	β-oxidation/cholesterol catabolism
EchA12	3QRE		Phospholipid (PIM) biosynthesis
EchA6	3HE2		Mycolate biosynthesis
EchA13		*fadE17, fadE18*	β-oxidation/cholesterol catabolism
EchA2		*mmpL4*	Mycobactin biosynthesis/recycling
EchA4		*fadE8, echA5, mmpl5*	
EchA5		*fadE8, echA4, mmpl5*	
EchA1	3QXI, 3R9T	*rv0221, tmaT*	Mycolate transport/TAG biosynthesis
EchA19	4F47	*fadD18, fadD19*	β-oxidation/cholesterol catabolism
EchA16	4JJT		Unknown
EchA3	4HC8, 4FNB		Unknown
EchA17	4DI1		Unknown
EchA14		*plsB2, plsC, rv2484c*	Phospholipid/Tag biosynthesis
EchA20		*chsE1, chsE2*	β-oxidation/cholesterol catabolism
EchA21	4LK5		Unknown
EchA18		*rv3771, otsB*	Trehalose/TAG biosynthesis
EchA8	3PZK, 3Q0J	*echA9*	Unknown

Figure 3.2: The phylogenetic tree of the 21 EchA proteins observed in *Mtb*. The figure details the different EchA enzymes found in *Mtb* with the structure IDs and notable genes surrounding the gene encoding the enzyme. The EchA enzymes highlighted in red are the only enzymes in the family that have catalytic residues in their structure.

Although some of these targets recur frequently and are promiscuous (for example DprE1), it is prudent to have a keen interest in novel unknown targets whose functions are not completely understood.

Enoyl CoA hydratases are involved in fatty acid β-oxidation and elongation of fatty acids in mammalian mitochondria (Fujita *et. al.*, 1980). The enoyl CoA hydratase belongs to the crotonase family, depicts a variable structural framework and has been found in prokaryotes, eukaryotes and archaea (Kinsella *et. al.*, 2003; Hamed *et. al.*, 2008). The hydratase enzyme found in animals' hydrates C_4-C_{16} enoyl CoAs while the enoyl CoA hydratase in *C. acetobutylicum* is incapable of hydrating those chain length enoyl CoAs. The enoyl CoA

hydratase is also found in *E. coli* and other mycobacterial strains (Fujita *et. al.*, 1980; Beckman and Kranz, 1991). In *M. smegmatis*, the enoyl CoA hydratase has two forms. As opposed to the enoyl CoA hydratase II, the enoyl CoA hydratase I am not involved in fatty acid chain elongation using acetyl CoA. It has been predicted that this form might instead be using malonyl CoA or be involved in amino acid metabolism (Shimakata *et. al.*, 1980). The *Mtb* enoyl CoA hydratase or the *Mtb*-EchA family consists of 21 enzymes which are probably involved in the fatty acid biosynthesis pathways (Mawuenyega *et. al.*, 2005) (figure 3.2).

It was noted that EchA16, EchA9 and EchA3 were isolated to the cytoplasm while EchA7, EchA12, EchA17, EchA20 and EchA21 were present in the membrane. EchA6 was found to be present in the cell wall, whereas the EchA10 was found to be both cytoplasm and present in the membrane (Mawuenyega *et. al.*, 2005). It was also interesting to note that the EchA12 proteins demonstrated strong functional linkages with the FadB2 and FadB3 enzymes, both of which are involved in fatty acid degradation (Mawuenyega *et. al.*, 2005). The gene encoding for the Fad proteins in *Mtb* are notably observed in the vicinity of the EchA encoding gene, potentially indicating their role in fatty acid biosynthesis. Among the EchA enzymes it was observed that the EchA1 enzyme contained a glutamate residue in the position 149 which correlates to the catalytic residues noted in *E.coli* (Humanes *et. al.*, 1999). The EchA19 and EchA21 proteins contain acidic residues which are active site residues, indicating that they are catalytic enzymes. EchA9 contains a glutamate and an aspartate residue in the catalytic site (Srivastava *et. al.*, 2015). These are the only four enzymes which are catalytic within the EchA family of proteins in mycobacteria. Although the *echA* genes have been predicted to be involved in fatty acid biosynthesis, the regulation of these genes can vary. The genes are expressed differently under various environmental conditions. The *echA8*, *echA11* and *echA12* genes are upregulated during nutrient starvation while the *echA10* and *echA21* genes are downregulated

during this process. The *echA* genes are also expressed variably based on infection, for example, the *echA19* gene is upregulated during macrophage infections in THP-1 cell lines while in the case of mouse infection, *echA7* is upregulated (Williams *et. al.*, 2011; Dubnau, 2002). It was also recently proved that EchA6 is a non-catalytic essential enzyme involved in phospholipid biosynthesis (Cox *et. al.*, 2016a).

In this chapter, we have discussed the mycobacterial enoyl CoA hydratase EchA12 which, as discussed in chapter 2, was discovered to be a target for florfenicol through spontaneous mutant generation. EchA12 has been found in the membrane fraction and Himar-I based mutagenesis has presented this gene to be non-essential *in vivo* (Sassetti *et. al.*, 2003; Mawuenyega *et. al.*, 2005). In this chapter, we have attempted to deconvolute the function of EchA12 in mycobacteria.

3.2 Results

3.2.1 Genetic synteny of the echA12 gene

A genomic alignment of the *echA12* genes was performed using ClustalOmega for 4 different mycobacterial species against the *Mtb echA12* gene. It was observed that the *echA12* gene from *M. bovis* (Mb1507) had a maximum genomic identity of 99.88% with the *echA12* (Rv1472) gene from *Mtb*.

The lowest identity of 70.6% was with the *M. leprae echA12* gene (ML1241), but despite this, it shared more than a 50% similarity, which could mean that the important bases required for the functions of the protein were conserved within the sequence. The *echA12* gene in *M. smegmatis* (MSMEG_3139/MSMEI_3508) shares only 74.7% similarity, closely followed by *M. leprae*. genome of different mycobacterial species was localised around the same position. In *Mtb* and *M. bovis* the genes upstream and downstream to the *echA12* gene were the same.

The genes upstream were *trxB1* and *trxA* (figure 3.3) which encode for thioredoxin molecules involved in redox reactions during oxidative stress in *Mtb* (Mehta *et. al.*, 2016). The gene ML1240c encodes for the first part of the transporter and ML1239c encodes the second part. In *M. smegmatis*, the genes that are present upstream and downstream to the *echA12* gene were the same as those observed in *Mtb* and *M. bovis*. With this observation, it is clear that the genetic synteny is conserved to a high degree between all the species of mycobacteria.

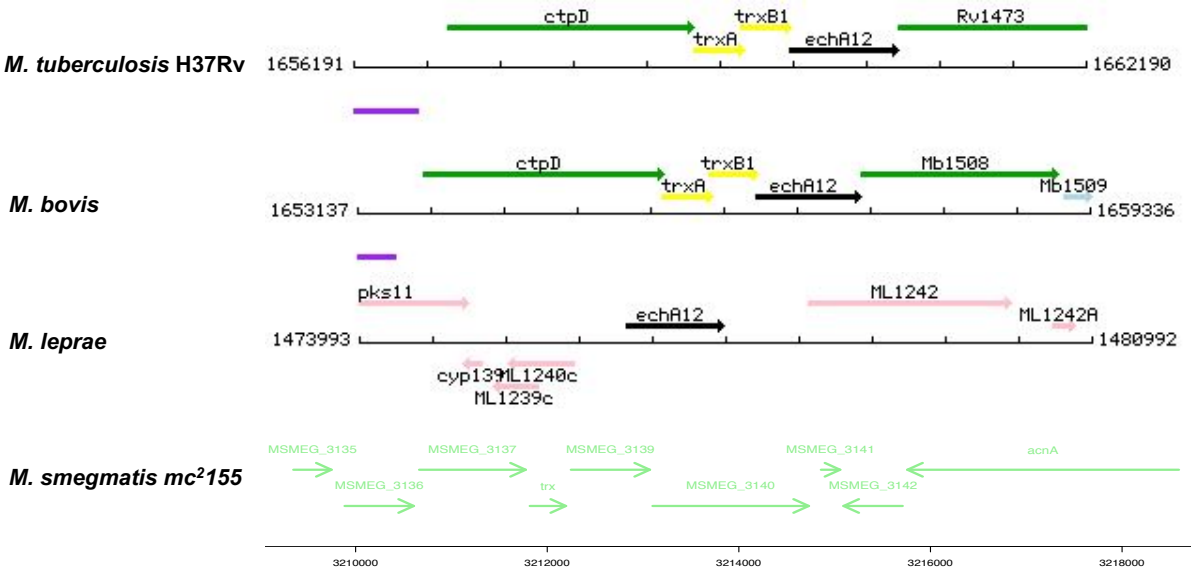

Species name	Notable gene upstream to *echA12*	Notable gene downstream to *echA12*
***M. tuberculosis* H37Rv**	***trxB1, trxA***	**Rv1473**
M. bovis	***trxB1, trxA***	**Mb1508**
M. leprae	**ML1240c**	**ML1242**
***M. smegmatis* mc²155**	***trx***	**MSMEG3140**

Figure 3.3: A comparative representation of the gene placement of the *echA12* gene across different mycobacterial species. The figure depicts the various genes found upstream and downstream of the *echA12* gene in different species of mycobacteria to represent the genetic synteny of *echA12*. The table below the diagram lists the prominent genes observed on either side of *echA12* in each of the mycobacterial species.

Based on the genes flanking it, it was observed that the position of the *echA12* gene within the

This includes *M. leprae* which has a reduced genome generated through reductive evolution to in order to conserve only the most important genes for survival and virulence. The gene downstream to the *echA12* gene encodes for an ABC transporter involved in the export of macrolides (figure 3.3). In the case of *M.leprae*, the genes encoding for the ABC transporter for macrolides are upstream to the *echA12* gene and are potentially the cause of macrolide resistance (Braibant *et. al.*, 2000).

3.2.2 Cloning of echA12 into pVV16 for constitutive overexpression.

The *echA12* gene from *M. tuberculosis* H37Rv, *M. bovis* BCG and the spontaneous mutant raised against florfenicol in *M. bovis* BCG (table 4, section 2.2.9) were cloned into the pVV16 vector (section 6.4.1.2) for constitutive overexpression of the gene.

The gene was amplified (figure 3.4A) and cloned into the vector through double digestion (figure 3.4B) (section 6.4). Once the cloned plasmids were sequenced, the plasmids were electroporated into *M. bovis* BCG and *M. smegmatis* (section 6.9.2.2).

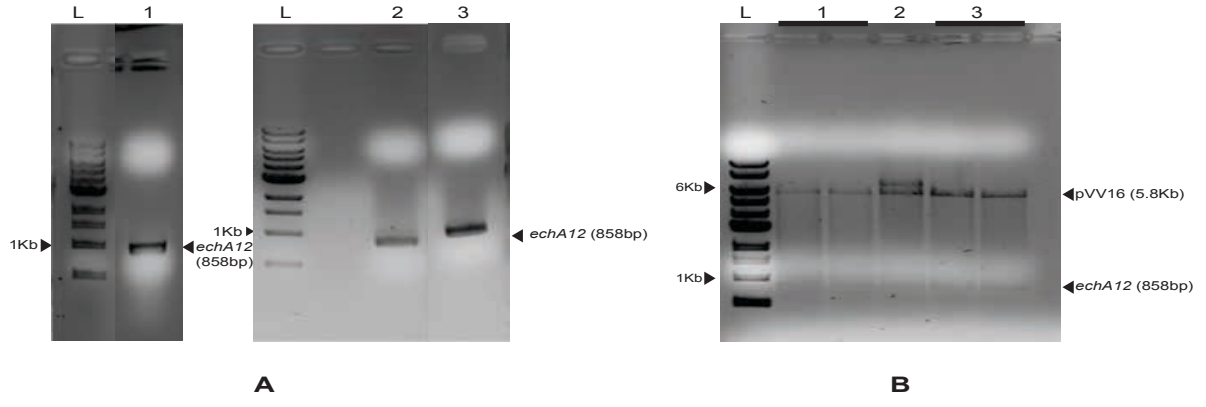

Figure 3.4: Cloning of the *echA12* (858bp) gene into the pVV16 (5.8Kb) vector. A. Represents the agarose gel of the PCR products of the *echA12* with a 1Kb ladder (L), 1. *echA12*_Rv, 2. *echA12_M. bovis* BCG, 3. *echA12*_G239R. B. Agarose gel depicting the double digest (HindIII and NdeII) products of a cloned pVV16 vector containing the *echA12* gene. The products were run alongside a 1Kb ladder (L), 1. pVV16_*echA12*_G239R, 2. pVV16_*echA12_M. bovis* BCG and 3. pVV16_*echA12*_Rv

3.2.3 Overexpression of *echA12* in *M. bovis* BCG and *M. smegmatis* to test resistance against florfenicol

The overexpression strains with constitutive expression of *echA12* were tested for resistance against florfenicol (Section 6.18.1). It was observed that the *echA12* overexpression strains with the different genes had a higher tolerance to florfenicol when compared to the strains containing the empty vector (figure 3.5). It was observed that the *echA12* overexpression strain with the amino acid substitution G239R had the highest tolerance to florfenicol, depicting approximately 70% survival percentage at the highest concentration of florfenicol in the *M. smegmatis* overexpressor.

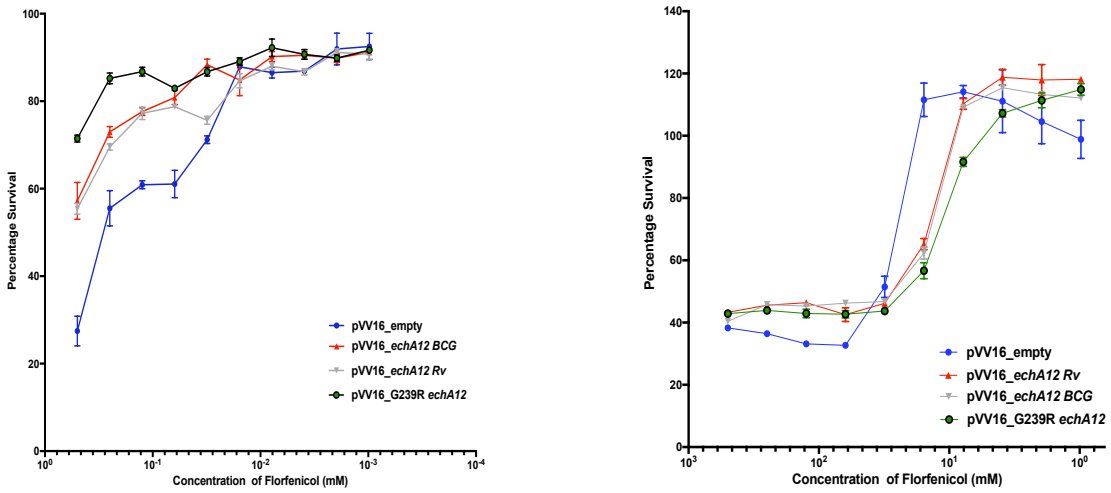

Figure 3.5: IC50 shift against florfenicol in echA12 overexpressing strains in *M. smegmatis* and M. *bovis* BCG. A. The figure represents the average survival percentage at various drug concentration leading to an IC50 shift in *echA12* overexpressing strains in *M. smegmatis* containing pVV16 plasmids with the e*chA12* gene from *M. tuberculosis* H37Rv, *M. bovis* BCG and the spontaneous resistant mutant raised in *M. bovis* BCG. B. The figure represents the average survival percentage at various drug concentration leading to an IC50 shift in *echA12* overexpressing strains in *M. bovis* BCG containing pVV16 plasmids with the e*chA12* gene from *M. tuberculosis* H37Rv, *M. bovis* BCG and the spontaneous resistant mutant raised in *M. bovis* BCG.

The *M. smegmatis* strain containing the H37Rv gene and the *M. bovis* BCG gene had similar growth profiles and survival percentages at the highest concentration of florfenicol (figure 3.5A). The overexpression strains in *M. bovis* BCG depicted similar profiles, albeit with higher tolerances as compared to the empty vector containing strain at the highest concentration of florfenicol (figure 3.5B). The percentage survivals for the strains were observed to be fairly high yet consistent, so this could perhaps be the effect of the vector, which has inherent antibiotic resistant markers. There is, however, a clear difference of an IC50 shift between the strain containing the empty vector when compared to the strains expressing the *echA12* gene (figure 3.5B).

3.2.4 Lipid analysis of the *echA12* overexpression strains in the presence of florfenicol

Lipid analysis was carried out using four different overexpression constructs electroporated in *M. smegmatis* and *M. bovis* BCG. The overexpression strains containing the pVV16_*echA12*_G239R, pVV16_*echA12*_*M. bovis* BCG and pVV16_*echA12*_Rv were compared with the empty vector containing strain. The extractions were performed after radiolabelling the *M. smegmatis* and *M. bovis* BCG cultures with C14-acetate and then extracting the lipids (section 6.18 to 6.19).

3.2.4.1 Apolar lipid analysis in *M. smegmatis echA12* overexpressors

In the apolar lipid extractions we generally observe free fatty acids, free mycolic acids, triacyl glycerols, trehalose monomycolate and trehalose dimycolate moieties based on the various solvent systems that are undertaken to perform the thin layer chromatography. When the apolar lipids were separated in different solvent systems on the 2-D TLCs (figure 3.6,3.7; appendix

11,12), there were no differences observed among the different overexpression strains compared to the empty vector strain.

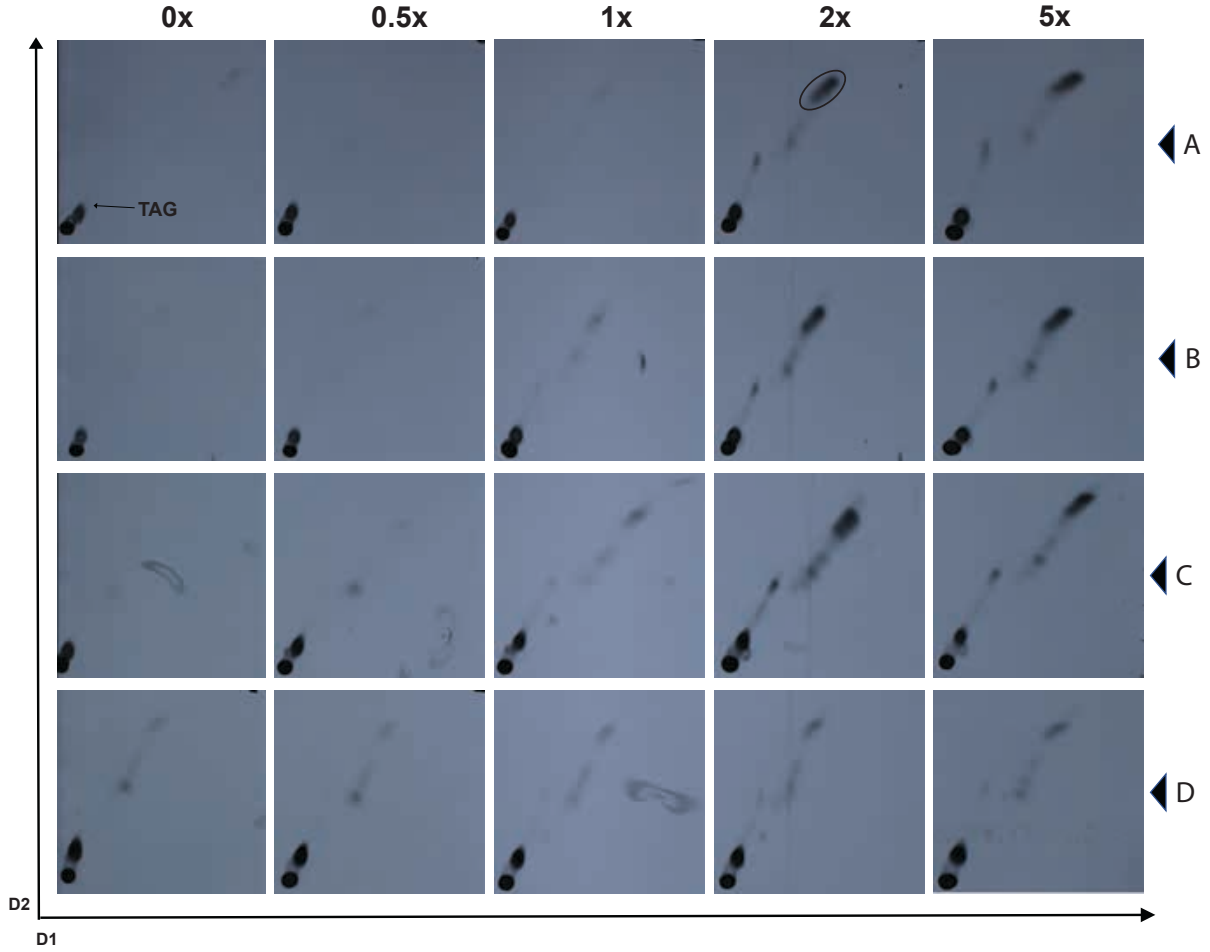

Figure 3.6: Apolar lipids separated by 2-D TLC on a silica gel plate using Petroleum ether: Ethyl acetate (98:2)x3 in direction one (D1) and Petroleum ether: Acetone (98:2) in direction two (D2). The TLC separation of apolar lipids from four different strains of *M. smegmatis* mc^2155 was carried out using two different solvent systems in two directions. The *M. smegmatis* strains used are depicted based on the overexpression plasmids they contain: A. mc^2155_pVV16, B. mc^2155_pVV16_*echA12*_Rv, C. mc^2155_pVV16_*echA12*_BCG, D. mc^2155_pVV16_G239_*echA12*. The strains were treated with 0x, 0.5x, 1x,2x and 5x MIC of florfenicol. TAG, triacylated glycerol; the spot encircled is a mixture or ketones.

Amongst the lipids separated in system A however, it was observed that there was an accumulation of a mixture of ketones that increased in abundance with the increase in the florfenicol concentration, as seen prominently in the 2x and 5x MICs (figure 3.6). These have

been previously described as a mixture of unsaturated branched ketones which are similar to tuberculenone from *M. tuberculosis*.

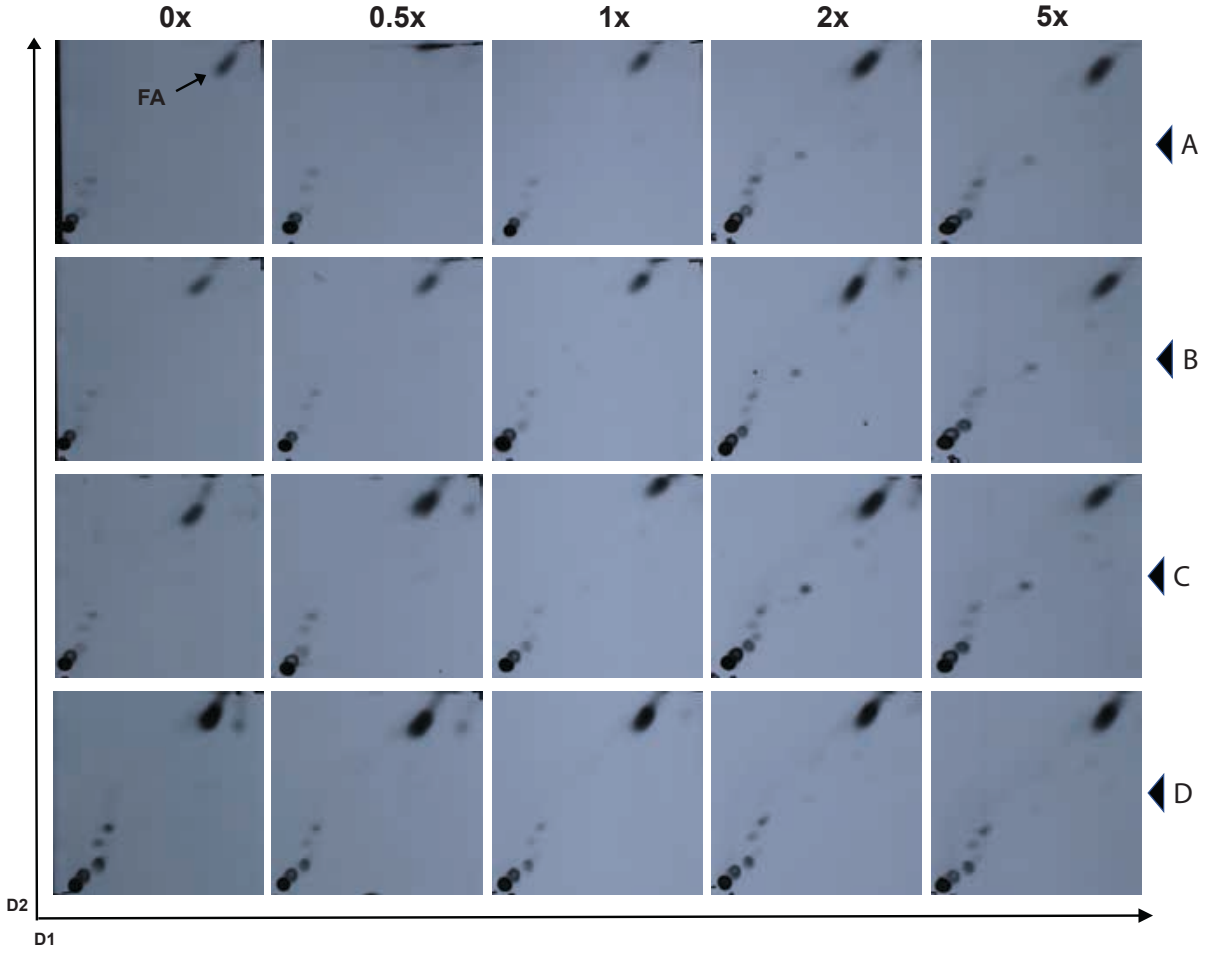

Figure 3.7: Apolar lipids separated by 2-D TLC on a silica gel plate using Petroleum ether: Acetone (98:2)x3 in direction one (D1) and Toluene: Acetone (95:5) in direction two (D2). The TLC separation of apolar lipids from four different strains of *M. smegmatis* mc^2155 was carried out using two different solvent systems in two directions. The *M. smegmatis* strains used are depicted based on the overexpression plasmids they contain: A. mc^2155_pVV16, B. mc^2155_pVV16_*echA12*_Rv, C. mc^2155_pVV16_*echA12*_BCG, D. mc^2155_pVV16_G239_*echA12*. The strains were treated with 0x, 0.5x, 1x,2x and 5x MIC of florfenicol. FA, fatty acids.

These ketones were potential shuttle products of mycolic acid precursors such as α-alkyl β-oxo fatty acids which undergo decarboxylation (Bhatt *et. al.*, 2008). This accumulation of ketones

was comparatively lower in the construct with the mutated *echA12* gene containing the amino acid substitution G293R. It was also observed that there was an accumulation of free fatty acids when the apolar lipids were separated using solvent system B (figure 3.7). When compared to all the other constructs of the *echA12* overexpression, there was comparatively less accumulation of the free fatty acids in the G239R substituted overexpression strain.

3.2.4.2 Polar lipid analysis in *M. smegmatis echA12* overexpressors

After the initial extraction of the apolar lipids from the mycobacterial overexpression strains,

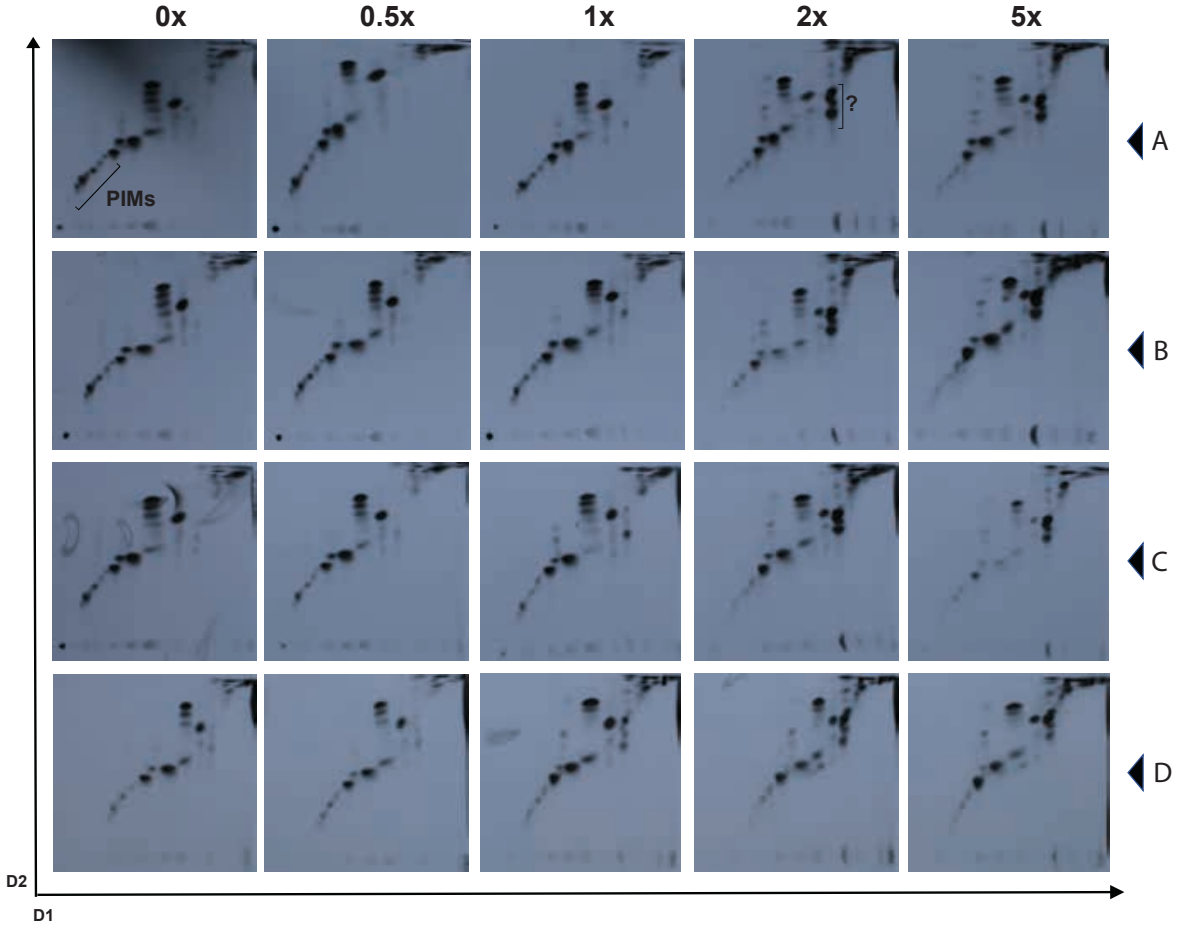

Figure 3.8: Polar lipids separated by 2-D TLC on a silica gel plate using Chloroform: Methanol: Water (60:30:6) in direction one (D1) and Chloroform: Acetone: Methanol: Water (40:25:3:6) in direction two (D2). The TLC separation of polar lipids from four different strains of *M. smegmatis* mc^2155 was carried out using two different solvent systems in two directions. The *M. smegmatis* strains used are depicted based on the overexpression

plasmids they contain: A. mc^2155_pVV16, B. mc^2155_pVV16_*echA12*_Rv, C. mc^2155_pVV16_*echA12*_BCG, D. mc^2155_pVV16_G239_*echA12*. The strains were treated with 0x, 0.5x, 1x,2x and 5x MIC of florfenicol. P, phospholipids; PI, phosphatidylinositol; Ac_1PIM_2, monoacylated phosphatidylinositol dimannoside; Ac_2PIM_2, diacylated phosphatidylinositol dimannoside; Ac_1PIM_6, monoacylated phosphatidylinositol hexamannoside; Ac_2PIM_6, diacylated phosphatidylinositol hexamannoside.

the polar lipids were extracted (section 6.18.5). The polar lipids were separated using solvent system E to visualise the acylated phosphatidylinositol mannosides, phoshpotidylinositols, phospholipids, trehalose monomycolates and trehalose dimycolates. A notable change in the phospholipid profile with the increase in the florfenicol concentration is seen at 2x and 5x MICs without any obvious change in the PIMs or phosphatidylinositol moieties (figure 3.8).

3.2.4.3 Apolar lipid analysis in *M. bovis* BCG *echA12* overexpressors

Apolar lipid extraction was carried out on overexpression strains in *M. bovis* BCG labelled with [^{14}C]-acetate in the presence of florfenicol. Here we observe triacylglycerols, free fatty acids, free mycolic acids, diacylglycerols, glucose monomycolate, trehalose dimycolate, diacylated trehalose, sulpholipid and phthiocerol dimycocerosate in different solvent systems (figure 3.9,3.10; appendix 13,14). There was no specific trend observed in apolar lipids in *M. bovis*

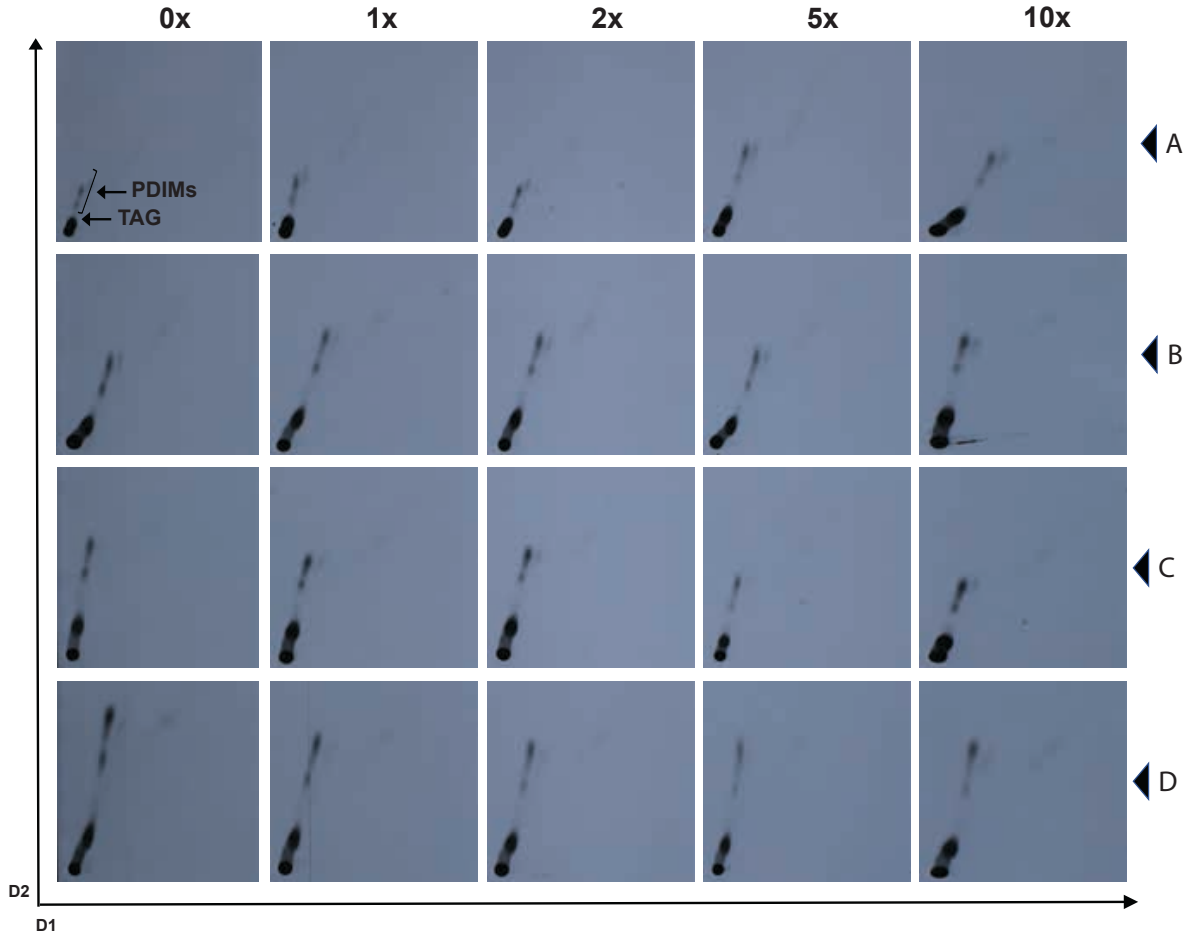

Figure 3.9: Apolar lipids separated by 2-D TLC on a silica gel plate using Petroleum ether: Ethyl acetate (98:2) x3 in direction one (D1) and Petroleum ether: Acetone (98:2) in direction two (D2). The TLC separation of apolar lipids from four different strains of *M. bovis* BCG was carried out using two different solvent systems in two directions. The *M. bovis* BCG strains used are depicted based on the overexpression plasmids they contain: A. *M. bovis* BCG_pVV16, B. *M. bovis* BCG_pVV16_*echA12*_Rv, C. *M. bovis* BCG_pVV16_*echA12*_BCG, D. *M. bovis* BCG_pVV16_G239_*echA12*. The strains were treated with 0x, 1x, 2x, 5x and 10x MIC of florfenicol. TAG, Triacyl Glycerol, PDIMs, Phthiocerol dimycocerosate.

BCG overexpressing *echA12* in the presence of florfenicol, except for the increased accumulation of triacyl glycerols and phthiocerol dimycocerosate in apolar lipids separated in system A. In the empty vector, an increase was observed in the triacyl glycerol with the increase in florfenicol as opposed to the consistent high expression of the triacyl glycerols in the overexpression strains (figure 3.9).

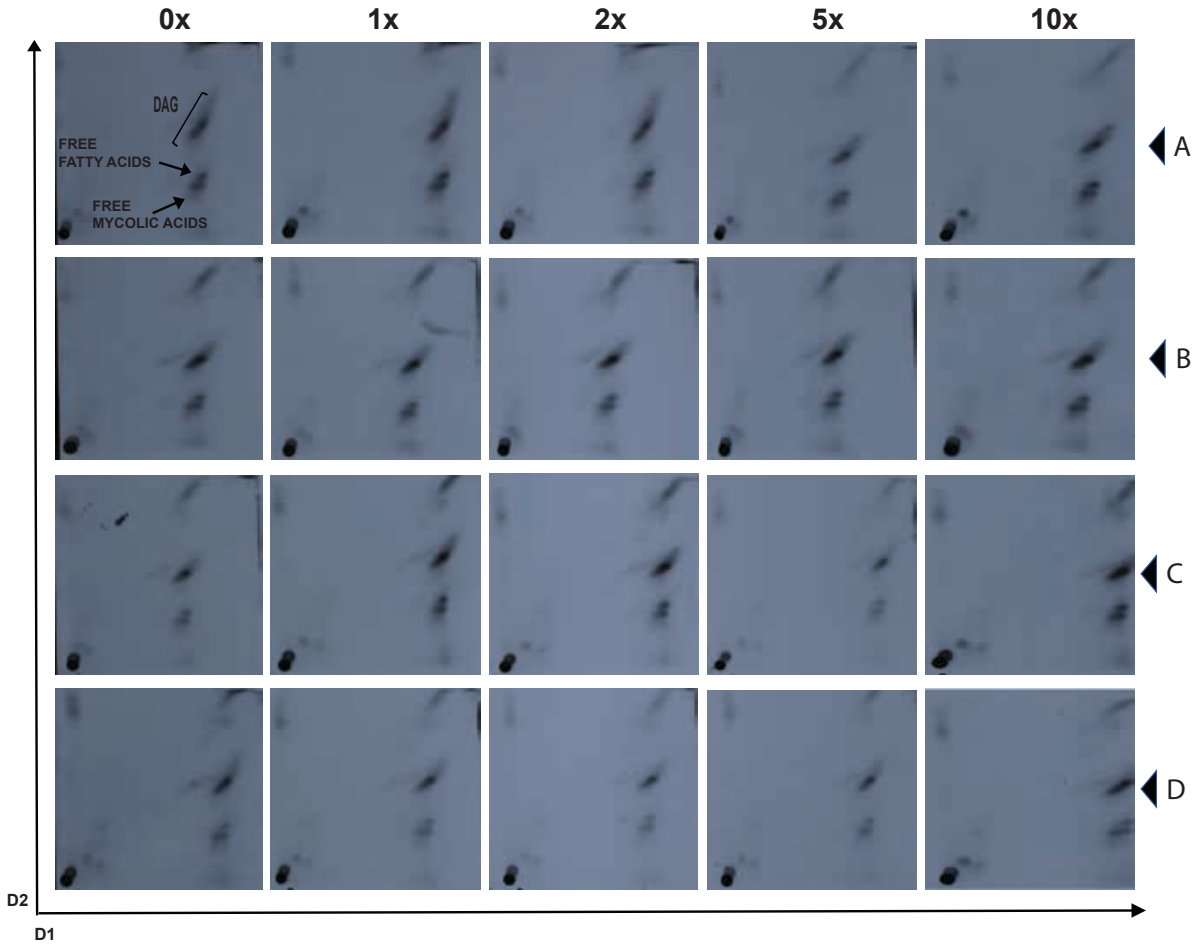

Figure 3.10: Apolar lipids separated by 2-D TLC on a silica gel plate using Petroleum ether: Acetone (98:2) x3 in direction one (D1) and Toluene: Acetone (95:5) in direction two (D2). The TLC separation of apolar lipids from four different strains of *M. bovis* BCG was carried out using two different solvent systems in two directions. The *M. bovis* BCG strains used are depicted based on the overexpression plasmids they contain: A. *M. bovis* BCG_pVV16, B. *M. bovis* BCG_pVV16_*echA12*_Rv, C. *M. bovis* BCG_pVV16_*echA12*_BCG, D. *M. bovis* BCG_pVV16_G239_*echA12*. The strains were treated with 0x, 1x, 2x, 5x and 10x MIC of florfenicol. DAG, Diacyl Glycerol.

3.2.4.4 Polar lipid analysis in *M. bovis* BCG *echA12* overexpressors

The polar lipid extractions that followed the apolar extractions were then separated on a 2-D TLC in system E. The system allows the visualisation of the acylated PIMs, phosphatidylinositol, phospholipids, trehalose mono- and di-mycolates. There were no changes observed in the presence of florfenicol in any of the strains (figure 3.11).

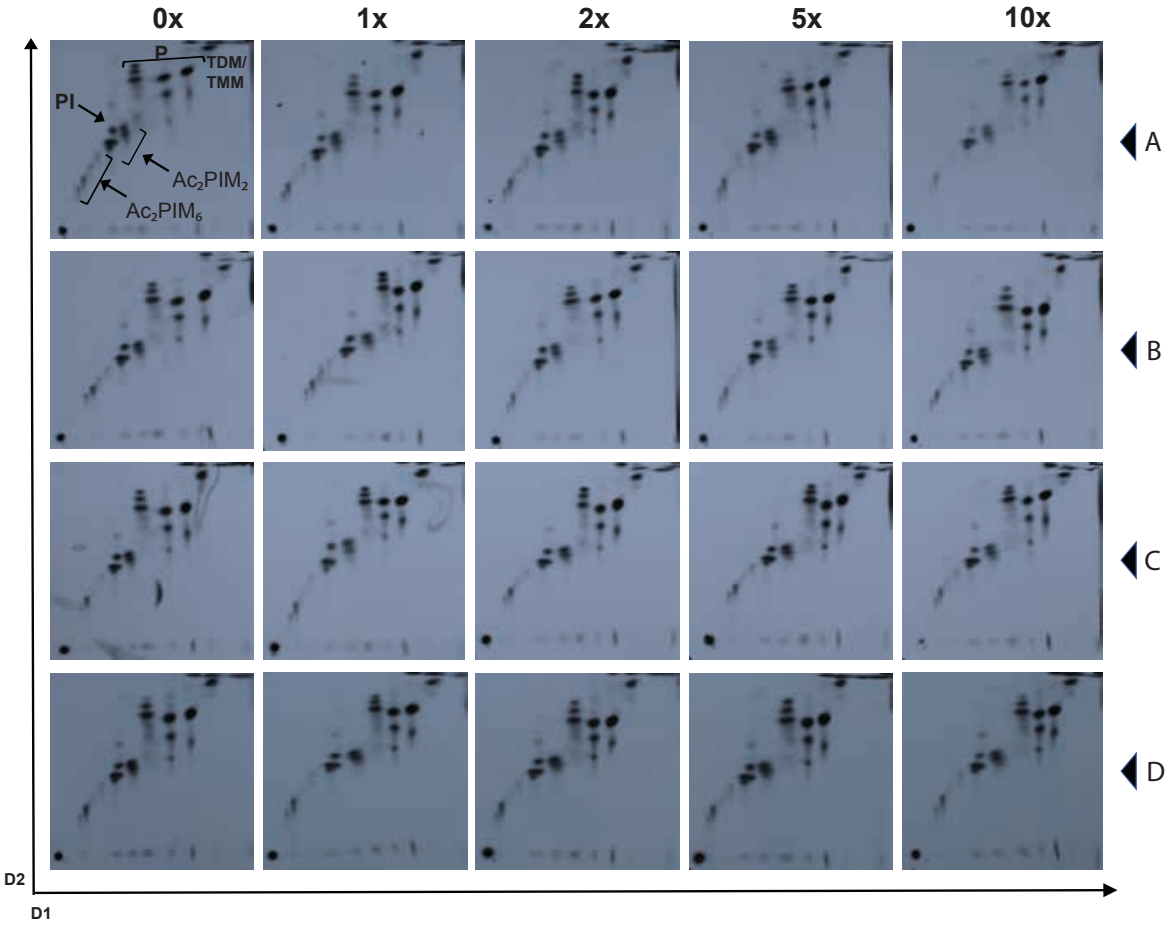

Figure 3.11: Polar lipids separated by 2-D TLC on a silica gel plate using Chloroform: Methanol: Water (60:30:6) in direction one (D1) and Chloroform: Acetone: Methanol: Water (40:25:3:6) in direction two (D2). The TLC separation of polar lipids from four different strains of *M. bovis* BCG was carried out using two different solvent systems in two directions. The *M. bovis* BCG strains used are depicted based on the overexpression plasmids they contain: A. *M. bovis* BCG_pVV16, B. *M. bovis* BCG_pVV16_*echA12*_Rv, C. *M. bovis* BCG_pVV16_*echA12*_BCG, D. *M. bovis* BCG_pVV16_G239_*echA12*. The strains were treated with 0x, 1x, 2x, 5x and 10x MIC of florfenicol. P, phospholipids; PI, phosphatidylinositol; Ac_1PIM_2 monoacylated phosphatidylinositol dimannoside; Ac_2PIM_2 diacylated phosphatidylinositol dimannoside; Ac_1PIM_6 monoacylated phosphatidylinositol hexamannoside; Ac_2PIM_6 diacylated phosphatidylinositol hexamannoside.

3.2.4.5 FAMEs and MAMEs analysis in *M. smegmatis* and *M. bovis* BCG *echA12* overexpressors

Extraction of the fatty acid methyl esters (FAMEs) and mycolic acid methyl esters (MAMEs) was performed on the delipidated cells and separated using the solvent system of petroleum

ether/acetone (95:5) on a 1-D TLC. There were no changes observed in any of the FAMEs and the α, α′, epoxy and the hydroxylated MAMEs in the *M. smegmatis* extracts (figure 3.12). Similarly, there were no changes observed in the *M. bovis* BCG extracts with the FAMEs and the α and keto MAMEs (figure3.12).

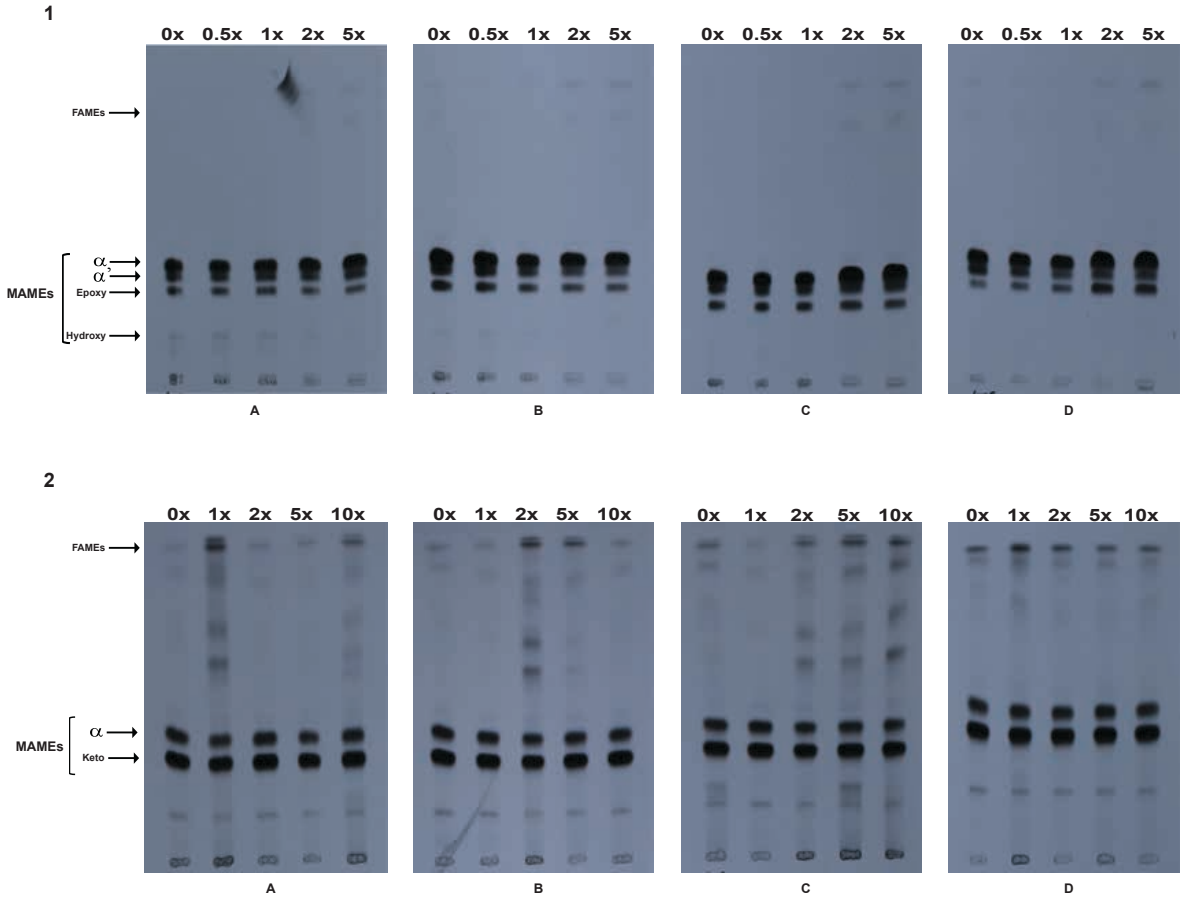

Figure 3.12: FAMES and MAMES extraction on a 1-D TLC separated on a solvent system containing petroleum ether/acetone (95:5, v/v). 1.The TLCs representing the cell wall bound lipids in the presence of 0x,0.5x,1x,2x and 5x of florfenicol in *M. smegmatis* mc^2155: A. mc^2155_pVV16, B. mc^2155_pVV16_*echA12*_Rv, C. mc^2155_pVV16_*echA12*_BCG, D. mc^2155_pVV16_G239_*echA12*constructs. 2. The TLCs representing the cell wall bound lipids in the presence of 0x,1x,2x,5x and 10x of florfenicol in *M. bovis* BCG; A. *M. bovis* BCG_pVV16, B. *M. bovis* BCG_pVV16_*echA12*_Rv, C. *M. bovis* BCG_pVV16_*echA12*_BCG, D. *M. bovis* BCG_pVV16_G239R_*echA12*
FAMEs, Fatty acid methyl esters; MAMEs, Mycolic acid methyl esters.

3.2.5 Generation of a knockout strain for *echA12*

In order to determine the essentiality of *echA12,* an attempt was made to generate a knockout mutant using specialised transduction (section 6.16) in *M. smegmatis* and *M. bovis* BCG. A knockout mutant was successfully generated.

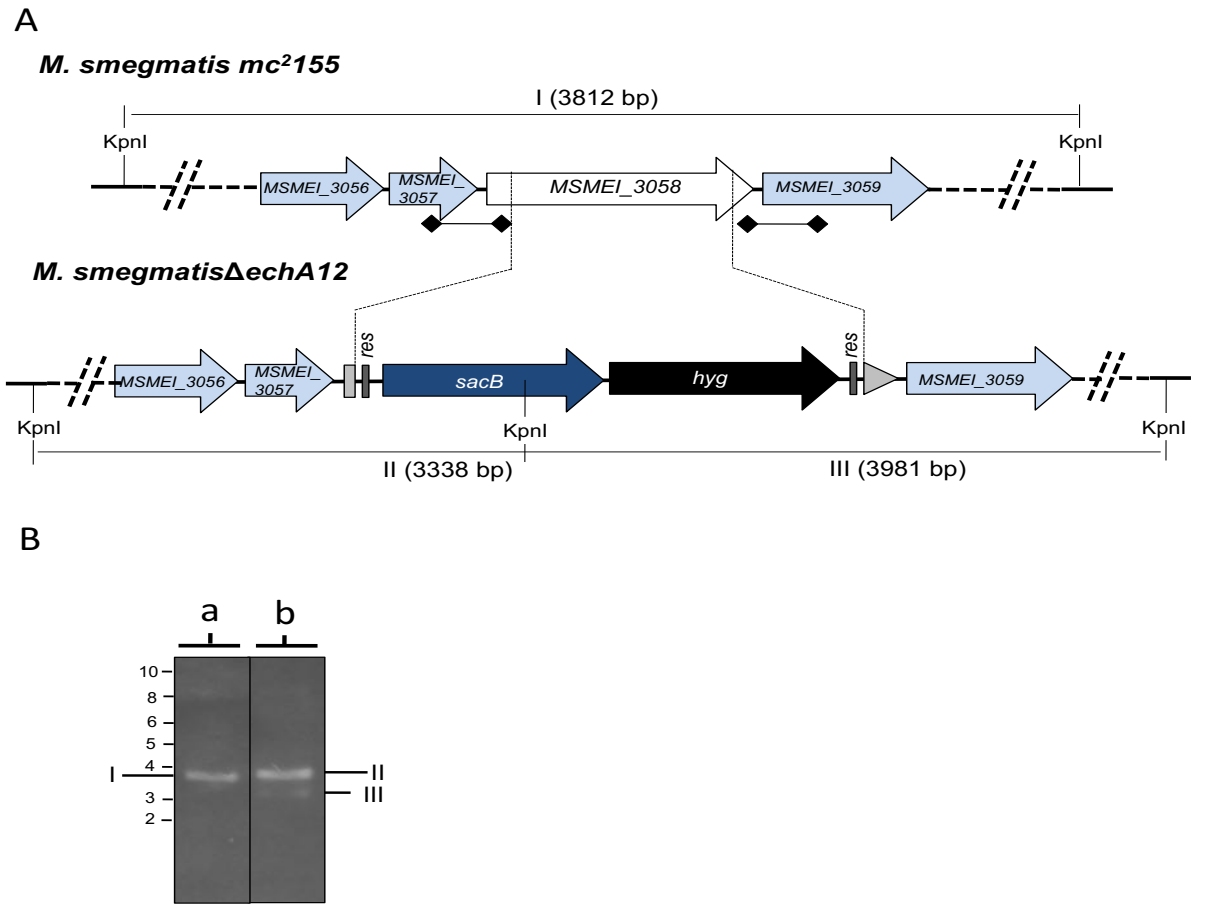

Figure 3.13: Generation of knockout mutants for echA12 in *M. smegmatis*. A. A schematic representation of the gene map corresponding to the *echA12* (MSMEI_3508) gene in *M smegmatis* along with flanking genes, following which is the map of the *M. smegmatisΔechA12* mutant. The dotted line cutting through the gene represents the region of the *echA12* gene replaced by the Hygromycin resistance gene (*hyg*) from *S. hygroscopicus* and the sucrose counter-selectable marker (*sacB)* from *B. subtilis*. Flanking DNA fragments upstream and downstream from the gene (~1Kb) linked with digoxigenin were used as molecular probes to construct the knockout plasmid; these are represented as solid lines with diamond shaped ends in the gene map of the *echA12* gene. The expected band sizes for each strain after digestion with KpnI enzyme are represented as I, II and III. B. The southern blot of the KpnI-digested genomic DNA from both the wild type strain (a) and knockout mutant (b) strain of *echA12* in *M smegmatis*. Bands I, II and III correspond to the expected sizes for the wild type and knockout mutant gene map.

As depicted in figure 3.13, the *M. smegmatis* gene MSMEI_3058, which is homologous to the *Mtb echA12* gene, was knocked out and replaced with a hygromycin antibiotic marker and sucrose counter selectable marker (figure 3.13A). A southern blot was performed, in order to check if the colonies observed for the knockout mutant were true mutants (section 6.17).

As depicted in figure 3.13A, the knockout mutant will produce two bands of 3.3Kb and 3.9Kb when the DNA is digested with a KpnI restriction endonuclease. It was confirmed with the southern blot that the mutants obtained had the *echA12* gene in *M. smegmatis* knocked out (figure 3.13B). As the gene was knocked out of the organism to produce a null mutant, it was inferred that *echA12* is not essential for the survival of mycobacterium.

3.2.6. A comparative growth curve analysis between the wild type and *echA12* null mutant in *M. smegmatis*

It was observed that although *echA12* is not essential for the survival of *M. smegmatis* due to

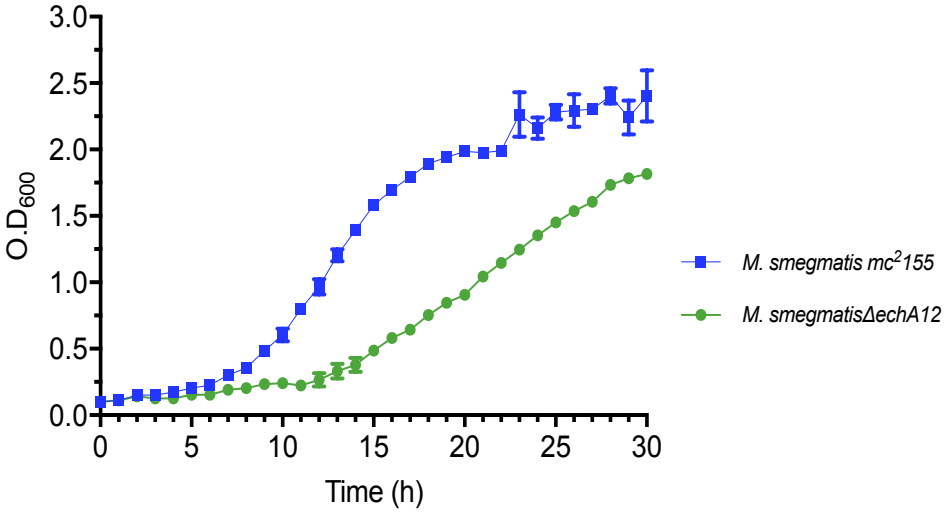

Figure 3.14: Graphical representation of a comparative growth curve between *M. smegmatis* mc²155 and *M. smegmatis*Δ*echA12*. The graph represents the growth of both the wild type and *echA12* null mutant by measuring the $O.D_{600}$ against time.

the successful generation of a knockout mutant, the absence of the gene caused a significant growth defect in the strain. The *echA12* knockout mutant had a slower growth rate when compared to wild type *M. smegmatis* mc^{2}155 (figure 3.14). The *echA12* mutant was almost twice as slow as the wild type *M. smegmatis*, for example, when the mutant reached an O. D_{600} of 1 the wild type *M. smegmatis* strain was reaching a growth plateau at an O. D_{600} of 2.0. This means that *echA12* has an important role in growth and multiplication of the cell despite being non-essential.

3.2.7 Morphological variation of the *M. smegmatis echA12* null mutant

In order to determine a morphological difference between the wild type and knock mutant of *echA12,* the strains were plated on to TSB agar plates in the presence and absence of tween (section 6.23)

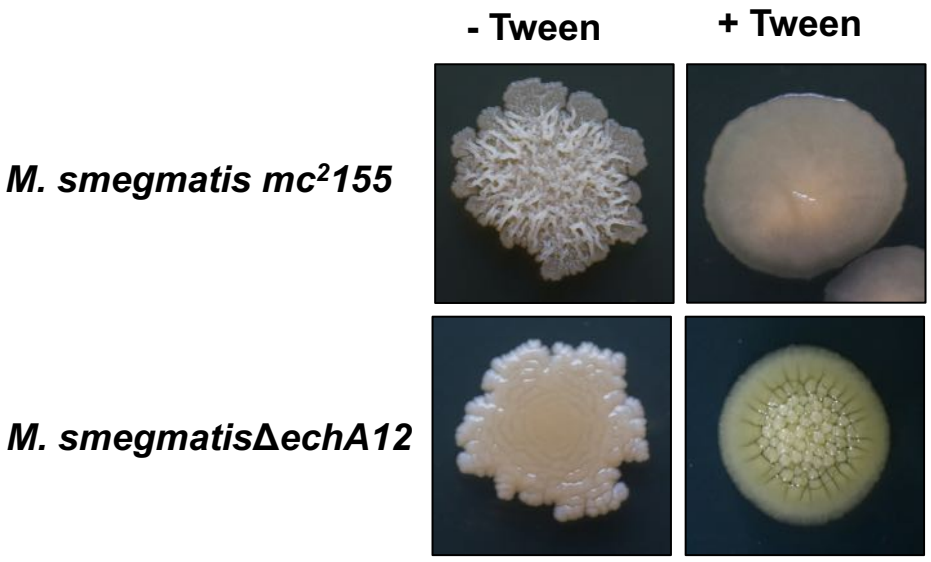

Figure 3.15: Morphological difference between *M. smegmatis* mc^{2}155 and *M. smegmatis*Δ*echA12* in the presence and absence of 0.05% Tween-80. Isolated single colonies grown on TSB agar with the addition of 0.0.5% Tween 80 in the column represented as +Tween.

The wild type *M. smegmatis* had the expected colony morphology with irregular edges and crenulated structures in the absence of tween, while the null mutant presented a glossier and less crenulated colony (figure 3.15). The difference was more prominent with the addition of 0.05% tween in the media. The null mutant showed an interesting nodulated colony morphology as opposed to the non-crenulated dome-shaped glossy colony of the wild type *M. smegmatis*. The growth of the bacteria on the agar plates mirrored the growth defect observed in liquid culture (section 3.2.6).

3.2.8 Loss of acid fastness in the null mutant of *echA12* in *M. smegmatis*

Mycobacteria are classified as acid fast bacteria and take up the stain of carbol fuchsin due to the high lipid content cell wall. The wild type *M. smegmatis* mc^2155 and the null mutant of *echA12* were stained using the Ziehl Neelson stain (section 6.22).

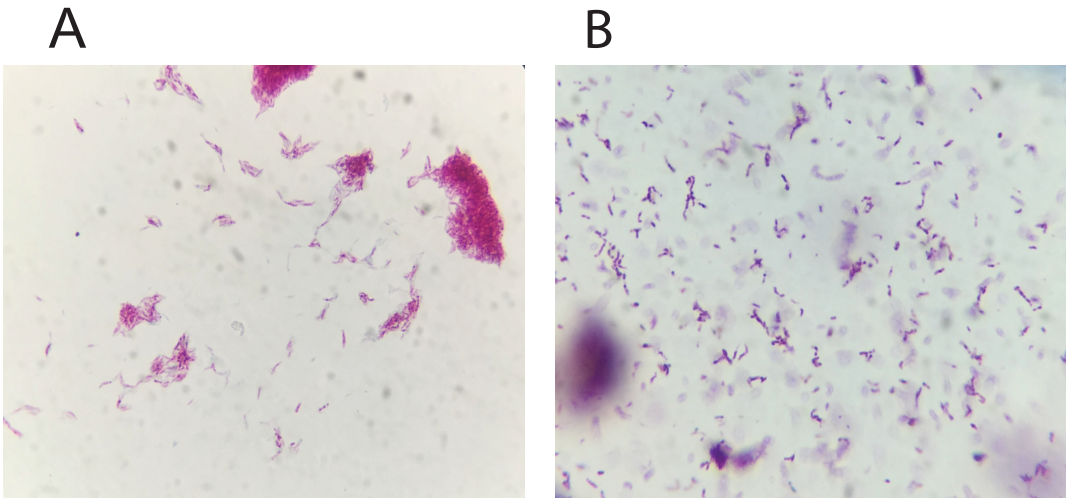

Figure 3.16: Acid fast staining of *M. smegmatis* mc^2155 and *M. smegmatis*Δ*echA12*. The *echA12* knockout mutant displays loss of acid fastness and decrease in cell size.

The *echA12* knockout mutant took up the secondary stain of methylene blue, causing the bacteria to look purple under the microscope, as opposed to the red stained bacteria for the wild

type *M. smegmatis* (figure 3.16). This therefore indicates loss of lipid content or modifications in the cell wall of the mutant which would lead to loss of the primary stain during washing. It was also observed that the cell size of the null mutant was smaller than the elongated cell structures of the wild type *M. smegmatis*. This further adds to the previous observation that change in colony morphology and growth rate of the cell are caused by the loss of the *echA12* gene in the null mutant.

3.2.9 Lipid analysis of the *echA12* null mutant

The lipid analysis was performed for the null mutant of *echA12* and compared against the wild type strain of *M.smegmatis* mc^2155. The apolar and polar lipid extractions did not depict any major variations when compared to the wild type. There was some loss of free fatty acids observed in system B when compared to the wild type strain (figure 3.17). As the cell bound lipids from the overexpression strains did not show any changes, the lipids were separated in a different solvent system which revealed phosphatidylinositols, phosphatidylethanolamine and cardiolipin moieties. There were no prominent changes that were noted in these species either.

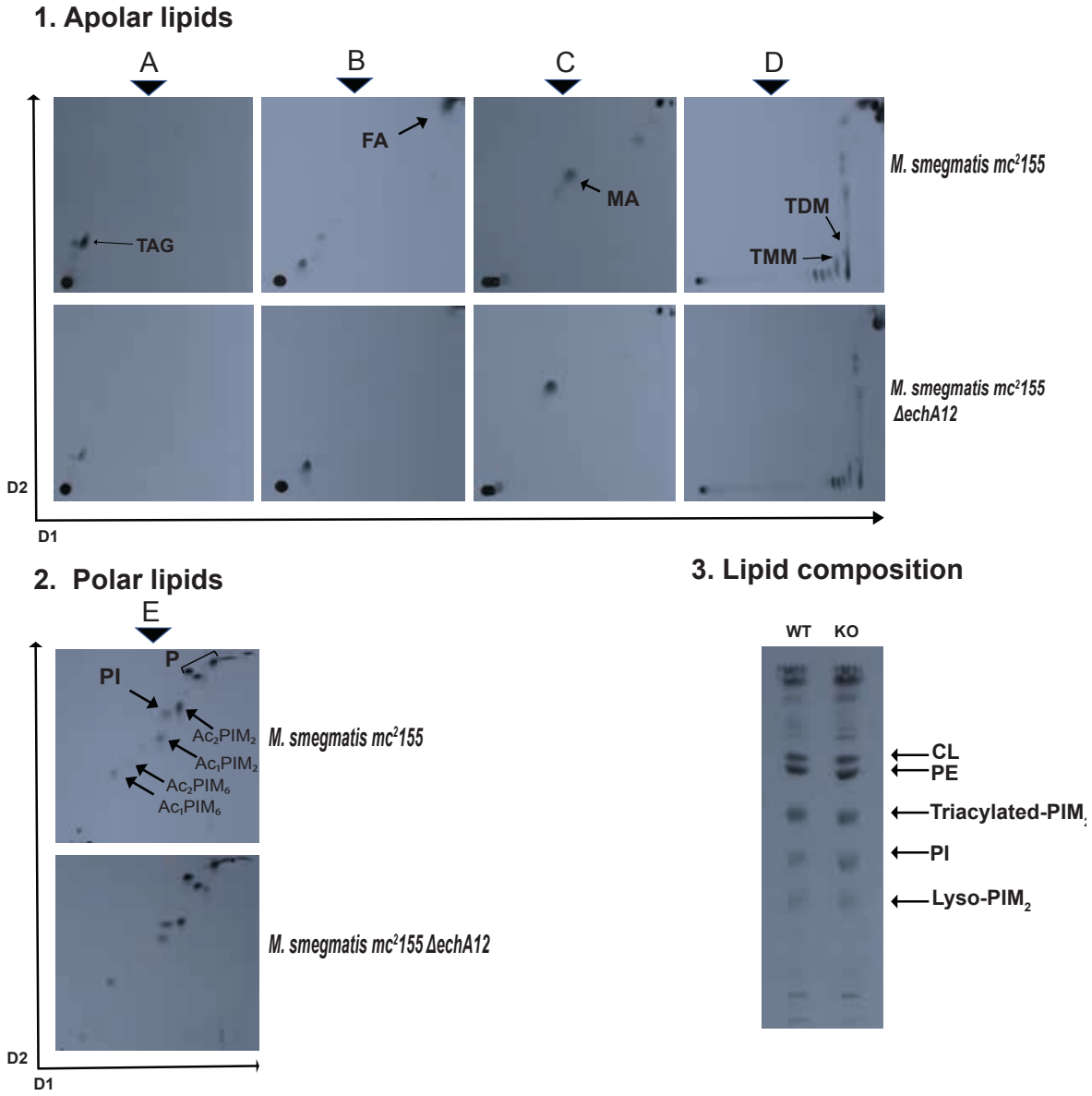

Figure 3.17: Lipid separation performed using 2-D TLC on a silica gel plate for apolar and polar lipids with System A, B, C, D (1. Apolar lipids) and E (2. Polar lipids). The TLC separation was performed for the wild type *M. smegmatis* mc^{2}155 (WT) and the *echA12* null mutant *M. smegmatis* mc^{2}155*ΔechA12* (KO). D1 and D2 represent the directions in which the TLCs were run in the solvent system. A 1-D TLC with lipids extracted using a 10:10:3 Chloroform: methanol: water (v/v/v) extraction was separated using a solvent system of CHCl3/CH3OH/NH4OH/H2O (65:25:0.5:3.6). P, phospholipids; PI, phosphatidylinositol; FA, Free Fatty Acids; TAG, Triacyl Glycerol; TDM, Trehalose dimycolate; TMM, Trehalose monomycolate; Ac_1PIM_2, monoacylated phosphatidylinositol dimannoside; Ac_2PIM_2, diacylated phosphatidylinositol dimannoside; Ac_1PIM_6, monoacylated phosphatidylinositol hexamannoside; Ac_2PIM_6, diacylated phosphatidylinositol hexamannoside, CL, cardiolipin; PE, phosphatidylethanolamine.

3.2.10 Liquid Extraction Surface Analysis (LESA)- Mass Spectrometry analysis of the null mutant of *echA12* in *M. smegmatis*

The extraction of lipids was performed by solvent extraction from colony surfaces using a surface based mass spectrometric technique.

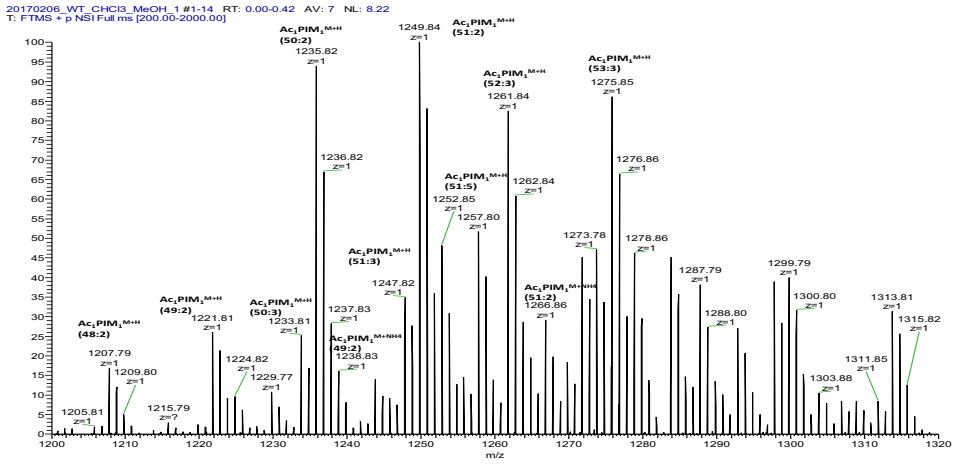

M. smegmatis mc²155

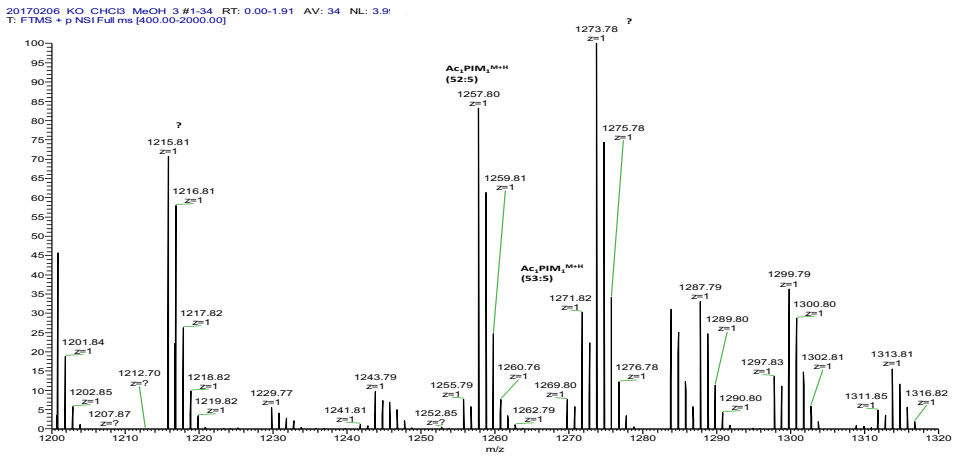

M. smegmatisΔechA12

Figure 3.18: The spectra from the LESA MS analysis of *M. smegmatis* wild type mc²155 and the *echA12* null mutant. The figure represents the mass spectrometry data with the masses and peak intensities of each peak. The spectras belong to the wild type *M. smegmatis* mc²155 and the *echA12* null mutant. The peaks have been annotated with the different Ac_1PIM_1 molecules containing a different number of carbon atoms and double bonds.

The analysis of the lipid moieties extracted from the *M. smegmatis* mc^2155 and *M. smegmatis echA12* null mutant was undertaken by assigning the peaks of observed masses from the MS analysis to different lipid molecules using LipidMaps Mass Spectrometry Peak Prediction software (Sartain *et. al.*, 2011) (figure 3.18). It was observed that in the *echA12* null mutant the Ac_1PIM_2 moieties were absent in all the different ionic states. Phosphatidylethanolamine (PE) was absent in the knockout null mutant in a C-38 form which contains two acyl groups with a total of 38 carbons and no double bonds. Other forms of Phosphatidylethanolamine that were present in both the strains were 34:1 and C-35 in a potassiated form, which meant that the molecule had two acyl groups containing a total of 34 carbons and 1 double bond and two acyl groups containing a total of 35 carbons without a double bond respectively.

Another important observation made was that Ac_1PIM_1 molecules in the knockout had acyl groups containing only a specific number of carbons and double bonds when compared to all the forms observed in the wild type *M. smegmatis*. In the hydrated state the null mutant had only 5 out of the 26 types of monoacylated PIMs observed in the wild type strain, while in the potassiated state the null mutant had 8 out of the 16 monoacylated PIMs observed in the wild type *M. smegmatis*. The number of monoacylated PIMs observed in the knockout mutant were the least in number in the sodiated adduct when compared to the wild type strain. After the analysing the spectra derived from the LESA-MS and assigning the peaks to the molecules based on their masses, it was observed that the *M. smegmatis* wild type mc^2155 strain had Ac_1PIM_1 molecules in the 50:2, 51:2, 52:3 and 53:3 at high intensities (figure 3.19). However, the other Ac_1PIM_1 molecules were not particularly intense, specifically 48:2, 49:2, 50:3, 51:3 and 51:5. In the case of the *echA12* null mutant Ac_1PIM_1 molecules were present in a low number and were only intense for the 52:5 form (figure 3.18).

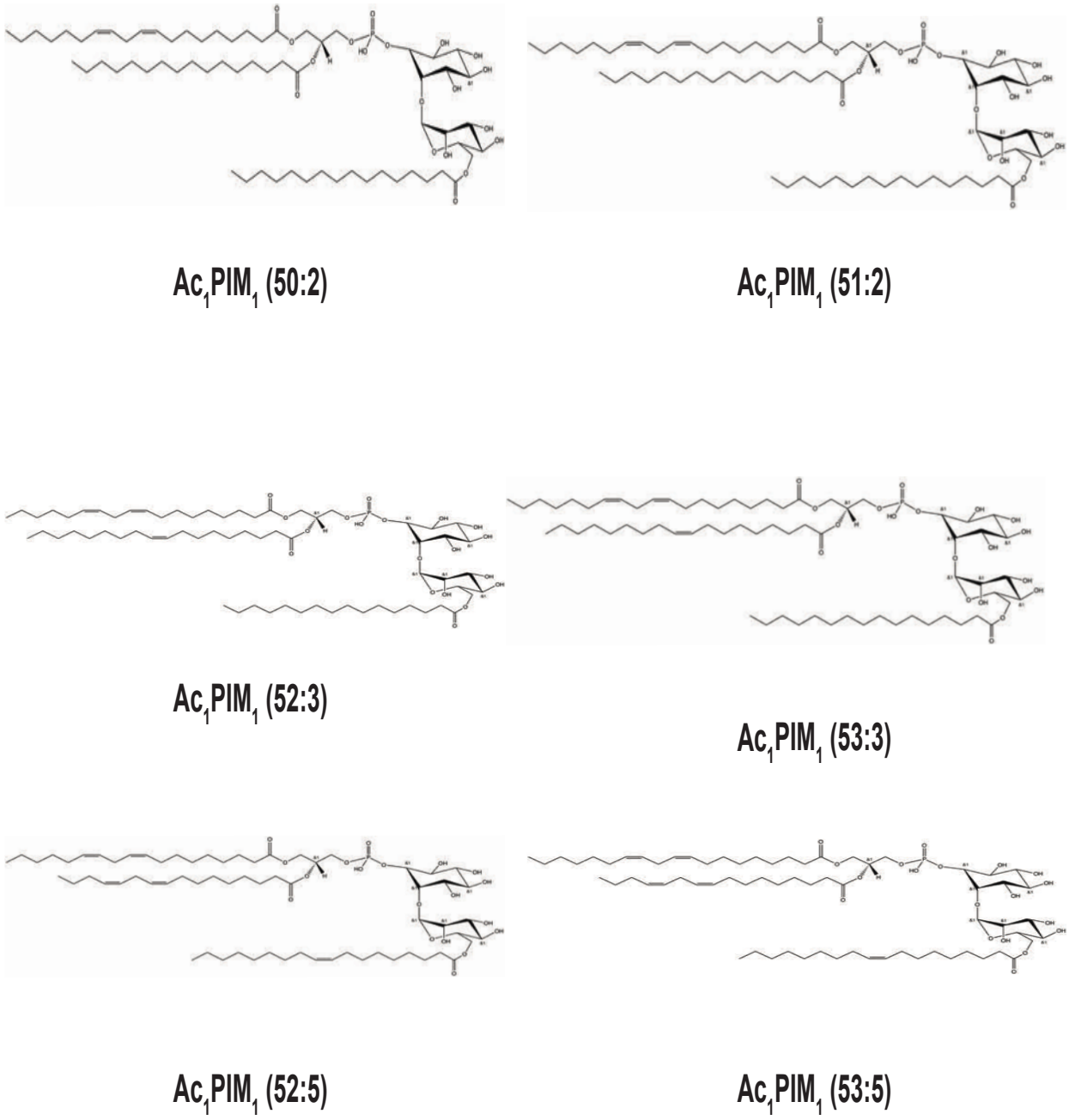

Figure 3.19: Structures of Ac1PIM1 molecules with different acylation states. The figure represents the structures of all the major Ac_1PIM_1 molecules observed in the wild type *M. smegmatis* which were absent in the *echA12* null mutant.

From the acetonitrile and ethanol/water extractions its was observed that the knockout did not contain lyso-Phosphatidyl inositol molecules with carbon chain length of 19 with one or two double bonds.

3.2.11 Amino acid alignment of *echA12* orthologs

The alignment of the amino acid sequence revealed similar results to the genomic alignment of *echA12* in *M. bovis*. The amino acid sequence showed a 99.65% match to the EchA12 amino acid sequence in *Mtb*. It lost 0.35% identity due to the amino acid substitution in the spontaneous mutation caused by florfenicol in *M. bovis* BCG at the 239 position where the glycine residue is obaserved (figure 3.20). It was interesting to observe that although the gene alignment depicted that the *M. smegmatis echA12* gene was only 74% (section 3.2.1) similar to

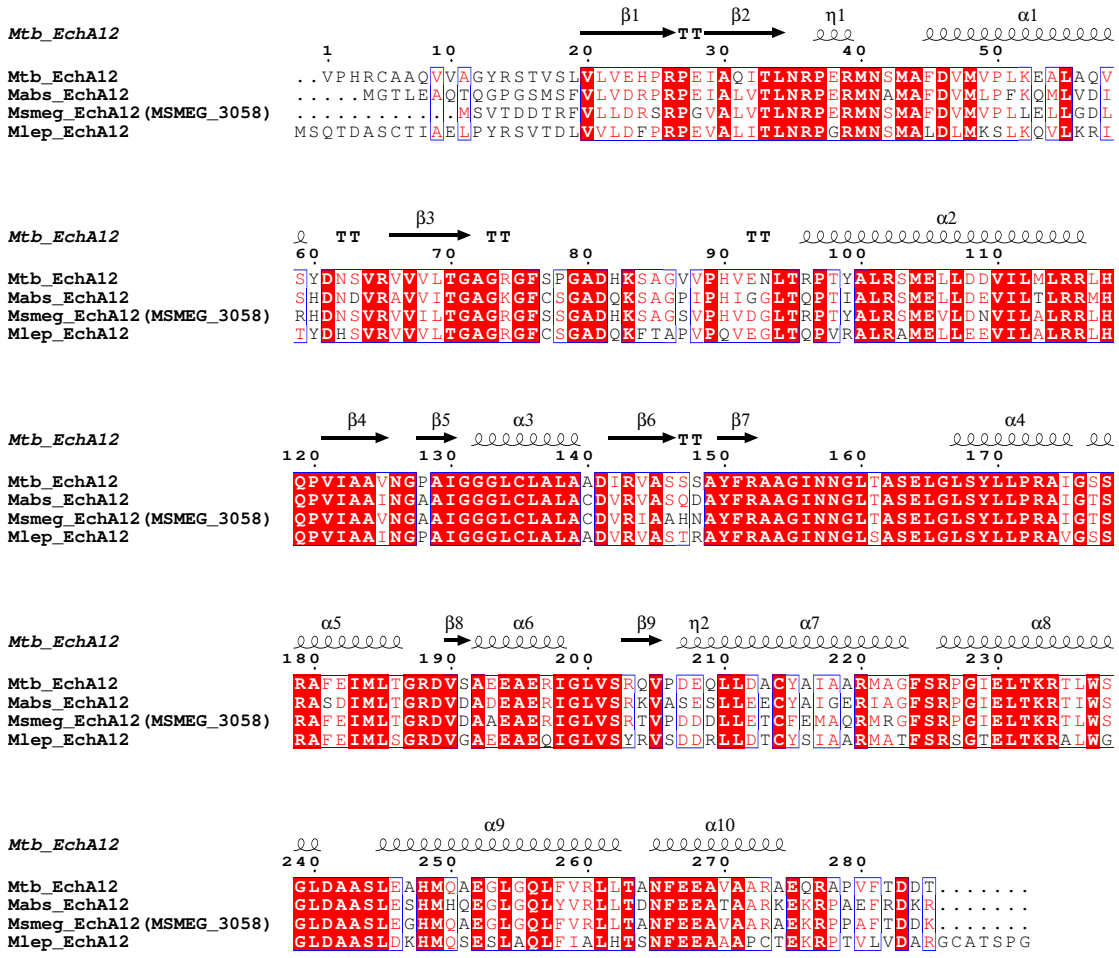

Figure 3.20: Protein sequence alignment of EchA12 from different species of mycobacteria. The sequence alignment highlights residues which are conserved throughout all the different mycobacterial species (in red) showing a high level of homology. The protein alignment has been annotated with the various secondary structures in the protein based on the crystal structure of the EchA12 protein from *M. abscessus* (Mabs_EchA12).

the *Mtb* e*chA12* gene, the amino acid sequence similarity was almost 80%. This potentially means that the protein structures might be fairly similar to each other. The secondary structure annotations revealed that the protein contains 10 α-helices and 9 β-sheets in its structure based on the crystal structure of *M. abscessus* EchA12 structure. The residue which underwent the amino acid substitution in response to florfenicol occurs in a α-helix loop (figure 3.20).

3.2.12 Purification of the EchA12 protein from the *M. smegmatis* overexpression strains

The EchA12 protein was purified from *M. smegmatis* overexpression strains containing the pVV16_*echA12*_Rv and the pVV16_G239_*echA12* constructs. The protein was initially extracted at a small scale and confirmed colourimetrically for size on a western blot. The EchA12 protein is 30.6KDa in size and presents a band on the SDS- gel and the blot just above the corresponding 25KDa band on the protein ladder (figure 3.21A). The protein purification was subsequently scaled up to get a higher amount of protein, although it was difficult to obtain the protein in very high concentrations due to its membrane bound nature and low affinity to the nickel column, which might be due to its structural nature. Both the EchA12 proteins elutes at imidazole concentrations of 150 and 200mM (figure 3.21 B1 and B2).

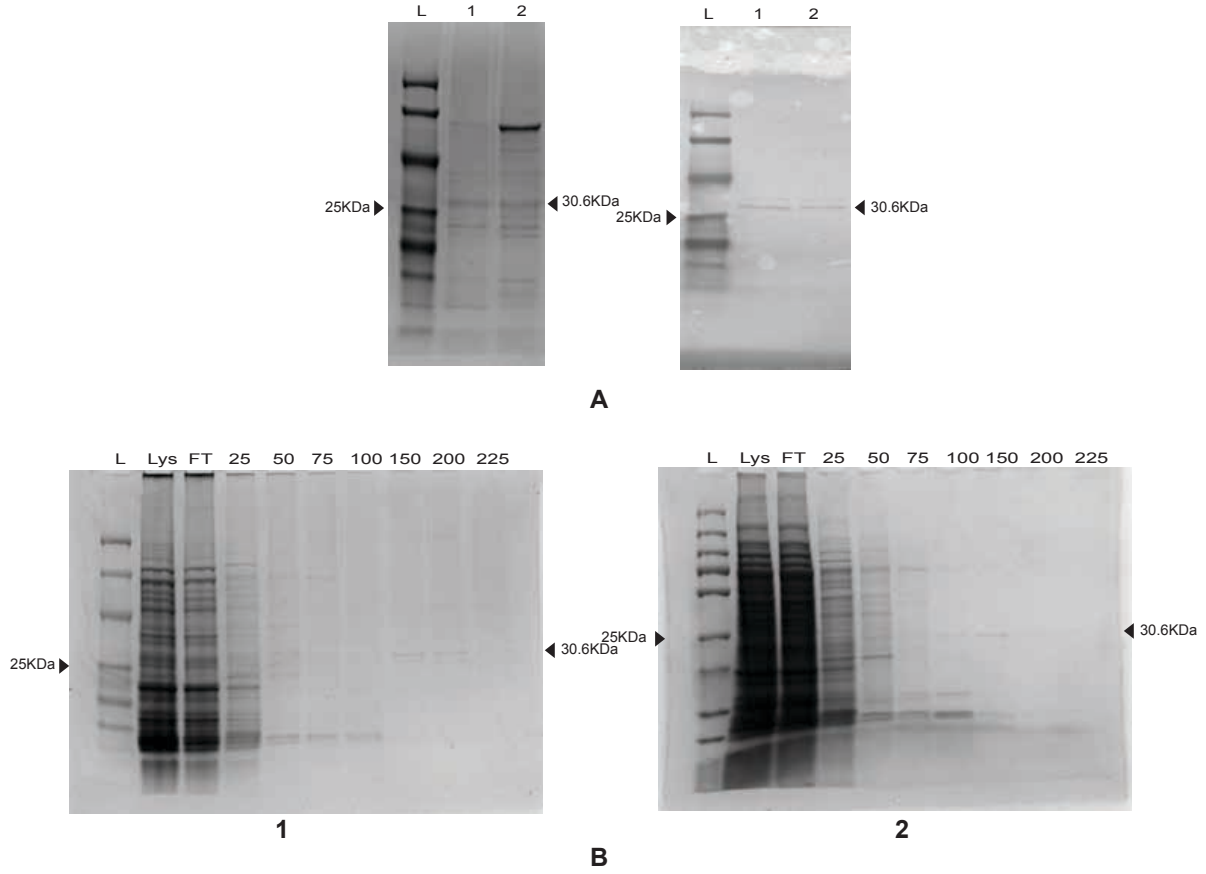

Figure 3.21: Protein expression of echA12 protein using the pVV16_EchA12_Rv and pVV16_EchA12_G239R construct in *M. smegmatis*. A. A SDS protein gel with a corresponding western blot depicting the protein fractions from a small-scale protein extraction. 1. EchA12 protein from the pVV16_*echA12*_Rv construct, 2. EchA12 protein from the pVV16_*echA12*_Rv construct. The band can be visualised at the 25kDa band on the protein ladder for the 30.6KDa EchA12 protein and colourimetrically on the western blot to confirm the histidine linked EchA12 protein. B SDS protein gels depicting the protein fractions at various imidazole concentrations collected during the large-scale protein expression. 1B. EchA12 protein from the pVV16_E- chA12_Rv construct; 2B. EchA12 protein from the pVV16_EchA12_Rv construct. The gel contains (from left to right) a protein ladder (L), cell lysate (Lys), flow through (FT), the wash fraction (W) at 25mM imidazole concentration and then the other fractions for imidazole concentrations 50mM, 75mM,100mM,150mM,200mM and 225mM. The Echa12 protein (30.6KDa) was eluted at imidazole concentrations 150mM and 200mM. B. The band can be visualised at the 25kDa band on the protein ladder.

3.2.13 EchA12 interaction with palmitoyl coenzyme A (Palmitoyl CoA)

Solvent extraction of the EchA12 protein revealed that the protein co-eluted with a coenzyme A molecule.

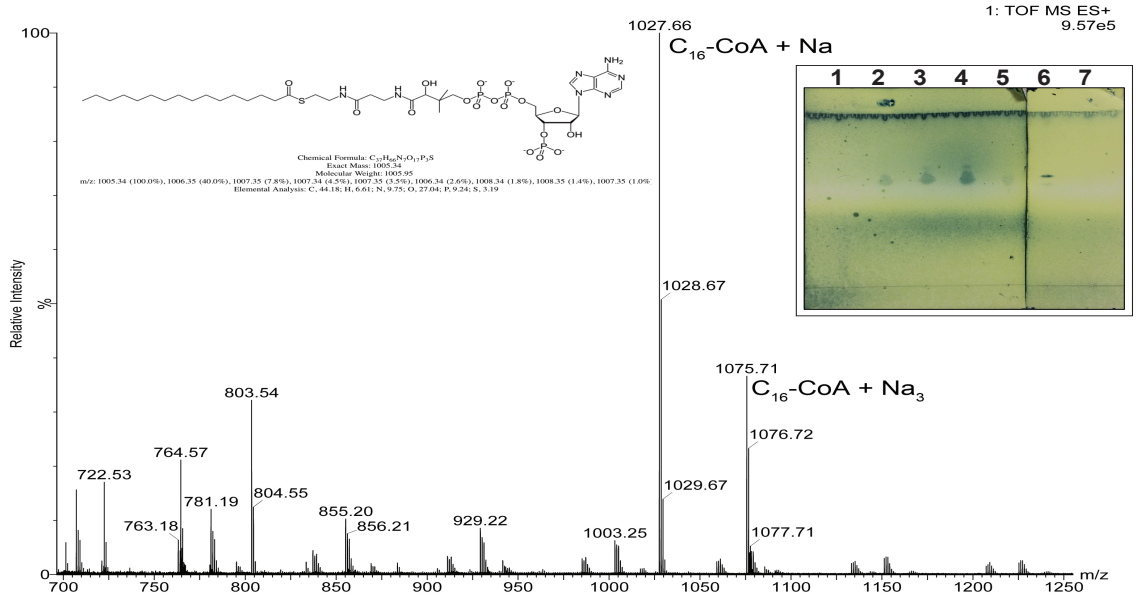

Figure 3.22: The mass spectrometric analysis of the EchA12 protein solvent extracted and run on a silica TLC (inset) with other controls on the TLC. 1. Coenzyme A, 2. C_8-Coenzyme A, 3. C_{12}- Coenzyme A, 4. C_{14}- Coenzyme A, 5. C_{16}- Coenzyme A, 6. EchA12 solvent extract, 7. Buffer control. The mass spectrometric analysis of the solvent extract of the protein depicts a peak with the m/z ratio of 1027.66 which correlates to the sodium adduct of C_{16}-Coenzyme A.

In order to determine the chain length of the eluted coenzyme A, standard CoA with different chain lengths were run alongside the solvent extracted EchA12 (figure 3.22 inset). The protein extract showed a spot in line with C_{12} to C_{16} coenzyme A and therefore in order to confirm the exact chain length, the spot was then extracted and tested using mass spectrometry. The mass spectrometric analysis confirmed that the EchA12 protein interacted and co-eluted with a plamitoyl coenzyme A (figure 3.22). The peak of the extract had a mass/size ratio of 1027.66 which corresponded to the sodium salt of the C_{16}-CoA.

3.2.14 EchA12 binds to Phosphatidylinositolmannosides (PIMs)

The EchA12 protein was purified from the *M. smegmatis* strains containing the pVV16_*echA12*_Rv and pVV16 G239R_*echA12* vectors (figure 3.23).

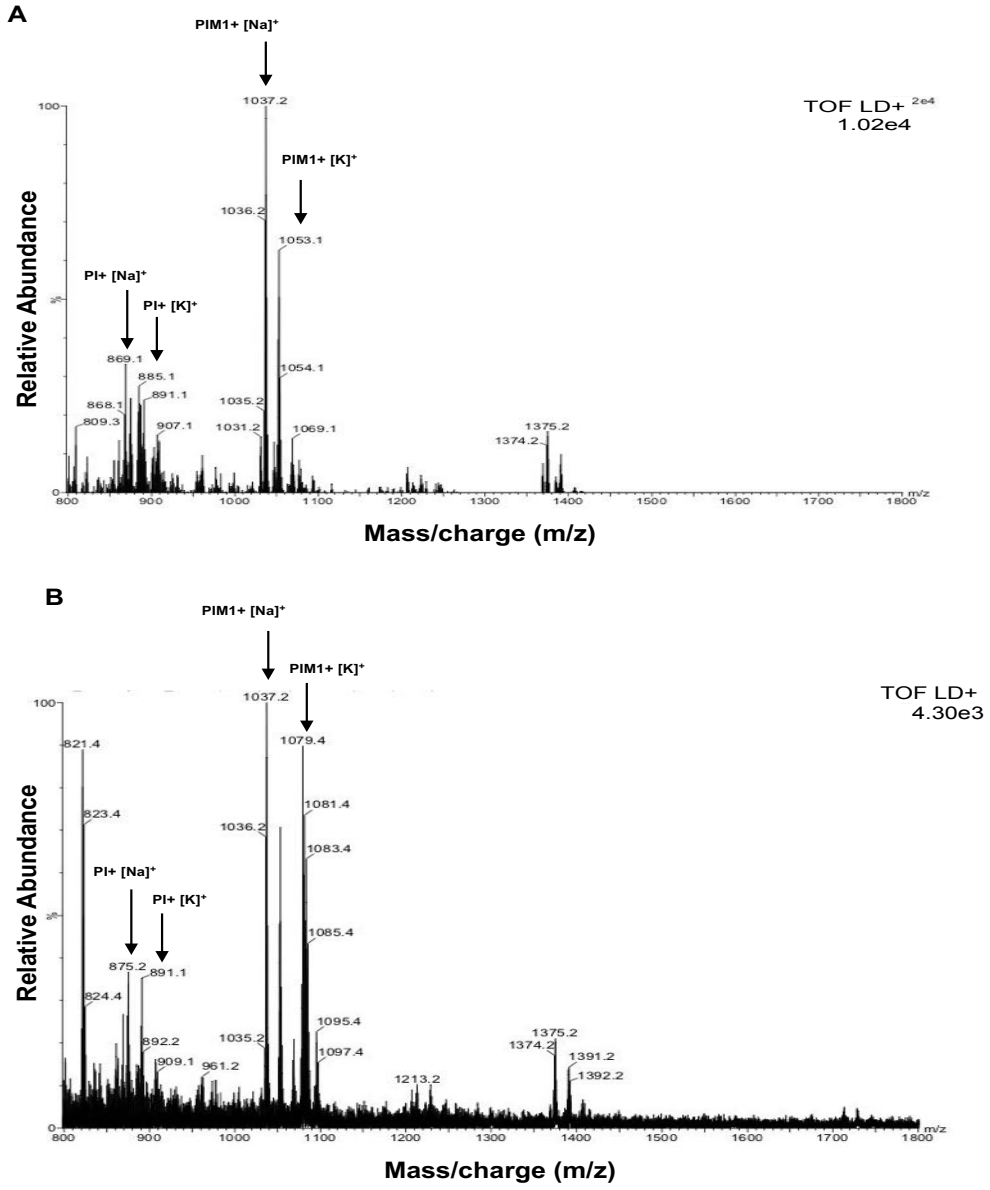

Figure 3.23: The mass spectrometric analysis of the solvent extract of EchA12 from *M. smegmatis*. The peaks show the sodium and potassium adducts of phosphatidylinositol (PI) and phosphatidylinositol mannoside (PIM_1). A. Represents the data for Echa12 from the pVV16_*echA12*_Rv construct and B. Represents the data for EchA12 from the pVV16_ G239R_*echA12* construct. C. Presents the structural details and formulas of PI and PIM_1.

Lipid extractions were performed on the proteins to determine the binding of the proteins with lipid moieties. The extracts were then sent for MALDI-TOF mass spectrometric analysis and it was observed that both EchA12_Rv (figure 3.23A) and EchA12_G239R (figure 3.23B) had phosphatidylinositol and phosphatidylinositolmannoside1 molecules.

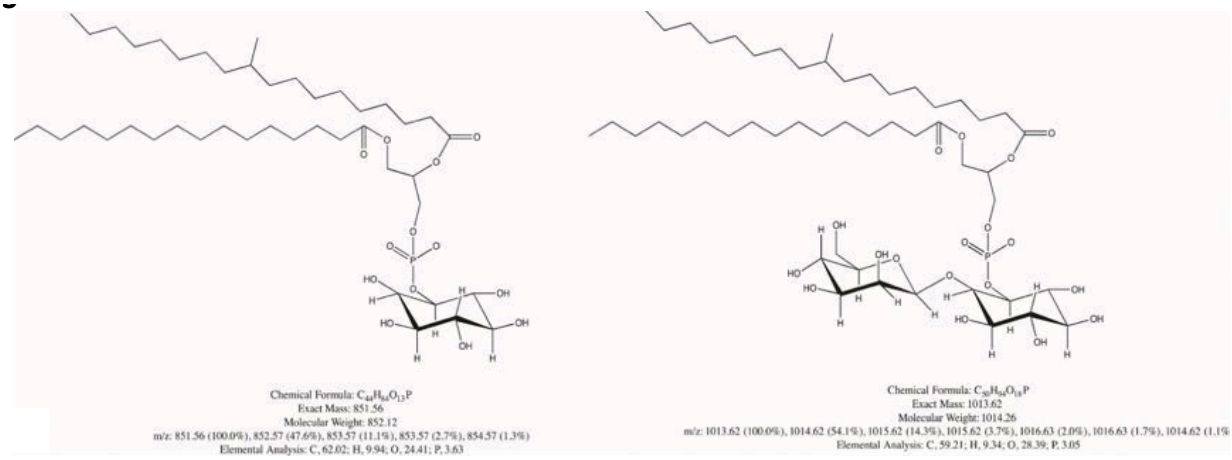

Figure 3.24: Structure of PI and PIM_1. Represents the data for EchA12 from the pVV16_ G239R_*echA12* construct. C. Presents the structural details and formulas of PI and PIM_1.

The peaks depicted in the mass spectrometry graph matched the sodium and potassium adducts of PI and PIM_1 (figure 3.23A and B). The molecular masses were confirmed to be the same when the molecular mass of sodium and potassium were deducted from the observed masses (figure 3.24).

3.2.15 Model structure of EchA12 illustrating site of mutation (likely interaction site with florfenicol) and Palmityl-CoA.

The structure of the EchA12 protein was determined using the **I**terative **T**hreading **ASSE**mbly **R**efinement method (I-TASSER).

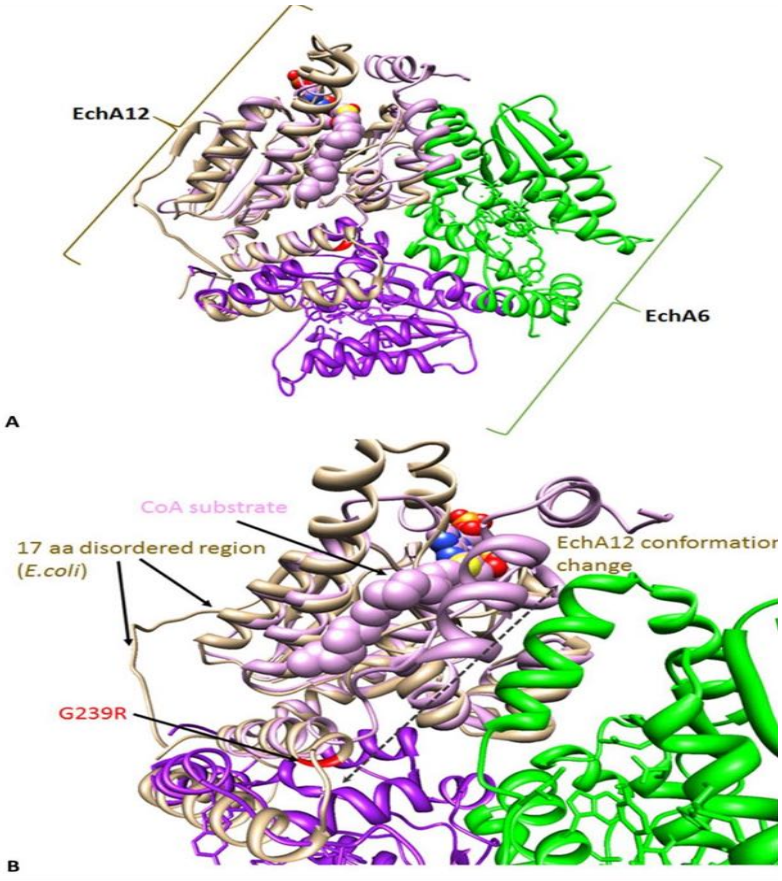

Figure 3.25: An I-TASSER model of the EchA12 protein using the EchA6 protein structure as a scaffold. A. The model structure of EchA12 in beige has been modelled on to one of the monomers of the EchA6 trimer, presented by the three monomers in pink, purple and green. On the EchA12 monomer, the red residue on the α-helix indicates the site of the mutation causing the G239R substitution. B. The model structure of the EchA12 monomer on the EchA6 scaffold with the palmitoyl CoA docked into the potential binding site. The mutation G239R has been highlighted in red on the hinge region of the α-helix loop.

We used the EchA6 protein model (Cox *et. al.*, 2016a) as a template to act as a scaffold to generate the EchA12 protein structure. The model represented here is of the monomer of the EchA12 protein superimposed on one of the monomers of the EchA6 trimer (figure 3.25A). The protein structure contains the mutated amino acid residue highlighted in red where there was substitution at the 239 position from glycine to an arginine residue.

I-TASSER utilises a template model to thread the predicted protein structure. The substitution occurs in the hinge region of the α-helix loop which has two other asparagine residues opposite

to the substituted residue. The binding pocket for the Palmitoyl CoA is situated above this α-helix loop (figure 3.25B). The predicted interaction of florfenicol seems to occur in the hinge region of this protein due to the occurrence of the mutation. The interaction potentially caused a disruption in the movement of the hinge in the α-helix loop which interacts with α-helix loop on another EchA12 protein, forming a dimer. This disruption of the α-helix interaction and movement of the hinge region could lead to the inability of the protein to interact with another EchA12 monomer and affect the docking of the Palmitoyl CoA into the binding site. The amino acid substitution probably causes a change in the interaction with florfenicol, while at the same increasing the hydrogen bonding with the neighbouring asparagine residues thereby increasing the stability of the enzyme.

3.3 Discussion

In understanding the functional and genetic importance of the enoyl CoA hydratase targeted by a chloramphenicol derivative (chapter 2), we have discovered that the *echA12* gene is a conserved gene between major classes of pathogenic and non-pathogenic mycobacteria. The gene has a highly-conserved region with *M. leprae,* which has the smallest genome in mycobacteria due to reductive evolution (Singh and Cole, 2011). This evidence, along with the presence of the gene in *M. bovis* and the saprophytic strain *M. smegmatis,* indicates that the gene might be important for the bacteria to grow or survive. Further investigations revealed that the gene was not required for survival and therefore was non-essential due to the generation of a null mutant of the gene. However, it was observed that the null mutant of the gene exhibited physiological changes such as change in the colony morphology, growth rate and loss of acid fastness. This suggested potential changes in the cell wall components or metabolism. Due to

its potential involvement in fatty acid biosynthesis (Beckman and Kranz, 1991), analysis of lipids from overexpression strains of *echA12* in *M. smegmatis* and *M. bovis* BCG was undertaken. This revealed that there was an accumulation of ketones and a change in phospholipid profiles in bound lipids. Solvent extractions of the proteins revealed that the protein interacted with PI and PIM_1. Phosphatidyl-*myo*-inositol is an essential phospholipid in the cytoplasmic membrane, it is synthesised from inositol by an enzyme PgsA (phosphatidylinositol synthase) (Jackson *et. al.*, 2000b) and acts a starting molecule for the formation of PIMs and LAM. PIMs are important cell wall molecules which are present in both mycobacteria and corynebacteria (Crellin *et. al.*, 2008). It has been observed that depletion of PI and PIMs does not affect the viability of mycobacteria, but depleting polar PIMs such as Ac_1PIM_6 and Ac_2PIM_6 does effect the viability by compromising the cell wall integrity. It is known that apolar PIMs are precursors to the synthesis of polar PIMs, yet reserves of PI and apolar PIMs (Ac_1PIM_2 and Ac_2PIM_2) are not necessary to maintain the synthesis of polar PIMs. *De novo* synthesis of PI or production of PI through the catabolism of lyso-PI is used as a supplement for the synthesis of PIMs and LM/LAM, circumventing the absence of apolar lipids (Haites *et. al.*, 2005). In the *echA12* null mutant, it was observed that apolar PIMs, along with Lyso-PI, were absent in certain chain lengths, yet the cells were viable albeit slow growing. This could be a possible reason as to why the cell wall integrity was not majorly affected in the absence of the apolar PIMs. Polar PIMs are synthesised in the plasma membrane and cell wall, the role of some of the enzymes involved in the biosynthetic pathway is to take the transitional components from the cytoplasmic face of the plasma membrane to the periplasmic side of the plasma membrane. This variation helps to regulate the synthesis of the cell wall and growth rate of the bacterium (Morita *et. al.*, 2005). It was noted that the Ac_1PIM_1 molecules observed in the *M. smegmatis* wild type strain in various acylated states had the presence of a palmitoyl group

attached to the mannose residue in the PIM molecule. However, this was not found to be the case when the analysis was performed for the acylated Ac_1PIM_1 molecules observed in the *echA12* null mutant. As our analysis showed that the EchA12 protein interacts and carries the palmitoyl CoA, it is therefore clear that due to the absence of the enzyme the metabolism was skewed towards non-palmitoyl CoA groups. PatA is a membrane associated acyl transferase which has been identified as the enzyme that transfers the palmitoyl CoA on to the 6^{th} position of the mannose ring in PIM_1 or PIM_2 molecule (Albesa-Jové *et. al.*, 2016). On the basis of our observations, it was inferred that PatA might be a promiscuous enzyme which, in the absence of a palmitoyl CoA donor, is able to incorporate non-palmitoyl CoA moieties on to the mannoside residue, driving the PIM biosynthesis forward. This would explain the presence of PIM molecules observed during the TLC analysis of lipids. The PIMs observed in that scenario were of a different acylation state not containing the palmitoyl moieties, therefore depicting no obvious variation. The metabolic shift in the lipid biosynthesis and variation in the lipid composition of the cell wall could therefore explain the loss of acid fastness and the slow growing null mutant.

Enzymes and molecules involved in cell division are contributing factors to cell growth. Cardiolipin is an acidic phospholipid synthesised by cardiolipin synthase which is present in the cell membrane of mycobacteria. A higher concentration of the lipid is observed at the septa in the middle of the cell and at the poles of actively dividing cells (Maloney *et. al.*, 2011). It has also been known to interact with gyrases and activates polymerases in the cell (Sarma *et. al.*, 1998). This indicates that it has a role in cell division (Maloney *et. al.*, 2011; Sarma *et. al.*, 1998). The lipid analysis of the *echA12* knockout revealed the absence of cardiolipin which would explain the slow growth of the mutant. The synthesis of cardiolipin has been predicted to involve that utilisation of phosphatidylethanolamine (Aktas *et. al.*, 2014), this might explain

the absence of cardiolipin in the *echA12* null mutant as the PE is absent in the mutant when observed via the LESA-MS analysis. This subtle change identified through the LESA study could explain why there were no obvious changes observed in the TLC analysis previously undertaken. The structural prediction studies and the analysis of the cell lipid content in the *echA12* null mutant indicate the role of the enzyme in shuttling the palmitoyl CoA molecule for PIM synthesis. The interaction of florfenicol with the enzyme might be hindering the binding of the palmitoyl CoA, leading to the enzyme's inability to carry the molecule. Although this causes a non-lethal change in the composition of the cell wall, it causes the bacterium to slow down and potentially leads to a more vulnerable pathogen, indicating that EchA12 could still be considered as a dug target for combinatorial drug development.

Chapter 4

Target based phenotypic screen of the GSK177 box set against *prsA*

4. Target based phenotypic screen of the GSK177 box set against *prsA*

4.1 Introduction

Target based drug screening is another approach in drug discovery which has been utilised to discover new antimicrobials. The target based drug discovery approach rests on a hypothesis that the target protein/ enzyme/ mechanism is potentially disease modifying. This method is technically less labour intensive when compared to a more genralised phenotypic screen which involves a longer and more tedious process of identifying targets of the identified inhibitors for a specific pathogen. Pathway specific screens and promoters are limited in many ways as they only work for specific metabolic pathways (Singh *et. al.*, 2013) and also affect drug interaction *in vivo* with a lower possibility of growth inhibition (Mdluli *et. al.*, 2014). Target based approaches have a high attrition rate which affect the efficiency of the screen in general (Singh *et. al.*, 2013). The prevailing methodology used in TB drug discovery is phenotypic screening as target based screening has largely been abandoned. The lack of detailed understanding of the cellular metabolism of *Mtb* during infection limits the target validation. Furthermore, the hydrophobic cell wall acts as a barrier which, when combined with the limited availability of chemically diverse groups, leads to issues with cell wall permeability at a later stage (Kana *et. al.*, 2014). It is therefore important to understand the initial criteria for target selection in order to avoid failure at a later stage of the drug discovery process. A good target should have important properties such as; essentiality to cell growth or viability *in vivo*, druggablility and location in a position easily accessible by the inhibitory molecule (Kana *et. al.*, 2014). In addition, there needs to be a clear understanding of whether it is a genetic target, which involves

one specific gene having a specific function during stages such as infection and host invasion, or a mechanistic target, which affects a chain of molecular events in a biosynthetic cycle (Sams-Dodd, 2005). This is important as *Mtb* has a genetic redundancy which probably increases the robustness of an organism and its ability to survive under stress (Kafri *et. al.*, 2006). For example, there are approximately 100 genes in the mycobacterial genome designated for the five biochemical reactions in the β-oxidation cycle. Although most of these genes are non-essential some of the genes which have been known to be essential via transposon mutagenesis are not essential when tested experimentally and vice versa (Williams *et. al.*, 2011). Another interesting thing about these paralogues is the roles that they play *in vivo* are different to the assigned or expected roles. The enzyme encoded by *fadB3* which catalyses the fourth reaction in the β-oxidation cycle and is the only one deemed as essential out of the five encoded by *Mtb* to be essential. Studies *in vivo* have depicted up- and down-regulation of *fadB3, fadB2, fadB4* and *fadB5* in the mice infections, macrophage infections, nutrient deprivation and acidic conditions. This clearly indicates towards a different role of these genes *in vivo* (Williams *et. al.*, 2011). *Mtb* and *C. glutamicum* multiple copies of the GroEL gene which are essential and conserved although seemingly accumulate non-conserved mutations which affect the structure and function of the protein (Goyal *et. al.*, 2006). Therefore, it is very important to have a clear understanding of the target in order to avoid a high attrition rate which is the main issue for target based drug discovery for tuberculosis.

Primarily there are three ways of validating the targets and confirming mode of actions of the compound active against a target in the drug discovery process. These are: 1) generation of spontaneous resistant mutants, 2) over or under-expressing the target gene in a conditional mutant and 3) culturing pooled mutants in the presence and absence of the compound to see phenotypic variation (Schnappinger, 2015). Once a drug target has been validated it can then

be used in a combined approach involving target based phenotypic screening. This allows the benefit of having a targeted screen but in a whole cell which minimizes the issues that occur downstream from a target based screen. There have been recent examples of compound hits generated against validated targets using this approach. Inosine monophosphate dehydrogenase (IMPDH) or GuaB2 is an enzyme involved in purine biosynthesis. A class of 7 chemical clusters were identified to be targeting this enzyme through *M. bovis* BCG overexpression strains (Cox *et. al.*, 2016b). A compound from the GSK library was identified against a CTP synthetase PyrG through a conditional knock strain generated for PyrG after target validation, The compound 4-(pyridine-2-yl)thiazole derivate showed a high inhibitory activity against mycobacterial CTP synthetase and a low activity against human CTP synthetase (Esposito *et. al.*, 2017). This is a potentially more feasible and effective approach which could generate a higher amount of lead compounds.

The current TB drug regimen includes drugs which inhibit the cell wall synthesis processes such as isoniazid and ethambutol (Breda *et. al.*, 2012; Alderwick *et. al.*, 2011), but in view of the emerging drug resistant strains newer drugs are required and the metabolic pathways involved in energy exchange mechanisms and cell wall synthesis are interesting targets. *DprE1* is the most prominent example of a target gene involved in cell wall synthesis which has led to a new class of drugs that have been approved for tuberculosis treatment. DprE1 is a vulnerable target involved in the epimerisation of decaprenylphosphoryl-β-D-ribose (DPR) to decaprenylphosphoryl-β-D-arabinose (DPA), the precursor to arabinose in the cell wall (figure 4.1) (Trefzer *et. al.*, 2010). With the deconvolution of the structure of the protein it was found that benzothiazinones (the class of drugs inhibiting the enzyme) interact with the protein through covalent bonding at the cysteine 387 residue and Van der Waals interaction between the triflouromethyl group of the inhibitor and protein backbone residues 132-134 (Batt *et. al.*,

2012). This target has now lead to the synthesis of new drug classes and modification of the current drug classes such as azaindoles, dinitrobenzamide and 8-pyrrole benzothiazinones all inhibiting the DprE1 enzyme (Trefzer *et. al.*, 2010; Shirude *et. al.*, 2013; Makarov *et. al.*, 2015).

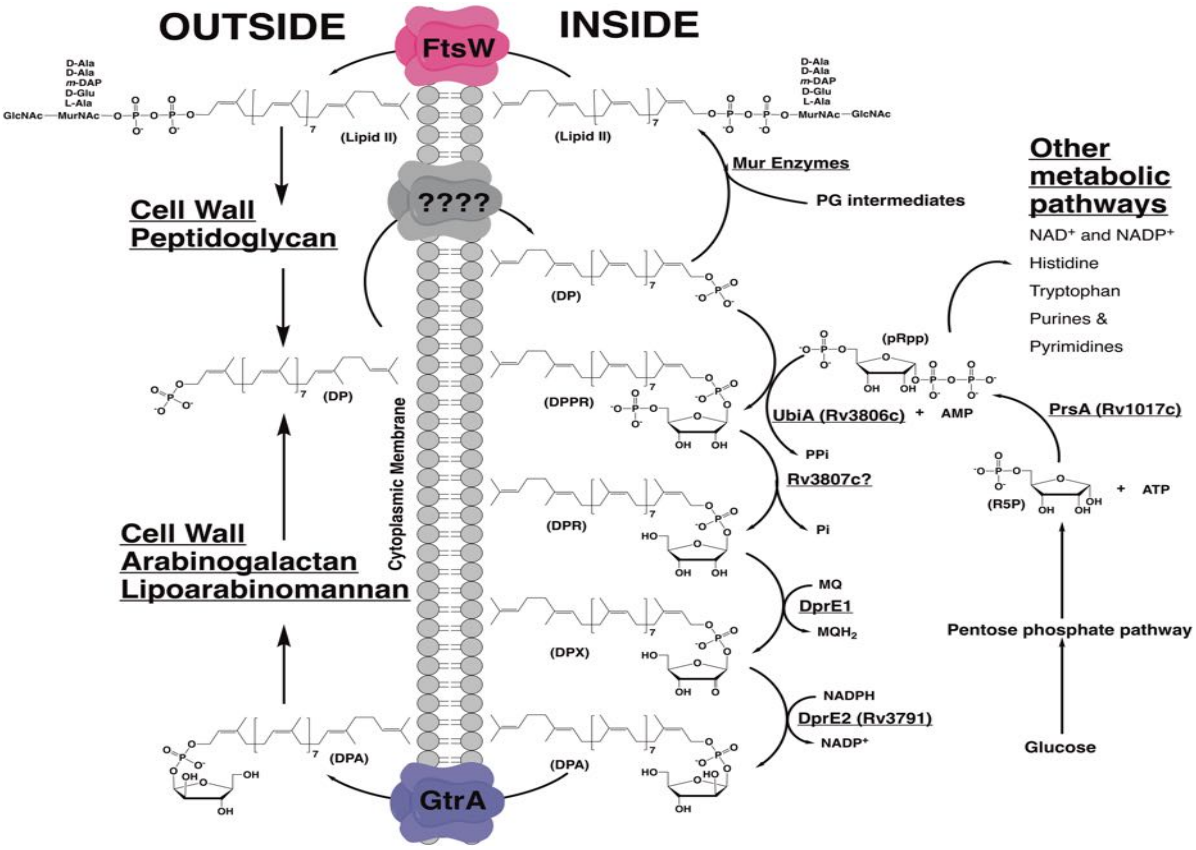

Figure 4.1: The biochemical pathway describing the synthesis of cell wall components. The figure details the synthesis of DPA through utilisation of ribose-5-phosphate by the PrsA enzyme and shuttling of the decaprenol-1-monophosphate 5-phosphoribosyltransferase into the extracellular space to be converted into cell wall macromolecules.
pRpp : Phospho-α-d-ribosyl-1-pyrophosphate; DP: decaprenol-1-monophosphate; DPR decaprenol-1-monophosphoribose; DPX: decaprenol-1-monophosphoryl-2-keto-β-*erythro*-pentofuranose; DPA: decaprenol-1-monophosphoarabinose (Alderwick *et. al.*, 2011)

PrsA is a phosphoribosylpyrophosphate synthase that is upstream of the DprE1 protein in the synthesis of the cell wall macromolecules (figure 4.1). The PrsA protein has been divided into three classes based on its molecular and kinetic characters (Alderwick *et. al.*, 2011). The mycobacterial PrsA has been defined as class I due to its hexameric structure which is very specific to its substrate and needs an inorganic phosphate for activation. The mycobacterial

PrsA depicts 40% identity to the three human PrsA isoforms although there are two major substitutions in the mycobacterial PrsA at the substrate binding site when compared to the human PrsA protein (Lucarelli *et. al.*, 2010; Breda *et. al.*, 2012).

Phospho-α-D-ribosyl-1-phosphate (pRpp) is the metabolite which links the pentose phosphate pathway to the *de novo* and salvage pathway for purine and pyrimidine production (Alderwick *et. al.*, 2011). The gene responsible for the production of the enzyme converting ribose-5-phosphate into pRpp in the presence of ATP is PrsA. The gene has been determined to be essential for the survival of the cell and a decrease in the product has a pleiotropic effect on the cell such as cell elongation and implosion (Kolly *et. al.*, 2014; Alderwick *et. al.*, 2011). This protein has therefore been validated as a suitable drug target that could be used in target-based drug discovery screen.

In this chapter, we screened a library of compounds synthesised by GlaxoSmithKline (GSK). This library contains 177 compounds depicting inhibitory activity against *M. bovis* BCG and *M. tuberculosis* H37Rv which were shortlisted from approximately $2x10^6$ chemical compounds after several iterations. The initial screen was performed against *M. bovis* BCG which has almost 99% similarity to the genome of *Mtb* H37Rv leading to a subset of approximately 20,000. These 20,000 compounds were selected from the hits based on permeability, stock availability within the company and followed the guidelines of a drug. These were then further assayed against *Mtb* H37Rv and *M. bovis* BCG to compare the hit rates. 127 hits from the primary screen inhibited *M. bovis* BCG and 112 compounds inhibited *Mtb* H37Rv. They also analysed which compounds where cross inhibiting both strains with two concentrations of the compounds which were 10μM and 25μM. They found a 97% increase in cross-reactivity for the compounds when they increased the concentration from 10μM to 25μM. The compounds were then further shortlisted based on inhibition percentage of >90%, log P vale of >6, presence

of new chemical cluster while discarding any known antibacterial structures and compounds with reactive groups. After the dose response studies and cytotoxicity testing against the HepG2 cells, 177 compounds were shortlisted which had MIC values of less than 10μM and a therapeutic index of more than 50. They were then tested for broad spectrum activity against 8 different bacterial strains where 7 specific chemical clusters depicted very high affinity for mycobacteria and were classified as potential leads. Although these compounds have shown a high antitubercular activity, it is still unclear as to what is the target of these chemical entities in *Mtb*. In an attempt to de-orphanise the GSK177 compound set we screened this library against a validated drug target which is essential for the survival of the mycobacteria and is involved in the synthesis of the cell wall using a target based phenotypic approach.

4.2 Results

4.2.1 Cloning of *Mtb-prsA* in pMV261 for the *Mtb-prsA* overexpression strain

In order to develop an overexpression strain of *Mtb-prsA* gene was cloned into a pMV261

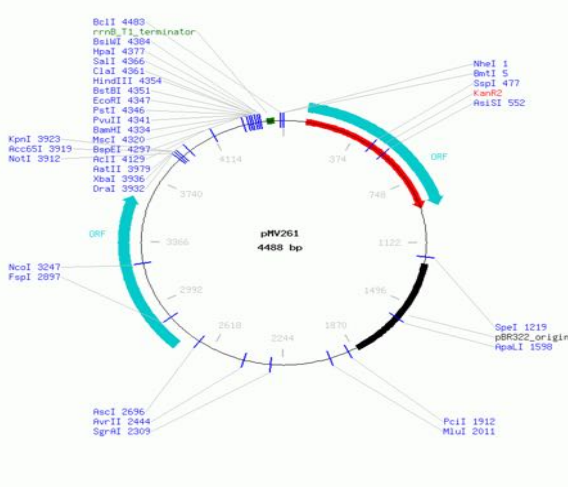

Figure 4.2: Plasmid map of the pMV261 vector. The pMV261 vector is a 4.5 Kb plasmid containing multiple cloning sites and a kanamycin antibiotic selection marker (Stover *et. al.*, 1991).

shuttle vector which replicates inside mycobacteria. The vector is derived from a pBR322 vector and contains three open reading frame with multiple cloning sites (MCS). The plasmid is 4.48Kb in size and contains a kanamycin antibiotic selection marker (figure 4.2).

The *Mtb-prsA* gene was amplified by PCR (figure 4.3A) and cloned into the mycobacterial vector pMV261 as mentioned in section 6.8.

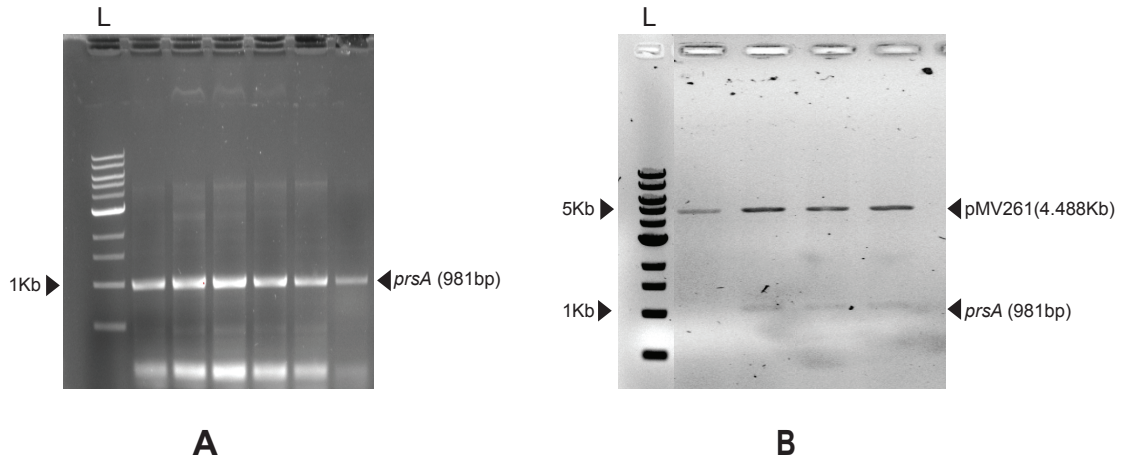

Figure 4.3: Cloning of the *Mtb-prsA* gene into the pVV16 vector. The figure shows agarose gel images of the amplified *Mtb-prsA* gene at 981bp (A) with respect to a 1Kb DNA ladder and double digest of gene cloned into to the pmV261 vector 4.45Kb (B).

The overexpression strains were generated in *M. smegmatis*, *M. smegmatis* _psMT3_eGFP, *M. bovis* BCG and *M. bovis* BCG_pSMT3_eGFP (section 6.9) once the clones were confirmed through double digestion (figure 4.3B) and sequencing the plasmid.

4.2.2 Screening the GSK177 library against *Mtb-prsA* overexpressing strains

An overexpression screen at single compound concentration was performed against an extended library of the GSK 177 collection containing 201 compounds (Appendix 16). The compounds from the library were re-distributed into three separate plates in order to accommodate columns for positive and negative controls. The compounds from the extended GSK177 library were screened, against A GFP fluorescing strain of *M. bovis* BCG overexpressing the *Mtb-prsA* gene, at a final concentration of 10μM with Z' score for all the plates being 0.7 on an average. Since there are no known inhibitors of the *Mtb*-PrsA enzyme it was not possible to have a control with an inhibitor for the overexpression screen. The overexpression of the pMV261_*prsA* containing strain was compared to a wild type GFP expressing *M. bovis* BCG strain. The average fold change (for the two replicates) was calculated after the data was normalised against the controls to determine percentage survival values and a cutoff of 1.5-fold change was set for *M. bovis* BCG (figure 4.4).

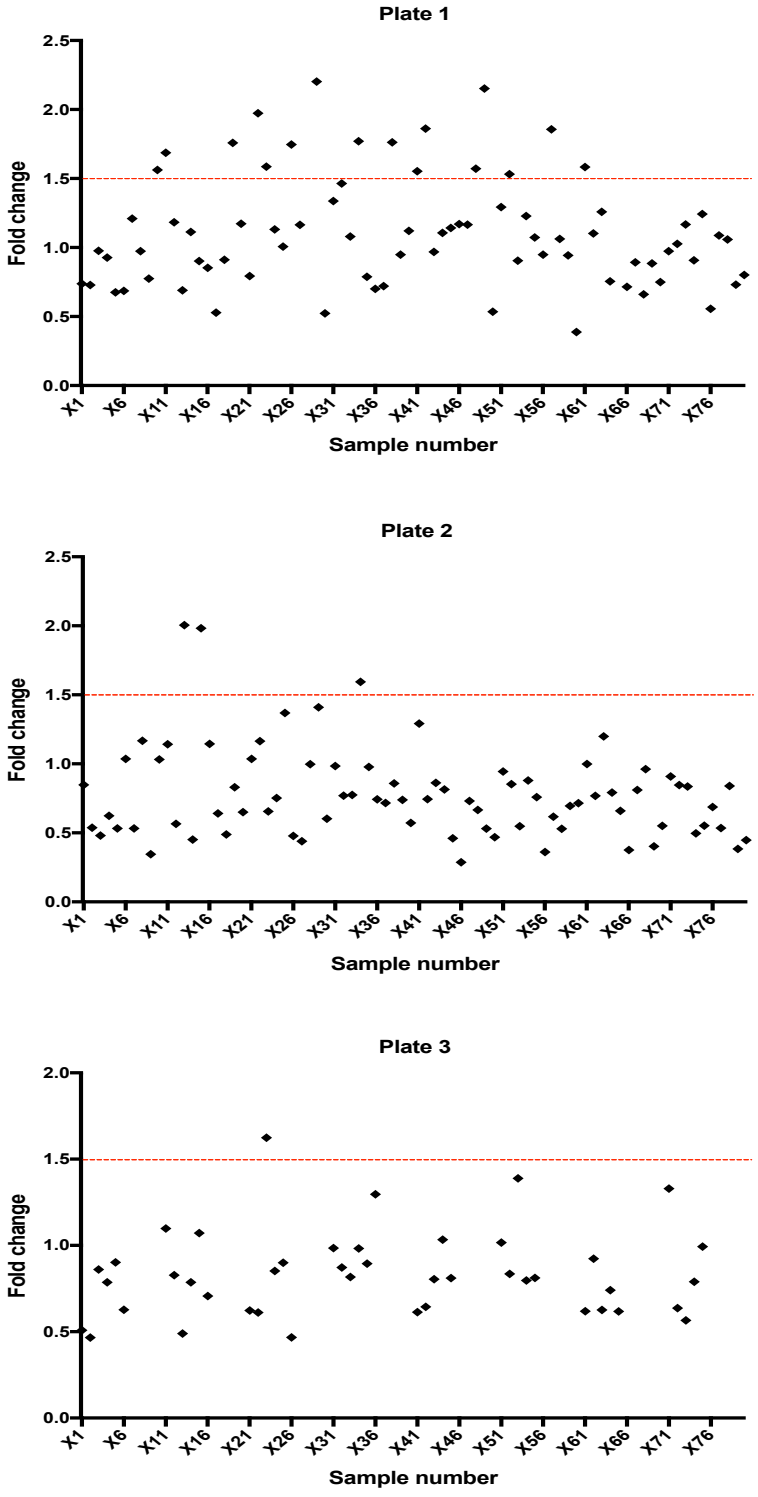

Figure 4.4: Fold change in survival percentages against the extended GSK177 compound library. The scatter graphs in the figure represent the average fold change of two replicate plates comparing the overexpression of the *Mtb-prsA* overexpression strains with respect to the empty vector containing strain. The X-axis represent the sample number in each plate against the fold change on the Y-axis. The cut-off for the fold change is marked by the red dotted line at 1.5.

20 hits were observed amongst the three plates containing the GSK compounds out of which GSK1051703A, GSK135487X and GSK1829728A had fold change of 2 or higher (table 4.1) indicating a strong possibility of the target of these compounds being the *Mtb*-PrsA enzyme. There were 4 other compounds which had a fold change of ~1.9 and therefore represented strong candidates as *Mtb*-PrsA inhibitors (table 4.1). The remaining compounds had fold change values of 1.6 or higher which could be either weak inhibitors or false positive values which would be confirmed through biochemical assays (Appendix 15).

Table 4.1: Table representing the compounds that showed activity against *Mtb-prsA* based on overexpression of the gene in a whole cell.

Plate number/ Sample number	Fold change	Plate bar code	Compound Identification	Well ID (Intermediate plate)
1/X10	1.56	G214G8D	GSK353071A	A11
1/X11	1.69	G214G8D	GSK1857145A	B2
1/X19	1.76	G214G8D	GSK921295A	B10
1/X22	1.97	G214G8D	GSK2059310A	C3
1/X23	1.59	G214G8D	GSK1329151A	C4
1/X26	1.75	G214G8D	GSK1783710A	C7
1/X29	2.20	G214G8D	GSK1051703A	C10
1/X34	1.77	G214G8D	GSK1985270A	D5
1/X38	1.76	G214G8D	GSK2379464A	D9
1/X41	1.55	G214G8D	GSK1925843A	E2
1/X42	1.86	G214G8D	GSK2215855A	E3
1/X48	1.57	G214G8D	GR153167X	E9
1/X49	2.15	G214G8D	GR135487X	E10
1/X52	1.53	G214G8D	GSK735816A	F3
1/X57	1.86	G214G8D	GSK2247256A	F8
1/X61	1.58	G214G8D	GSK1829729A	G2
2/X13	2.00	G214G8E	GSK1829728A	B4
2/X15	1.98	G214G8E	GSK810016A	B6
2/X34	1.59	G214G8E	GSK2200160A	D5
3/X23	1.62	G214FNZ	GSK2595882A	C4

4.2.2 Cloning the *Mtb-prsA* gene into a pET-SUMO expression vector

The *Mtb-prsA* was cloned into a pET-SUMO expression vector which was used as an expression vector for the production of the *Mtb*-PrsA protein.

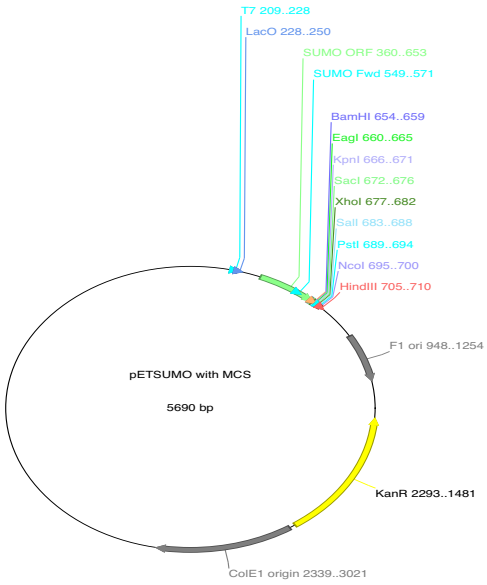

Figure 4.5: Plasmid map of the pET-SUMO vector. The pET-SUMO vector contains a region with multiple cloning sites (MCS) which is placed downstream to the lac operon and the SUMO gene. The plasmid has an antibiotic marker for kanamycin.

The protein production could be induced with isopropyl β-D-1-thiogalactopyranoside (IPTG) under the control of the lac operon (figure 4.5) and the plasmid containing colonies could be selected with the kanamycin antibiotic marker.

The *Mtb-prsA* gene was amplified using PCR to give 918bp amplified fragments of the gene (figure 4.6A). This gene was then ligated to the pET-SUMO vector after double digestion and the positively selected colonies containing the kanamycin resistance gene were tested for the presence of the plasmid containing the *Mtb-prsA* gene through double digestion (figure 4.6 B).

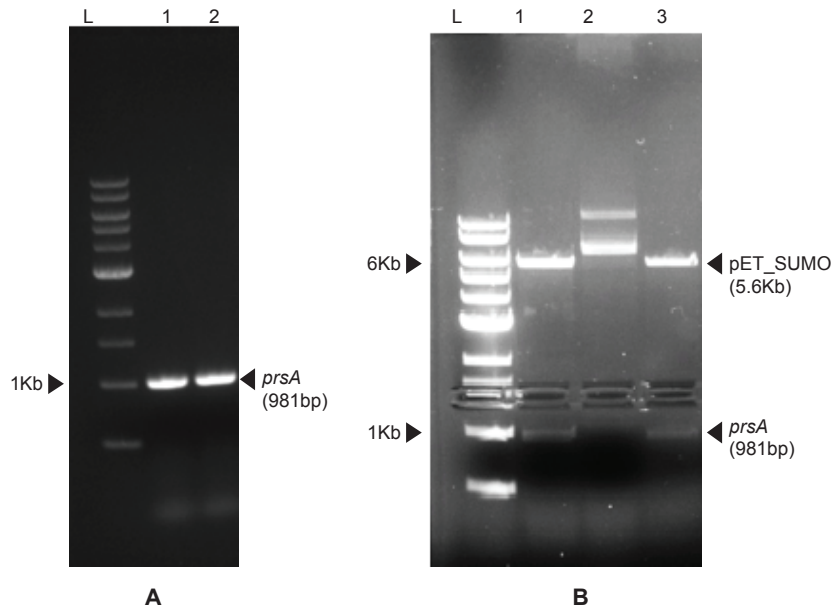

Figure 4.6: Cloning of the *Mtb-prsA* gene in the pET-SUMO expression vector. A. Represents the PCR amplified *Mtb-prsA* gene (981bp) product on an agarose gel. The PCR product is separated with a 1Kb ladder and the amplified bands can be seen lined up next to the 1Kb band on the ladder. B. Represents an agarose gel of the double digested plasmids isolated from positively selected colonies. Lane 1 and 3 show the presence of the *Mtb-prsA* gene at the 1Kb band on the ladder while the pET-SUMO vector (5.6Kb) can be observed next to the 6Kb band on the ladder. Lane 2 represents a negative result with the absence of the gene drop out.

Plasmids containing the *Mtb-prsA* genes were sent for sequencing for further confirmation before use for producing expression strains.

4.2.3 Expression and purification of the *Mtb*-PrsA enzyme

The *Mtb*-PrsA enzyme was expressed and purified as mentioned in section 6.13.1, for target based screening against the GSK177 library. As shown in figure 4.7A, the enzyme elutes (35.459KDa) at 200mM and 225mM on the imidazole concentration gradient. The histidine tagged protein was confirmed by a western blot (figure 4.7B) and stored for further experiments.

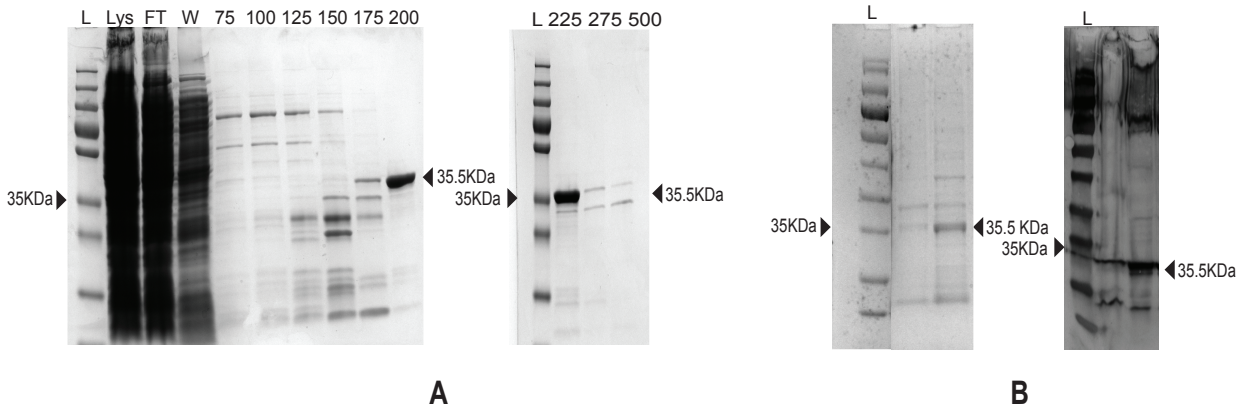

Figure 4.7: Protein expression of *Mtb*-PrsA using the pET-SUMO_*prsA* construct. A. SDS protein gels depicting the protein fractions at various imidazole concentrations collected during the large-scale protein expression. The gel contains (from left to right) a protein ladder (L), cell lysate (Lys), flow through (FT), the wash fraction (W) at 50mM imidazole concentration and then the other fractions for imidazole concentrations 75mM, 100mM, 125mM, 150mM, 175mM, 200mM, 225mM, 275mM and 500mM. The *Mtb*-PrsA protein (35.459KDa) was eluted at imidazole concentrations 200mM and 225mM. B. The figure depicts a SDS gel and a western blot to confirm the histidine linked *Mtb*-PrsA protein through a colorimetric detection procedure. The band can be visualised at the 35kDa band on the protein ladder.

4.2.4 Optimisation of the *Mtb*-PrsA enzyme assay

The purified protein was tested for activity and titrated to monitor substrate utilisation in order to extend the length of the assay. The enzyme was titrated to approximately 0.1μg/μL so that the substrate conversion could take place over approximately half an hour. As mentioned in section 4.2.3, the enzyme was used to screen the GSK177 library for target protein inhibition. In order to be able to analyse the inhibition of the enzyme with the compounds in the GSK177 library, an enzyme titration was performed to enable measurement of NADH conversion over a reasonable period of time. The *Mtb*-PrsA enzyme was titrated at 0.75μg/μL, 0.5μg/μL and

0.1µg/µL and tested for NADH conversion till the fluorescence level reached zero indicating utilisation of the substrates.

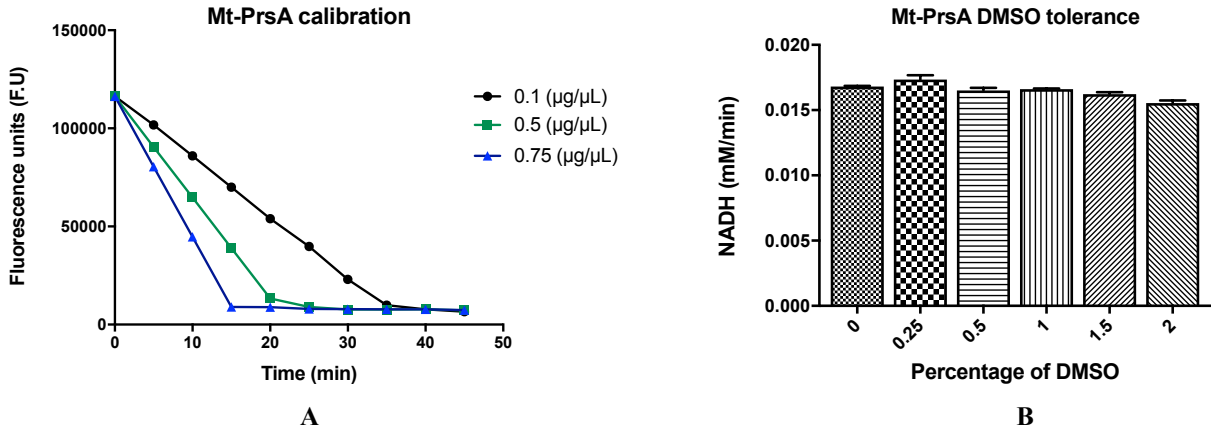

Figure 4.8: Optimisation of *Mtb*-PrsA and DMSO concentration in the enzyme assay. A. Represents the conversion of NADH by *Mtb*-PrsA enzyme at different concentration measured in fluorescence units. B. Represents the rate of conversion of NADH in the enzyme couple at different DMSO concentrations relating its effect on *Mtb*-PrsA enzyme activity.

It was observed that 0.1µg/µL was the optimum enzyme concentration to be used as it allowed for the reaction to progress for nearly half an hour while at other two concentrations the enzyme utilizes the substrate within 10-20mins (figure 4.8A).

The compounds that were screened against *Mtb*-PrsA were solubilised in DMSO and therefore it was imperative to test the effect of the solvent on the activity of the enzyme. The activity of the enzyme was studied by its ability to be able to convert substrates and measured by the rate of depletion of the NADH. Five different concentrations of DMSO were tested in the assay at 0.25%, 0.5%, 1%, 1.5% and 2%. The rate of NADH depletion remained fairly stable at 0.016mM/min at DMSO concentrations of 0.25%, 5%, 1% and 1.5% matching the rate in the absence of DMSO. The rate decreased at 2% DMSO concentration to 0.015mM/min (figure 4.9B).

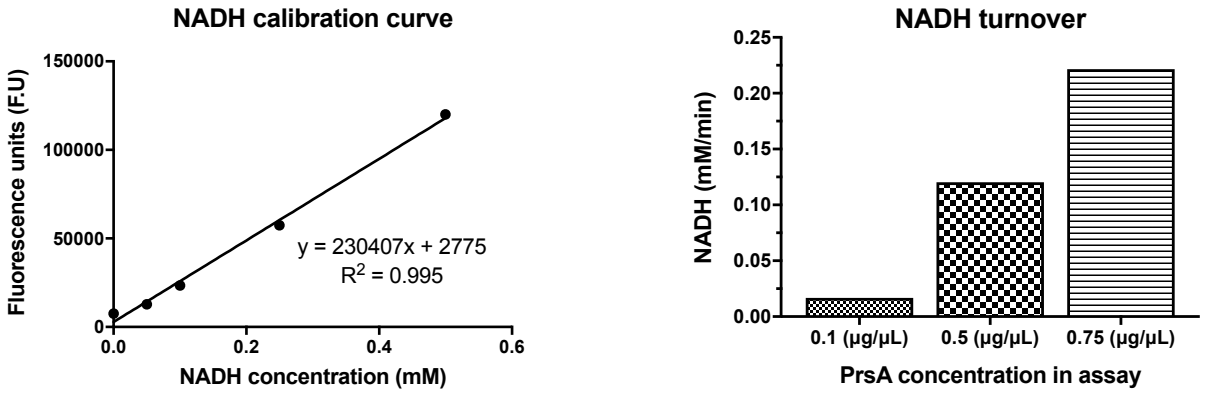

Figure 4.9: Calibration of NADH concentration and conversion in the assay. A. Represents the fluorescence units of NADH at different NADH concentration in the assay mixture relating the amount of fluorescence to the amount of NADH added into the mixture. B. The rate of NADH conversion at different *Mtb*-PrsA enzyme concentrations.

In order to determine the amount fluorescence emitted by NADH in a concentration dependant manner the fluorescence units were measured against the NADH concentration in the assay. The fluorescence follows a concentration dependant linear pattern (figure 4.9A) and was helpful in determining the upper limit of the fluorescence when normalising the enzyme screen data. The NADH turnover was tested with different concentrations of the *Mtb*-PrsA enzyme in order to confirm that the concentration of *Mtb*-PrsA enzyme being considered was appropriate. The NADH turnover rate at 0.1µg/µL was 0.016mM/min while the rates for 0.5µg/µL and 0.75µg/µL were 0.12mM/min and 0.22mM/min respectively. The rate was 7.5 time faster at an enzyme concentration of 0.75µg/µL in comparison to 0.1µg/µL which explains the relatively quick decline in fluorescence units observed before (figure 4.9A). It was therefore confirmed that 0.1µg/µL was the most suitable concentration to be used for the assay.

4.2.4 GSK177 compound screens against *Mtb*-PrsA enzyme

The GSK177 compound library was reintroduced into new intermediate plates for use with new annotations to include columns for positive and negative controls (Appendix 17). Two separate sets of compound screenings were performed against the *Mtb*-PrsA enzyme with the final compound concentration of 20μM in 30% DMSO therefore making the final DMSO concentration 1.5% in the assay along with both positive and negative controls (section 6.14.2). Since there are no known inhibitors of the *Mtb*-PrsA enzyme it was not possible to have a control with an inhibitor. The compounds were incubated initially with the substrate and read as an end point assay after incubation with the *Mtb*-PrsA enzyme for ~30mins.

4.2.4.1 GSK177 compound screen against *Mtb*-PrsA enzyme

Hits were shortlisted based on their ability to limit enzyme activity to or below 50% (figure 4.10, 4.12). The initial set of biochemical screening against the GSK 177 library did not reveal as many hits as observed from the overexpression screen. The screen also depicted fairly high (almost 100%) activity percentages against most of the compounds. Although two hits were observed from plate 1 of the GSK 177 plate GSK1829727A and GR135487X which inhibited the enzyme activity to 45% and 24% respectively. GR135487X was one of the compounds that was highlighted as inhibiting the *Mtb*-PrsA enzyme in the overexpression screen performed again *M. bovis* BCG. This proved that this particular compound is potentially a strong inhibitor of the enzyme both in the biochemical assay and a target based whole cell assay.

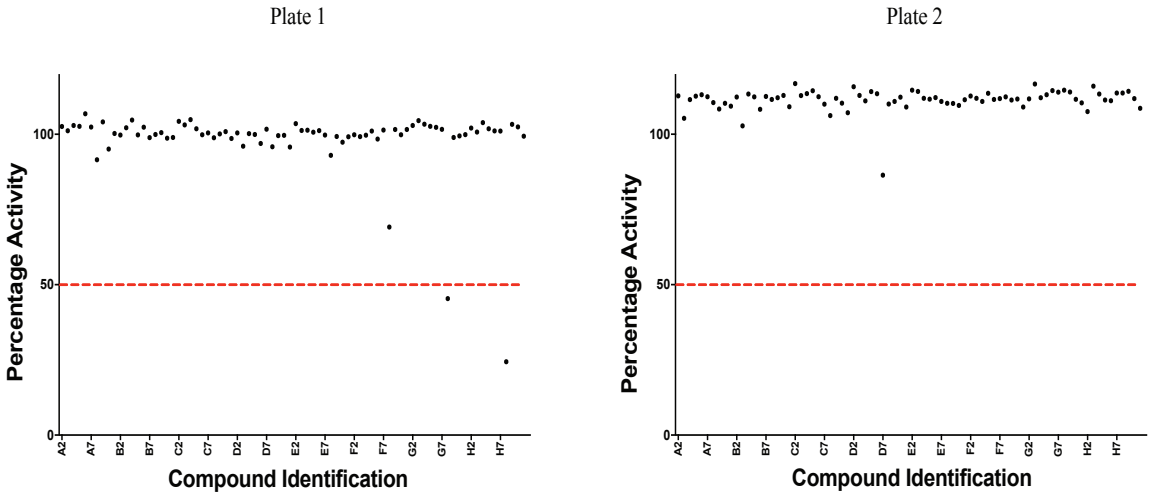

Well ID	Compound Identification	Percentage Activity
G8	GSK1829727A	45.37280278
H8	GR135487X	24.40757357

Figure 4.10: Biochemical screen of the GSK177 library against *Mtb*-PrsA.The scatter graph represents the average percentage activity of the *Mtb*-PrsA enzyme against 20µM concentration (in 30% DMSO) of the GSK 177 drug library. The table below each scatter graph lists the hits with details of the compound identification and percentage activity.

4.2.4.2 IC_{50} analysis of the compound GR135487X

The IC_{50} analysis was performed for the compound GR135487X which displayed a very strong inhibitory activity in both the whole cell screen and the biochemical assay against *Mtb*-PrsA. The GR135487X IC_{50} was 0.62µM against the *Mtb*-PrsA enzyme. The IC_{50} value observed here was much lower to the *in vivo* inhibitory concentration (MIC90) observed against H37Rv was 2.2µM (Sorrentino *et. al.*, 2015). The compound was tested against intracellular mycobacteria in the THP-1 macrophage cell line where the MIC90 was found to be 0.6µM indicating that the

compound is potent at clearing the bacterial load within macrophages at a very low concentration (Sorrentino *et. al.*, 2015).

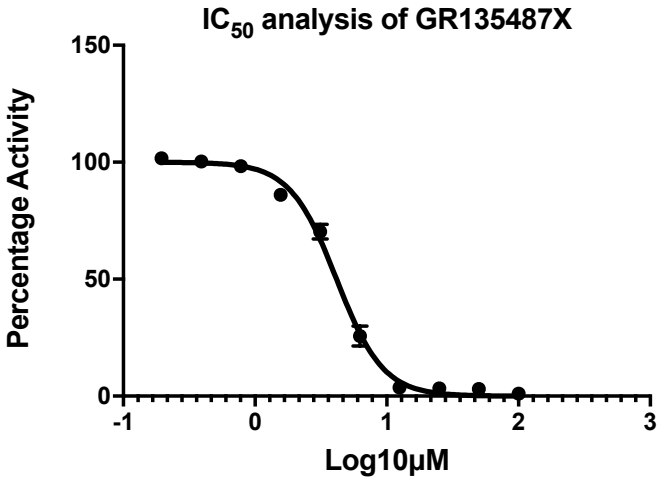

Figure 4.11: IC50 analysis of the compound GR135487X. The graph depicts the normalised percentage activity of the *Mtb*-PrsA enzyme in presence of the serially diluted compound GR135487X.

4.2.4.3 GSK177 compound screen against *Mtb*-PrsA enzyme repeat

There was an expected drop in the hits as the screen was performed against the smaller and original set of the GSK 177 collection. Another set of biochemical screens was performed to check if the compounds depicted any inhibitory activity against the *Mtb*-PrsA enzyme using a fresh purified preparation of the enzyme and plating out the compounds in new intermediate plates. More hits were observed in this screen against the *Mtb*-PrsA enzyme (figure 4.12).

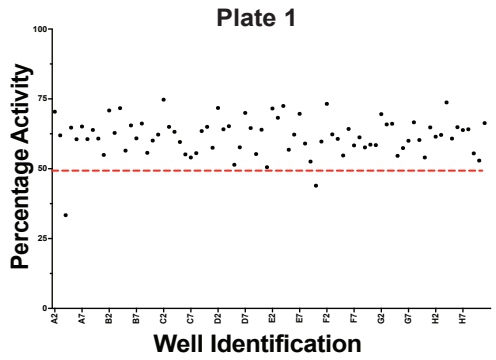

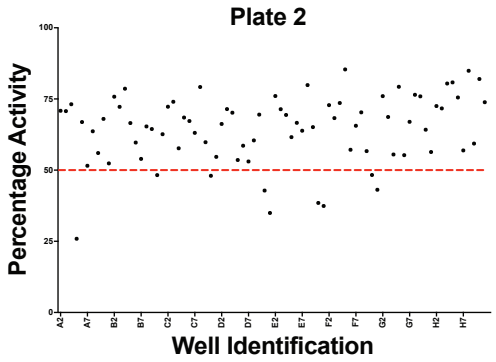

Well ID	Compound identification	Percentage activity
A4	SB-204804-A	33.387
E10	GSK1788487A	43.949

Well ID	Compound identification	Percentage activity
A5	GW664700A	25.915
D10	GSK237561A	42.825
D11	SB-746177	34.97
E11	GSK353069A	37.435
F10	GR153167X	48.287
F11	BRL-10988SA	43.129

Figure 4.12: Biochemical screen of the GSK177 library against *Mtb*-PrsA. The scatter graph represents the average percentage activity of the *Mtb*-PrsA enzyme against 20µM concentration (in 30% DMSO) of the GSK 177 drug library. The table below each scatter graph lists the hits with details of the compound identification and percentage activity.

The most potent inhibitor in the second set of biochemical screens was GW664700A which limited the activity of the enzyme to 25% (figure 4.12). The other compounds were either inhibiting enzyme activity to approximately 30-37% and 40-48% (figure 4.12). Once the inhibitory activity was confirmed to be against *Mtb*-PrsA alone within the multienzyme biochemical assay the drugs were then screened against a *Mtb-prsA* overexpression strain in *M. bovis* BCG.

4.2.5 Whole cell overexpression screens of the GSK177 compound library

In order to test the inhibitors that were revealed in the second biochemical screen against *Mtb*-PrsA (section 4.2.4.3), an overexpression screen was performed against the hits observed.

4.2.5.1 *Mtb-prsA* overexpressing screen using the GFP expressing strains of *M. bovis* BCG

The overexpression screen was initially performed using the GFP fluorescing strain of *M. bovis* BCG overexpressing the *Mtb*-PrsA enzyme (section 6.15.1). The results observed from this screen did not particularly reflect the results observed in the biochemical screen. There was no resistance observed in the *Mtb-prsA* overexpressing strain against the selected inhibitors (figure 4.13). This is depicted by a higher survival percentage of the overexpression strains with respect to a strain without the overexpression plasmid. The discrepancy between the biochemical screen and target based whole cell screening was deemed to be caused by the molecular interactions of two plasmids in the cell or characteristics of the GFP molecule. The compounds have been tested for whole cell activity in *M. bovis* BCG (Ballell *et. al.*, 2013) and therefore the permeability of the drug would not have been an issue. The screens were then repeated further using the non-fluorescing strain of *M. bovis* BCG.

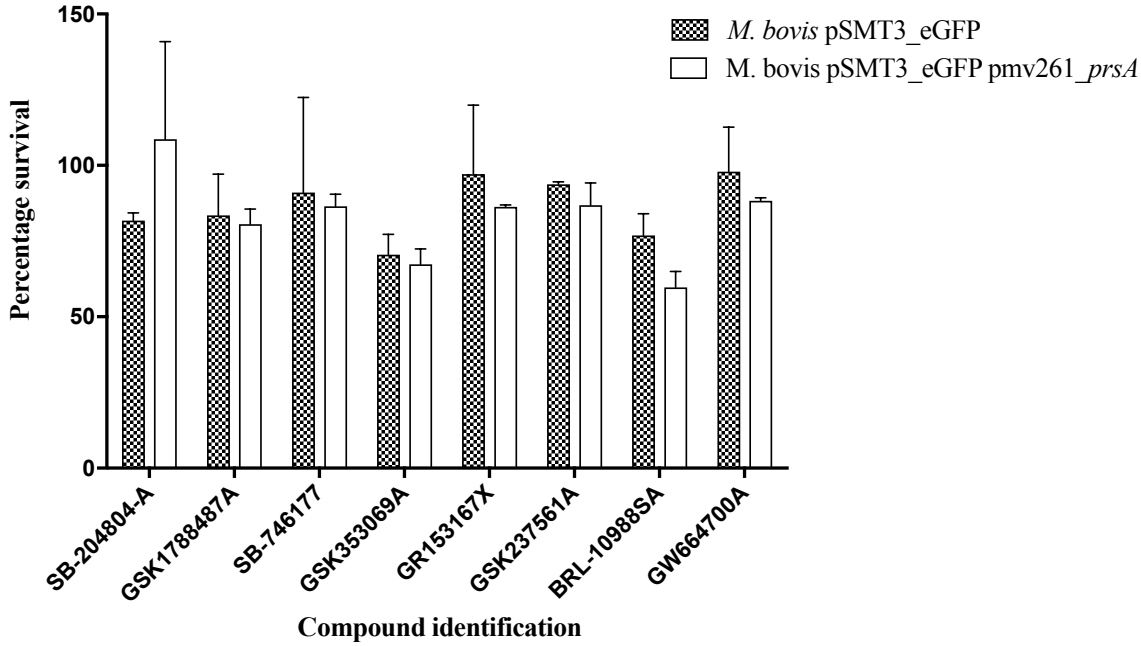

Figure 4.13: Whole cell overexpression screen using the fluorescing strain of *M. bovis* BCG. The bar graph represents the average percentage survival (from duplicates) for both the empty vector (pMV261) and cloned vector (pMV261_*prsA*) containing strains.

4.2.5.1 *Mtb-prsA* overexpressing screen using the end point luminescence cell viability assay

The overexpression screen was then repeated at an initial concentration of 20μM and then at a lower concentration of 10μM for selected compounds against a non-GFP expressing strain of *M. bovis* BCG containing the pMV261_*prsA* vector. The overexpression of the *Mtb-prsA* strain was compared to the strain containing an empty pMV261 vector and the results were observed using an end point Cell Titer Glo assay (section 6.15.2).

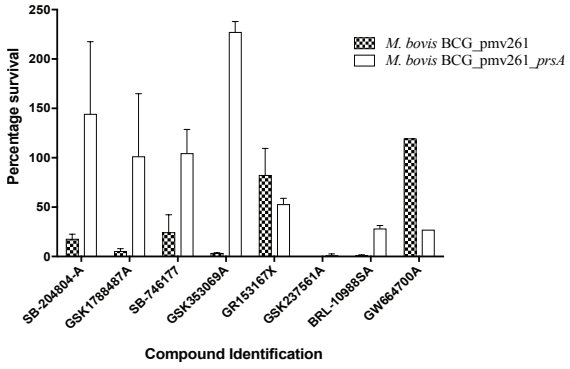

Compound Identification	Fold overexpression
SB-204804-A	8 fold
GSK1788487A	18 fold
SB-746177	~6 fold
GSK353069A	62 fold
GR153167X	0.6 fold
GSK237561A	99 fold
BRL-10988SA	19 fold
GW664700A	0.22 fold

A

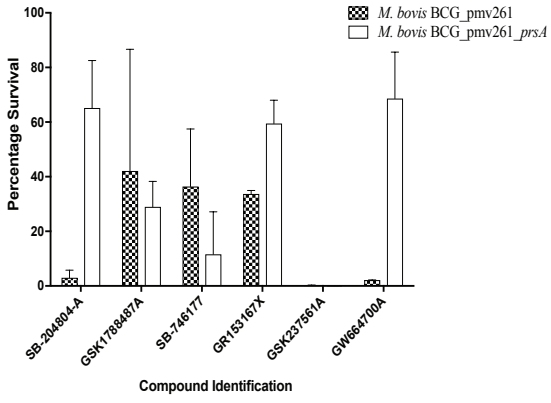

Compound Identification	Fold overexpression
SB-204804-A	21 fold
GSK1788487A	0.68 fold
SB-746177	0.32 fold
GR153167X	~2 fold
GSK237561A	0.4 fold
GW664700A	~32 fold

B

Figure 4.14: End point whole cell overexpression screen using *M. bovis* BCG and the Cell Titer Glo assay. The bar graph depicts the average percentage survival (from duplicates) of the *M. bovis* BCG strain containing the empty vector versus the strain containing the *Mtb-prsA* overexpression plasmid and the survival percentages against each selected compound. Below the graph the table lists the fold change observed for each drug. A. Drugs were tested at 20μM concentration against *M. bovis* BCG, B. Drugs were tested at 10μM concentration against *M. bovis* BCG

In the initial screen at 20μm compound concentration, it was observed that GSK237561A had a 99-fold overexpression in the presence of the inhibitor. This resistance against the inhibitor from the overexpression strain indicated a strong possibility of the compound targeting the *Mtb*-PrsA enzyme. Alongside the above-mentioned inhibitor, GSK353069A, BRL-10988SA, GSK1788487A and SB-204804-A depicted a fold difference of 62, 19,18 and 8 respectively with respect to the non-overexpressing strain (figure 4.14A).

Based on the results observed in this initial screen at 20μM, the screen was repeated at 10μM concentrations against selected inhibitors based on the high fold changes and the availability of the inhibitors

It was seen that although SB-204804-A had high fold change at 20μM, the inhibitor fold change increased with a corresponding decrease in concentration, this could be due to the high error bars observed for the inhibitor in the first screen (figure 4.14B). It was observed that the fold change was concentration dependent for the inhibitors GSK1788487A, SB-746177 and GSK237561A. This combined with the biochemical screen data indicated that the target for these inhibitors was the *Mtb*-PrsA enzyme. The compounds displayed potency by inhibiting the enzyme in both the biochemical and whole cell screen. Not all the potential hits identified during the *Mtb*-PrsA enzyme assay could be screened due to the unavailability of some specific compounds from the library.

4.2.6 Potential hits against *Mtb-prsA* from the GSK177 compound library

9 potential hits were shortlisted against *Mtb*-PrsA based on the biochemical and whole cell overexpression screens (figure 4.15). The compound GR135487X is seemingly the most potent inhibitor which has been analysed in detail to determine the IC_{50} values. The other hits

mentioned here were observed during a second biochemical assay performed against *Mtb*-PrsA and confirmed for activity in a whole cell phenotypic overexpression assay.

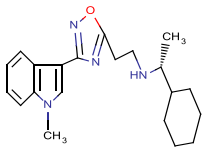

SB-204804-A
8 fold

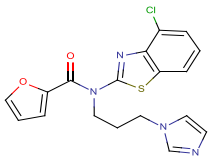

GSK1788487A
18 fold

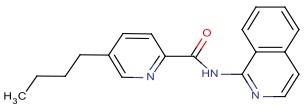

SB-746177
~6 fold

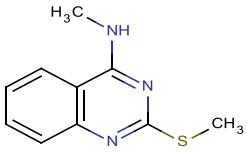

GSK353069A
62 fold

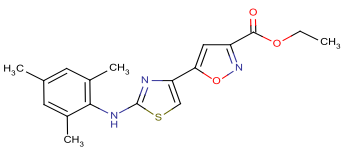

GR153167X
0.6 fold

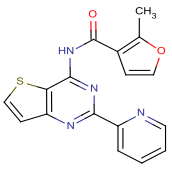

GSK237561A
99fold

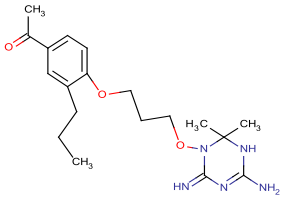

BRL-10988SA
19 fold

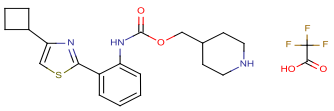

GW664700A
0.22 fold

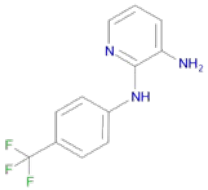

GR135487X
2.15 fold

Figure 4.15: Hits from the GSK177 screen against *Mtb-prsA*. The figure represents structures of the potential hits from the GSK177 screen with the structures and fold changes for each compound. The fold change of GR135487X mentioned here is from the initial overexpression screen against the extended GSK177 library while the fold changes for all the other compounds was based on the results from the end point luminescent assay at 10µM final concentration.

It was observed that SB-746177, GSK1788487A and GR135487X have molecular weights of 305.4, 386.9 and 253.2 respectively. All of these compounds also had logP values of less than 5. Therefore, these drugs obey the Lipinski's rule of 5 and could potentially be probable drug like inhibitor molecules targeting *Mtb*-PrsA.

4.3 Discussion

There have been some target based screening programmes that have produced potential molecular scaffolds and groups useful against a specific target in *Mtb.* As an example, FtsZ is a protein that has been deemed as an important target for target based drug discovery. The FtsZ protein is involved in cell division and cytokinesis by utilizing GTP to form a polymeric ring (Ojima *et. al.*, 2017). This temperature sensitive filamentous protein is homologous to the eukaryotic tubulin. Compound screens have been performed against this protein using a 20,000-compound containing library to reveal a compound 297F which had inhibitory activity on the protein leading to a decrease in the polymers formed. The compound had low cytotoxicity and maintained specificity against *Mtb* as it did not show activity against any other gram negative or gram positive bacteria (Lin *et. al.*, 2014). There have been developments in generating a class of compounds that are effective against this protein by combining pharmacological study with the protein structure and a generic screening of the compound classes against the protein to detect inhibitory activity. A fluorinated benzimidazole has been designed as a possible contender which stops the polymerisation and aggregation of the protein in a dose dependent manner (Ojima *et. al.*, 2017).

PanC is another example of a target based approach for *Mtb* drug discovery. The gene encodes for pantothenate synthetase which is responsible for ATP-dependent condensation of pantoate and β-alanine into panthothenate with the release of AMP and pyrophosphate molecules. This gene has been known to be essential both for *in vitro* growth and *in vivo* as tested in mouse models. A new class of compounds was discovered that inhibited this enzyme both in biochemical assays and whole cell screening against *Mtb.* The screen was executed against a library of 4080 compound from which two compounds showed activity against the enzyme and

belonged to the 3-biphenyl-4-cyanopyrrole-2-carboxylic acid class (Kumar *et. al.*, 2013).

Due to the pitfalls of target based assays there has been a certain level of interest in developing specialised whole cell based assays which target a specific gene or enzyme considered to be a possible drug target (Mdluli *et. al.*, 2015). In order to test the activity of compounds against PanC and other targets, conditional mutants were designed to underexpress the protein and were then screened against a library of 600 compounds, out of which 37 presented activity against the PanC enzyme. Out of these hits, 4 were commercially available flavones which had almost 16 fold activity against the under-expressing mutant (Abrahams *et. al.*, 2012).

The target based study involving the *Mtb*-PrsA enzyme as a potential drug target revealed compounds from the GSK177 collection with activity against the protein. The compounds identified as most promising by comparing the fold change of wild type *M. bovis* BCG against *M. bovis* BCG overexpression strain were GSK 1788487A, SB-746177 and GSK 237561A with MIC90 values of 8.4μM, 9.2μM and 4μM against *Mtb* H37Rv (Sorrentino *et. al.*, 2015). These compounds depicted a dose dependent activity against *M. bovis* BCG. The target of these compounds was therefore validated to be the *Mtb*-PrsA enzyme. GW664700A has been predicted to target a serine/threonine kinase (*Rv0014c)* (Martínez-Jiménez *et. al.*, 2013) with a MIC90 of 5.55μM in *Mtb* H37Rv (Sorrentino *et. al.*, 2015). The compound GR135487X also depicted a strong potential to be a *Mtb*-PrsA inhibitor based on the biochemical and overexpression study performed with a low MIC value of 0.6μM against the enzyme and a MIC90 of 2.2μM (Sorrentino *et. al.*, 2015). Some of these compounds were also tested for activity against intracellular *Mtb* H37Rv infecting THP-1 cells, a macrophage cell line. GSK 1788487A, SB-746177 and GSK 237561A depicted an intracellular MIC90 of 50μM, 1.85μM and 1.85μM respectively (Sorrentino *et. al.*, 2015).

Unfortunately, attempts to crystallise the enzyme failed due to issues with enzyme quantity during purification and salt crystal formation. It would have been useful to understand the interaction between these compounds and the protein structurally in order to decipher the mechanism of inhibition. Recently the PrsA enzyme from *M. smegmatis* was crystallised and the structure was as expected for a class I phosphoribosylpyrophosphate synthase. The crystal presented with a quaternary hexamer, whose oligomerisation is a requirement for complete enzymatic activity. The enzyme has a catalytic and allosteric regulatory site which has conserved residues to the nearby subunits (Donini *et. al.*, 2017). It is 88% similar to the *Mtb* PrsA and 43% similar to the human isoform. The protein requires phosphate and magnesium ions for activity. The major differences observed between the *M. smegmatis* PrsA and the human isoform was the substitution of the glutamic residue to alanine in the human PrsA and the change from Glycine 236 to Cysteine 226 in the ribose-5-phosphate binding site (Donini *et. al.*, 2017). These differences are important to design compounds that are specific to the mycobacterial protein in order to inhibit the cell wall synthesis.

An understanding of the structural interaction of the GSK 177 compounds which depict activity against *M. bovis* BCG would help to gauge the feasibility of using these compounds and/or their structural scaffolds as drugs or potential drug classes, chemical modification of the latter can improve activity. Toxicity studies and structure activity relationship data could provide information regarding the suitability of the compounds. Although more work needs to be done on these compounds and how they interact with the protein, here we have successfully screened a compound library against a potential drug target, isolating compounds showing inhibitory activity both in a biochemical assay and a target based whole cell assay.

Chapter 5

General Discussion

5.1 Conclusion and future work

Tuberculosis is currently a major global health concern and the continual increase in the number of drug resistant cases is exacerbating the situation. Given the steady rise in the number of MDR, XDR and TDR cases, it has become imperative to understand the cause of resistance in TB and have new ammunition to combat it. *Mtb* is a very robust bacterium and its ability to survive within the host is largely due to the unique structural nature of its cell wall. This structure allows the bacterium to sustain itself for prolonged periods in the presence of environmental pressure (caused by immune cells and physiological conditions) and evolve to resist inhibitory antibiotics. In view of the current crisis, progress is largely dependent on understanding how the bacteria survive within the host, this includes a better understanding of cell wall functions. Although numerous efforts have been made to develop new drugs for TB treatment, few have successfully transitioned from bench to bedside. Furthermore, although a lot of studies have been carried out on the various biosynthetic pathways of *Mtb*, there are still some pathways that are not completely understood.

In light of this information, the aim of this thesis was to employ various methods of drug discovery to generate inhibitors against mycobacteria and understand how they inhibit the bacteria. In chapter 2, we attempted to shorten the time from bench to bedside by screening a library of FDA approved drugs to see if they inhibited two strains of mycobacteria. We observed that similar numbers of drugs were inhibiting both the fast and slow growing strains of mycobacteria. Some known inhibitors of *Mtb*, which included antitubercular drugs and some newly discovered inhibitors such as Auranofin and Ebselen (Favrot *et. al.*, 2013; Harbut *et. al.*, 2015), came through as hits in the screening assay that we performed, validating the screening process that we utilised. The process of deconvolution of the drug targets for the shortlisted

drugs led to a lot of interesting targets. Among the targets observed, it would have been fascinating to further investigate the function of the enzyme targeted by the GBR12909 drug. The enzyme AroB is a dehydroquinate synthase involved in the shikimate pathway (Cheng *et. al.*, 2012; de Mendonça *et. al.*, 2007) and could be an attractive drug target for further development using the GBR12909 as a scaffold for designing compounds. It is also necessary to understand that the *in vitro* assays do not replicate the heterogeneity and metabolic state of the bacteria *in vivo* during infection or under the selective pressure of antimicrobials. Utilising *in vitro* models to mimic the state of the bacterium *in vivo* through various stimuli is a good way of investigating the efficacy of the drug in a real-world scenario (Evangelopoulos *et. al.*, 2015). It would be useful to have insights into the efficacy of the hits observed during this screen in cell lines, or under stress conditions that imitate the *in vivo* pressures the bacterium faces. A combinatorial approach to this drug screen could help to identify any synergistic properties that the hits or the drugs in the library could contribute to the existing drug set.

It was interesting to observe that a chloramphenicol derivative inhibited an enoyl CoA hydratase as a secondary target. Chloramphenicol has been proven to interact and bind at the 2451 and 2452 of the 23SrRNA in the 50S ribosomal subunit (Schifano *et. al.*, 2013), therefore causing a disruption in the biosynthesis of proteins. During the mode of action study of florfenicol (the chloramphenicol derivative), it was observed that the drug not only inhibited protein biosynthesis but also targeted the EchA12 protein in *M. bovis* BCG. After analysing various drug targets revealed during the mode of actions studies, a further investigation into the role of EchA12 was undertaken.

In chapter 3, we investigated the role of EchA12 in mycobacteria. It was recently determined that EchA6 (an enoyl CoA hydratase) was actually essential due to the inability to obtain a null mutant for the gene (Cox *et. al.*, 2016a), despite being predicted to be non-essential through

Himar-I based transposon mutagenesis (Sassetti *et. al.*, 2003). The *echA6* gene was revealed to be an important target due to its involvement in mycolic acid synthesis where the enzyme encoded is an acyl CoA carrier to the FAS-II cycle. A new set of chemical inhibitors were found to be active against this particular enzyme, causing a disruption in the mycolic acid synthesis (Cox *et. al.*, 2016a). The essentiality testing of *echA12* revealed that the gene was non-essential as we were able to generate a null mutant in *M. smegmatis*. Further testing did not reveal a clear function of the enzyme in the biosynthetic pathway. A detailed investigation of the lipids using surface solvent extraction and mass spectrometry uncovered that the enzyme was involved in shuttling the palmitoyl CoA which is added on to the mannose sugar in the PIM molecule. The change in acylation states in the null mutant confirmed that the EchA12 is the carrier protein for palmitoyl CoA, although the absence of the palmitoyl CoA only redirected the PIM synthesis pathway towards differently acylated molecules. Although this change in the lipid composition was not lethal, it triggered a morphological change causing the null mutant to be slower than the wild type *M. smegmatis*. We also developed a protein structure model in I-TASSER using the solved protein structure of EchA6 (Cox *et. al.*, 2016a). The EchA12 monomer was modeled on to one of the EchA6 monomers and illustrated that the mutation generated against florfenicol in the protein was present in the hinge of an α-helix loop. The increased hydrogen bonding, caused due to the amino acid substitution from a glycine to an arginine (Borders Jr *et. al.*, 2008) , would therefore allow the protein to keep the hinge region in operation. We docked the palmitoyl CoA into the binding pocket to understand the interaction of the protein with the coenzyme A. The protein appears to be quite difficult to isolate and purify under *in vitro* conditions. This limited our ability to generate feasible crystals for the protein and potentially perform a ligand binding assay, although the shift in IC_{50} against the drug confirms the interaction of the ligand with the protein. It would be interesting to be

able to generate a crystal structure of this protein in order to improve the understanding of the binding pockets and interaction of the drug with the protein. PatA is an acyltransferase enzyme which is regulated by cyclic AMP and helps the bacteria adapt to change in carbon sources. It also plays a role in assisting the bacteria to slow down its growth rate, which is helpful for the bacteria to reach a non-replicating state. It would be intriguing to see what other enzymes PatA interacts with given the fact that in our study it was proven to have a promiscuous nature. Although a lot is now known about the PIM pathway, there are still holes in the models surrounding acylations of the PIMs and it is still debated if the acylation of the PIM_1 molecule comes before the mannosylation of PIM_1 into PIM_2 (Albesa-Jové *et. al.*, 2016; Guerin *et. al.*, 2009). A two-hybrid analysis of protein-protein interaction could unravel a part of the protein network involved in the biosynthesis of PIMs.

In chapter 4, we explored another area of drug discovery by looking for inhibitors against a validated target. The *Mtb*-PrsA enzyme has been determined as essential for the survival of the bacterium as in its absence the cell wall biosynthetic pathway breaks down, causing the bacterial cell to collapse (Alderwick *et. al.*, 2011; Donini *et. al.*, 2017). This target was screened against a compound library of inhibitors with confirmed activity against *Mtb* but without known modes of action. In this chapter ww to utilised a target based phenotypic assay to allow the cell wall barrier to be present while still targeting the desired enzyme target. This allowed us to isolate compounds that inhibited the target, but were also active within a whole cell as opposed to a purely biochemical approach. Several compounds depicted activity against the target but we could perform detailed analysis of only one compound due to limited supply of the compounds. The *Mtb*-PrsA protein purified extremely well with a phosphate based purification buffer however this caused issues during the crystallisation process. The *Mtb*-EchA12 protein structure has been predicted through homology modelling against the *Bacillus subtilis* PrsA,

which is 43% homologous to the *Mtb*-PrsA. The enzyme has been predicted to have a hexameric form with each monomer containing two subunits. The residues involved in the catalytic domain of the enzyme are conserved and retain important residues such as Asp42. It contains a His109 in a flexible loop which ranges from Lys108 to Arg112, helping it to form hydrogen bonds with the ATP substrate (Alderwick *et. al.*, 2011). The ability to crystallise and consequently deconvolute the crystal structure of the *Mtb*-PrsA enzyme would be of notable importance. This would help in understanding not only the interaction of the enzyme with its substrate, but also the newly found ligands from this screen. It would be also be of significant value to be able to perform the IC_{50} analysis of the enzyme with all the other compounds that seem to inhibit the enzyme both in the biochemical assay and in the phenotypic assay.

Here we have presented a phenotypic drug discovery model involving two major strategies which have revealed inhibitors and drugs active against the surrogate models of *Mtb*. The analysis of one of the targets investigated through the phenotypic screens revealed its role in the biosynthetic pathway of cell wall glycolipids. The strategy employing targeted drug screening de-orphaned some inhibitors with known antimycobacterial activity.

Chapter 6

Materials and Methods

6. Materials and Methods

6.1 Media Preparation

6.1.1 Luria – Bertani (LB) broth

37g LB (Merck Millipore) broth powder was added to 1l water and autoclaved at 121°C for 15 min.

6.1.2 Luria – Bertani (LB) agar

37g LB broth powder (Merck Millipore) and 12g Bacto Agar (BD, Difco) was added to 1l water and autoclaved at 121°C for 15 min. Once autoclaved the media was kept at 55°C and then poured into 90 mm petri dishes (25mL/petri dish).

6.1.3 Tryptic Soy broth (TSB)

30g TSB powder (BD, Difco) was added to 1L water and autoclaved at 121°C for 15 min.

6.1.3 Tryptic Soy agar (TSA)

30g TSB powder (BD, Difco) and 12g Bacto Agar (BD, Difco) was added to 1L water and autoclaved at 121°C for 15 min. Once autoclaved the media was kept at 55°C and then poured into 90mm petri dishes (25mL/petri dish).

6.1.4 Middlebrook 7H9 broth

1.31g Middlebrook 7H9 (BD, Difco) in 225mL of water. To this solution 556µL 100% Glycerol, 25mL OADC enrichment and 125µL Tween 80 was added. The solution was thoroughly mixed and then filter sterilsed through a filteration unit containing a 0.2µm pore size filter.

6.1.5 Middlebrook 7H9 basal agar

4.7g Middlebrooke 7H9 powder (BD, Difco) and 12g Bacto Agar (BD, Difco) in 1L of water was autoclaved at 121°C for 15 min.

6.1.6 Top agar

4.7g Middlebrook 7H9 Broth (BD, Difco), 6 g Bacto Agar (BD, Difco) in 1L water (without ADC supplement) was autoclaved at 121°C for 15 min.

6.1.7 Terrific broth

47.6g terrific broth powder (Merck Millipore) and 4mL of 100% glycerol in 1L of water. The solution was dissolved and autoclaved at 121°C for 15 min.

6.1.8 Terrific salts

23.1g Potassium dihydrogen phosphate (KH_2PO_4) and 125.4g Dipotassium hydrogen phosphate (K_2HPO_4) were dissolved in 1L of water and autoclaved at 121°C for 15 min. The solution was added to terrific broth in a 9:1 (Terrific broth: Terrific salts) ratio before use.

6.1.9 Tween- 80 (10%)

A 10% tween-80 solution was prepared by dissolving 10mL of tween-80 in 90mL of water followed by filter sterilisation using a 0.2μm pore size filter. The solution was used at 0.05% in liquid media to culture mycobacterial strains.

6.1.10 Transformation Buffers

6.1.10.1 Transformation buffer I (TFBI)

30mM Potassium acetate (KAc), 10mM calcium chloride ($CaCl_2$), 50mM manganese chloride ($MnCl_2$), 100mM Rubidium chloride ($RbCl_2$) and 15% glycerol (v/v) were prepared in water. The solution was adjusted to a pH of 5.8 and filter sterilized.

6.1.10.2 Transformation buffer II (TFBII)

10mM MOPS, 75mM Calcium chloride ($CaCl_2$), 10mM Rubidium chloride ($RbCl_2$) and 15% glycerol (v/v) were prepared in water. The solution was adjusted to a pH of 6.5 and filter sterilized.

6.1.11 Protein Purification buffers

6.1.11.1 Protein Purification buffer 1

100mM potassium dihydrogen phosphate (KH_2PO_4) and 600mM sodium chloride (NaCl) were dissolved in water and the pH was adjusted to 7.9.

6.1.11.2 Protein Purification buffer 2

1M Tris and 300mM sodium chloride (NaCl) were dissolved in water and the pH was adjusted to 7.8.

6.1.12 Dialysis Buffer

6.1.12.1 Dialysis buffer 1

50mM potassium dihydrogen phosphate pH 7.9, 150mM sodium chloride (NaCl), 5mM EDTA pH 7.5 and 1mM DTT were prepared in water.

6.1.12.2 Dialysis buffer 2

50mM potassium dihydrogen phosphate pH 7.9, 150mM sodium chloride (NaCl), 10% glycerol and 1mM DTT were prepared in water.

6.1.12.3 Dialysis buffer 3

1M Tris, 100mM of sodium chloride (NaCl), 5mM of EDTA and 1mM DTT were dissolved in water and the pH was adjusted to 7.8.

6.1.12.4 Dialysis buffer 4

1M Tris, 100mM of sodium chloride (NaCl) and 1mM DTT were dissolved in water and the pH was adjusted to 7.8.

6.1.13 Western blot transfer buffer

3.03g of Tris, 14.4g Glycine pH 7.5 and 100ml methanol were dissolved in 1l of water.

6.1.14 Tris Buffered Saline (TBS)

2.42g of Tris and 8g of sodium chloride (NaCl) were dissolved in 500ml of water. An addition of 0.05% Tween 20 was done to make Tris Buffered Saline with Tween (TBS-T).

6.1.15 Mycobacteriophage (MP) buffer

50mM Tris HCl pH 7.6, 150mM sodium chloride (NaCl), 10mM magnesium chloride ($MgCl_2$), 2mM calcium chloride ($CaCl_2$) were dissolved in water and filter sterilised.

6.1.16 Southern blotting buffers

6.1.16.1 Depurination buffer

0.25M hydrochloric acid (HCl) was prepared in water.

6.1.16.2 Denaturation buffer

1.5 M of sodium chloride (NaCl) and 0.5 M sodium hydroxide (NaOH) was prepared in water.

6.1.16.3 Neutralisation buffer

0.5M Tris HCl and 1M sodium chloride (NaCl) were dissolved in water and the pH adjusted to 7.2.

6.1.16.4 SSC buffer (20x)

3M sodium chloride (NaCl) and 0.3 M sodium citrate were dissolved in water and the pH was adjusted to 7.

The 20x was diluted to 2x and 0.5x with an addition of 0.1% sodium dodecyl sulphate (SDS).

6.1.16.5 Maleic acid buffer

0.1M Maleic acid and 0.15M sodium chloride (NaCl) were dissolved in water and adjusted to a pH of 7.5.

6.1.16.6 Detection buffer

0.1M Tris HCl and 0.1M sodium chloride (NaCl) were dissolved in water and adjusted to a pH of 9.5.

6.2 Antibiotic stocks

Antibiotics were prepared as stocks at higher concentrations to be diluted out to lower concentrations during screens.

6.2.2 FDA Drugs

To prepare 250 µL of 10mM stocks of the FDA approved antibiotics the quantity of antibiotics in table 6.1 were weighed out. The FDA drugs were prepared in 10mM stocks in 100% DMSO except for Phentermine which was available is a solution in methanol. The stocks were used to prepare intermediate plates having 3-fold dilutions of the drugs in 30% DMSO.

Table 6.1: Stock preparation of FDA approved drugs. The table enlists the weight of the antibiotics to be measured out to make a 10mM stock solution.

Antibiotic Name (Sigma)	Molecular weight (g/mol)	Weight (mg)
Josamycin	827.99	2.069
Pentamidine isethionate	592.68	1.48
Thonzonium bromide	591.71	1.479
Florfenicol	358.21	0.895
Glipizide	445.54	1.113
Granisetron	348.87	0.872
Olopatadine hydrochloride	373.87	0.934
Astemizole	458.57	1.146
Tripelennamine	291.82	0.729
Rosiglitazone	357.43	0.893
Pinaverium bromide	511.51	1.47
Phentermine	149.23	1mg/mL
Meclocyline sulfosalicylate	695.05	1.738
Auranofin	**678.48**	1.696
Chlorhexidine	**505.45**	1.263
Alexidine dihydrochloride	**581.71**	1.454
Clomiphene citrate	**598.08**	1.495

Ebselen	**274.18**	0.618
Raloxifen hydrochloride	**510.04**	1.275
Toremifene citrate salt	**598.08**	1.495
Tamoxifen	**371.51**	1.409
GBR12909 dihydrochloride	**523.49**	1.309
Fendiline hydrochloride	**351.91**	0.88
Suloctidil	**337.56**	0.844
Apomorphine hydrochloride	**312.79**	0.782
Nisoldipine	**388.41**	0.971
Sertraline hydrochloride	**342.69**	0.857
Fluspirelene	**475.57**	1.19

6.2.2 Stock antibiotics for screening transformed *M. smegmatis*, *M. bovis* BCG and *E. coli* (Top 10, BL21 DE3)

For Kanamycin (Sigma) stocks and Hygromycin B stock (Thermofisher). Kanamycin was prepared as a stock solution of 50mg/mL in water and was filter sterilized using a 0.2µm pore size filter. The working concentration of Kanamycin was 25µg/mL for *M. smegmatis*, *M. bovis* BCG and 50µg/mL for *E. coli* strains . Hygromycin B was available as a stock solution in PBS at a concentration of 50mg/mL and was used at a working concentration of 20µg/mL for *M. smegmatis* and *M. bovis* BCG.

6.3 Preparation of competent cells

6.3.1 Preparation of chemically competent *E. coli* cells

E. coli cells (Top 10 or BL21 DE3 strains) were grown for 4 h to an $O.D_{600}$-0.4 to 0.5 and then incubated on ice for 10mins. The cells were then pelleted by centrifugation at 4000 rpm for 15mins. The supernatant was discarded and the cells were re-suspended in 400µL of cold TFB1 and incubated on ice for 15mins. The cells were then centrifuged at 4000rpm for 15mins at 4°C and the supernatant was discarded. The cells were then re-suspended in 200µL of TFB2 and incubated for 30mins on ice. The cells were then aliquoted into cryovials or microcentrifuge tubes then flash frozen in liquid nitrogen and stored at -80°C until use.

6.3.2 Preparation of electrocompetent mycobacteria cells

To produce genetically modified strains of *M. smegmatis* and *M. bovis* BCG expressing green fluorescence protein for HTS screening of drugs and overexpressing genes. The procedure involved producing electrocompetent cells to electroporate the said plasmid (such as pSMT3_eGFP, pVV16 empty vector, pVV16_*echA12*_Rv, pVV16_*echA12*_BCG and pVV16_G239_echA12) and then screening out the transformed cells. A 50mL culture of the appropriate mycobacterial strain (*M. smegmatis* and *M. bovis* BCG) was cultured in 7H9 (with tween-80 and OADC). The cells were allowed to grow to an appropriate $O.D_{600}$ of 0.4-0.5 at 37°C. The grown culture was then incubated on ice for 1.5h and centrifuged at 3000g for 10mins. The cell pellets were then consecutively washed in 10% cold glycerol decreasing the volume everytime. For a 50mL culture the pattern of incubation, centrifugation and

resuspension with 12.5mL, 5mL to a final 2.5mL of 10% ice-cold glycerol continued. The electrocompetent cells were then aliquoted and stored at -80°C after flash freezing with liquid nitrogen (-196°C).

6.3.3 Glycerol Stocks

Glycerol stocks were prepared using fresh cultures with an $O.D_{600}$ of 0.5-0.6. The stocks were prepared by adding 1mL of bacterial culture, 357 µL of sterile glycerol (70%) so that the final concentration of glycerol reaches 25% in the culture. The cryovials were then flash frozen using liquid nitrogen (-196°C) and then stored at - 80°C.

6.4 Polymerase chain reaction

6.4.1 Primers used for PCR amplification of genes for different vectors

6.4.1.1 Primer pairs for *Mtb*-prsA overexpression plasmid

Table 6.2: PCR primers for pMV261 cloning of *Mtb-prsA*

Primer	Sequence	Restriction enzyme site
pMV261 Forward	5'-GATCGATCGGATCCATGTTGAGCCACGACTGGACCGATA-3'	BamHI
pMV261 Reverse	5'-GATCGATCAAGCTTTCATGCGTCCCCGTCGAAAAGT-3	HindIII

6.4.1.2 Primer pairs for *echA12* overexpression plasmid

Table 6.3: PCR primers for pVV16 cloning of echA12

Primer	Sequence	Restriction enzyme site
pVV16_*echA12* Forward	5'-GATCGATCCATATGGCTGTGCCCCACCGCTGC-3'	NdeI
pVV16_*echA12* Reverse	5'-GATCGATCAAGCTTCGTGTCATCGGTGAACACCGG-3'	Hind III

6.4.1.6 Primer pairs for *Mtb-prsA* protein expression plasmid

Table 6.4: PCR primers for pET-SUMO cloning of *Mtb-prsA*

Primer	Sequence	Restriction enzyme site
pET SUMO forward	5'-GATCGATCAAGCTTTGCGTCCCCGTCGAAAAGTCCT-3'	HindIII
pET23b reverse	5'-GATCGATCGGATCCATGTTGAGCCACGACTGGACCGATA-3'	BamHI

6.4.2 PCR conditions

The PCR mastermix comprised of the components in table 6.5. Each tube had a 20µL of the PCR mix. It was ensured that the Phusion enzyme was added as the last component to the mix.

Table 6.5: PCR mastermix. The table details the two mastermix combinations used to conduct amplification of genes.

Component (for a strip of 12)	Condition 1	Condition 2
F. Primer (100 pmol/µL)	1.12 µL	1.12 µL
R. Primer (100 pmol/µL)	1.12 µL	1.12 µL
Genomic DNA (~0.05-0.1 µg/µL)	5.6 µL	5.6 µL
dNTPs (0.001µmol/µL)	5.6 µL	5.6 µL
GC Buffer (5x)	56 µL	56 µL
DMSO (100%)	14 µL	14 µL
$MgCl_2$ (50mM)	0 µL	5.6 µL
Phusion enzyme (2U/ µL)	2.8 µL	2.8 µL
dH_2O	193.76 µL	188.16 µL

6.4.3 PCR programme

The PCR programme used for the amplification of the genes is detailed in table 6.6.

Table 6.6: PCR amplification programme. The table details the PCR amplification conditions in terms of the amplification time and temperatures used.

Step	Temperature	Time	Go To	Passes	Gradient
1	98.0°C	60s		1	
2	98.0°C	30s		35	
3	60.0°C	60s		35	10
4	72.0°C	60s	2	35	
5	72.0°C	10min		1	
6	4.0°C	∞		1	

6.5 Agarose Gel Electrophoresis

The agarose gel was prepared at a percentage of 0.8% by adding 0.8g of agarose powder to 100mL of 1x TAE buffer (40mM Tris acetate, 1mM EDTA buffer, pH 8.0) and heated till dissolved. The solution was then cooled to approximately 50°C. To this warm solution, midori

green 5% (v/v) was added, dissolved and poured into the gel tray. The gel was allowed to solidify and the samples loaded with a loading dye (5% glycerol (v/v), 0.4% Bromophenol blue) into the wells. The gel was run in 1x TAE at 140V, 400mA for 50mins and visualised using a Gel Doc XR (Bio-Rad) with Image Lab software.

6.6 DNA extraction from Agarose Gels

DNA was extracted from the agarose gel using the QIAquick gel extraction kit. The DNA band was carefully excised from the agarose gel using a scalpel and weighed. The QG buffer was added in three times volume of the weight of the gel slice and placed on a heating block at 50°C. The tube was mixed frequently for 10mins until the gel slice was completely dissolved. The pH of the mixture was checked by ensuring that it was yellow in colour (indicator shows pH ≤ 7.5). One volume of isopropanol was added to the solution and mixed. The dissolved mixture was then added to a QIAquick column provided in the kit and spun at 13,000rpm for 1min. The flowthrough was discarded and 0.75mL of PE buffer was added to the QIAquick column and centrifuged for 1min. After discarding the flowthrough the column was centrifuged again for 1min to remove residual buffer and ethanol. The column was then placed in a new microcentrifuge tube and 30µL of EB buffer was added to the center of the column and allowed to stand for 1min. The tube along with the column was centrifuged for a minute at 13,000rpm. The extracted DNA was stored at -20°C for later use.

6.7 Plasmid DNA extraction

Plasmid DNA was extracted from a 5mL overnight bacterial culture using the QIAprep spin miniprep kit (Qiagen). The cells from the overnight bacterial culture were pelleted by centrifugation at 5000rpm for 15min. After the supernatant was discarded the pellet was resuspended in 250μL of Buffer P1 containing RNAse (Qiagen) and transferred to a microcentrifuge tube. After transferring the suspension, 250 μL of Buffer P2 (Qiagen) was added to the tube and gently mixed by inverting the tube a few times. Following this 350 μL of Buffer N3 (Qiagen) was added to the tube and mixed by inversion. This mixture was then centrifuged at 13000rpm for 10mins. The supernatant from this tube was transferred to a miniprep spin column (Qiagen) and centrifuged at 13000rpm for 1min and the flow through was then discarded. The column was then washed with 500 μL of Buffer PB (Qiagen) by centrifuging at 13,000rpm for 1min and the flow through was discarded. The column was then washed using 750 μL of Buffer PE (Qiagen) and centrifuged at 13000rpm for 1 min with the flow through being discarded. The spin column was then centrifuged again at 13,000rpm for 1min to remove any residual buffer which was then discarded. The spin column was then transferred to a new microcentrifuge tube and then 50 μL of EB buffer was added to the centre of the column. The column was allowed to sit for 1min and then centrifuged at 13000rpm for 1min. The extracted plasmid DNA in the eluate was stored at -20°C.

6.8 Cloning of genes into plasmid vectors

6.8.1 Double digestion of PCR products and plasmids

The PCR products and plasmids had to be double digested to get sticky ends and ligated to get clones.

Table 6.7: Restriction digest mastermix.

DNA (~0.5-0.1 ng/µL)	10.0 µL
Restriction buffer (10x NEBuffer)	2.0 µL
Restriction enzyme 1	0.5 µL
Restriction enzyme 2	0.5 µL
Water	7.0 µL
	20.0 µL

For pMV261

Restriction enzyme 1(NEB) - BamHI (20U/µL)

Restriction enzyme 2 (NEB) - HindIII (20U/µL)

For pVV16

Restriction enzyme 1 (NEB) - NdeI (20U/µL)

Restriction enzyme 2 (NEB) - HindIII (20U/µL)

For pET SUMO

Restriction enzyme 1 (NEB) - HindIII (20U/µL)

Restriction enzyme 2 (NEB) - BamHI (20U/µL)

The double digest mixture was incubated for 2h at 37°C. The double digested products for plasmids were run on an agarose gel and purified through gel extraction to be used for ligation.

6.8.2 Ligation of digested and purified PCR products and plasmids

The digested plasmid were ligated to the digested PCR products using a T4 DNA ligase. Three conditions were prepared for ligation (table 6.8).

Table 6.8: Ligation mastermix.

Components	Condition 1	Condition 2	Condition 3
Insert (~30 ng)	16 µL	5 µL	0 µL
Water	0 µL	11 µL	16 µL
Plasmid/Vector (~50 ng)	1 µL	1 µL	1 µL
T4 DNA ligase (400 U/µL) (NEB)	1 µL	1 µL	1 µL
T4 DNA ligase buffer (10x) (NEB)	2 µL	2 µL	2 µL

Condition 3 was used to see the presence of self-ligation for the plasmid DNA. The ligation was carried out overnight at 4°C. The next day the ligated products were transformed as per section 6.9. The presence of colonies for conditions 1 and 2 would be suggestive of presence of clones, which was confirmed by double digesting plasmids, isolated form colonies.

6.9 Transformation of bacterial cells

6.9.1 Transformation of *E. coli* cells by heat shock method

100µL of chemically competent *E .coli* (Top10 or BL21_DE3) were added to 1µL of the pET23b_*prsA* plasmid and incubated on ice for 15mins. The mixture was then subjected to a heat shock of 42°C for 1min. The cells are then incubated on ice for 2 mins and recovered at 37°C after the addition of 250µL of LB broth for 1h. The suspension was then plated at various

volumes (50µL and 100µL) on LB agar plates containing kanamycin (50µg/mL) and incubated overnight at 37°C.

6.9.2 Transformation of mycobacterial cell by electroporation

6.9.2.1 *Mtb-prsA* overexpression strains in *M. smegmatis* and *M. bovis* BCG

5µL of plasmid DNA at approximately 0.2-1mg/mL (pMV261 plasmid and pMV261_*prsA* plasmid) was added to 200 µL of electrocompetent cells (*M. smegmatis* mc^2155, *M. smegmatis* pSMT3_eGFP, *M. bovis* BCG, *M. bovis* BCG pSMT3_eGFP) and kept in ice for 10minutes. An electroporation cuvette (0.2cm gap electrodes) was put on ice until cold and the cells were then transferred to the sterile cuvette ensuring that no bubbles are produced. The bubbles reduce the efficiency of electroporation. A single pulse of 1.8kV with pulse controller resistance set at 1000Ω resistance was given to the cells. The cuvette was then placed back onto ice for 10min. 5mL of TSA with tween (for *M. smegmatis*) and 7H9 with tween (for *M. bovis* BCG) was added to recover the cells. The cells were allowed to incubate at 37°C for 4h. They were then plated out onto TSA (for *M. smegmatis*) and 7H10 plates containing OADC (for *M. bovis* BCG) and selective antibiotic (kanamycin 25µg/mL) for each plasmid and strain and incubated at 37°C for 2-3 days for *M. smegmatis* and 7-10 days for *M. bovis* BCG till colonies appeared.

6.9.2.2 Tranformation of *echA12* overexpression plasmid into *M. smegmatis* and *M. bovis* BCG

5µL of plasmid DNA at approximately 0.2-1mg/mL (pVV16 empty vector, pVV16_*echA12*_Rv, pVV16_*echA12*_BCG and pVV16_G239_*echA12*) was added to 200 µL of electrocompetent cells (*M. smegmatis* mc^2155, *M. smegmatis* pSMT3_eGFP, *M. bovis* BCG, *M. bovis* BCG pSMT3_eGFP) and kept in ice for 10 min. An electroporation cuvette (0.2cm gap electrodes) was put on ice until cold and the cells were then transferred to the sterile cuvette ensuring that no bubbles are produced. The bubbles reduce the efficiency of electroporation. A single pulse of 1.8kV with pulse controller resistance set at 1000Ω resistance was given to the cells. The cuvette was then placed back onto ice for 10minutes. 5mL of TSB with tween (for *M. smegmatis*) and 7H9 with tween (for *M. bovis* BCG) was added to recover the cells. The cells were allowed to incubate at 37°C for 4h. They were then plated out onto TSA (for *M. smegmatis*) and 7H10 plates containing OADC (for *M. bovis* BCG) and selective antibiotic (kanamycin 25µg/mL) for each plasmid and strain and incubated at 37°C for 2-3 days for *M. smegmatis* and 7-10 days for *M. bovis* BCG till colonies appeared.

6.10 Genomic DNA extraction from *M. smegmatis* and *M. bovis* BCG

25mL of a mid-log cell culture of the specific mycobacterial species was centrifuged at 5000rpm for 10mins and the pellet was resuspended in 450µL GTE-RNAse buffer [200 µL RNase A + 20 mL GTE buffer (25mM Tris pH8, 10 mM EDTA pH8, 50 mM glucose)]. 10 µL

of lysozyme was added and the mixture was then incubated at 37°C overnight without shaking. To the overnight incubated mixture, 10 µL of 10% SDS and 20µL of Proteinase K (15mg/ml) was sequentially added. The mixture was then incubated at 55°C for 3h. After the incubation, 200 µL of 5M NaCl, 1mL of chloroform: isoamylalcohol (24:1) was added and centrifuged at 13,000rpm for 5-10mins. The aqueous layer was carefully transferred to a new eppendorf tube and an additional 1mL of chloroform: isoamyalcohol (24:1) was added. The mixture was then centrifuged again at 13,000rpm for 10mins. The aqueous layer was again carefully transferred to a new tube and 0.7 volumes of ice-cold isopropanol was added to the tube and gently mixed by inverting the tube. The tube and reagents were kept cold from this step onwards. The mixture was then centrifuge at 4°C, 13,000rpm for 30mins. The supernatant was decanted and the pellet was washed with 700 µL of 70% ice cold ethanol. The tube was centrifuged again at 4°C, 13,000rpm for 30mins-1h. The supernatant was carefully pipetted out and the DNA pellet was left to dry. After the pellet was completely dry, it was resuspended in 20µL of water. The DNA was quantified using a nanodrop.

6.11 Screening Assays against *M. bovis* BCG (pSMT3_eGFP) and *M. smegmatis* (pSMT3_eGFP)

6.11.1 Screening the Prestwick library against *M. bovis* BCG (pSMT3_eGFP) and *M. smegmatis* (pSMT3_eGFP)

The FDA screen was performed using GFP expressing strains of *M. smegmatis* and *M. bovis* BCG containing the pSMT3_eGFP plasmid (provided by Dr. Apoorva Bhatt, University of

Birmingham, UK). The pSMT3_eGFP plasmid used to get GFP fluorescent strains of *M. smegmatis* and *M. bovis* BCG has a shuttle vector pSMT3 for Mycobacterium with a hsp60 promoter (Hayward *et. al.*, 1999). The plasmid has been cloned with an enhanced GFP codon and an antibiotic marker for hyrgromycin. The expression of GFP is independent of hygromycin B induction and is constitutively expressed under the hsp60 promoter (Hayward *et. al.*, 1999). Assay plates were prepared to have a drug concentration of 0.05mM by dispensing 10µL of the drug in the assay plate from an intermediate plate containing the drugs at a concentration of 1mM.The first column as the negative control (only media, 7H9 and OADC with 10µL 30% DMSO) and the last column as a positive control (culture with 10µL 30% DMSO). 200µL of the culture ($O.D_{600}$ – 0.2) without any Hygromycin B was dispensed and the plates were then incubated statically at 37°C and read over a period of 48h.

6.11.2 Dose response study of the hits from the Prestwick library against *M. bovis* BCG (pSMT3_eGFP) and *M. smegmatis* (pSMT3_eGFP)

For the dose response study concentrations, a 3-fold dilution were performed using the highest drug concentration of 0.5mM in the stock plate; which presented concentrations as 0.167mM as the maximum concentration as 10µL of the drug was added to the assay plate and then moving on to ten 3-fold dilutions of the same from well 2 to 11 in 30% DMSO. The plate had the first column as the negative control (only media, 7H9 and OADC with 10µL 30% DMSO) and the last column as a positive control (culture with 10µL 30% DMSO). 190µL of cells ($O.D_{600}$- 0.2) were added to the plates containing the drugs without any hygromycin B in the media. The plates were incubated statically at 37°C and read over a period of 48h.

6.11.3 MIC determination on solid media against *M. bovis* BCG and *M. smegmatis*

Stocks of 10mM antibiotics were dispensed in 2-fold concentrations and mixed with 2mL of liquid agar into a partitioned petri dish. This was done for 5 wells each of every concentration. After the media had solidified, 10 µL of cells ($0.D_{600}$-0.2) were inoculated onto the agar containing the 5 different antibiotic concentrations and incubated for 2 days for *M. smegmatis* and 7-10 days for *M. bovis* BCG.

6.11.4 Statistical Validation of Assays

The statistical validation of the assay was carried using the Z` factor analysis. The Z` factor is the value depicting the total variation between the negative and positive control which generally defines the assay signal window. The formula for calculating the Z` factor is:

$$Z` = 1 - \left(\frac{3\sigma_{+c} + 3\sigma_{-c}}{| \mu_{-c} - \mu_{+c} |} \right)$$

Where, σ_{+c}, σ_{-c}, μ_{+c} and μ_{-c} are the standard deviation (σ) and the averages (µ), respectively of the negative (-*c*) controls. positive (+c) and negative (-c) controls.

The Z` factor describes the assay quality and reliability of the assay results. For an assay to be reliable and the data to be validated the Z' factor should at least be 0.5. An assay with a Z` factor ≥ 0.6 is considered very good while an assay quality is considered poor when the value is less than 0.5. The Z` factor value of 1 is considered as an ideal value.

6.12 Generation of Spontaneous resistant mutants

Mutants were generation based on solid MIC values (appendix). Drugs were mixed into 20mL of 7H10 or TSB agar for *M. bovis* BCG and *M. smegmatis*, respectively in concentrations of 2.5x, 5x and 10x the MIC values. Cells from a mid-log culture ($O.D_{600}$-0.6) were plated at a concentration of $1x10^8$ cells per plate and incubated at 37°C until colonies were observed. Once the colonies were observed they were inoculated in liquid media and cultured in the absence of drug. Once the cultures were grown the cells were streaked on the same plate (containing antibiotics) with the wild type strain and growth was compared. This was done in order to validate true mutants. After the mutants were validated the genomic DNA extraction was performed for each mutant strain and glycerol stocks were prepared. The genomic DNA was sent for genome sequencing and sequence analysis to MicrobesNG for detection of SNPs.

6.13 Protein Expression and Purification

6.13.1 Expression and Purification of the *Mtb*-PrsA protein from the transformed BL21 (pET-SUMO *prsA*) strain

A single colony of *E. coli* (BL21 cells transformed with plasmids) was inoculated in 5mL of LB broth with the appropriate antibiotic (kanamycin 50µg/mL) and incubated at 37°C, 180rpm overnight. 2mL of the overnight culture was then added to 1L of terrific broth (For each 1L of the broth – 900mL terrific broth + 100mL terrific salts). The inoculated culture was incubated

at 37°C, 180rpm for 4-5 h until the $O.D_{600}$ had reached ~0.5. 1mL of IPTG was added to every 1L of the culture and incubated at 16°C, 180rpm overnight.

The overnight-induced culture was pelleted down at 5000rpm for 25mins at 4°C. The pellets were resuspended in ~30-35mL of PBS and pelleted again at 4000rpm for 15mins at 4°C. The supernatant was discarded. The pellet was immediately used but can also be stored at -20°C for processing later.

The cell pellet was then resuspended in the lysis buffer (Purification buffer with 20mM imidazole + proteinase inhibitor). The cells were then lysed using a sonicator (soniprep 150) (30s on, 30s off; 10 cycles). The lysed cell suspension was centrifuged at 15,000rpm for 40mins at 4°C.

Column preparation: A 5mL HiTrap chelating HP column (GE Healthcare) was charged with 0.1M $NiCl_2$ until the flow through ran green. The excess $NiCl_2$ was washed using 50mLs of water. The column was then equilibrated with the lysis buffer to provide the same environment as the sample to be loaded onto it.

After centrifugation, the supernatant was loaded on to the column with a flow rate of 1mL/min. After the clarified lysate was run through the column was washed using the wash buffer (1x purification buffer + 50mM imidazole). An imidazole gradient was run through and 5mL fractions were collected for each gradient concentration. The gradient concentrations were run as 75mM, 100mM, 125mM, 150mM, 175mM, 200mM, 225mM, 275mM and 500mM of imidazole in the purification buffer.

The protein was added to a dialysis membrane (prepared by boiling and cooling it in 500mM EDTA and 300mL water). The fraction containing the band with the required protein was dialysed overnight in the dialysis buffer a. (2L) overnight at 4°C. The protein was transferred

to the dialysis buffer b. (1L) for 5-6 h the next day. The purified protein was then concentrated and quantified by A_{280} value and stored at 35-40% glycerol at -20°C.

6.13.1 Expression and Purification of EchA12 protein from the transformed strain on *M. smegmatis* containing the pVV16_*echA12*_Rv and pVV16_*echA12*_G239R

A single colony of the *M. smegmatis* mc^2155_pVV16_*echA12*_Rv and *M. smegmatis* mc^2155_pVV16_*echA12*_G239R was inoculated in 5mL of TSB broth with the appropriate antibiotic (kanamycin 25µg/mL) and incubated at 37°C, 180rpm overnight. 2mL of the overnight culture was then added to 1L of TSB broth with kanamycin 25µg/mL. The inoculated culture was incubated at 37°C, 180rpm overnight at 37°C.

The overnight culture was pelleted down at 5000rpm for 25mins at 4°C. The pellets were resuspended in ~30-35mL of PBS and pelleted again at 4000rpm for 15mins at 4°C. The supernatant was discarded. The pellet was immediately used but can also be stored at -20°C.

The cell pellet was then resuspended in the lysis buffer (Purification buffer with 20mM imidazole + proteinase inhibitor). The cells were then lysed using a French press at ~20,000MPa and repeated three times. The lysed cell suspension was centrifuged at 15,000rpm for 40mins at 4°C.

Column preparation: A 5mL HiTrap chelating HP column (GE Healthcare) was charged with 0.1M $NiCl_2$ until the flow through ran green. The excess $NiCl_2$ was washed using 50mLs of water. The column was then equilibrated with the lysis buffer to provide the same environment as the sample to be loaded onto it.

After centrifugation, the supernatant was loaded on to the column with a flow rate of 1mL/min. After the clarified lysate had run through, the column was washed using the wash buffer (1x

purification buffer 2 + 25mM imidazole). An imidazole gradient was run through and 5mL fractions were collected for each gradient concentration. The gradient concentrations were run as 50mM, 75mM, 100mM, 150mM, 200mM and 225mM of imidazole in the purification buffer.

The protein was added to a dialysis membrane (prepared by boiling and cooling it in 500mM EDTA and 300mL water). The fraction containing the band with the required protein was dialysed overnight in the dialysis buffer 3 (2L) overnight at 4°C. The protein was transferred to the dialysis buffer 4 (1L) for 5-6 h the next day.

6.13.3 SDS-PAGE and western blotting

The protein fractions were run onto a SDS PAGE, 10µL of each sample (prepared by boiling with the SDS loading buffer) was run at 200V, 25-30mA until the dye front reached the end of the gel. The gel was then stained using Instant blue for 10-20 mins and diluted with water to view.

The samples run on the SDS-PAGE gel were then transferred onto a nitrocellulose membrane using a western blot cassette.The western blot cassette was submerged in the western transfer buffer and run at 20V, 300mA for 1h. The membrane was then blocked using a 5% skimmed milk solution made in TBS-T followed by incubation at room temperature in 0.1% skimmed milk. The primary antibody (mouse anti-His, Qiagen) was added (1:1000) to the membrane and incubated at room temperature. The membrane was then washed with TBS-T followed by the addition of the secondary antibody (goat anti-mouse, Sigma Aldrich) at 1: 25,000. The

membrane was washed with TBS-T and then in TBS. The bands were developed colourimetrically using a BCIP (5-Bromo-4-chloro-3-indolyl phosphate) solution.

6.14 Enzyme Assay with *Mtb*-PrsA

The enzyme assay for *Mtb*-PrsA enzyme is based on a coupled reaction with other enzymes. The reaction proceeds with the conversion of ribose-5-phosphate utilizing ATP to produce Prpp with AMP. The AMP with another ATP is converted by a kinase enzyme to ADP, which is used to produce pyruvate molecules from phosphoenol pyruvate regenerating ATP molecules. The pyruvate is then converted to lactate utilizing the NADH molecule, which is detected via fluorescence. Therefore, the reduction of NADH fluorescence acts as an indication of *Mtb*-PrsA enzyme activity (figure 6.1).

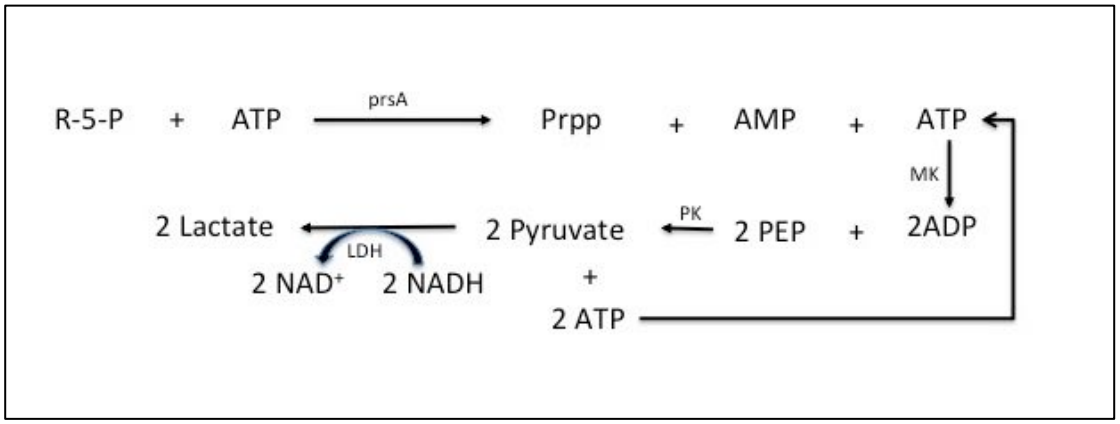

Figure 6.1: The *Mtb*-PrsA enzyme couple for the biochemical assay. The flowchart depicts the coupled reaction in the enzyme assay which is used to detect the activity of the *Mtb*-PrsA enzyme by the fluorescence of NADH. Phosphoenol pyruvate [PEP], Myokinase (MK), PyruvateKinase/LacatateDehydrogenase [PK/LDH], Ribose-5-phosphate [R-5-P]

6.14.1 Optimisation of the *Mtb*-PrsA enzyme assay

Components required for the assay were ATP (100mM), Phosphoenol pyruvate [PEP] (100mM), NADH (100mM), Ribose-5-phosphate [R-5-P] (100mM), Myokinase (MK), PyruvateKinase/LacatateDehydrogenase (PK/LDH), 4x Assay Buffer (150mM NaCl, 1mM KH_2PO_4, 1mM $MgCl_2$), DTT (1M), $MgCl_2$.

An enzyme mix was prepared with various concentrations of the purified enzyme to determine the lowest volume needed which showed activity. Injecting ribose-5-phosphate through a period of approximately 30mins induced the enzyme reaction. The activity was determined by detection of decrease in fluorescence by the NADH utilised during the reaction through a fluorescence spectrophotometer (PHERAstar FS, BMG LabTech).

6.14.1.1 Optimisation of enzyme activity

The enzyme assay was tested for activity, at an enzyme concentration of 0.1µg/µL which gave a consistent fluorescence for a period of at least ~30mins.

For testing effect of DMSO on enzyme activity

The decided enzyme volume was used with three conditions that were absence of DMSO (positive control), 30% DMSO and 100% DMSO and a negative control without the enzyme.

Table 6.9: *Mtb*-PrsA biochemical enzyme assay mix.

Components	Stock concentration	Final concentration	Volume
ATP	100mM	0.5mM	2 µL
PEP	100mM	4mM	2 µL
NADH	100mM	0.5mM	0.5 µL
R-5-P	100mM	4mM	4 µL

MK	1,500-3,000 U/mg		0.25 µL
PK/LDH	0.6-1U/µL (PK) 0.9-1.4U/µL (LDH)		0.25 µL
4x Buffer			25 µL
DTT	1000mM	10mM	1 µL
$MgCl_2$	1000mM	10mM	1 µL
DMSO 30%			5 µL
Water			60.5 µL
Mtb-PrsA		0.1 µg/ µL	2.5 µL

6.14.2 GSK177 compound screen against the *Mtb*-PrsA enzyme

A drug screen was performed against the purified enzyme to detect possible compound interaction. The drug screen was performed with a library of 177 drugs (GSK_177) which were identified as potent compounds with anti-tubercular activity by GSK (Mdluli *et. al.*, 2014; Ballell *et. al.*, 2013). 5µL of drugs (400µM) were added to the assay plate and 96µL of enzyme mixture was added to each well keeping the first column for negative control and last column for positive control. The final compound concentration on the assay plate would be 20µM. Injecting ribose-5-phosphate same as previously mentioned (6.14.1) induced the enzyme activity. The assay plate had a positive control and a negative control. The negative control had no enzyme present while positive control had enzyme without any compound. The screen was performed in duplicates.

The enzyme mix for the GSK 177 compound screen is mentioned in table 6.10.

Table 6.10: *Mtb*-PrsA biochemical enzyme assay mix for the GSK177 screen.

Components	Stock concentration	Final concentration	Volume
ATP	100mM	0.5mM	2 µL
PEP	100mM	4mM	2 µL
NADH	100mM	0.5mM	0.5 µL
R-5-P	100mM	4mM	4 µL
MK	1,500-3,000 U/mg		0.25 µL

PK/LDH	0.6-1U/µL (PK) 0.9-1.4U/µL (LDH)		0.25 µL
4x Buffer			25 µL
DTT	1000mM	10mM	1 µL
$MgCl_2$	1000mM	10mM	1 µL
Compound in DMSO 30%			5 µL
Compound	10mM	20 µM	5 µL
Mtb-PrsA		0.1 µg/ µL	2.5 µL
Water			60.5 µL

6.14.3 IC_{50} analysis of the compound GR135487X

The IC_{50} analysis of GR135487X was performed by serially diluting the drug 3-fold in 30% DMSO from a starting concentration of 20µM. 5µL of the serially diluted compounds were added to the assay plate with the assay mastermix (section 6.14.2). The compounds were incubated with the drugs before the addition of the *Mtb-prsA* enzyme. The assay was incubated for 30mins after the addition of the enzyme and was read as an end point assay through a fluorescence spectrophotometer (PHERAstar FS, BMG LabTech).

6.15 GSK177 overexpression screens

6.15.1 GSK177 overexpression screen with the *M. bovis* BCG pSMT3_eGFP

The hits that came off from the biochemical screen from the *Mtb*-PrsA biochemical screen were tested in whole cell overexpression strains. The percentage survival of the fluorescent overexpression strains was compared to the empty pMV261 containing fluorescent strains.

The pMV261 vector is a mycobacterial shuttle vector which constitutively expresses the integrated gene under a hsp60 promoter (Stover *et. al.*, 1991). Therefore, the cells added to the assay did not contain any kanamycin. The compounds were plated at a concentration of 20μM onto the assay plate with the cell volume at 200μL. The cells were incubated for 2 days at 37°C and read as an end point assay.

6.15.2 GSK177 overexpression screen using Cell Titer Glo

The hits that came off from the biochemical screen from the *Mtb*-PrsA biochemical screen were tested in whole cell overexpression strains. The percentage survival of the overexpression strains was compared to the empty pMV261 strain.

The compounds were plated in an appropriate 96-well plate for luminescence at a concentration of 20μM onto the assay plate with the cell (O.D- 0.2) volume at 100μL. The cells were incubated for 2 days at 37°C and read as an end point assay using the CellTiter-Glo® Luminescent Cell Viability Assay (Promega). The reagents were thawed to room temperature before use. The Cell Titer Glo substrate was solubilised using the 100mL of the Cell Titre Glo buffer. The substrate was mixed thoroughly by vortexing. The reagents were titrated to be used at $1/8^{th}$ the prescribed concentration. To the incubated cells 100μL of the reagent (diluted by 1/8) was added and incubated for 60mins at 37°C. The plates were then read in a spectrophotometer to record the luminescence.

6.16 Generation of the *echA12* gene knockout mutant

In order to generate a knockout mutant for the gene of interest, a 1kB flanking region both up and downstream of the gene were amplified. These amplified flanking fragments were then digested using Van91I and then ligated into a Van91I digested p0004S plasmid (a gift from T. Hsu and W. R. Jacobs Jr., Albert Einstein College of Medicine, New York). The correctly cloned plasmids were then digested using PacI and packaged into a temperature sensitive mycobacteriophage phAE159 to yield the knockout phage containing the phasmid DNA. *In vitro* packaging was done by adding 5µL of the ligation mixture to the MaxPlax packaging extract and then incubated the mix at RT for 1hour. The reaction was then stopped using 200 µL of MP buffer and incubating the mix at RT for 30min. After the incubation period 100 µL of prepared HB101 (*E.coli*) host cells were added to the mix and incubated at 30 ^{o}C for 1h. The cells were then centrifuged at 13000rpm for a minute and the pellet was then resuspended in 1mL of fresh LB media. The cells were then plated onto LB agar plates containing hygromycin (150 µg/mL) and incubated at 37 ^{o}C overnight. Colonies were selected the next day and cultured for plasmid isolation. Once the plasmids were isolated they were digested with PacI to select for the required phasmid DNA.

The phasmid DNA was then electroplated into electrocompetent *M. smegmatis* mc^{2}155 strain and recovered in 1mL of TSB at 30^{o}C for 4h. After the incubation period, two dilutions were setup: A. 300 µL of the transformed cells were mixed with 200 µL of freshly cultured *M. smegmatis* mc^{2}155 cells and B. 100 µL of the transformed cells were mixed with 200 µL of freshly cultured *M. smegmatis* mc^{2}155 cells. These dilutions were then added to 4mL of molten top agar in separate tubes, mixed gently and poured on top of pre-warmed 7H9 agar plates. The plates were incubated at 30 ^{o}C for 3 days until plaques are observed. The plaques were then

picked out using a sterile pipette tip and soaked into 200 µL of MP buffer and allowed to recover at room temperature for 1.5 h and then stored at 4 ^{o}C.

In order to calculate the phage titre, 4mL of top agar was mixed with 400 µL of actively growing *M. smegmatis* mc^{2}155 cells and overlayed on top of 7H9 basal agar. 10-fold dilutions of the phage from the afore mentioned soak was made using MP buffer (dilutions upto 10^{-6}). 10 µL of these dilutions were spotted onto the overlayed plate and incubated for 3 days at 30 ^{o}C until plaques were observed in the spot zones. The plaque zones were used to calculate the plaque forming units (PFU) per mL of the 'soak'.

The plates were then overlayed in triplicate containing 400 µL of actively growing *M. smegmatis* mc^{2}155 cells and the appropriate dilution of the soak and incubated at 30^{o}C for 3 days. Ideally the plates would yield a lacy pattern at the appropriate 1000 pfu/mL due to confluent lysis. The plates were then soaked with 3-4mL of MP buffer and incubated at RT for 3-4h. The MP buffer was then pipetted out and filtered using a 2-micron filter to get a sterile phage filtrate and stored at 4^{o}C.

In order to transduce mycobacterial strains; a 50mL culture was prepared to an O. D_{600} of 0.8-1. The cells were pelleted at 4000rpm for 15mins. The pellet was then resuspended in 5mL MP buffer and then further diluted by the addition of 45mL of MP buffer. The suspension was centrifuged again at 4000rpm for 15mins. The pellet was then resuspended in 5mL of MP buffer. 2mL of this cell suspension was mixed with 2mL of the high titre knockout phage lysate. A negative control was setup using 2mL of MP buffer instead of the phage. The mix was then incubated at 37 ^{o}C for 1h to allow infection. The tubes were then spun at 4000rpm for 15mins. The supernatant was decanted and the pellet was resuspended in 400 µL TSB + 0.05% Tween 80 and incubated at 37 ^{o}C for 3h. 50 µL of the suspension was spread on TSB agar plates

containing 100 µg/mL hygromycin. The entire suspension was distributed among 8 plates. All plates were incubated for 3 days at 37 ºC.

6.17 Confirmation of the *echA12* null mutant by southern blotting

A southern blot was performed in order to confirm the gene knockout in *M. smegmatis*. The genomic DNA was extracted from all the colonies observed and confirmed from the TSB plates containing hygromycin B (20µg/µL) (ThermoFisher). The genomic DNA for both possible knockouts and wild type was then digested using KpnI (NEB) overnight. On the following day, the digested genomic DNAs were run on an agarose gel with a 1kb DNA ladder (NEB). This gel was then used to blot the DNA onto a nylon membrane by a southern blot transfer setup using transfer buffer overnight. The DNA was transferred onto the nylon membrane using the capillary effect generated by the southern blot setup.

A DNA probe was prepared using the flanking region PCR products 4 µL each of the upstream and downstream products. To this mix, 8 µL of milliq water was added and boiled at 95 ºC for 10mins. The tubes were then snap frozen on dry ice. To this frozen mix, 4 µL of the DIG- High Prime (Roche) was added and mixed gently until thawed. This mixture was then incubated at 37 ºC overnight.

Once the DNA had been transferred onto the nylon membrane, it was crosslinked to the membrane by exposing the membrane to UV light for 5mins. 10mL of preheated DIG Easy Hyb buffer was added to a hybridisation bottle along with the membrane and incubated with gentle rotation at 42 ºC for 30mins. Meanwhile, a probe hybridisation mixture was prepared using 10mL of pre-heated DIG Easy Hyb buffer and 20 µL of the probe prepared earlier. This

mixture was added to the hybridisation bottle after the initial incubation period and was incubated overnight at 42 °C.

After the incubation period, the membrane was washed twice for 5mins each using 50mL of 2x SSC buffer containing 0.1% SDS at 68 °C with gentle agitation. The membrane was then washed twice using 0.5x SSC buffer containing 0.1% SDS at 68 °C for 15mins each.

The membrane was washed for 2mins in 10mL of washing buffer and then incubated with 100mL of blocking buffer for 30mins at 50 °C. After which the membrane was incubated with 20mL of antibody solution for 30min at 50 °C. Following this, two consecutive washes were performed for 15mins each using 100mL of washing buffer. The membrane was then equilibrated with 20mL of detection buffer for 5mins and bands were observed by incubating the membrane with 20mLs of CPID tablets dissolved in detetction buffer for 30mins. The membrane was then imaged using a BioRad gel doc XR+ imager.

6.18 Analysis of strains overexpressing *echA12* and the *echA12* null mutant

6.18.1 Analysis of the *echA12* overexpressing strains in the presence of florfenicol

The overexpression strains of *echA12* in *M. smegmatis* and *M. bovis* BCG containing plasmids pVV16_empty, pVV16_*echA12*_G239R, pVV16_*echA12*_BCG and 3. pVV16_*echA12*_Rv. The pVV16 vector is a mycobacterial shuttle vector which constitutively expresses the gene inserted (in this instance *echA12)* under the hsp60 promoter (O'Gaora, 1998). The cell culture therefore added to this assay did not contain any kanamycin. These vectors containing strains

were tested for overexpression to observe a shift in IC_{50} values against florfenicol. The assay plate contained a 3-fold dilution of florfenicol in 30% DMSO from a 10mM stock. 10µL of the drug was added to the assay plate with a positive and a negative control column containing 10µL of 30% DMSO. The positive control column had cells while the negative control column only contained media.190µL of the cells from each individual strain were added to the assay plate at an O.D of 0.1. The cells were incubated overnight for *M. smegmatis* and 4 days for *M. bovis* BCG at 37°C. To the incubated plates 0.01% (w/v) of sterile resazurin was added and further incubated at 37°C for 24h. The plates were then read as an end point viability assay at Exc530/Em590 nm.

6.18.3 Treatment of the overexpression strains with florfenicol for lipid analysis

The overexpression strains of *echA12* in *M. bovis* and *M. bovis* BCG were prepared grown in liquid culture in 10mL tubes in TSB broth for *M. smegmatis* and 7H9 for *M. bovis* BCG in the absence of kanamycin. The cultures were grown to a log phase to which florfenciol was added in concentrations of 0x, 0.5x, 1x, 2x, 5x the liquid MIC as observed from the liquid MIC testing earlier. In *M. bovis* BCG strains, florfenicol was added in concentrations of 0x,1x,2x,5x and 10x the MIC. The cultures were labelled with [^{14}C] by the addition of [^{14}C]-acetate to the culture before incubating the cultures overnight at 37°C, 180rpm.

6.18.4 Apolar Lipid extraction from overexpression strains of *echA12* and *echA12* null mutant

Lipid extractions were performed using cell cultures of the *echA12* overexpression strains in *M. smegmatis* and *M. bovis* BCG strains and *echA12* null mutant in *M. smegmatis*. The [^{14}C]-acetate radiolabelled cells (using C-14 acetate) were harvested by centrifuging the cultures in glass tubes with lids fitted with Teflon lined stoppers at 3000rpm for 10 minutes. To the dried pellet 2mL of Methanol:0.3% NaCl :: 10:1(v/v) was added, followed by 1mL petroleum ether (60-80°C). The tube was mixed on a rotary mixer for 15mins and then centrifuged at 3000rpm for 5mins. The upper layer from this tube was then transferred over to another tube labelled B using a glass Pasteur pipette. To the remaining lower layer in the initial tube A 1mL of petroleum ether was added and mixed for 15mins. The tube was then centrifuged again at 3000rom for 5mins. The upper layer was then transferred to tube B containing the upper layer from before. The contents of the tube were then dried by placing the tube on a heating block at 50°C under nitrogen. This tube contained the apolar lipids.

6.18.5 Polar lipid extraction from overexpression strains of *echA12* and *echA12* null mutant

To the tube A from 6.18.4, 2.3mL of chloroform: methanol:0.3%NaCl:9:10:3 (v/v/v) was added and mixed on a rotary mixer for 60mins. The tubes were then spun at 3000rpm for 5mins. The supernatant was then transferred to a fresh tube C. To the pellet in tube A, 750µL of chloroform: methanol:0.3%NaCl:5:10:4(v/v/v) was added and mixed for 30mins.The tube was centrifuged at 3000rpm for 5mins and then supernatant was transferred to tube C. The last step was repeated

one more time and the supernatant added to the tube C. To the pooled extract in tube C, 1.3mL of chloroform and 1.3mL of 0.3% NaCl was added. The tube was then mixed for 5mins and then spun at 3000rpm for 5mins. The lower layer of the biphase was transferred over to a fresh tube, labelled as tube D. The tube D containing the polar lipids extract was then dried at 50°C under nitrogen. The remaining cells here are delipidated cells containing non-extractable lipids and used for extraction of mycolates.

6.18.6 Extraction of mycolates from overexpression strains of *echA12* and *echA12* null mutant

To the delipidated pellet from section 6.18.5, 750µL of 0.5% methanolic KOH was added and incubated at 37°C for 3 days. The cells were then centrifuged at 3000rpm for 5mins and the supernatant discarded. The cells were then washed using 375µL methanol twice with the supernatant discarded each time. The mycolic esters were then extracted using 500µL of diethyl ether incubated at room temperature for 5mins. The ether phase was collected into a separate tube after centrifuging the tube at 3000rpm for 5mins. This step was repeated three times. The ether phase in the new tube now contained crude mycolates from the cells. The ether phase was dried and resuspended in 2:1::chloroform:methanol (v/v). The samples were then visualised through thin layer chromatography described in section 6.19.

6.19 Thin Layer Chromatography of lipid extracts

Analysis of samples was done by separating samples on a silica plate run in different solvent systems. Polar and apolar lipids were analysed through a 2-D TLC run in different solvent

systems as mentioned in table 6.11. Apolar lipids were analysed using system A, B, C and D while polar lipids were analysed using systems D and E.

For analysing radiolabelled lipid extracts 10,000-50,000cpm (measured using a liquid scintillation analyser, Tri-Carb 2700TR by mixing sample with scintillation fluid in a tube) were loaded onto a silica plate and run in the respective solvent systems. Once the TLCs were dried and the solvent had evaporated the TLCs were placed in a shielded cassette with an X-ray radiograph and left for 24-48h depending on the amount of counts loaded. After the exposure period the x-ray radiographs were developed. Samples that were not labelled with radioactive carbon acetate were stained with phosphomolybdic acid (PMA) and visualised under UV light.

Table 6.11: Solvent systems used to analyse lipid extract on 1-D and 2-D TLCs.

System	Direction	Solvent	Proportions	Number of runs
A	1	petroleum ether 60-80°C/ethyl acetate	98:2 (v/v)	3
A	2	petroleum ether 60-80°C/acetone	92:8 (v/v)	1
B	1	petroleum ether 60-80°C/acetone	92:8 (v/v)	3
B	2	toluene/acetone	95:5 (v/v)	1
C	1	chloroform/methanol	96:4 (v/v)	1
C	2	toluene/acetone	80:20 (v/v)	1
D	1	chloroform/methanol/water	14:0.8 (v/v/v)	1
D	2	chloroform/acetone/methanol/water	50:60:2.5:3 (v/v/v/v)	1
E	1	chloroform/methanol/water	60:30:6 (v/v/v)	1
E	2	chloroform/acetone/methanol/water	40:25:3:6 (v/v/v/v)	1
FAMEs and MAMEs	1	petroleum ether 60-80°C/acetone	95:5 (v/v)	1
FAMEs and MAMEs	1	Chloroform/methanol/ammonium hydroxide/water	65:25:0.5:3.6	1

6.20 Solvent extraction of the EchA12 protein

The solvent extraction of the EchA12 protein involved mixing 2mL of the purified protein (~1mg/mL) with 2mL of chloroform: methanol (2:1, v/v). The mixture was then centrifuged at 3000rpm for 10mins. The organic phase (lower phase) was removed and transferred to a separate tube. The tube containing the organic phase was dried in the presence of nitrogen at 50°C. The dried residue was then resuspended in 200µL of chloroform. This dissolved residue was then subjected to electrospray mass spectrometry in the positive mode on a Micromass LCT mass spectrometer.

6.21 Growth curve analysis of the *echA12* null mutant in *M. smegmatis*

A growth curve analysis was performed on *M. smegmatis* mc^2155 and the *echA12* null mutant in *M. smegmatis*. A single colony was inoculated into tubes containing 10mL of TSB media. The overnight cultures were then inoculated into fresh 100mL TSB flasks in triplicate to get a starting $O.D_{600}$ of 0.1 and incubated at 37°C, 180rpm. The $O.D_{600}$ was then measured using a spectrophotometer every hour for 30h.

6.22 Acid fast staining of the *echA12* null mutant in *M. smegmatis*

Acid fast staining was performed on *M. smegmatis* mc^2155 and the *echA12* null mutant in *M. smegmatis* . Smears were prepared and heat fixed on standard clear glass slides. The smear was flooded with TB Carbolfuchsin KF for 4mins without heating. The smear was then washed and

decolourised using the TB decolorizer for 3 to 5s. The smear was washed with water again and counterstained with TB Brilliant Green K for 30s. The smear was then washed and air dried. The slides were visualised at 40X magnification and then 100X magnification with oil immersion. Acid fast bacilli appear as red stained bacteria on a blue background.

6.23 Cell morphology analysis in the presence and absence of tween-80 of the *echA12* null mutant in *M. smegmatis*

Colony morphology was analysed for *M. smegmatis* mc^2155 and the *echA12* null mutant in *M. smegmatis.* TSB agar plates were prepared with 0.05% tween and without tween. An overnight liquid culture was prepared by inoculating a single colony in the TSB and incubating at 37°C, 180rpm. The culture was streaked onto plates containing 0.05% tween and ones without tween for each strain and incubated in a static incubator at 37°C. Once single colonies appeared they were photographed to depict the variation in morphology observed.

6.24 Liquid extraction surface mass spectrometry analysis (LESA) of the *echA12* null mutant in *M. smegmatis*

A LESA analysis was performed on colonies of *M. smegmatis* mc^2155 and the *echA12* null mutant in *M. smegmatis.* A single colony was inoculated into a 10mL TSB media containing tube and incubated overnight at 37°C, 180rpm. 1-5µL of the culture was plated onto TSB agar containing 30mm petri plates. Once the colonies appeared, the colonies were used to perform

surface extraction using various solvent combinations such as chloroform: methanol (2:1, v/v), ethanol: water and acetonitrile and analysed mass spectroscopically using a native LESA (University of Birmingham, UK) for solubilised lipid moieties.

References

Abassi, Y.A., Xi, B., Zhang, W., Ye, P., Kirstein, S.L., Gaylord, M.R., Feinstein, S.C., Wang, X. and Xu, X. (2009) Kinetic Cell-Based Morphological Screening: Prediction of Mechanism of Compound Action and Off-Target Effects. *Chemistry and Biology*, 16 (7): 712–723.

Abrahams, G.L., Kumar, A., Savvi, S., Hung, A.W., Wen, S., Abell, C., Barry, C.E., Sherman, D.R., Boshoff, H.I.M. and Mizrahi, V. (2012) Pathway-selective sensitisation of *Mycobacterium tuberculosis* for target-based whole-cell screening. *Chemistry and Biology*, 19 (7): 844–854.

Abrahams, K.A. and Besra, G.S. (2016) Mycobacterial cell wall biosynthesis: a multifaceted antibiotic target. *Parasitology*, 7: 1–18.

Acharya, P.V. and Goldman, D.S. (1970) Chemical composition of the cell wall of the H37Ra strain of *Mycobacterium tuberculosis*. *Journal of Bacteriology*, 102 (3): 733–739.

Ahmad, Z., Minkowski, A., Peloquin, C.A., Williams, K.N., Mdluli, K.E., Grosset, J.H. and Nuermberger, E.L. (2011) Activity of the fluoroquinolone DC-159a in the initial and continuation phases of treatment of murine tuberculosis. *Antimicrobial agents and chemotherapy*, 55 (4): 1781–1783.

Aínsa, J.A., Pérez, E., Pelicic, V., Berthet, F.X., Gicquel, B. and Martin, C. (1997) Aminoglycoside 2'-N-acetyltransferase genes are universally present in mycobacteria: characterisation of the aac(2“)-Ic gene from *Mycobacterium tuberculosis* and the aac(2”)-Id gene from *Mycobacterium smegmatis*. *Molecular microbiology*, 24 (2): 431–441.

Aktas, M., Danne, L., Möller, P. and Narberhaus, F. (2014) Membrane lipids in Agrobacterium tumefaciens: biosynthetic pathways and importance for pathogenesis. *Frontiers in plant science*, 5 (20130810): 109.

Al-Balas, Q., Anthony, N.G., Al-Jaidi, B., Alnimr, A., Abbott, G., Brown, A.K., Taylor, R.C., Besra, G.S., McHugh, T.D., Gillespie, S.H., Johnston, B.F., Mackay, S.P. and Coxon, G.D. (2009) Identification of 2-aminothiazole-4-carboxylate derivatives active against *Mycobacterium tuberculosis* H37Rv and the beta-ketoacyl-ACP synthase mtFabH. Todd, M.H. (ed.). *PLoS ONE*, 4 (5): e5617.

Albesa-Jové, D., Svetlíková, Z., Tersa, M., Sancho-Vaello, E., Carreras-González, A., Bonnet, P., Arrasate, P., Eguskiza, A., Angala, S.K., Cifuente, J.O., Kordulakova, J., Jackson, M., Mikušová, K. and Guerin, M.E. (2016) Structural basis for selective recognition of acyl chains by the membrane-associated acyltransferase PatA. *Nature Communications*, 7: 10906–12.

Alderwick, L.J., Lloyd, G.S., Lloyd, A.J., Lovering, A.L., Eggeling, L. and Besra, G.S. (2011) Biochemical characterisation of the *Mycobacterium tuberculosis* phosphoribosyl-1-pyrophosphate synthetase. *Glycobiology*, 21 (4): 410–425.

Alderwick, L.J., Radmacher, E., Seidel, M., Gande, R., Hitchen, P.G., Morris, H.R., Dell, A., Sahm, H., Eggeling, L. and Besra, G.S. (2005) Deletion of Cg-emb in corynebacterianeae leads

to a novel truncated cell wall arabinogalactan, whereas inactivation of Cg-ubiA results in an arabinan-deficient mutant with a cell wall galactan core. *Journal of Biological Chemistry*, 280 (37): 32362–32371.

Alderwick, L.J., Seidel, M., Sahm, H., Besra, G.S. and Eggeling, L. (2006) Identification of a novel arabinofuranosyltransferase (AftA) involved in cell wall arabinan biosynthesis in *Mycobacterium tuberculosis*. *Journal of Biological Chemistry*, 281 (23): 15653–15661.

Almeida, D., Converse, P.J., Ahmad, Z., Dooley, K.E., Nuermberger, E.L. and Grosset, J.H. (2011) Activities of Rifampin, Rifapentine and Clarithromycin Alone and in Combination against *Mycobacterium ulcerans* Disease in Mice. *PLoS Neglected Tropical Diseases*, 5 (1): e933–7.

Altaf, M., Miller, C.H., Bellows, D.S. and O'Toole, R. (2010) Evaluation of the *Mycobacterium smegmatis* and BCG models for the discovery of *Mycobacterium tuberculosis* inhibitors. *Tuberculosis (Edinburgh, Scotland)*, 90 (6): 333–337.

Amin, A.G., Goude, R., Shi, L., Zhang, J., Chatterjee, D. and Parish, T. (2008) EmbA is an essential arabinosyltransferase in *Mycobacterium tuberculosis*. *Microbiology*, 154 (Pt 1): 240–248.

Andersen, P.H. (1989) The dopamine inhibitor GBR 12909: selectivity and molecular mechanism of action. *European journal of pharmacology*, 166 (3): 493–504.

Andries, K., Verhasselt, P., Guillemont, J., Göhlmann, H.W.H., Neefs, J.-M., Winkler, H., Van Gestel, J., Timmerman, P., Zhu, M., Lee, E., Williams, P., de Chaffoy, D., Huitric, E., Hoffner, S., Cambau, E., Truffot-Pernot, C., Lounis, N. and Jarlier, V. (2005) A diarylquinoline drug active on the ATP synthase of *Mycobacterium tuberculosis*. *Science*, 307 (5707): 223–227.

Anthony T Podany, S.S. (2016) Current strategies to treat tuberculosis. *F1000Research*, 5: 2579.

Arias, C.A., Vallejo, M., Reyes, J., Panesso, D., Moreno, J., Castañeda, E., Villegas, M.V., Murray, B.E. and Quinn, J.P. (2008) Clinical and microbiological aspects of linezolid resistance mediated by the cfr gene encoding a 23S rRNA methyltransferase. *Journal of Clinical Microbiology*, 46 (3): 892–896.

Arjona, A. and Castañer, R. (2008) TMC-207. *Drugs of the Future*, 33 (12): 1018.

Arsic, B., Barber, J., Čikoš, A., Mladenovic, M., Stankovic, N. and Novak, P. (2017) 16-Membered Macrolide Antibiotics: a Review. *International journal of antimicrobial agents*.

Baell, J. and Walters, M.A. (2014) Chemical con artists foil drug discovery. *Nature*, 513(7519): 481-483.

Baell, J.B. and Holloway, G.A. (2010) New Substructure Filters for Removal of Pan Assay Interference Compounds (PAINS) from Screening Libraries and for Their Exclusion in Bioassays. *Journal of Medicinal Chemistry*, 53 (7): 2719–2740.

Ballell, L., Bates, R.H., Young, R.J., Alvarez-Gomez, D., Alvarez-Ruiz, E., Barroso, V., Blanco, D., Crespo, B., Escribano, J., González, R., Lozano, S., Huss, S., Santos-Villarejo, A., Martín-Plaza, J.J., Mendoza, A., Rebollo-López, M.J., Remuiñan-Blanco, M., Lavandera, J.L., Pérez-Herran, E., Gamo-Benito, F.J., García-Bustos, J.F., Barros, D., Castro, J.P. and Cammack, N. (2013) Fueling open-source drug discovery: 177 small-molecule leads against tuberculosis. *ChemMedChem*, 8 (2): 313–321.

Ballou, C.E., Vilkas, E. and Lederer, E. (1963) Structural studies on the myo-inositol phospholipids of *Mycobacterium tuberculosis* (var. bovis, strain BCG). *Journal of Biological Chemistry*, 238 (1): 69–76.

Bártfai, Z., Somoskovi, A., Ködmön, C., Szabó, N., Puskás, E., Kosztolányi, L., Faragó, E., Mester, J., Parsons, L.M. and Salfinger, M. (2001) Molecular characterisation of rifampin-resistant isolates of *Mycobacterium tuberculosis* from Hungary by DNA sequencing and the line probe assay. *Journal of Clinical Microbiology*, 39 (10): 3736–3739.

Basu, J. (2004) Mycobacteria within its intracellular niche: survival of the pathogen or its host? *Current science-bangalore*, 86 (1): 103-110.

Batt, S.M., Jabeen, T., Bhowruth, V., Quill, L., Lund, P.A., Eggeling, L., Alderwick, L.J., Fütterer, K. and Besra, G.S. (2012) Structural basis of inhibition of *Mycobacterium tuberculosis* DprE1 by benzothiazinone inhibitors. *Proceedings of the National Academy of Sciences of the United States of America*, 109 (28): 11354–11359.

Bearson, B.L., Allen, H.K., Brunelle, B.W., Lee, I.S., Casjens, S.R. and Stanton, T.B. (2014) The agricultural antibiotic carbadox induces phage-mediated gene transfer in *Salmonella*. *Frontiers in Microbiology*, 5: 52.

Beckman, D.L. and Kranz, R.G. (1991) A bacterial homolog to the mitochondrial enoyl-CoA hydratase. *Gene*, 107 (1): 171–172.

Belanova, M., Dianiskova, P., Brennan, P.J., Completo, G.C., Rose, N.L., Lowary, T.L. and Mikušová, K. (2008) Galactosyl transferases in mycobacterial cell wall synthesis. *Journal of Bacteriology*, 190 (3): 1141–1145.

Belisle, J.T., Vissa, V.D., Sievert, T., Takayama, K., Brennan, P.J. and Besra, G.S. (1997) Role of the Major Antigen of *Mycobacterium tuberculosis* in Cell Wall Biogenesis. *Science*, 276 (5317): 1420–1422.

Bernstein, J., Lott, W.A., Steinberg, B.A. and Yale, H.L. (1952) Chemotherapy of experimental tuberculosis. V. Isonicotinic acid hydrazide (nydrazid) and related compounds. *American review of tuberculosis*, 65 (4): 357–364.

Bhatt, A., Brown, A.K., Singh, A., Minnikin, D.E. and Besra, G.S. (2008) Loss of a mycobacterial gene encoding a reductase leads to an altered cell wall containing beta-oxo-mycolic acid analogs and accumulation of ketones. *Chemistry and Biology*, 15 (9): 930–939.

Bhatt, A., Fujiwara, N., Bhatt, K., Gurcha, S.S., Kremer, L., Chen, B., Chan, J., Porcelli, S.A., Kobayashi, K., Besra, G.S. and Jacobs, W.R., Jr (2007a) Deletion of kasB in *Mycobacterium tuberculosis* causes loss of acid-fastness and subclinical latent tuberculosis in immunocompetent mice. *Proceedings of the National Academy of Sciences of the United States of America*, 104 (12): 5157–5162.

Bhatt, A., Kremer, L., Dai, A.Z., Sacchettini, J.C. and Jacobs, W.R. (2005) Conditional Depletion of KasA, a Key Enzyme of Mycolic Acid Biosynthesis, Leads to Mycobacterial Cell Lysis. *Journal of Bacteriology*, 187 (22): 7596–7606.

Bhatt, A., Molle, V., Besra, G.S., Jacobs, W.R., Jr and Kremer, L. (2007b) The Mycobacterium tuberculosis FAS-II condensing enzymes: their role in mycolic acid biosynthesis, acid-fastness, pathogenesis and in future drug development. *Molecular microbiology*, 64 (6): 1442–1454.

Birch, H.L., Alderwick, L.J., Appelmelk, B.J., Maaskant, J., Bhatt, A., Singh, A., Nigou, J., Eggeling, L., Geurtsen, J. and Besra, G.S. (2010) A truncated lipoglycan from mycobacteria with altered immunological properties. *Proceedings of the National Academy of Sciences of the United States of America*, 107 (6): 2634–2639.

Birch, H.L., Alderwick, L.J., Bhatt, A., Rittmann, D., Krumbach, K., Singh, A., Bai, Y., Lowary, T.L., Eggeling, L. and Besra, G.S. (2008) Biosynthesis of mycobacterial arabinogalactan: identification of a novel alpha (1-->3) arabinofuranosyltransferase. *Molecular microbiology*, 69 (5): 1191–1206.

Blanchard, J.S. (1996) Molecular Mechanisms of Drug Resistance in *Mycobacterium tuberculosis*. *Annual Review of Biochemistry*, 65:215-39.

Bloch, K. (2006) "Control Mechanisms for Fatty Acid Synthesis in *Mycobacterium smegmatis*." *In Advances in Enzymology and Related Areas of Molecular Biology. Meister/Advances. vol. Hoboken, NJ, USA: John Wiley & Sons*, Inc. pp. 1–84.

Books, LLC General Books LLC (2010) *Veterinary Drugs. Books LLC*, Wiki Series.

Boostanfar, R., Jain, J.K., Mishell, D.R. and Paulson, R.J. (2001) A prospective randomised trial comparing clomiphene citrate with tamoxifen citrate for ovulation induction. *Fertility and sterility*, 75 (5): 1024–1026.

Boshoff, H.I.M., Myers, T.G., Copp, B.R., McNeil, M.R., Wilson, M.A. and Barry, C.E. (2004) The transcriptional responses of Mycobacterium tuberculosis to inhibitors of metabolism: novel insights into drug mechanisms of action. *Journal of Biological Chemistry*, 279 (38): 40174–40184.

Braibant, M., Gilot, P. and Content, J. (2000) The ATP binding cassette (ABC) transport systems of *Mycobacterium tuberculosis*. *FEMS Microbiology Reviews*, 24 (4): 449–467.

Breda, A., Martinelli, L.K.B., Bizarro, C.V., Rosado, L.A., Borges, C.B., Santos, D.S. and Basso, L.A. (2012) Wild-type phosphoribosylpyrophosphate synthase (PRS) from *Mycobacterium tuberculosis*: a bacterial class II PRS? Tyagi, A.K. (ed.). *PLoS ONE*, 7 (6): e39245.

Brennan, P.J. (2003) Structure, function, and biogenesis of the cell wall of *Mycobacterium tuberculosis*. *Tuberculosis*, 83 (1-3): 91–97.

Brennan, P.J. and Besra, G.S. (1997) Structure, function and biogenesis of the mycobacterial cell wall. *Biochemical Society Transactions*, 25 (1): 188–194.

Brennan, P.J. and Nikaido, H. (1995) The envelope of mycobacteria. *Annual review of biochemistry*, 64 (1): 29–63.

Cambau, E. and Drancourt, M. (2014) Steps towards the discovery of *Mycobacterium tuberculosis* by Robert Koch, 1882. *Clinical Microbiology and Infection*, 20 (3): 196–201.

Cantaloube, S., Veyron-Churlet, R., Haddache, N., Daffé, M. and Zerbib, D. (2011) The *Mycobacterium tuberculosis* FAS-II Dehydratases and Methyltransferases Define the Specificity of the Mycolic Acid Elongation Complexes Cardona, P.-J. (ed.). *PLoS ONE*, 6 (12):

Carbadox (2014). *Antibacterials* pp. 216.

Cavanagh, R., Begon, M., Bennett, M., Ergon, T., Graham, I.M., De Haas, P.E.W., Hart, C.A., Koedam, M., Kremer, K., Lambin, X., Roholl, P. and Soolingen Dv, D.V. (2002) *Mycobacterium microti* infection (vole tuberculosis) in wild rodent populations. *Journal of Clinical Microbiology*, 40 (9): 3281–3285.

Cave, A.J.E. and Demonstrator, A. (1939) The evidence for the incidence of tuberculosis in ancient Egypt. *British Journal of Tuberculosis*, 33 (3): 142–152.

Chafetz, L., Greenough, R.C. and Frank, J. (1986) Thermal decomposition of thonzonium bromide. *Pharmaceutical research*, 3 (5): 298–301.

Chahine, E.B., Karaoui, L.R. and Mansour, H. (2013) Bedaquiline. *Annals of Pharmacotherapy*, 48 (1): 107–115.

Chambers, H.F., Moreau, D., Yajko, D., Miick, C., Wagner, C., Hackbarth, C., Kocagoz, S., Rosenberg, E., Hadley, W.K. and Nikaido, H. (1995) Can penicillins and other beta-lactam antibiotics be used to treat tuberculosis? *Antimicrobial agents and chemotherapy*, 39 (12): 2620–2624.

Chambers, H.F., Turner, J., Schecter, G.F., Kawamura, M. and Hopewell, P.C. (2005) Imipenem for treatment of tuberculosis in mice and humans. *Antimicrobial agents and chemotherapy*, 49 (7): 2816–2821.

Chan, C.-Y., Prudom, C., Raines, S.M., Charkhzarrin, S., Melman, S.D., De Haro, L.P., Allen, C., Lee, S.A., Sklar, L.A. and Parra, K.J. (2012) Inhibitors of V-ATPase proton transport reveal

uncoupling functions of tether linking cytosolic and membrane domains of V0 subunit a (Vph1p). *The Journal of biological chemistry*, 287 (13): 10236–10250.

Chang, Y.H., Labgold, M.R. and Richards, J.H. (1990) Altering enzymatic activity: recruitment of carboxypeptidase activity into an RTEM beta-lactamase/penicillin-binding protein 5 chimera. *Proceedings of the National Academy of Sciences*, 87 (7): 2823–2827.

Chatterjee, D. (1997) The mycobacterial cell wall: structure, biosynthesis and sites of drug action. *Current opinion in chemical biology*, 1 (4): 579–588.

Cho, S.H., Warit, S., Wan, B., Hwang, C.H., Pauli, G.F. and Franzblau, S.G. (2007) Low-oxygen-recovery assay for high-throughput screening of compounds against nonreplicating Mycobacterium tuberculosis. *Antimicrobial agents and chemotherapy*, 51 (4): 1380–1385.

Christen, M.O. (1990) Action of pinaverium bromide, a calcium-antagonist, on gastrointestinal motility disorders. *General pharmacology*, 21 (6): 821–825.

Christophe, T., Jackson, M., Jeon, H.K., Fenistein, D., Contreras-Dominguez, M., Kim, J., Genovesio, A., Carralot, J.-P., Ewann, F., Kim, E.H., Lee, S.Y., Kang, S., Seo, M.J., Park, E.J., Škovierová, H., Pham, H., Riccardi, G., Nam, J.Y., Marsollier, L., Kempf, M., Joly-Guillou, M.-L., Oh, T., Shin, W.K., No, Z., Nehrbass, U., Brosch, R., Cole, S.T. and Brodin, P. (2009) High Content Screening Identifies Decaprenyl-Phosphoribose 2′ Epimerase as a Target for Intracellular Antimycobacterial Inhibitors Bishai, W. (ed.). *PLoS Pathogens*, 5 (10): e1000645.

Clark-Curtiss, J.E. and Haydel, S.E. (2003) Molecular Genetics of *Mycobacterium tuberculosis Pathogenesis*. 57 (1): 517–549.

Cole, S.T. (1994) *Mycobacterium tuberculosis*: drug-resistance mechanisms. *Trends in microbiology*, 2 (10): 411–415.

Cole, S.T. (2016) Inhibiting *Mycobacterium tuberculosis* within and without. *Philosophical Transactions of the Royal Society: Biological Sciences*, 371 (1707): 20150506–8.

Cole, S.T. and Riccardi, G. (2011) New tuberculosis drugs on the horizon. *Current opinion in microbiology*, 14 (5): 570–576.

Collins, L. and Franzblau, S.G. (1997) Microplate alamar blue assay versus BACTEC 460 system for high-throughput screening of compounds against *Mycobacterium tuberculosis* and *Mycobacterium avium*. *Antimicrobial agents and chemotherapy*, 41 (5): 1004–1009.

Cooksey, R.C., Crawford, J.T., Jacobs, W.R., Jr and Shinnick, T.M. (1993) A rapid method for screening antimicrobial agents for activities against a strain of *Mycobacterium tuberculosis* expressing firefly luciferase. *Antimicrobial agents and chemotherapy*, 37 (6): 1348–1352.

Cooper, C.B. (2013) Development of *Mycobacterium tuberculosis* Whole Cell Screening Hits as Potential Antituberculosis Agents. *Journal of Medicinal Chemistry*, 56 (20): 7755–7760.

Cousins, D.V. (2003) Tuberculosis in seals caused by a novel member of the *Mycobacterium tuberculosis* complex: *Mycobacterium pinnipedii* sp. nov. *International journal of systematic and evolutionary microbiology*, 53 (5): 1305–1314.

Cox, J.A.G., Abrahams, K.A., Alemparte, C., Ghidelli-Disse, S., Rullas, J., Angulo-Barturen, I., Singh, A., Gurcha, S.S., Nataraj, V., Bethell, S., Remuiñán, M.J., Encinas, L., Jervis, P.J., Cammack, N.C., Bhatt, A., Kruse, U., Bantscheff, M., Fütterer, K., Barros, D., Ballell, L., Drewes, G. and Besra, G.S. (2016) THPP target assignment reveals EchA6 as an essential fatty acid shuttle in mycobacteria. *Nature microbiology*, 1 (2): 15006–15010.

Cox, J.A.G., Mugumbate, G., Del Peral, L.V.-G., Jankute, M., Abrahams, K.A., Jervis, P., Jackenkroll, S., Perez, A., Alemparte, C., Esquivias, J., Lelièvre, J., Ramon, F., Barros, D., Ballell, L. and Besra, G.S. (2016) Novel inhibitors of *Mycobacterium tuberculosis* GuaB2 identified by a target based high-throughput phenotypic screen. *Scientific Reports*, 6 (1): 420.

Crellin, P.K., Brammananth, R. and Coppel, R.L. (2011) Decaprenylphosphoryl-β-D-Ribose 2′-Epimerase, the Target of Benzothiazinones and Dinitrobenzamides, Is an Essential Enzyme in *Mycobacterium smegmatis*. *PLoS ONE*, 6 (2): e16869.

Crellin, P.K., Kovacevic, S., Martin, K.L., Brammananth, R., Morita, Y.S., Billman-Jacobe, H., McConville, M.J. and Coppel, R.L. (2008) Mutations in pimE restore lipoarabinomannan synthesis and growth in a *Mycobacterium smegmatis* lpqW mutant. *Journal of Bacteriology*, 190 (10): 3690–3699.

CROFTON, J. and Mitchison, D.A. (1948) Streptomycin resistance in pulmonary tuberculosis. *British medical journal*, 2 (4588): 1009–1015.

Daffé, M. and Lanéelle, M.-A. (2001) "Analysis of the Capsule of *Mycobacterium tuberculosis*." *In Mycobacterium tuberculosis Protocols. vol. New Jersey: Humana Press. pp*. 217–227.

Daffe, M., Brennan, P.J. and McNeil, M. (1990) Predominant structural features of the cell wall arabinogalactan of *Mycobacterium tuberculosis* as revealed through characterisation of oligoglycosyl alditol fragments by gas chromatography/mass spectrometry and by 1H and 13C NMR analyses. *Journal of Biological Chemistry*, 265 (12): 6734–6743.

de Mendonça, J.D., Ely, F., Palma, M.S., Frazzon, J., Basso, L.A. and Santos, D.S. (2007) Functional characterisation by genetic complementation of aroB-encoded dehydroquinate synthase from *Mycobacterium tuberculosis* H37Rv and its heterologous expression and purification. *Journal of Bacteriology*, 189 (17): 6246–6252.

Deoxyribonucleic acid relatedness among selected strains of *Mycobacterium tuberculosis*, *Mycobacterium bovis*, *Mycobacterium bovis* BCG, *Mycobacterium microti*, and *Mycobacterium africanum* (1986). *Clinical Microbiology Newsletter*, 8 (2): 14.

Diacon, A.H., van der Merwe, L., Barnard, M., Groote-Bidlingmaier, von, F., Lange, C., García-Basteiro, A.L., Sevene, E., Ballell, L. and Barros-Aguirre, D. (2016) β-Lactams against

Tuberculosis — New Trick for an Old Dog? *New England Journal of Medicine*, 375 (4): 393–394.

Dogra, M., Palmer, B.D., Bashiri, G., Tingle, M.D., Shinde, S.S., Anderson, R.F., O'Toole, R., Baker, E.N., Denny, W.A. and Helsby, N.A. (2010) Comparative bioactivation of the novel anti-tuberculosis agent PA-824 in Mycobacteria and a subcellular fraction of human liver. *British Journal of Pharmacology*, 162 (1): 226–236.

Domenech, P., Rog, A., Moolji, J. U. D., Radomski, N., Fallow, A., Leon-Solis, L., Bowes, J., Behr, M.A. and Reed, M.B. (2014) Origins of a 350-kilobase genomic duplication in Mycobacterium tuberculosis and its impact on virulence. *Infection and immunity*, 82 (7): 2902–2912.

Donini, S., Garavaglia, S., Ferraris, D.M., Miggiano, R., Mori, S., Shibayama, K. and Rizzi, M. (2017) Biochemical and structural investigations on phosphoribosylpyrophosphate synthetase from *Mycobacterium smegmatis*. Permyakov, E.A. (ed.). *PLoS ONE*, 12 (4): e0175815.

Dorey, L., Hobson, S. and Lees, P. (2016) Activity of florfenicol for Actinobacillus pleuropneumoniae and Pasteurella multocida using standardised versus non-standardised methodology. *Veterinary journal (London, England: 1997)*, 218: 65–70.

Dorlo, T.P.C. and Kager, P.A. (2008) Pentamidine dosage: a base/salt confusion. Utzinger, J. (ed.). *PLoS Neglected Tropical Diseases*, 2 (5): e225.

Draper, P., Khoo, K.-H., Chatterjee, D., Dell, A. and Morris, R.H. (1997) Galactosamine in walls of slow-growing mycobacteria. *Biochemical Journal*, 327 (2): 519–525.

Dubée, V., Triboulet, S., Mainardi, J.-L., Ethève-Quelquejeu, M., Gutmann, L., Marie, A., Dubost, L., Hugonnet, J. E. and Arthur, M. (2012) Inactivation of *Mycobacterium tuberculosis* l,d-transpeptidase $LdtMt_1$ by carbapenems and cephalosporins. *Antimicrobial agents and chemotherapy*, 56 (8): 4189–4195.

Dubnau, E. (2002) *Mycobacterium tuberculosis* Genes Induced during Infection of Human Macrophages. *Infection and immunity*, 70 (6): 2787–2795.

Dubnau, E., Chan, J., Raynaud, C., Mohan, V.P., Lanéelle, M.-A., Yu, K., Quémard, A., Smith, I. and Daffé, M. (2002) Oxygenated mycolic acids are necessary for virulence of Mycobacterium tuberculosis in mice. *Molecular microbiology*, 36 (3): 630–637.

Ekins, S., Casey, A.C., Roberts, D., Parish, T. and Bunin, B.A. (2014) Bayesian models for screening and TB Mobile for target inference with *Mycobacterium tuberculosis*. *Tuberculosis*, 94 (2): 162–169.

Engohang-Ndong, J. (2012) Antimycobacterial drugs currently in Phase II clinical trials and preclinical phase for tuberculosis treatment. *Expert Opinion on Investigational Drugs*, 21 (12): 1789–1800.

Escuyer, V.E., Lety, M.A., Torrelles, J.B., Khoo, K.H., Tang, J.B., Rithner, C.D., Frehel, C., McNeil, M.R., Brennan, P.J. and Chatterjee, D. (2001) The role of the embA and embB gene products in the biosynthesis of the terminal hexaarabinofuranosyl motif of *Mycobacterium smegmatis* arabinogalactan. *Journal of Biological Chemistry*, 276 (52): 48854–48862.

Esposito, M., Szadocka, S., Degiacomi, G., Orena, B.S., Mori, G., Piano, V., Boldrin, F., Zemanová, J., Huszár, S., Barros, D., Ekins, S., Lelièvre, J., Manganelli, R., Mattevi, A., Pasca, M.R., Riccardi, G., Ballell, L., Mikušová, K. and Chiarelli, L.R. (2017) A Phenotypic Based Target Screening Approach Delivers New Antitubercular CTP Synthetase Inhibitors. *ACS Infectious Diseases*, 3 (6): 428–437.

Evangelopoulos, D., da Fonseca, J.D. and Waddell, S.J. (2015) Understanding anti-tuberculosis drug efficacy: rethinking bacterial populations and how we model them. *International journal of infectious diseases : IJID : official publication of the International Society for Infectious Diseases*, 32: 76–80.

Farnia, P., Mohammad, R.M., Merza, M.A., Tabarsi, P., Zhavnerko, G.K., Ibrahim, T.A., Kuan, H.O., Ghanavei, J., Farnia, P., Ranjbar, R., Poleschuyk, N.N., Titov, L.P., Owlia, P., Kazampour, M., Setareh, M., sheikolslami, M., Migliori, G.B. and Velayati, A.A. (2010) Growth and cell-division in extensive (XDR) and extremely drug resistant (XXDR) tuberculosis strains: transmission and atomic force observation. *International Journal of Clinical and Experimental Medicine*, 3 (4): 308–314.

Feng, Z. and Barletta, R.G. (2003) Roles of *Mycobacterium smegmatis* D-alanine:D-alanine ligase and D-alanine racemase in the mechanisms of action of and resistance to the peptidoglycan inhibitor D-cycloserine. *Antimicrobial agents and chemotherapy*, 47 (1): 283–291.

Fenner, L., Egger, M., Bodmer, T., Altpeter, E., Zwahlen, M., Jaton, K., Pfyffer, G.E., Borrell, S., Dubuis, O., Bruderer, T., Siegrist, H.H., Furrer, H., Calmy, A., Fehr, J., Stalder, J.M., Ninet, B., Böttger, E.C., Gagneux, S.Swiss HIV Cohort Study and the Swiss Molecular Epidemiology of Tuberculosis Study Group (2012) Effect of mutation and genetic background on drug resistance in *Mycobacterium tuberculosis*. *Antimicrobial agents and chemotherapy*, 56 (6): 3047–3053.

Fleischman, J.K., MD and Greenberg, H.E., MD (1998) Tuberculosis. *Medical Update for Psychiatrists*, 3 (1): 16–21.

Flores, A.R. (2005) Genetic analysis of the β-lactamases of *Mycobacterium tuberculosis* and *Mycobacterium smegmatis* and susceptibility to β-lactam antibiotics. *Microbiology*, 151 (2): 521–532.

Flynn, J.L. and Chan, J. (2001) Tuberculosis: latency and reactivation. *Infection and immunity*, 69 (7): 4195–4201.

Freiberg, C. and Brötz-Oesterhelt, H. (2005) Functional genomics in antibacterial drug discovery. *Drug Discovery Today*, 10 (13): 927–935.

Fritzler, J.M. and Zhu, G. (2012) Novel anti-Cryptosporidium activity of known drugs identified by high-throughput screening against parasite fatty acyl-CoA binding protein (ACBP). *The Journal of antimicrobial chemotherapy*, 67 (3): 609–617.

Fujita, Y., Shimakata, T. and Kusaka, T. (1980) Purification of Two Forms of Enoyl-CoA Hydratase from *Mycobacterium smegmatis*. *Journal of biochemistry*, 88 (4): 1045–1050.

Gande, R., Gibson, K.J.C., Brown, A.K., Krumbach, K., Dover, L.G., Sahm, H., Shioyama, S., Oikawa, T., Besra, G.S. and Eggeling, L. (2004) Acyl-CoA carboxylases (accD2 and accD3), together with a unique polyketide synthase (Cg-pks), are key to mycolic acid biosynthesis in Corynebacterianeae such as *Corynebacterium glutamicum* and *Mycobacterium tuberculosis*. *Journal of Biological Chemistry*, 279 (43): 44847–44857.

Gangwar, S.P., Meena, S.R. and Saxena, A.K. (2014) Comparison of four different crystal forms of the *Mycobacterium tuberculosis* ESX-1 secreted protein regulator EspR. Acta crystallographica. *Structural biology communications*, 70:433–437.

Garbe, T., Servos, S., Hawkins, A., Dimitriadis, G., Young, D., Dougan, G. and Charles, I. (1991) The *Mycobacterium tuberculosis* shikimate pathway genes: evolutionary relationship between biosynthetic and catabolic 3-dehydroquinases. *Molecular & general genetics*, 228 (3): 385–392.

Ghuysen, J.M. (1991) Serine Beta-Lactamases and Penicillin-Binding Proteins. *Annual Review of Microbiology*, 45 (1): 37–67.

Gillespie, S.H. (2016) The role of moxifloxacin in tuberculosis therapy. *European respiratory review: an official journal of the European Respiratory Society*, 25 (139): 19–28.

Glickman, M.S. and Jacobs, W.R. (2001) Microbial pathogenesis of *Mycobacterium tuberculosis*: dawn of a discipline. *Cell*, 104 (4): 477–485.

Glickman, M.S., Cahill, S.M. and Jacobs, W.R. (2001) The *Mycobacterium tuberculosis* cmaA2 gene encodes a mycolic acid trans-cyclopropane synthetase. *Journal of Biological Chemistry*, 276 (3): 2228–2233.

Glickman, M.S., Cox, J.S. and Jacobs, W.R., Jr (2000) A Novel Mycolic Acid Cyclopropane Synthetase Is Required for Cording, Persistence, and Virulence of *Mycobacterium tuberculosis*. *Molecular Cell*, 5 (4): 717–727.

Gold, B., Smith, R., Nguyen, Q., Roberts, J., Ling, Y., Lopez Quezada, L., Somersan, S., Warrier, T., Little, D., Pingle, M., Zhang, D., Ballinger, E., Zimmerman, M., Dartois, V., Hanson, P., Mitscher, L.A., Porubsky, P., Rogers, S., Schoenen, F.J., Nathan, C. and Aubé, J. (2016) Novel Cephalosporins Selectively Active on Nonreplicating *Mycobacterium tuberculosis*. *Journal of Medicinal Chemistry*, 59 (13): 6027–6044.

Goldman, R.C. (2013) Why are membrane targets discovered by phenotypic screens and genome sequencing in *Mycobacterium tuberculosis*? *Tuberculosis*, 93 (6): 569–588.

Goyal, K., Qamra, R. and Mande, S.C. (2006) Multiple gene duplication and rapid evolution in the groEL gene: functional implications. *Journal of molecular evolution*, 63 (6): 781–787.

Grant, S.S., Kawate, T., Nag, P.P., Silvis, M.R., Gordon, K., Stanley, S.A., Kazyanskaya, E., Nietupski, R., Golas, A., Fitzgerald, M., Cho, S., Franzblau, S.G. and Hung, D.T. (2013) Identification of Novel Inhibitors of Nonreplicating *Mycobacterium tuberculosis* Using a Carbon Starvation Model. *ACS Chemical Biology*, 8 (10): 2224–2234.

Griffith, R.S. (1981) Introduction to vancomycin. *Reviews of infectious diseases*, 3 suppl: S200–4.

Grundy, D., Blackshaw, L.A. and Hillsley, K. (1994) Role of 5-hydroxytryptamine in gastrointestinal chemosensitivity. *Digestive diseases and sciences*, 39 (12 Suppl): 44S–47S.

Grzegorzewicz, A.E., de Sousa-d'Auria, C., McNeil, M.R., Huc-Claustre, E., Jones, V., Petit, C., Angala, S.K., Zemanová, J., Wang, Q., Belardinelli, J.M., Gao, Q., Ishizaki, Y., Mikušová, K., Brennan, P.J., Ronning, D.R., Chami, M., Houssin, C. and Jackson, M. (2016) Assembling of the *Mycobacterium tuberculosis* Cell Wall Core. *The Journal of biological chemistry*, 291 (36): 18867–18879.

Gupta, A., Kaul, A., Tsolaki, A.G., Kishore, U. and Bhakta, S. (2012) *Mycobacterium tuberculosis*: immune evasion, latency and reactivation. *Immunobiology*, 217 (3): 363–374.

Gupta, R., Kim, J.Y., Espinal, M.A., Caudron, J.M., Pecoul, B., Farmer, P.E. and Raviglione, M.C. (2001) Public health. Responding to market failures in tuberculosis control. *Science*, 293 (5532): 1049–1051.

Haites, R.E., Morita, Y.S., McConville, M.J. and Billman-Jacobe, H. (2005) Function of phosphatidylinositol in mycobacteria. *Journal of Biological Chemistry*, 280 (12): 10981–10987.

Hamed, R.B., Batchelar, E.T., Clifton, I.J. and Schofield, C.J. (2008) Mechanisms and structures of crotonase superfamily enzymes – How nature controls enolate and oxyanion reactivity. *Cellular and Molecular Life Sciences*, 65 (16): 2507–2527.

Harrison, J., Lloyd, G., Joe, M., Lowary, T.L., Reynolds, E., Walters-Morgan, H., Bhatt, A., Lovering, A., Besra, G.S. and Alderwick, L.J. (2016) Lcp1 is a phosphotransferase responsible for ligating arabinogalactan to peptidoglycan in *Mycobacterium tuberculosis*. *mBio*, 7 (4).

Hayman, J. (1984) *Mycobacterium ulcerans*: an infection from Jurassic time? *Lancet*, 2 (8410): 1015–1016.

Hayward C. M., O'Gaora P., Young D. B., Griffin G. E., Thole J., Hirst T. R., Castello-Branco L. R., Lewis D. J. (1999) Construction and murine immunogenicity of recombinant Bacille Calmette Guerin vaccines expressing the B subunit of *Escherichia coli* heat labile enterotoxin. *Vaccine*, 17, 1272–1281

Hazbón, M.H., Brimacombe, M., Bobadilla del Valle, M., Cavatore, M., Guerrero, M.I., Varma-Basil, M., Billman-Jacobe, H., Lavender, C., Fyfe, J., García-García, L., León, C.I., Bose, M., Chaves, F., Murray, M., Eisenach, K.D., Sifuentes-Osornio, J., Cave, M.D., Ponce de León, A. and Alland, D. (2006) Population genetics study of isoniazid resistance mutations and evolution of multidrug-resistant *Mycobacterium tuberculosis*. *Antimicrobial agents and chemotherapy*, 50 (8): 2640–2649.

He, S., Zhou, Z., Liu, Y., Cao, Y., Meng, K., Shi, P., Yao, B. and Ringø, E. (2010) Effects of the antibiotic growth promoters flavomycin and florfenicol on the autochthonous intestinal microbiota of hybrid tilapia (Oreochromis niloticus ♀ × O. aureus ♂). *Archives of microbiology*, 192 (12): 985–994.

Hett, E.C., Chao, M.C. and Rubin, E.J. (2010) Interaction and Modulation of Two Antagonistic Cell Wall Enzymes of Mycobacteria. *PLoS Pathogens*, 6 (7): e1001020.

Hu, Y.-Q., Zhang, S., Zhao, F., Gao, C., Feng, L.-S., Lv, Z.-S., Xu, Z. and Wu, X. (2017) Isoniazid derivatives and their anti-tubercular activity. *European Journal of Medicinal Chemistry*, 133: 255–267.

Huard, R.C., Fabre, M., de Haas, P., Lazzarini, L.C.O., van Soolingen, D., Cousins, D. and Ho, J.L. (2006) Novel genetic polymorphisms that further delineate the phylogeny of the *Mycobacterium tuberculosis* complex. *Journal of Bacteriology*, 188 (12): 4271–4287.

Humanes, L., García-Fernández, J.M., Roldán, J.M. and Diez, J. (1999) Cloning of an ORF with homology to Mycobacterium echA1, encoding the enoyl-CoA hydratase, in *Rhodococcus fascians*. *DNA sequence: the journal of DNA sequencing and mapping*, 10 (4-5): 309–315.

Hunter, S.W. and Brennan, P.J. (1990) Evidence for the presence of a phosphatidylinositol anchor on the lipoarabinomannan and lipomannan of *Mycobacterium tuberculosis*. *Journal of Biological Chemistry*, 265 (16): 9272–9279.

Hwang, H.-H., Moon, P.-G., Lee, J.-E., Kim, J.-G., Lee, W., Ryu, S.-H. and Baek, M.-C. (2011) Identification of the target proteins of rosiglitazone in 3T3-L1 adipocytes through proteomic analysis of cytosolic and secreted proteins. *Molecules and cells*, 31 (3): 239–246.

Jackson, C.J., Lamb, D.C., Kelly, D.E. and Kelly, S.L. (2000) Bactericidal and inhibitory effects of azole antifungal compounds on *Mycobacterium smegmatis*. *FEMS Microbiology Letters*, 192 (2): 159–162.

Jackson, M., Crick, D.C. and Brennan, P.J. (2000) Phosphatidylinositol Is an Essential Phospholipid of Mycobacteria. *Journal of Biological Chemistry*, 275 (39): 30092–30099.

Jadaun, A., Sudhakar D, R., Subbarao, N. and Dixit, A. (2015) Correction: In Silico Screening for Novel Inhibitors of DNA Polymerase III Alpha Subunit of *Mycobacterium tuberculosis* (*Mtb*DnaE2, H37Rv). *PLoS ONE*, 10 (5): e0128613.

James, B.W., Williams, A. and Marsh, P.D. (2000) The physiology and pathogenicity of *Mycobacterium tuberculosis* grown under controlled conditions in a defined medium. *Journal of Applied Microbiology*, 88 (4): 669–677.

Jankute, M., Cox, J.A.G., Harrison, J. and Besra, G.S. (2015) Assembly of the Mycobacterial Cell Wall. *Annual Review of Microbiology*, 69 (1): 405–423.

Jankute, M., Grover, S., Birch, H.L. and Besra, G.S. (2014) Genetics of mycobacterial arabinogalactan and lipoarabinomannan assembly. *Microbiology Spectrum*, 2 (4).

Jarlier, V. and Nikaido, H. (1994) Mycobacterial cell wall: structure and role in natural resistance to antibiotics. *FEMS Microbiology Letters*, 123 (1-2): 11–18.

Jawed Ahsan, M., Yousuf Ansari, M., Yasmin, S., Singh Jadav, S., Kumar, P., Kumar Garg, S., Aseri, A. and Khalilullah, H. (2015) Tuberculosis: Current Treatment, Diagnostics, and Newer Antitubercular Agents in Clinical Trials. *Infectious Disorders- Drug Targets*, 15(1): 32-41.

Ji, B., Chauffour, A., Andries, K. and Jarlier, V. (2006) Bactericidal activities of R207910 and other newer antimicrobial agents against *Mycobacterium leprae* in mice. *Antimicrobial agents and chemotherapy*, 50 (4): 1558–1560.

Jiang, T., He, L., Zhan, Y., Zang, S., Ma, Y., Zhao, X., Zhang, C. and Xin, Y. (2011) The effect of MSMEG_6402 gene disruption on the cell wall structure of *Mycobacterium smegmatis*. *Microbial Pathogenesis*, 51 (3): 156–160.

Jin, Y., Xin, Y., Zhang, W. and Ma, Y. (2010) *Mycobacterium tuberculosis* Rv1302 and Mycobacterium smegmatis MSMEG___4947 have WecA function and MSMEG__4947 is required for the growth of *M. smegmatis*. *FEMS Microbiology Letters*, 310 (1): 54–61.

Jureen, P., Werngren, J., Toro, J.-C. and Hoffner, S. (2008) Pyrazinamide resistance and pncA gene mutations in *Mycobacterium tuberculosis*. *Antimicrobial agents and chemotherapy*, 52 (5): 1852–1854.

Kafri, R., Levy, M. and Pilpel, Y. (2006) The regulatory utilisation of genetic redundancy through responsive backup circuits. *Proceedings of the National Academy of Sciences*, 103 (31): 11653–11658.

Kana, B.D., Karakousis, P.C., Parish, T. and Dick, T. (2014) Future target-based drug discovery for tuberculosis? *Tuberculosis (Edinburgh, Scotland)*, 94 (6): 551–556.

Kaur, D., Guerin, M.E., Škovierová, H., Brennan, P.J. and Jackson, M. (2009) Chapter 2: Biogenesis of the cell wall and other glycoconjugates of *Mycobacterium tuberculosis*. *Advances in applied microbiology*, 69: 23–78.

Keating, L.A., Wheeler, P.R., Mansoor, H., Inwald, J.K., Dale, J., Hewinson, R.G. and Gordon, S.V. (2005) The pyruvate requirement of some members of the *Mycobacterium tuberculosis* complex is due to an inactive pyruvate kinase: implications for *in vivo* growth. *Molecular microbiology*, 56 (1): 163–174.

Khovidhunkit, W. and Shoback, D.M. (1999) Clinical effects of raloxifene hydrochloride in women. *Annals of internal medicine*, 130 (5): 431–439.

Kinsella, R.J., Fitzpatrick, D.A., Creevey, C.J. and McInerney, J.O. (2003) Fatty acid biosynthesis in *Mycobacterium tuberculosis*: lateral gene transfer, adaptive evolution, and gene duplication. *Proceedings of the National Academy of Sciences*, 100 (18): 10320–10325.

Knechel, N.A. (2009) Tuberculosis: pathophysiology, clinical features, and diagnosis. *Critical care nurse*, 29 (2): 34–43.

Koch, R. (1982) The Etiology of Tuberculosis. *Clinical Infectious Diseases*, 4 (6): 1270–1274.

Koeck, J.L., Fabre, M., Simon, F., Daffe, M., Garnotel, É., Matan, A.B., Gérôme, P., Bernatas, J.J., Buisson, Y. and Pourcel, C. (2011) Clinical characteristics of the smooth tubercle bacilli '*Mycobacterium canettii*' infection suggest the existence of an environmental reservoir. *Clinical Microbiology and Infection*, 17 (7): 1013–1019.

Kolattukudy, P.E., Fernandes, N.D., Azad, A.K., Fitzmaurice, A.M. and Sirakova, T.D. (1997) Biochemistry and molecular genetics of cell-wall lipid biosynthesis in mycobacteria. *Molecular microbiology*, 24 (2): 263–270.

Kolattukudy, P.E., Fernandes, N.D., Azad, A.K., Fitzmaurice, A.M. and Sirakova, T.D. (1997) Biochemistry and molecular genetics of cell-wall lipid biosynthesis in mycobacteria. *Molecular microbiology*, 24 (2): 263–270.

Konno, K., Feldmann, F.M. and McDermott, W. (1967) Pyrazinamide susceptibility and amidase activity of tubercle bacilli. *The American review of respiratory disease*, 95 (3): 461–469.

Kordulakova, J., Gilleron, M., Mikušová, K., Puzo, G., Brennan, P.J., Gicquel, B. and Jackson, M. (2002) Definition of the First Mannosylation Step in Phosphatidylinositol Mannoside Synthesis PimA is essential for growth of mycobacteria. *Journal of Biological Chemistry*, 277 (35): 31335–31344.

Kordulakova, J., Gilleron, M., Puzo, G., Brennan, P.J., Gicquel, B., Mikušová, K. and Jackson, M. (2003) Identification of the required acyltransferase step in the biosynthesis of the phosphatidylinositol mannosides of mycobacterium species. *Journal of Biological Chemistry*, 278 (38): 36285–36295.

Koul, A., Arnoult, E., Lounis, N., Guillemont, J. and Andries, K. (2011) The challenge of new drug discovery for tuberculosis. *Nature*, 469 (7331): 483–490.

Koul, A., Dendouga, N., Vergauwen, K., Molenberghs, B., Vranckx, L., Willebrords, R., Ristic, Z., Lill, H., Dorange, I., Guillemont, J., Bald, D. and Andries, K. (2007) Diarylquinolines target subunit c of mycobacterial ATP synthase. *Nature Chemical Biology*, 3 (6): 323–324.

Kremer, L., Dover, L.G., Morbidoni, H.R., Vilcheze, C., Maughan, W.N., Baulard, A., Tu, S.-C., Honoré, N., Deretic, V., Sacchettini, J.C., Locht, C., Jacobs, W.R. and Besra, G.S. (2003) Inhibition of InhA activity, but not KasA activity, induces formation of a KasA-containing complex in mycobacteria. *Journal of Biological Chemistry*, 278 (23): 20547–20554.

Kremer, L., Dover, L.G., Morehouse, C., Hitchin, P., Everett, M., Morris, H.R., Dell, A., Brennan, P.J., McNeil, M.R., Flaherty, C., Duncan, K. and Besra, G.S. (2001) Galactan Biosynthesis in *Mycobacterium tuberculosis* identification of a bifunctional udp-galactofuranosyltransferase. *Journal of Biological Chemistry*, 276 (28): 26430–26440.

Kumar, A., Casey, A., Odingo, J., Kesicki, E.A., Abrahams, G., Vieth, M., Masquelin, T., Mizrahi, V., Hipskind, P.A., Sherman, D.R. and Parish, T. (2013) A high-throughput screen against pantothenate synthetase (PanC) identifies 3-biphenyl-4-cyanopyrrole-2-carboxylic acids as a new class of inhibitor with activity against *Mycobacterium tuberculosis*. *PLoS ONE*, 8 (11): e72786.

Kumar, A., Zhang, M., Zhu, L., Liao, R.P., Mutai, C., Hafsat, S., Sherman, D.R. and Wang, M.W. (2012) High-throughput Screening and Sensitized Bacteria Identify an *M. tuberculosis* Dihydrofolate Reductase Inhibitor with Whole Cell Activity Roe, A.J. (ed.). *PLoS ONE*, 7 (6): e39961.

Kurosu, M., Mahapatra, S., Narayanasamy, P. and Crick, D.C. (2007) Chemoenzymatic synthesis of Park's nucleotide: toward the development of high-throughput screening for MraY inhibitors. *Tetrahedron Letters*, 48 (5): 799–803.

Labesse, G., Daffé, M., Quémard, A., Emorine, L., Charpentier, X., Marrakchi, H., Montrozier, H., Margeat, E. and Ducasse, S. (2002) MabA (FabG1), a *Mycobacterium tuberculosis* protein involved in the long-chain fatty acid elongation system FAS-II. *Microbiology*, 148 (4): 951–960.

Lalloo, U.G. and Ambaram, A. (2010) New antituberculous drugs in development. *Current HIV/AIDS reports*, 7 (3): 143–151.

Lapage, G. (1947) Tuberculosis of Voles and Shrews. *Nature*, 160 (4072): 687–687.

Lea-Smith, D.J., Martin, K.L., Pyke, J.S., Tull, D., McConville, M.J., Coppel, R.L. and Crellin, P.K. (2008) Analysis of a new mannosyltransferase required for the synthesis of phosphatidylinositol mannosides and lipoarbinomannan reveals two lipomannan pools in corynebacterineae. *Journal of Biological Chemistry*, 283 (11): 6773–6782.

Lechartier, B., Hartkoorn, R.C. and Cole, S.T. (2012) In vitro combination studies of benzothiazinone lead compound BTZ043 against *Mycobacterium tuberculosis*. *Antimicrobial agents and chemotherapy*, 56 (11): 5790–5793.

Lechartier, B., Rybniker, J., Zumla, A. and Cole, S.T. (2014) Tuberculosis drug discovery in the post-post-genomic era. *EMBO molecular medicine*, 6 (2): 158–168.

Lee, M.-Y., Hung, W.-P. and Tsai, S.-H. (2017) Improvement of shikimic acid production in Escherichia coli with growth phase-dependent regulation in the biosynthetic pathway from glycerol. *World journal of microbiology & biotechnology*, 33 (2): 25.

Lee, M., Lee, J., Carroll, M.W., Choi, H., Min, S., Song, T., Via, L.E., Goldfeder, L.C., Kang, E., Jin, B., Park, H., Kwak, H., Kim, H., Jeon, H.-S., Jeong, I., Joh, J.S., Chen, R.Y., Olivier, K.N., Shaw, P.A., Follmann, D., Song, S.D., Lee, J.-K., Lee, D., Kim, C.T., Dartois, V., Park, S.-K., Cho, S.-N. and Barry, C.E. (2012) Linezolid for treatment of chronic extensively drug-resistant tuberculosis. *The New England journal of medicine*, 367 (16): 1508–1518.

Lee, O.Y.-C., Wu, H.H.T., Besra, G.S., Rothschild, B.M., Spigelman, M., Hershkovitz, I., Bar-Gal, G.K., Donoghue, H.D. and Minnikin, D.E. (2015) Lipid biomarkers provide evolutionary signposts for the oldest known cases of tuberculosis. *Tuberculosis (Edinburgh, Scotland)*,95 Suppl 1: S127–32.

Lewis, K. (2013) Platforms for antibiotic discovery. *Nature Publishing Group*, 12 (5): 371–387.

Li, X.-Z., Zhang, L. and Nikaido, H. (2004) Efflux pump-mediated intrinsic drug resistance in *Mycobacterium smegmatis*. *Antimicrobial agents and chemotherapy*, 48 (7): 2415–2423.

Lin, Y., Zhu, N., Han, Y., Jiang, J. and Si, S. (2014) Identification of anti-tuberculosis agents that target the cell-division protein FtsZ. *The Journal of antibiotics*, 67 (9): 671–676.

Lipinski, C.A. (2004) Lead- and drug-like compounds: the rule-of-five revolution. *Drug Discovery Today: Technologies*, 1 (4): 337–341.

Lounis, N., Veziris, N., Chauffour, A., Truffot-Pernot, C., Andries, K. and Jarlier, V. (2006) Combinations of R207910 with Drugs Used To Treat Multidrug-Resistant Tuberculosis Have the Potential To Shorten Treatment Duration. *Antimicrobial agents and chemotherapy*, 50 (11): 3543–3547.

Lucarelli, A.P., Buroni, S., Pasca, M.R., Rizzi, M., Cavagnino, A., Valentini, G., Riccardi, G. and Chiarelli, L.R. (2010) *Mycobacterium tuberculosis* phosphoribosylpyrophosphate synthetase: biochemical features of a crucial enzyme for mycobacterial cell wall biosynthesis. *PLoS ONE*, 5 (11): e15494.

Luna-Herrera, J., Reddy, V.M., Daneluzzi, D. and Gangadharam, P.R. (1995) Antituberculosis activity of clarithromycin. *Antimicrobial agents and chemotherapy*, 39 (12): 2692–2695.

Ma, Z., Lienhardt, C., McIlleron, H., Nunn, A.J. and Wang, X. (2010) Global tuberculosis drug development pipeline: the need and the reality. *Lancet*, 375 (9731): 2100–2109.

Magdalena, J., Supply, P. and Locht, C. (1998) Specific differentiation between *Mycobacterium bovis* BCG and virulent strains of the *Mycobacterium tuberculosis* complex. *Journal of Clinical Microbiology*, 36 (9): 2471–2476.

Mah, F.S., O'Brien, T., Kim, T. and Torkildsen, G. (2008) Evaluation of the effects of olopatadine ophthalmic solution, 0.2% on the ocular surface of patients with allergic conjunctivitis and dry eye. *Current medical research and opinion*, 24 (2): 441–447.

Mahairas, G.G., Sabo, P.J., Hickey, M.J., Singh, D.C. and Stover, C.K. (1996) Molecular analysis of genetic differences between *Mycobacterium bovis* BCG and virulent *M. bovis*. *Journal of Bacteriology*, 178 (5): 1274–1282.

Mahapatra, S., Crick, D.C. and Brennan, P.J. (2000) Comparison of the UDP-N-acetylmuramate:L-alanine ligase enzymes from *Mycobacterium tuberculosis* and *Mycobacterium leprae*. *Journal of Bacteriology*, 182 (23): 6827–6830.

Maiga, M., Agarwal, N., Ammerman, N.C., Gupta, R., Guo, H., Maiga, M.C., Lun, S. and Bishai, W.R. (2012) Successful shortening of tuberculosis treatment using adjuvant host-directed therapy with FDA-approved phosphodiesterase inhibitors in the mouse model. *PLoS ONE*, 7 (2): e30749.

Maitra, A., Bates, S., Kolvekar, T., Devarajan, P.V., Guzman, J.D. and Bhakta, S. (2015) Repurposing—a ray of hope in tackling extensively drug resistance in tuberculosis. *International Journal of Infectious Diseases*, 32: 50–55.

Mak, P.A., Rao, S.P.S., Tan, M.P., Lin, X., Chyba, J., Tay, J., Ng, S.H., Tan, B.H., Cherian, J., Duraiswamy, J., Bifani, P., Lim, V., Lee, B.H., Ma, N.L., Beer, D., Thayalan, P., Kuhen, K., Chatterjee, A., Supek, F., Glynne, R., Zheng, J., Boshoff, H.I., Clifton E Barry, 3., Dick, T., Pethe, K. and Camacho, L.R. (2012) A High-Throughput Screen To Identify Inhibitors of ATP Homeostasis in Non-replicating *Mycobacterium tuberculosis*. *ACS Chemical Biology*, 7 (7): 1190–1197.

Makarov, V., Manina, G., Mikušová, K., Möllmann, U., Ryabova, O., Saint-Joanis, B., Dhar, N., Pasca, M.R., Buroni, S., Lucarelli, A.P., Milano, A., De Rossi, E., Belanova, M., Bobovska, A., Dianiskova, P., Kordulakova, J., Sala, C., Fullam, E., Schneider, P., McKinney, J.D., Brodin, P., Christophe, T., Waddell, S., Butcher, P., Albrethsen, J., Rosenkrands, I., Brosch, R., Nandi, V., Bharath, S., Gaonkar, S., Shandil, R.K., Balasubramanian, V., Balganesh, T., Tyagi, S., Grosset, J., Riccardi, G. and Cole, S.T. (2009) Benzothiazinones kill Mycobacterium tuberculosis by blocking arabinan synthesis. *Science*, 324 (5928): 801–804.

Makarov, V., Neres, J., Hartkoorn, R.C., Ryabova, O.B., Kazakova, E., Šarkan, M., Huszár, S., Piton, J., Kolly, G.S., Vocat, A., Conroy, T.M., Mikušová, K. and Cole, S.T. (2015) The 8-Pyrrole-Benzothiazinones Are Noncovalent Inhibitors of DprE1 from *Mycobacterium tuberculosis*. *Antimicrobial agents and chemotherapy*, 59 (8): 4446–4452.

Maloney, E., Madiraju, S.C., Rajagopalan, M. and Madiraju, M. (2011) Localisation of acidic phospholipid cardiolipin and DnaA in mycobacteria. *Tuberculosis*, 91: S150–S155.

Manjunatha, U., Boshoff, H.I. and Barry, C.E. (2009) The mechanism of action of PA-824: Novel insights from transcriptional profiling. *Communicative & integrative biology*, 2 (3): 215–218.

Manjunatha, U., Boshoff, H.I. and Barry, C.E. (2009) The mechanism of action of PA-824: Novel insights from transcriptional profiling. *Communicative & integrative biology*, 2 (3): 215–218.

Marrakchi, H., Lanéelle, G. and Quemard, A. (2000) InhA, a target of the antituberculous drug isoniazid, is involved in a mycobacterial fatty acid elongation system, FAS-II. *Microbiology*, 146 (Pt 2) (2): 289–296.

Martínez-Jiménez, F., Papadatos, G., Yang, L., Wallace, I.M., Kumar, V., Pieper, U., Sali, A., Brown, J.R., Overington, J.P. and Marti-Renom, M.A. (2013) Target prediction for an open access set of compounds active against *Mycobacterium tuberculosis*. MacKerell, A.D. (ed.). *PLoS computational biology*, 9 (10): e1003253.

Matsumoto, M., Hashizume, H., Tomishige, T., Kawasaki, M., Tsubouchi, H., Sasaki, H., Shimokawa, Y. and Komatsu, M. (2006) OPC-67683, a nitro-dihydro-imidazooxazole derivative with promising action against tuberculosis in vitro and in mice. Hopewell, P. (ed.). *PLoS Medicine*, 3 (11): e466.

Matthew B Soellner, Katherine A Rawls, Christoph Grundner, Tom Alber, A. Jonathan A Ellman (2007) Fragment-Based Substrate Activity Screening Method for the Identification of Potent Inhibitors of the *Mycobacterium tuberculosis* Phosphatase PtpB. *American Chemical Society,* 129(31): 9613-15.

Mawuenyega, K.G., Forst, C.V., Dobos, K.M., Belisle, J.T., Chen, J., Bradbury, E.M., Bradbury, A.R.M. and Chen, X. (2005) Mycobacterium tuberculosis functional network analysis by global subcellular protein profiling. *Molecular biology of the cell*, 16 (1): 396–404.

McCaleb, M.L., Maloff, B.L., Nowak, S.M. and Lockwood, D.H. (1984) Sulfonylurea effects on target tissues for insulin. *Diabetes care*, 7(1): 42–46.

McClure, W.R. and Cech, C.L. (1978) On the mechanism of rifampicin inhibition of RNA synthesis. *Journal of Biological Chemistry*, 253 (24): 8949–8956.

McDonnell, G. and Russell, A.D. (1999) Antiseptics and disinfectants: activity, action, and resistance. *Clinical Microbiology Reviews*, 12 (1): 147–179.

McNeil, M., Daffe, M. and Brennan, P.J. (1990) Evidence for the nature of the link between the arabinogalactan and peptidoglycan of mycobacterial cell walls. *Journal of Biological Chemistry*, 265 (30): 18200–18206.

McNeil, M., Daffe, M. and Brennan, P.J. (1991) Location of the mycolyl ester substituents in the cell walls of mycobacteria. *Journal of Biological Chemistry*, 266 (20): 13217–13223.

McNeil, M., Wallner, S.J., Hunter, S.W. and Brennan, P.J. (1987) Demonstration that the galactosyl and arabinosyl residues in the cell-wall arabinogalactan of *Mycobacterium leprae* and *Mycobacterium tuberculosis* are furanoid. *Carbohydrate Research*, 166 (2): 299–308.

Mdluli, K., Kaneko, T. and Upton, A. (2014) Tuberculosis drug discovery and emerging targets. *Annals of the New York Academy of Sciences*, 1323 (1): 56–75.

Meeske, A.J., Sham, L.-T., Kimsey, H., Koo, B.-M., Gross, C.A., Bernhardt, T.G. and Rudner, D.Z. (2015) MurJ and a novel lipid II flippase are required for cell wall biogenesis in *Bacillus subtilis*. *Proceedings of the National Academy of Sciences of the United States of America*, 112 (20): 6437–6442.

Mehta, M., Rajmani, R.S. and Singh, A. (2016) *Mycobacterium tuberculosis* WhiB3 Responds to Vacuolar pH-induced Changes in Mycothiol Redox Potential to Modulate Phagosomal Maturation and Virulence. *The Journal of biological chemistry*, 291 (6): 2888–2903.

Meniche, X., de Sousa-d'Auria, C., Van-der-Rest, B., Bhamidi, S., Huc, E., Huang, H., De Paepe, D., Tropis, M., McNeil, M., Daffé, M. and Houssin, C. (2008) Partial redundancy in the synthesis of the d-arabinose incorporated in the cell wall arabinan of Corynebacterineae. *Microbiology (Reading, England)*, 154 (8): 2315–2326.

Middlebrook, G. and cohn, M.L. (1953) Some observations on the pathogenicity of isoniazid-resistant variants of tubercle bacilli. *Science*, 118 (3063): 297–299.

Mikušová, K. and Ekins, S. (2017) Learning from the past for TB drug discovery in the future. Drug Discovery Today, 22 (3): 534–545.

Mikušová, K., Mikus, M., Besra, G.S., Hancock, I. and Brennan, P.J. (1996) Biosynthesis of the Linkage Region of the Mycobacterial Cell Wall. *Journal of Biological Chemistry*, 271 (13): 7820–7828.

Mikusova, K., Slayden, R.A., Besra, G.S. and Brennan, P.J. (1995) Biogenesis of the mycobacterial cell wall and the site of action of ethambutol. *Antimicrobial agents and chemotherapy*, 39 (11): 2484–2489.

Mills, J.A., Motichka, K., Jucker, M., Wu, H.P., Uhlik, B.C., Stern, R.J., Scherman, M.S., Vissa, V.D., Pan, F., Kundu, M., Ma, Y.F. and McNeil, M. (2004) Inactivation of the mycobacterial rhamnosyltransferase, which is needed for the formation of the arabinogalactan-peptidoglycan linker, leads to irreversible loss of viability. *Journal of Biological Chemistry*, 279 (42): 43540–43546.

Minnikin, D.E. (1982) Complex lipids: their chemistry, biosynthesis and roles. *The biology of mycobacteria*, pp. 94–184.

Mishra, A.K., Driessen, N.N., Appelmelk, B.J. and Besra, G.S. (2011) Lipoarabinomannan and related glycoconjugates: Structure, biogenesis and role in *Mycobacterium tuberculosis* physiology and host-pathogen interaction. *FEMS Microbiology Reviews*, 35 (6): 1126–1157.

Mishra, A.K., Klein, C., Gurcha, S.S., Alderwick, L.J., Babu, P., Hitchen, P.G., Morris, H.R., Dell, A., Besra, G.S. and Eggeling, L. (2008) Structural characterisation and functional properties of a novel lipomannan variant isolated from a *Corynebacterium glutamicum* pimB′ mutant. *Antonie van Leeuwenhoek*, 94 (2): 277–287.

Mitchison, D.A. (1979) Basic Mechanisms of Chemotherapy. *Chest*, 76 (6): 771–780.

Mitchison, D.A. (1985) The action of antituberculosis drugs in short-course chemotherapy. *Tubercle*, 66 (3): 219–225.

Morayya, S., Awasthy, D., Yadav, R., Ambady, A. and Sharma, U. (2015) Revisiting the essentiality of glutamate racemase in *Mycobacterium tuberculosis*. *Gene*, 555 (2): 269–276.

Moreland, R.B., Goldstein, I. and Traish, A. (1998) Sildenafil, a novel inhibitor of phosphodiesterase type 5 in human corpus cavernosum smooth muscle cells. *Life sciences*, 62 (20): PL 309–18.

Morita, Y.S., Velasquez, R., Taig, E., Waller, R.F., Patterson, J.H., Tull, D., Williams, S.J., Billman-Jacobe, H. and McConville, M.J. (2005) Compartmentalisation of lipid biosynthesis in mycobacteria. *Journal of Biological Chemistry*, 280 (22): 21645–21652.

MORSE, D., BROTHWELL, D.R. and UCKO, P.J. (1964) Tuberculosis in ancient Egypt. *The American review of respiratory disease*, 90: 524–541.

Motiwala, A.S., Dai, Y., Jones-López, E.C., Hwang, S.-H., Lee, J.S., Cho, S.-N., Via, L.E., Barry, C.E. and Alland, D. (2010) Mutations in extensively drug-resistant *Mycobacterium tuberculosis* that do not code for known drug-resistance mechanisms. *The Journal of infectious diseases*, 201 (6): 881–888.

Mulabagal, V. and Calderón, A.I. (2010) Development of an Ultrafiltration-Liquid Chromatography/Mass Spectrometry (UF-LC/MS) Based Ligand-Binding Assay and an LC/MS Based Functional Assay for *Mycobacterium tuberculosis* Shikimate Kinase. *Analytical Chemistry*, 82 (9): 3616–3621.

Munro, S.A., Lewin, S.A., Smith, H.J., Engel, M.E., Fretheim, A. and Volmink, J. (2007) Patient Adherence to Tuberculosis Treatment: A Systematic Review of Qualitative Research. *PLoS Medicine*, 4 (7): e238.

Munshi, T., Gupta, A., Evangelopoulos, D., Guzman, J.D., Gibbons, S., Keep, N.H. and Bhakta, S. (2013) Characterisation of ATP-Dependent Mur Ligases Involved in the Biogenesis of Cell Wall Peptidoglycan in *Mycobacterium tuberculosis*. *PLoS ONE*, 8 (3): e60143.

Munsiff, S.S., Kambili, C. and Ahuja, S.D. (2006) Rifapentine for the treatment of pulmonary tuberculosis. *Clinical Infectious Diseases*, 43 (11): 1468–1475.

Nataraj, V., Varela, C., Javid, A., Singh, A., Besra, G.S. and Bhatt, A. (2015) Mycolic acids: deciphering and targeting the Achilles' heel of the tubercle bacillus. *Molecular microbiology*, 98 (1): 7–16.

Navari, R.M., Kaplan, H.G., Gralla, R.J., Grunberg, S.M., Palmer, R. and Fitts, D. (1994) Efficacy and safety of granisetron, a selective 5-hydroxytryptamine-3 receptor antagonist, in the prevention of nausea and vomiting induced by high-dose cisplatin. *Journal of clinical oncology: official journal of the American Society of Clinical Oncology*, 12 (10): 2204–2210.

O'Gaora P. *Expression of genes in mycobacteria*. (1998) Mycobacteria Protocols. Totowa: Humana Press; pp. 261–273.

Ojima, I., Awasthi, D., Wei, L. and Haranahalli, K. (2017) Strategic incorporation of fluorine in the drug discovery of new-generation antitubercular agents targeting bacterial cell division protein FtsZ. *Journal of Fluorine Chemistry*, 196: 44–56.

Pang, Y., Lu, J., Wang, Y., Song, Y., Wang, S. and Zhao, Y. (2013) Study of the rifampin monoresistance mechanism in *Mycobacterium tuberculosis*. *Antimicrobial agents and chemotherapy*, 57 (2): 893–900.

Pease, A.S. (1940) Some Remarks on the Diagnosis and Treatment of Tuberculosis in Antiquity. *Isis*, 31 (2): 380–393.

Pethe, K., Sequeira, P.C., Agarwalla, S., Rhee, K., Kuhen, K., Phong, W.Y., Patel, V., Beer, D., Walker, J.R., Duraiswamy, J., Jiricek, J., Keller, T.H., Chatterjee, A., Tan, M.P., Ujjini, M., Rao, S.P.S., Camacho, L., Bifani, P., Mak, P.A., Ma, I., Barnes, S.W., Chen, Z., Plouffe, D., Thayalan, P., Ng, S.H., Au, M., Lee, B.H., Tan, B.H., Ravindran, S., Nanjundappa, M., Lin, X., Goh, A., Lakshminarayana, S.B., Shoen, C., Cynamon, M., Kreiswirth, B., Dartois, V., Peters, E.C., Glynne, R., Brenner, S. and Dick, T. (2010) A chemical genetic screen in *Mycobacterium tuberculosis* identifies carbon-source-dependent growth inhibitors devoid of in vivo efficacy. *Nature Communications*, 1 (5): 1–8.

Pipkorn, P., Costantini, C., Reynolds, C., Wall, M., Drake, M., Sanico, A., Proud, D. and Togias, A. (2008) The effects of the nasal antihistamines olopatadine and azelastine in nasal allergen provocation. *Annals of allergy, asthma & immunology: official publication of the American College of Allergy, Asthma, & Immunology*, 101 (1): 82–89.

Pontiroli, A.E., Alberetto, M., Bertoletti, A., Baio, G. and Pozza, G. (1984) Sulfonylureas enhance in vivo the effectiveness of insulin in type 1 (insulin dependent) diabetes mellitus. *Hormone and metabolic research*, 16(S 1): 167–170.

Portevin, D., de Sousa-d'Auria, C., Houssin, C., Grimaldi, C., Chami, M., Daffé, M. and Guilhot, C. (2004) A polyketide synthase catalyses the last condensation step of mycolic acid biosynthesis in mycobacteria and related organisms. *Proceedings of the National Academy of Sciences*, 101 (1): 314–319.

Protopopova, M., Hanrahan, C., Nikonenko, B., Samala, R., Chen, P., Gearhart, J., Einck, L. and Nacy, C.A. (2005) Identification of a new antitubercular drug candidate, SQ109, from a combinatorial library of 1,2-ethylenediamines. *Journal of Antimicrobial Chemotherapy*, 56 (5): 968–974.

Raghavan, S., Manzanillo, P., Chan, K., Dovey, C. and Cox, J.S. (2008) Secreted transcription factor controls *Mycobacterium tuberculosis* virulence. *Nature*, 454 (7205): 717–721.

Raimunda, D., Long, J.E., Padilla-Benavides, T., Sassetti, C.M. and Argüello, J.M. (2014) Differential roles for the Co(2+) /Ni(2+) transporting ATPases, CtpD and CtpJ, in *Mycobacterium tuberculosis* virulence. *Molecular microbiology*, 91 (1): 185–197.

Ramaswamy, S. and Musser, J.M. (1998) Molecular genetic basis of antimicrobial agent resistance in *Mycobacterium tuberculosis*: 1998 update. *Tubercle and lung disease: the official journal of the International Union against Tuberculosis and Lung Disease*, 79 (1): 3–29.

Ramaswamy, S.V., Reich, R., Dou, S.-J., Jasperse, L., Pan, X., Wanger, A., Quitugua, T. and Graviss, E.A. (2003) Single nucleotide polymorphisms in genes associated with isoniazid resistance in *Mycobacterium tuberculosis*. *Antimicrobial agents and chemotherapy*, 47 (4): 1241–1250.

Ramón-García, S., González del Río, R., Villarejo, A.S., Sweet, G.D., Cunningham, F., Barros, D., Ballell, L., Mendoza-Losana, A., Ferrer-Bazaga, S. and Thompson, C.J. (2016) Repurposing clinically approved cephalosporins for tuberculosis therapy. *Scientific Reports*, 6 (1): 19.

Rattan, A., Kalia, A. and Ahmad, N. (1998) Multidrug-resistant *Mycobacterium tuberculosis*: molecular perspectives. *Emerging infectious diseases*, 4 (2): 195–209.

Rawat, R., Whitty, A. and Tonge, P.J. (2003) The isoniazid-NAD adduct is a slow, tight-binding inhibitor of InhA, the *Mycobacterium tuberculosis* enoyl reductase: adduct affinity and drug resistance. *Proceedings of the National Academy of Sciences*, 100 (24): 13881–13886.

Raymond, J.B., Mahapatra, S., Crick, D.C. and Pavelka, M.S. (2005) Identification of the namH gene, encoding the hydroxylase responsible for the N-glycolylation of the mycobacterial peptidoglycan. *Journal of Biological Chemistry*, 280 (1): 326–333.

Reddy, V.M., Dubuisson, T., Einck, L., Wallis, R.S., Jakubiec, W., Ladukto, L., Campbell, S. and Nacy, C.A. (2012) SQ109 and PNU-100480 interact to kill Mycobacterium tuberculosis in vitro. *The Journal of antimicrobial chemotherapy*, 67 (5): 1163–1166.

Reddy, V.M., Einck, L., Andries, K. and Nacy, C.A. (2010) In vitro interactions between new antitubercular drug candidates SQ109 and TMC207. *Antimicrobial agents and chemotherapy*, 54 (7): 2840–2846.

Rehren, G., Walters, S., Fontan, P., Smith, I. and Zárraga, A.M. (2007) Differential gene expression between *Mycobacterium bovis* and *Mycobacterium tuberculosis*. *Tuberculosis*, 87 (4): 347–359.

Riddle, M.C. (1999) Oral pharmacologic management of type 2 diabetes. *American family physician*, 60 (9): 2613–2620.

Rinder, H., Mieskes, K.T. and Löscher, T. (2001) Heteroresistance in *Mycobacterium tuberculosis*. *The international journal of tuberculosis and lung disease: the official journal of the International Union against Tuberculosis and Lung Disease*, 5 (4): 339–345.

Rodrigues, L., Villellas, C., Bailo, R., Viveiros, M. and Aínsa, J.A. (2013) Role of the Mmr efflux pump in drug resistance in *Mycobacterium tuberculosis*. *Antimicrobial agents and chemotherapy*, 57 (2): 751–757.

Rook, G.A.W. and Bloom, B.R. (1994) “Mechanisms of Pathogenesis in Tuberculosis.” In Tuberculosis. *American Society of Microbiology*. pp. 485–502.

Ruan, Q., Liu, Q., Sun, F., Shao, L., Jin, J., Yu, S., Ai, J., Zhang, B. and Zhang, W. (2016) Moxifloxacin and gatifloxacin for initial therapy of tuberculosis: a meta-analysis of randomised clinical trials. *Emerging microbes & infections*, 5 (2): e12.

Safi, H., Lingaraju, S., Amin, A., Kim, S., Jones, M., Holmes, M., McNeil, M., Peterson, S.N., Chatterjee, D., Fleischmann, R. and Alland, D. (2013) Evolution of high-level ethambutol-resistant tuberculosis through interacting mutations in decaprenylphosphoryl-β-D-arabinose biosynthetic and utilisation pathway genes. *Nature genetics*, 45 (10): 1190–1197.

Sala, C. and Hartkoorn, R.C. (2011) Tuberculosis drugs: new candidates and how to find more. *Future microbiology*, 6 (6): 617–633.

Sams-Dodd, F. (2005) Target-based drug discovery: is something wrong? *Drug Discovery Today*, 10 (2): 139–147.

Sarma, P.V.G.K., Usha Sarma, P. and Murthy, P.S. (1998) Isolation, purification and characterisation of intracellular calmodulin like protein (CALP) from *Mycobacterium phlei*. *FEMS Microbiology Letters*, 159 (1): 27–34.

Sartain, M.J., Dick, D.L., Rithner, C.D., Crick, D.C. and Belisle, J.T. (2011) Lipidomic analyses of *Mycobacterium tuberculosis* based on accurate mass measurements and the novel "*Mtb* LipidDB". *Journal of lipid research*, 52 (5): 861–872.

Sassetti, C.M., Boyd, D.H. and Rubin, E.J. (2003) Genes required for mycobacterial growth defined by high density mutagenesis. *Molecular microbiology*, 48 (1): 77–84.

Sbardella, G., Mai, A., Artico, M., Loddo, R., Setzu, M.G. and La Colla, P. (2004) Synthesis and in vitro antimycobacterial activity of novel 3-(1H-pyrrol-1-yl)-2-oxazolidinone analogues of PNU-100480. *Bioorganic and Medicinal Chemistry Letters*, 14 (6): 1537–1541.

Schifano, J.M., Edifor, R., Sharp, J.D., Ouyang, M., Konkimalla, A., Husson, R.N. and Woychik, N.A. (2013) Mycobacterial toxin MazF-mt6 inhibits translation through cleavage of 23S rRNA at the ribosomal A site. *Proceedings of the National Academy of Sciences of the United States of America*, 110 (21): 8501–8506.

Schnappinger, D. (2015) Genetic Approaches to Facilitate Antibacterial Drug Development. *Cold Spring Harbor perspectives in medicine*, 5 (7): a021139.

Scorpio, A. and Zhang, Y. (1996) Mutations in pncA, a gene encoding pyrazinamidase/nicotinamidase, cause resistance to the antituberculous drug pyrazinamide in tubercle bacillus. *Nature Medicine*, 2 (6): 662–667.

Scorpio, A., Lindholm-Levy, P., Heifets, L., Gilman, R., Siddiqi, S., Cynamon, M. and Zhang, Y. (1997) Characterisation of pncA mutations in pyrazinamide-resistant *Mycobacterium tuberculosis*. *Antimicrobial agents and chemotherapy*, 41 (3): 540–543.

Segura-Cabrera, A. and Rodríguez-Pérez, M.A. (2008) Structure-based prediction of *Mycobacterium tuberculosis* shikimate kinase inhibitors by high-throughput virtual screening. *Bioorganic and Medicinal Chemistry Letters*, 18 (11): 3152–3157.

Shah, N.S., Wright, A., Bai, G.-H., Barrera, L., Boulahbal, F., Martín-Casabona, N., Drobniewski, F., Gilpin, C., Havelková, M., Lepe, R., Lumb, R., Metchock, B., Portaels, F., Rodrigues, M.F., Rüsch-Gerdes, S., Van Deun, A., Vincent, V., Laserson, K., Wells, C. and Cegielski, J.P. (2007) Worldwide Emergence of Extensively Drug-resistant Tuberculosis. *Emerging infectious diseases*, 13 (3): 380–387.

Shaw, K.J. and Barbachyn, M.R. (2011) The oxazolidinones: past, present, and future. *Annals of the New York Academy of Sciences*, 1241 (1): 48–70.

Shi, L., Zhou, R., Liu, Z., Lowary, T.L., Seeberger, P.H., Stocker, B.L., Crick, D.C., Khoo, K.-H. and Chatterjee, D. (2008) Transfer of the first arabinofuranose residue to galactan is essential for *Mycobacterium smegmatis* viability. *Journal of Bacteriology*, 190 (15): 5248–5255.

Shi, W., Zhang, X., Jiang, X., Yuan, H., Lee, J.S., Barry, C.E., Wang, H., Zhang, W. and Zhang, Y. (2011) Pyrazinamide inhibits trans-translation in *Mycobacterium tuberculosis*. *Science*, 333 (6049): 1630–1632.

Shimakata, T., Fujita, Y. and Kusaka, T. (1980) Involvement of one of two enoyl-CoA hydratases and enoyl-CoA reductase in the acetyl-CoA-dependent elongation of medium chain fatty acids by *Mycobacterium smegmatis*. *Journal of biochemistry*, 88 (4): 1051–1058.

Shirude, P.S., Shandil, R., Sadler, C., Naik, M., Hosagrahara, V., Hameed, S., Shinde, V., Bathula, C., Humnabadkar, V., Kumar, N., Reddy, J., Panduga, V., Sharma, S., Ambady, A., Hegde, N., Whiteaker, J., McLaughlin, R.E., Gardner, H., Madhavapeddi, P., Ramachandran, V., Kaur, P., Narayan, A., Guptha, S., Awasthy, D., Narayan, C., Mahadevaswamy, J., Vishwas, K.G., Ahuja, V., Srivastava, A., Prabhakar, K.R., Bharath, S., Kale, R., Ramaiah, M., Choudhury, N.R., Sambandamurthy, V.K., Solapure, S., Iyer, P.S., Narayanan, S. and Chatterji, M. (2013) Azaindoles: noncovalent DprE1 inhibitors from scaffold morphing efforts, kill *Mycobacterium tuberculosis* and are efficacious *in vivo*. *Journal of Medicinal Chemistry*, 56 (23): 9701–9708.

Silva, M.S.N., Senna, S.G., Ribeiro, M.O., Valim, A.R.M., Telles, M.A., Kritski, A., Morlock, G.P., Cooksey, R.C., Zaha, A. and Rossetti, M.L.R. (2003) Mutations in katG, inhA, and ahpC genes of Brazilian isoniazid-resistant isolates of *Mycobacterium tuberculosis*. *Journal of Clinical Microbiology*, 41 (9): 4471–4474.

Singh, G. and Dey, C.S. (2007) Induction of apoptosis-like cell death by pentamidine and doxorubicin through differential inhibition of topoisomerase II in arsenite-resistant L. donovani. *Acta tropica*, 103 (3): 172–185.

Singh, P. and Cole, S.T. (2011) *Mycobacterium leprae*: genes, pseudogenes and genetic diversity. *Future microbiology*, 6 (1): 57–71.

Singh, R., Manjunatha, U., Boshoff, H.I.M., Ha, Y.H., Niyomrattanakit, P., Ledwidge, R., Dowd, C.S., Lee, I.Y., Kim, P., Zhang, L., Kang, S., Keller, T.H., Jiricek, J. and Barry, C.E. (2008) PA-824 kills nonreplicating *Mycobacterium tuberculosis* by intracellular NO release. *Science*, 322 (5906): 1392–1395.

Smith, I. (2003) *Mycobacterium tuberculosis* pathogenesis and molecular determinants of virulence. *Clinical Microbiology Reviews*, 16 (3): 463–496.

Somoskovi, A., Parsons, L.M. and Salfinger, M. (2001) The molecular basis of resistance to isoniazid, rifampin, and pyrazinamide in *Mycobacterium tuberculosis*. *Respiratory research*, 2 (3): 164–168.

Soro, O., Pesce, A., Raggi, M., Debbia, E.A. and Schito, G.C. (1997) Selection of rifampicin-resistant *Mycobacterium tuberculosis* does not occur in the presence of low concentrations of rifaximin. *Clinical microbiology and infection: the official publication of the European Society of Clinical Microbiology and Infectious Diseases*, 3 (1): 147–151.

Sorrentino, F., González del Río, R., Zheng, X., Presa Matilla, J., Torres Gomez, P., Martinez Hoyos, M., Perez Herran, M.E., Mendoza-Losana, A. and Av-Gay, Y. (2015) Development of an Intracellular Screen for New Compounds Able to Inhibit *Mycobacterium tuberculosis* Growth in Human Macrophages. *Antimicrobial agents and chemotherapy*, 60 (1): 640–645.

Sreevatsan, S., Stockbauer, K.E., Pan, X., Kreiswirth, B.N., Moghazeh, S.L., Jacobs, W.R., Telenti, A. and Musser, J.M. (1997) Ethambutol resistance in *Mycobacterium tuberculosis*: critical role of embB mutations. *Antimicrobial agents and chemotherapy*, 41 (8): 1677–1681.

Srivastava, S., Ayyagari, A., Dhole, T.N., Nyati, K.K. and Dwivedi, S.K. (2009) emb nucleotide polymorphisms and the role of embB306 mutations in *Mycobacterium tuberculosis* resistance to ethambutol. *International journal of medical microbiology*, 299 (4): 269–280.

Srivastava, S., Chaudhary, S., Thukral, L., Shi, C., Gupta, R.D., Gupta, R., Priyadarshan, K., Vats, A., Haque, A.S., Sankaranarayanan, R., Natarajan, V.T., Sharma, R., Aldrich, C.C. and Gokhale, R.S. (2015) Unsaturated Lipid Assimilation by Mycobacteria Requires Auxiliary cis-trans Enoyl CoA Isomerase. *Chemistry and Biology*, 22 (12): 1577–1587.

Srivastava, S., Musuka, S., Sherman, C., Meek, C., Leff, R. and Gumbo, T. (2010) Efflux-pump-derived multiple drug resistance to ethambutol monotherapy in *Mycobacterium tuberculosis* and the pharmacokinetics and pharmacodynamics of ethambutol. *The Journal of infectious diseases*, 201 (8): 1225–1231.

Stehr, M., Elamin, A.A. and Singh, M. (2014) Filling the pipeline - new drugs for an old disease. *Current Topics in Medicinal*, 14 (1): 110–129.

Sterling, T.R., Scott, N.A., Miro, J.M., Calvet, G., La Rosa, A., Infante, R., Chen, M.P., Benator, D.A., Gordin, F., Benson, C.A., Chaisson, R.E., Villarino, M.E.Tuberculosis Trials Consortium, the AIDS Clinical Trials Group for the PREVENT TB Trial (TBTC Study 26ACTG 5259) The investigators of the TB Trials Consortium and the AIDS Clinical Trials Group for the PREVENT TB Trial are listed in the Supplement, item 17 (2016) Three months

of weekly rifapentine and isoniazid for treatment of Mycobacterium tuberculosis infection in HIV-coinfected persons. *AIDS (London, England)*, 30 (10): 1607–1615.

Sterling, T.R., Villarino, M.E., Borisov, A.S., Shang, N., Gordin, F., Bliven-Sizemore, E., Hackman, J., Hamilton, C.D., Menzies, D., Kerrigan, A., Weis, S.E., Weiner, M., Wing, D., Conde, M.B., Bozeman, L., Horsburgh, C.R., Chaisson, R.E.TB Trials Consortium PREVENT TB Study Team (2011) Three months of rifapentine and isoniazid for latent tuberculosis infection. *The New England journal of medicine*, 365 (23): 2155–2166.

Stover, C.K., la Cruz, de, V.F., Fuerst, T.R., Burlein, J.E., Benson, L.A., Bennett, L.T., Bansal, G.P., Young, J.F., Lee, M.H. and Hatfull, G.F. (1991) New use of BCG for recombinant vaccines. *Nature*, 351 (6326): 456–460.

Stover, C.K., Warrener, P., VanDevanter, D.R., Sherman, D.R., Arain, T.M., Langhorne, M.H., Anderson, S.W., Towell, J.A., Yuan, Y., McMurray, D.N., Kreiswirth, B.N., Barry, C.E. and Baker, W.R. (2000) A small-molecule nitroimidazopyran drug candidate for the treatment of tuberculosis. *Nature*, 405 (6789): 962–966.

Syriopoulou, V.P., Harding, A.L., Goldmann, D.A. and Smith, A.L. (1981) In vitro antibacterial activity of fluorinated analogs of chloramphenicol and thiamphenicol. *Antimicrobial agents and chemotherapy*, 19 (2): 294–297.

Takayama, K., Armstrong, E.L., Kunugi, K.A. and Kilburn, J.O. (1979) Inhibition by ethambutol of mycolic acid transfer into the cell wall of *Mycobacterium smegmatis*. *Antimicrobial agents and chemotherapy*, 16 (2): 240–242.

Takayama, K., Wang, C. and Besra, G.S. (2005) Pathway to Synthesis and Processing of Mycolic Acids in *Mycobacterium tuberculosis*. *Clinical Microbiology Reviews*, 18 (1): 81–101.

Tam, P.-H. and Lowary, T.L. (2009) Recent advances in mycobacterial cell wall glycan biosynthesis. *Current opinion in chemical biology*, 13 (5-6): 618–625.

Tardioli, S., Buijs, J., Gooijer, C. and van der Zwan, G. (2012) pH-dependent complexation of histamine H1 receptor antagonists and human serum albumin studied by UV resonance Raman spectroscopy. *The journal of physical chemistry*. B, 116 (12): 3808–3815.

Tatituri, R.V.V., Alderwick, L.J., Mishra, A.K., Nigou, J., Gilleron, M., Krumbach, K., Hitchen, P., Giordano, A., Morris, H.R., Dell, A., Eggeling, L. and Besra, G.S. (2007) Structural characterisation of a partially arabinosylated lipoarabinomannan variant isolated from a *Corynebacterium glutamicum* ubiA mutant. *Microbiology (Reading, England),* 153 (8): 2621–2629.

Telenti, A., Philipp, W.J., Sreevatsan, S., Bernasconi, C., Stockbauer, K.E., Wieles, B., Musser, J.M. and Jacobs, W.R. (1997) The emb operon, a gene cluster of *Mycobacterium tuberculosis* involved in resistance to ethambutol. *Nature Medicine*, 3 (5): 567–570.

Traore, H., Fissette, K., Bastian, I., Devleeschouwer, M. and Portaels, F. (2000) Detection of rifampicin resistance in *Mycobacterium tuberculosis* isolates from diverse countries by a

commercial line probe assay as an initial indicator of multidrug resistance. *International Journal of Tuberculosis and Lung Disease*, 4 (5):481-484.

Trefzer, C., Rengifo-Gonzalez, M., Hinner, M.J., Schneider, P., Makarov, V., Cole, S.T. and Johnsson, K. (2010) Benzothiazinones: prodrugs that covalently modify the decaprenylphosphoryl-β-D-ribose 2'-epimerase DprE1 of *Mycobacterium tuberculosis*. *Journal of the American Chemical Society*, 132 (39): 13663–13665.

Tufariello, J.M., Chan, J. and Flynn, J.L. (2003) Latent tuberculosis: mechanisms of host and bacillus that contribute to persistent infection. *The Lancet. Infectious diseases*, 3 (9): 578–590.

Van Soolingen, D., Hoogenboezem, T., De Haas, P.E.W., Hermans, P.W.M., Koedam, M.A., Teppema, K.S., Brennan, P.J., Besra, G.S., Portaels, F., Top, J., Schouls, L.M. and Van Embden, J.D.A. (1997) A Novel Pathogenic Taxon of the *Mycobacterium tuberculosis* Complex, Canetti: Characterisation of an Exceptional Isolate from Africa. *International Journal of Systematic Bacteriology*, 47 (4): 1236–1245.

Verschoor, J.A., Baird, M.S. and Grooten, J. (2012) Towards understanding the functional diversity of cell wall mycolic acids of *Mycobacterium tuberculosis*. *Progress in Lipid Research*, 51 (4): 325–339.

Vilchèze, C., Morbidoni, H.R., Weisbrod, T.R., Iwamoto, H., Kuo, M., Sacchettini, J.C. and Jacobs, W.R. (2000) Inactivation of the inhA-encoded fatty acid synthase II (FASII) enoyl-acyl carrier protein reductase induces accumulation of the FASI end products and cell lysis of *Mycobacterium smegmatis*. *Journal of Bacteriology*, 182 (14): 4059–4067.

Viljoen, A., Dubois, V., Girard-Misguich, F., Blaise, M., Herrmann, J.L. and Kremer, L. (2017) The diverse family of MmpL transporters in mycobacteria: from regulation to antimicrobial developments. *Molecular microbiology*, 104 (6): 889–904.

Warrilow, A.G.S., Jackson, C.J., Parker, J.E., Marczylo, T.H., Kelly, D.E., Lamb, D.C. and Kelly, S.L. (2009) Identification, characterisation, and azole-binding properties of *Mycobacterium smegmatis* CYP164A2, a homolog of ML2088, the sole cytochrome P450 gene of *Mycobacterium leprae*. *Antimicrobial agents and chemotherapy*, 53 (3): 1157–1164.

Watrous, J., Burns, K., Liu, W.-T., Patel, A., Hook, V., Bafna, V., Barry, C.E., Bark, S. and Dorrestein, P.C. (2010) Expansion of the mycobacterial "PUPylome". *Molecular bioSystems*, 6 (2): 376–385.

Wayne, L.G. and Hayes, L.G. (1996) An in vitro model for sequential study of shift down of *Mycobacterium tuberculosis* through two stages of non-replicating persistence. *Infection and immunity*, 64 (6): 2062–2069.

Williams, K.J., Boshoff, H.I., Krishnan, N., Gonzales, J., Schnappinger, D. and Robertson, B.D. (2011) The *Mycobacterium tuberculosis* β-oxidation genes echA5 and fadB3 are dispensable for growth *in vitro* and *in vivo*. *Tuberculosis (Edinburgh, Scotland)*, 91 (6): 549–555.

Williams, K.N., Brickner, S.J., Stover, C.K., Zhu, T., Ogden, A., Tasneen, R., Tyagi, S., Grosset, J.H. and Nuermberger, E.L. (2009) Addition of PNU-100480 to first-line drugs shortens the time needed to cure murine tuberculosis. *American Journal of Respiratory and Critical Care Medicine*, 180 (4): 371–376.

Winder, F.G. and Collins, P.B. (1970) Inhibition by isoniazid of synthesis of mycolic acids in *Mycobacterium tuberculosis*. *Journal of general microbiology*, 63 (1): 41–48.

Wolfe, L.M., Mahaffey, S.B., Kruh, N.A. and Dobos, K.M. (2010) Proteomic definition of the cell wall of *Mycobacterium tuberculosis*. *Journal of proteome research*, 9 (11): 5816–5826.

Wolucka, B.A. (2008) Biosynthesis of D-arabinose in mycobacteria - a novel bacterial pathway with implications for antimycobacterial therapy. *The FEBS journal*, 275 (11): 2691–2711.

Wolucka, B.A., McNeil, M.R., de Hoffmann, E., Chojnacki, T. and Brennan, P.J. (1994) Recognition of the lipid intermediate for arabinogalactan/arabinomannan biosynthesis and its relation to the mode of action of ethambutol on mycobacteria. *Journal of Biological Chemistry*, 269 (37): 23328–23335.

Young, D.B., Duncan, K., Gallagher, A., Kempsell, K.E. and De Smet, K.A.L. (1999) Alteration of a single amino acid residue reverses fosfomycin resistance of recombinant MurA from *Mycobacterium tuberculosis*. *Microbiology*, 145 (11): 3177–3184.

Zabinski, R.F. and Blanchard, J.S. (1997) The Requirement for Manganese and Oxygen in the Isoniazid-Dependent Inactivation of *Mycobacterium tuberculosis* Enoyl Reductase. *Journal of the American Chemical Society*, 119 (9): 2331–2332.

Zhang, B., Zhou, N., Liu, Y.-M., Liu, C., Lou, C.-B., Jiang, C.-Y. and Liu, S.-J. (2015) Ribosome binding site libraries and pathway modules for shikimic acid synthesis with *Corynebacterium glutamicum*. *Microbial cell factories*, 14 (1): 71.

Zhang, Y., Wade, M.M., Scorpio, A., Zhang, H. and Sun, Z. (2003) Mode of action of pyrazinamide: disruption of *Mycobacterium tuberculosis* membrane transport and energetics by pyrazinoic acid. *Journal of Antimicrobial Chemotherapy*, 52 (5): 790–795.

Zhu, X., Gao, J.J., Landao-Bassonga, E., Pavlos, N.J., Qin, A., Steer, J.H., Zheng, M.H., Dong, Y. and Cheng, T.S. (2016) Thonzonium bromide inhibits RANKL-induced osteoclast formation and bone resorption in vitro and prevents LPS-induced bone loss *in vivo*. *Biochemical pharmacology*, 104: 118–130.

Zimhony, O., Vilcheze, C., Arai, M., Welch, J.T. and Jacobs, W.R. (2007) Pyrazinoic acid and its n-propyl ester inhibit fatty acid synthase type I in replicating tubercle bacilli. *Antimicrobial agents and chemotherapy*, 51 (2): 752–754.

Appendix

Appendix 1: Scatter graphs representing averages of normalised survival percentages (from duplicates) of *M. smegmatis*_pSMT3_eGFP during the preliminary high throughput screening of the Prestwick library.

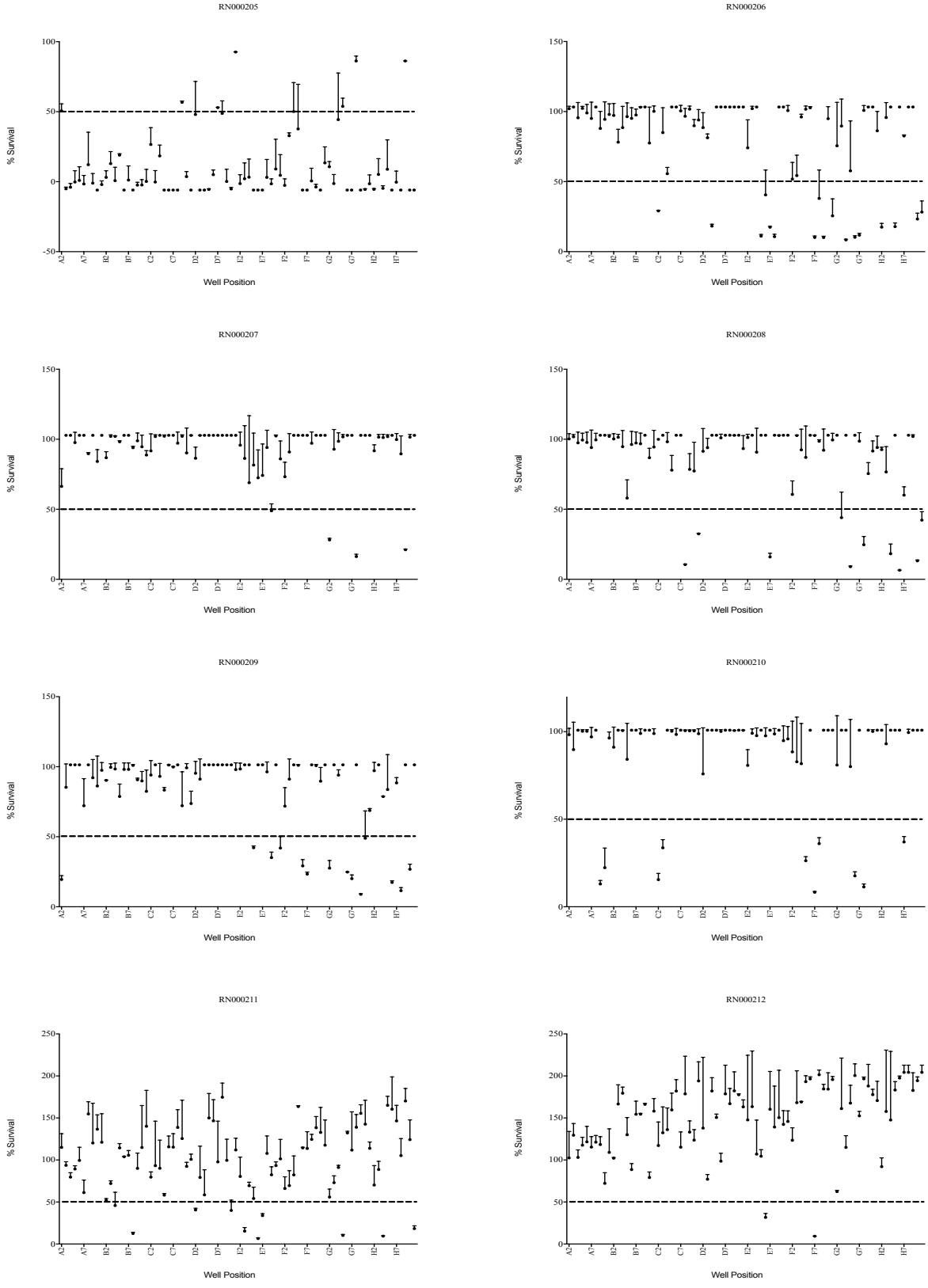

RN000213

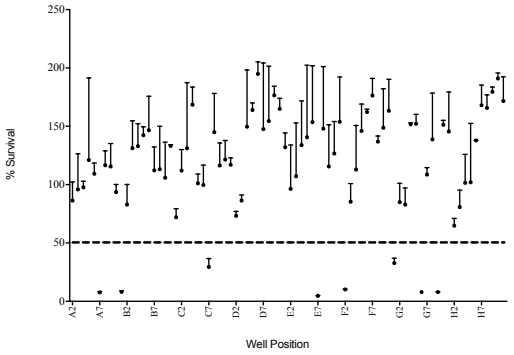

RN000214

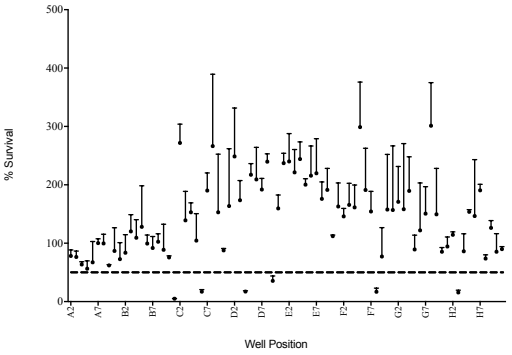

RN000215

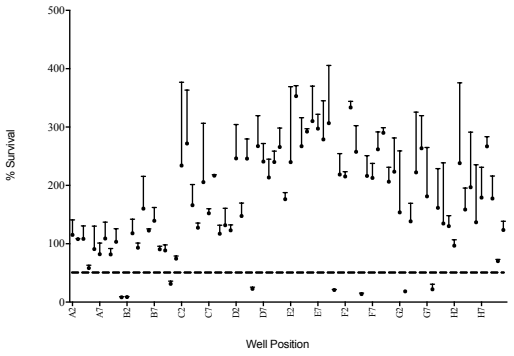

RN000216

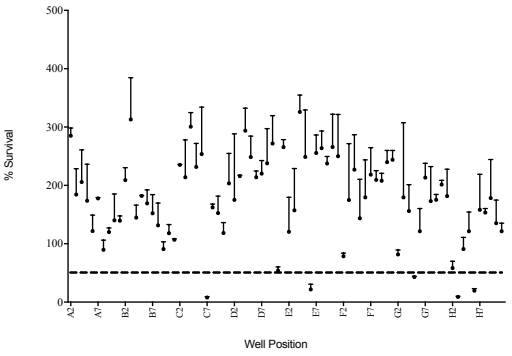

RN000217

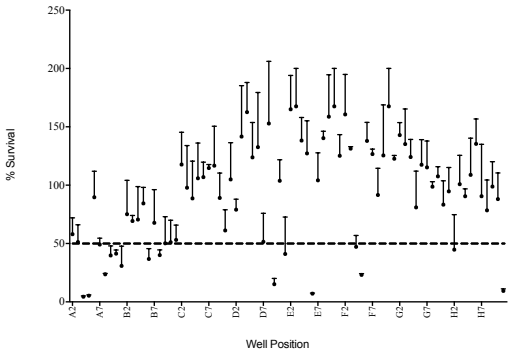

RN000218

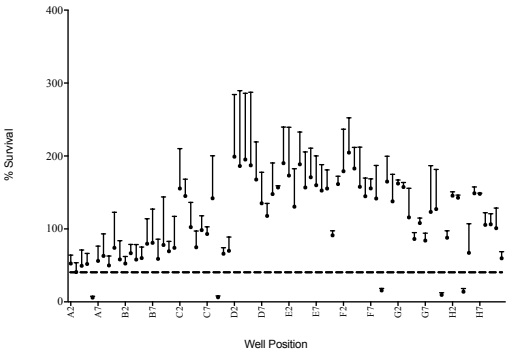

RN000219

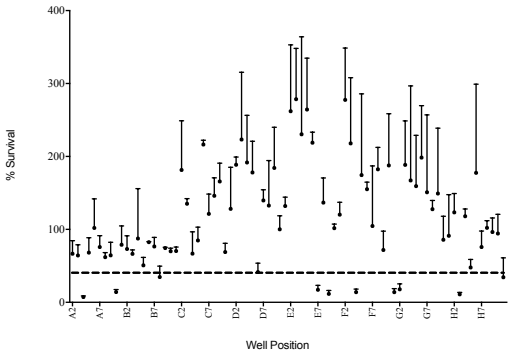

Appendix 2: Scatter graphs representing averages of normalised survival percentages (from duplicates) of *M. bovis* BCG_pSMT3_eGFP during the preliminary high throughput screening of the Prestwick library.

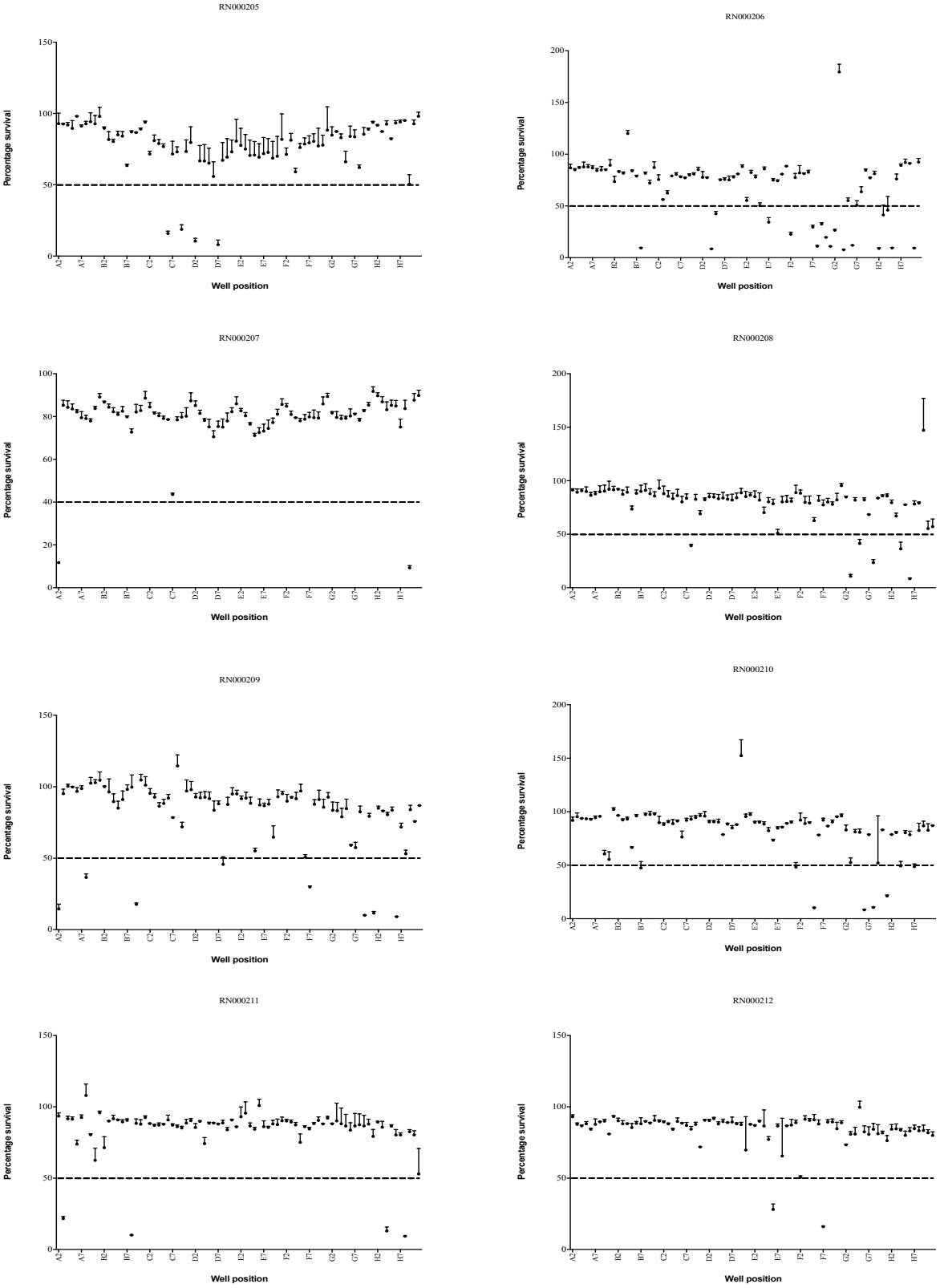

RN000213

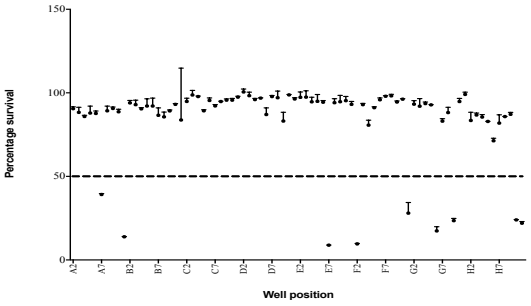

RN000214

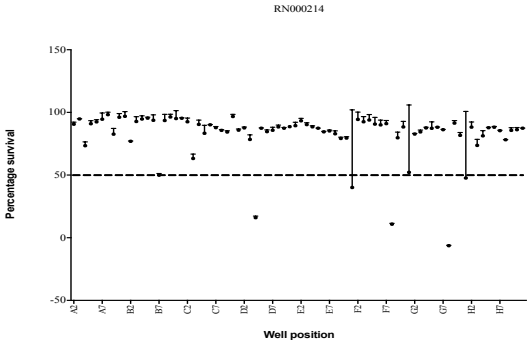

RN000215

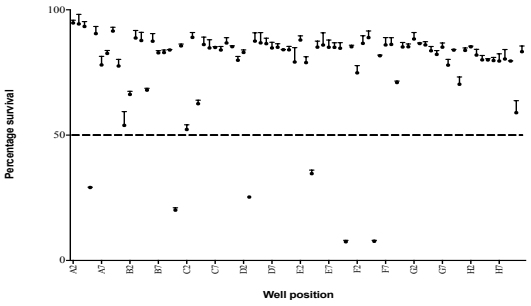

RN000216

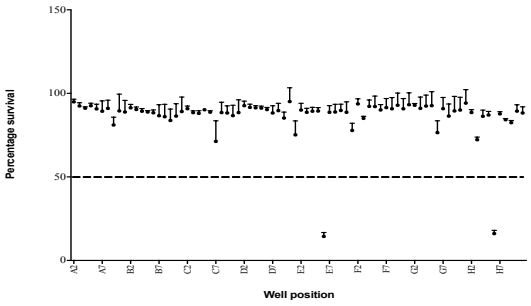

RN000217

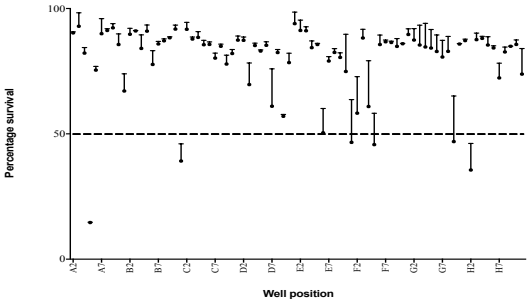

RN000218

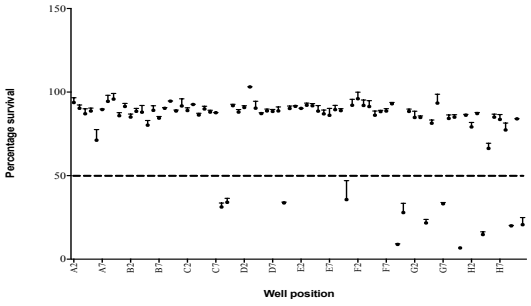

RN000219

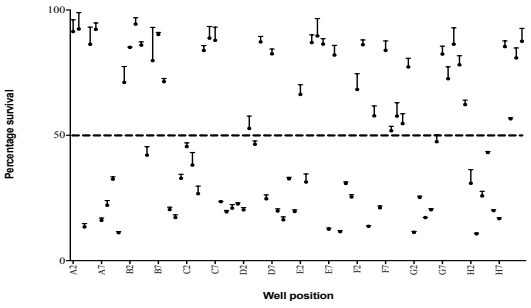

Appendix 3: Table listing all the hits with the survival percentages of *M. smegmatis* and M.bovis BCG generated during the preliminary screen

Primary Screen Hits (*M. smegmatis*)	% Survival	Primary Screen Hits (*M. bovis* BCG)	% Survival
Sertaconazole nitrate	3.45	**Merbromin**	6.34
Thiethylperazine dimalate	3.71	**Rifabutin**	6.73
Enilconazole	4.42	**Clinafloxacin**	7.47
Thimerosal	4.84	**Chlorhexidine**	7.61
Methacycline hydrochloride	5.35	**Roxithromycin**	7.76
Ebselen	5.57	**Troleandomycin**	7.99
Rifabutin	5.67	**Tosufloxacin**	8.32
Minocycline hydrochloride	6.51	**Minocycline**	8.41
Doxycycline hydrochloride	6.62	**Ciprofloxacin**	8.43
Rifampicin	7.05	**Sarafloxacin**	8.83
Apramycin	7.07	**Thimerosal**	8.83
Niclosamide	7.33	**Erythromycin**	8.93
Oxiconazole Nitrate	7.85	**Amikacin**	9.11
Sulconazole nitrate	8.03	**Josamycin**	9.21
Methyl benzethonium chloride	8.12	**Lomefloxacin**	9.27
Viomycin sulfate	8.14	**Dihydrostreptomycin**	9.29
Benzethonium chloride	8.17	**Dirithromycin**	9.32
Meclocycline sulfosalicylate	8.3	**Disulfiram**	9.33
Chlorhexidine	8.36	**Tylosin**	9.63
Pinaverium bromide	8.37	**Dequalinium**	10.1
Auranofin	8.44	**Linezolid**	10.1
Dequalinium dichloride	8.89	**Vancomycin**	10.14
Econazole nitrate	9.05	**Chloramphenicol**	10.5
Demecarium bromide	9.3	**Rifapentine**	10.58
Sarafloxacin	9.32	**Lincomycin**	10.67
Pyrvinium pamoate	9.42	**Moxifloxacin**	10.68
Moxifloxacin	10.06	**Alexidine**	10.82
Pentamidine isethionate	10.07	**Tetracycline**	10.93
Terfenadine	10.08	**Clindamycin hydrochloride**	11.03
Astemizole	10.14	**Rifaximin**	11.16
Chlorotetracycline hydrochloride	10.25	**Gatifloxacin**	11.27
Clotrimazole	10.48	**Clarithromycin**	11.56

Tylosin	10.5	**Fusidic acid**	11.61
Isoconazole	10.74	**Isoniazid**	11.74
Clarithromycin	10.85	**Chlortetracycline**	11.96
Tobramycin	11.02	**Sparfloxacin**	12.56
Tioconazole	11.05	**Pentamidine**	13
Rifapentine	11.32	**Doxycycline**	13.45
Clomiphene citrate	11.48	**Azithromycin**	13.67
Tamoxifen citrate	11.77	**Pinaverium**	13.87
Azithromycin	12.39	**Thonzonium**	14.39
Fluspirilen	12.4	**Streptomycin**	14.5
Bifonazole	12.89	**Methacycline**	14.63
Butoconazole nitrate	13.01	**Viomycin**	14.75
Rifaximin	13.02	**Thiamphenicol**	15.8
Clofilium tosylate	13.18	**Florfenicol**	16.01
Vancomycin hydrochloride	13.37	**Demecarium**	16.02
Roxithromycin	13.47	**Clavulanate**	16.04
Miconazole	13.76	**Demeclocycline**	16.09
Thioridazine hydrochloride	13.77	**Granisetron**	16.31
Toremifene	14.12	**Rosiglitazone**	16.75
Zuclopenthixol dihydrochloride	15.17	**Phentermine**	17.19
Suloctidil	15.5	**Gemcitabine**	17.2
Sparfloxacin	15.99	**Methyl benzethonium chloride**	17.4
Perhexiline maleate	15.99	**N6-methyladenosine**	17.7
Thiostrepton	16.27	**Ethambutol**	18.75
Clemizole hydrochloride	16.3	**Cladribine**	19.48
Gatifloxacin	16.7	**Lamotrigine**	19.62
Propidium iodide	17.24	**Cefotaxime**	19.65
Amikacin hydrate	17.38	**Olopatadine**	19.82
Mitoxantrone dihydrochloride	17.38	**Cefepime**	19.94
Mefloquine hydrochloride	17.46	**Pravastatin**	19.95
Erythromycin	17.51	**5-fluorouracil**	20.25
Tosufloxacin hydrochloride	17.66	**Olmesartan**	20.29
Josamycin	17.87	**Methenamine**	20.39
Raloxifene hydrochloride	17.92	**Nadifloxacin**	20.64
Ciprofloxacin hydrochloride monohydrate	18.27	**Vardenafil**	20.95

Trifluoperazine dihydrochloride	18.29	**Losartan**	21.08
Alexidine dihydrochloride	18.32	**Ceforanide**	21.31
Spiramycin	18.71	**Cefotiam**	21.63
Demeclocycline hydrochloride	18.91	**4-aminosalicylic acid**	21.72
Streptomycin sulfate	19.49	**Cefuroxime**	22.01
Prenylamine lactate	19.61	**Moxalactam**	22.07
GBR 12909 dihydrochloride	20.1	**Valproic**	22.09
Clinafloxacin	20.22	**Fluconazole**	22.63
Lomefloxacin hydrochloride	21.15	**Glipizide**	22.63
Paromomycin sulfate	21.2	**Pimozide**	23.44
Novobiocin sodium salt	22.17	**Benzethonium**	23.5
Amiodarone hydrochloride	22.32	**Fludarabine**	23.55
Sertraline	23.18	**Cephalothin**	23.9
Dihydrostreptomycin sulfate	23.29	**Triclosan**	24.66
Clofazimine	23.34	**Bosentan**	25.22
Gestrinone	23.59	**Cefoxitin**	25.28
Tridihexethyl chloride	23.98	**Tulobuterol**	25.41
Oxytetracycline dihydrate	24.7	**Formoterol**	25.84
Tetracycline hydrochloride	25.57	**Verapamil**	26.44
Linezolid	26.3	**Carprofen**	26.75
Prochlorperazine dimaleate	26.79	**Nialamide**	27.9
Lidoflazine	27.58	**Cefmetazole**	28.03
Norfloxacin	28.13	**Carbadox**	28.13
Gentamicin sulfate	28.27	**Spectinomycin**	29.1
R(-) Apomorphine hydrochloride hemihydrate	29.05	**Astemizole**	29.47
Methiothepin maleate	29.18	**Clofazimine**	29.89
Nisoldipine	30.41	**Tripelennamine**	30.8
Moxalactam disodium salt	30.53	**Imatinib**	30.86
Indatraline hydrochloride	30.79	**Ticarcillin**	31.25
Florfenicol	30.93	**Cyclophosphamide**	31.36
Carbadox	31.68	**Terfenadine**	32.46
Carvedilol	32.41	**Mepivacaine**	32.49
Fendiline hydrochloride	32.45	**Anthralin**	32.67
Hexachlorophene	32.85	**Diclazuril**	32.87
Thonzonium bromide	33.25	**Meropenem**	33.15
Zotepine	33.67	**Benzylpenicillin**	33.7

Cefmetazole sodium salt	33.8	**Thiethylperazine**	34.02
Bepridil hydrochloride	35.07	**Mefloquine hydrochloride**	34.24
Meclozine dihydrochloride	36.07	**Nafcillin**	34.6
Ethionamide	36.5	**Halofantrine**	35.56
Naftopidil dihydrochloride	36.76	**Cycloserine**	35.67
Primaquine diphosphate	37.02	**Trifluoperazine**	36.32
Clindamycin hydrochloride	38	**Cefoperazone**	36.52
Triclosan	38.39	**Dopamine**	38.11
Ribostamycin sulfate	38.94	**Piribedil**	39.15
Decamethonium bromide	39.76	**Oxiconazole**	39.2
Zardaverine	40.04	**Clotrimazole**	39.34
Perphenazine	40.52	**Isopropamide**	40.01
Lymecycline	41.08	**Chloroxine**	41.26
Darifenacin hydrobromide	41.35	**Econazole**	41.29
Benzbromarone	41.95	**Anethole-trithione**	42.07
Metergoline	42.18	**Ampicillin**	42.3
Fluphenazine dihydrochloride	42.29	**Rufloxacin**	43.12
ethambutol	43.33	**Cloxacillin**	43.58
Imipenem	43.65	**Sertraline**	45.7
Fluoxetine hydrochloride	43.81	**Amoxicillin**	45.73
Rufloxacin	43.97	**Didanosine**	45.96
Lincomycin hydrochloride	44.03	**Talampicillin**	46.59
Halofantrine hydrochloride	44.77	**Benzathine benzylpenicillin**	46.9
Chlorpromazine hydrochloride	46.21	**Bacampicillin**	47.43
Anethole-trithione	46.58	**Cycloheximide**	47.6
Troleandomycin	47.05	**Dicloxacillin**	48.29
Deptropine citrate	47.23	**Primaquine**	48.7
Omeprazole	48.44	**Cefotetan**	49.32
Trimethoprim	48.95	**Cefazolin**	49.9
Azaguanine-8	49.43	**Tioconazole**	50.4
		Apramycin	50.4
		Thioridazine hydrochloride	50.42
		Tamoxifen	50.63
		Methiothepin	50.69
		Perhexiline	50.88

Appendix 4: Scatter graph representing correlation analysis between plate A and B during the preliminary screen of the Prestwick library against *M. smegmatis*_pSMT3_eGFP

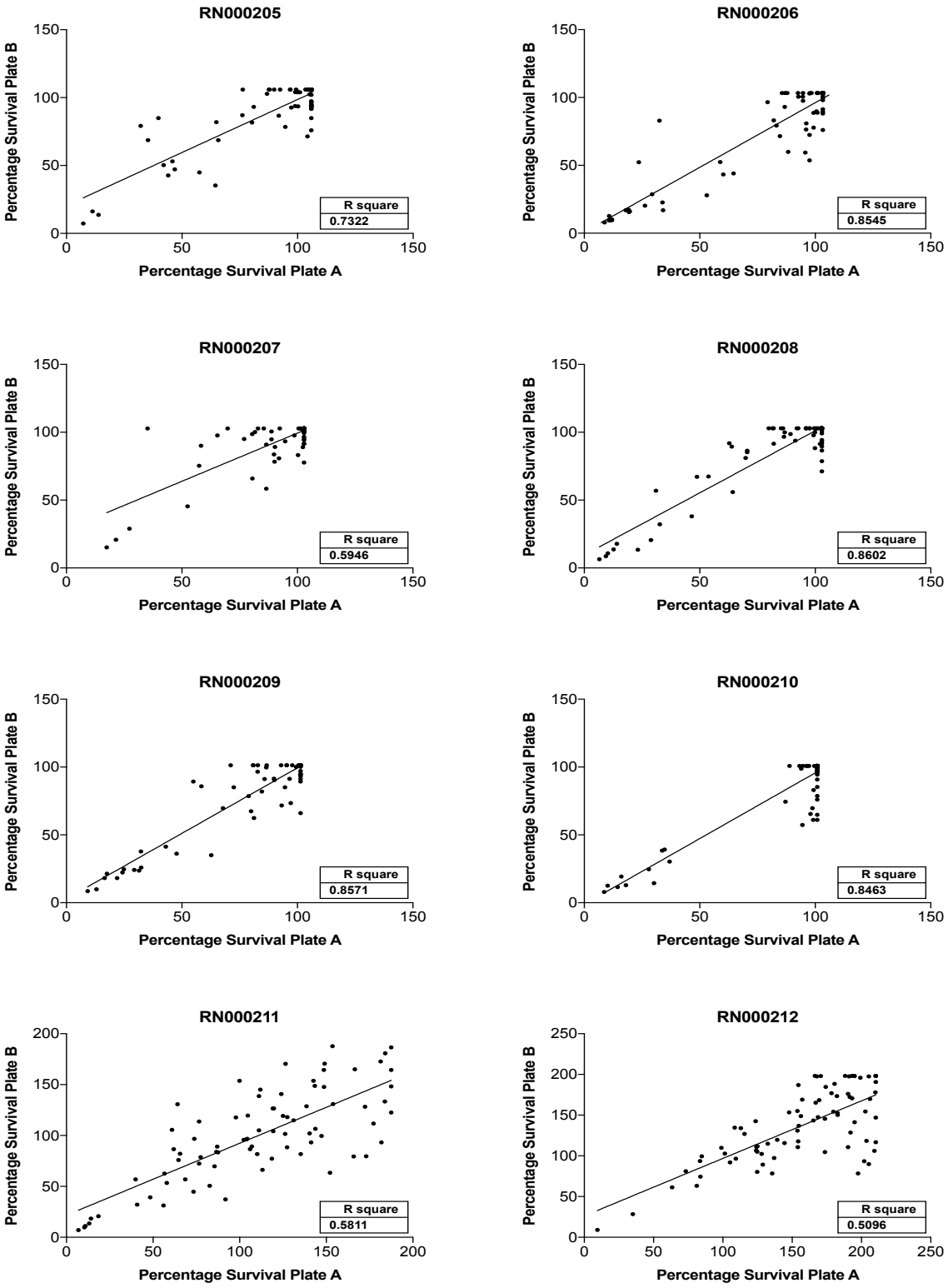

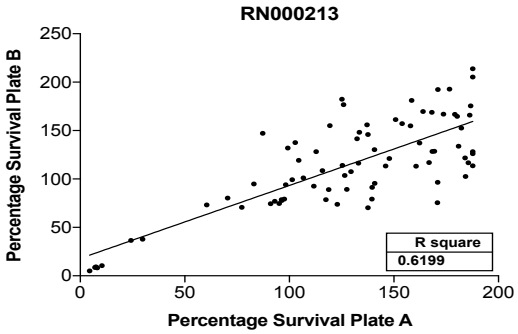
RN000213
Percentage Survival Plate B
Percentage Survival Plate A
R square
0.6199

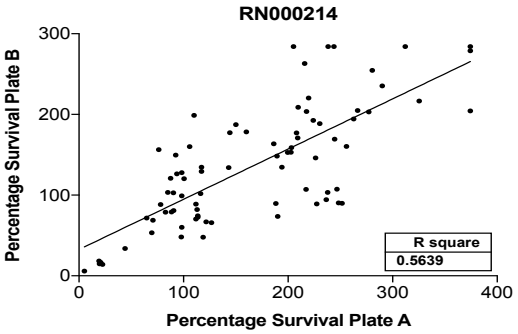
RN000214
Percentage Survival Plate B
Percentage Survival Plate A
R square
0.5639

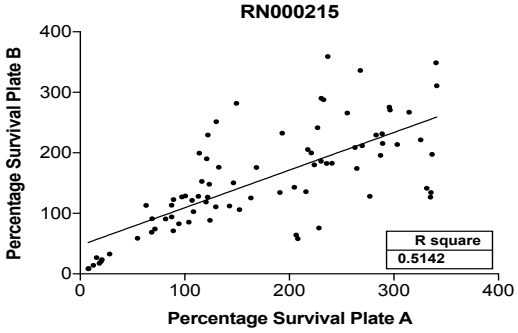
RN000215
Percentage Survival Plate B
Percentage Survival Plate A
R square
0.5142

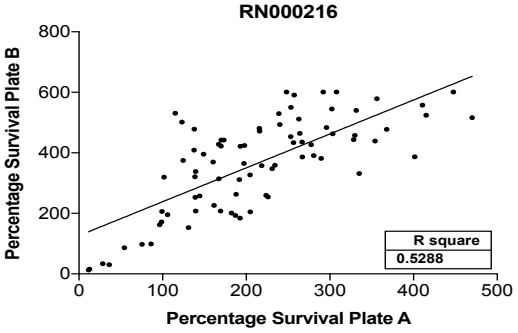
RN000216
Percentage Survival Plate B
Percentage Survival Plate A
R square
0.5288

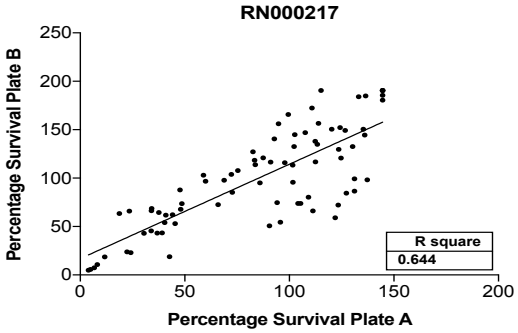
RN000217
Percentage Survival Plate B
Percentage Survival Plate A
R square
0.644

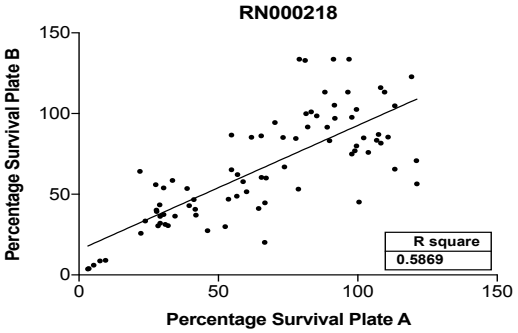
RN000218
Percentage Survival Plate B
Percentage Survival Plate A
R square
0.5869

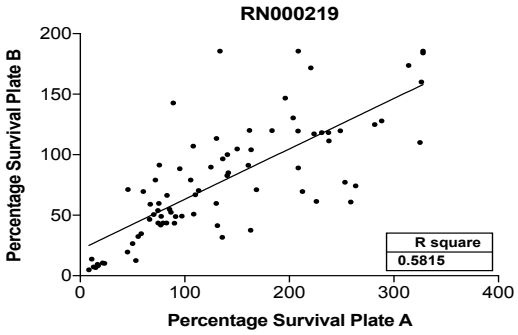
RN000219
Percentage Survival Plate B
Percentage Survival Plate A
R square
0.5815

Appendix 5: Scatter graph representing correlation analysis between plate A and B during the preliminary screen of the Prestwick library against *M. bovis* BCG_pSMT3_eGFP

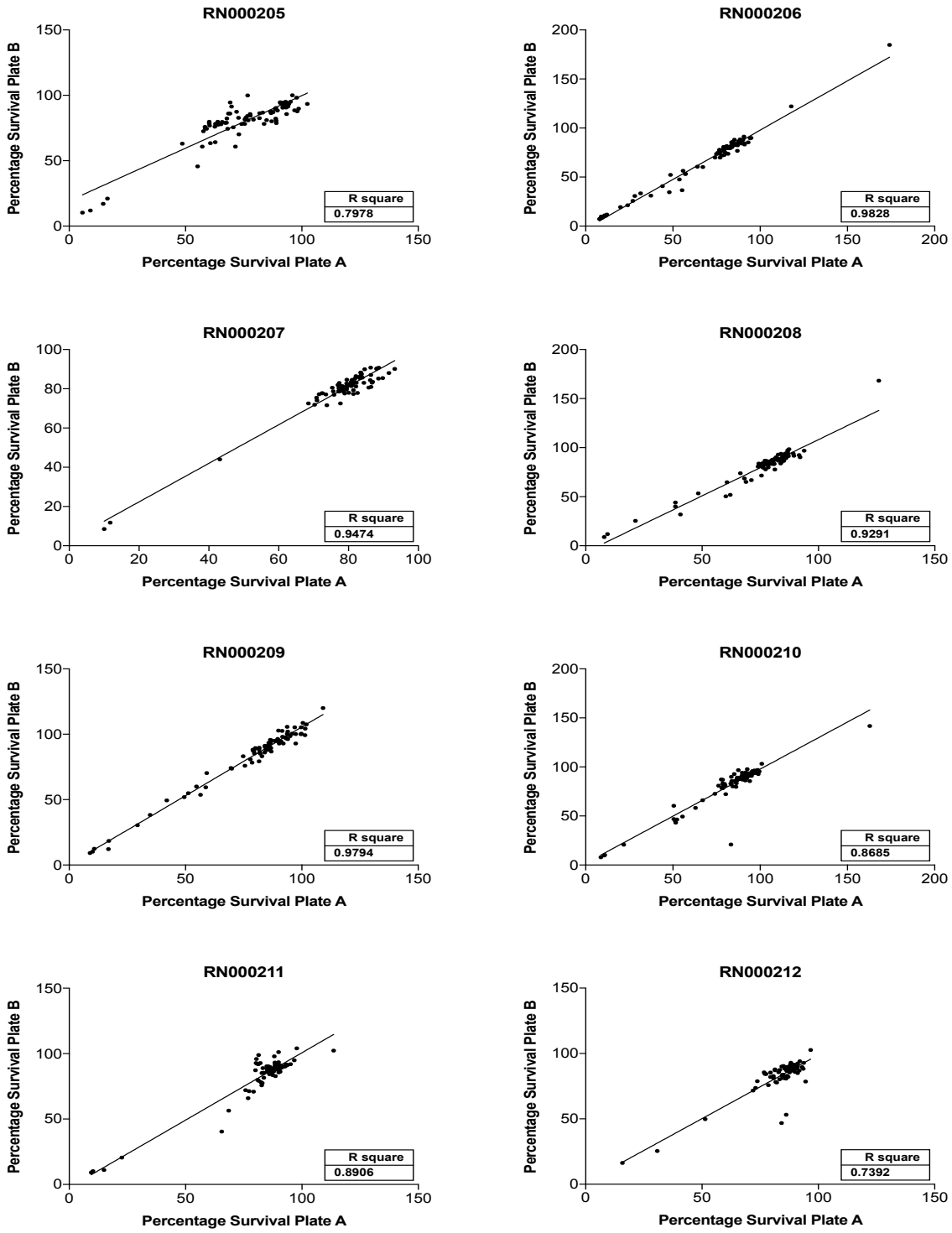

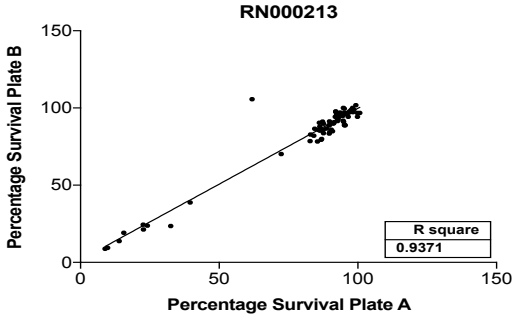
RN000213
Percentage Survival Plate B
Percentage Survival Plate A
R square
0.9371

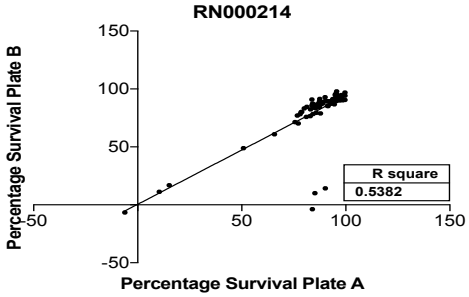
RN000214
Percentage Survival Plate B
Percentage Survival Plate A
R square
0.5382

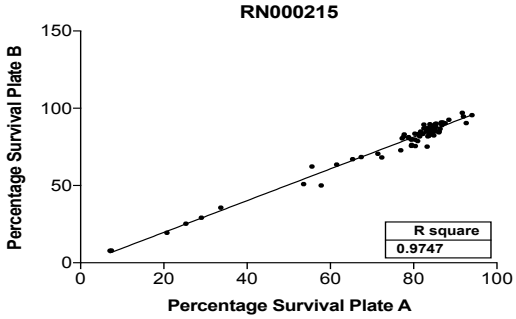
RN000215
Percentage Survival Plate B
Percentage Survival Plate A
R square
0.9747

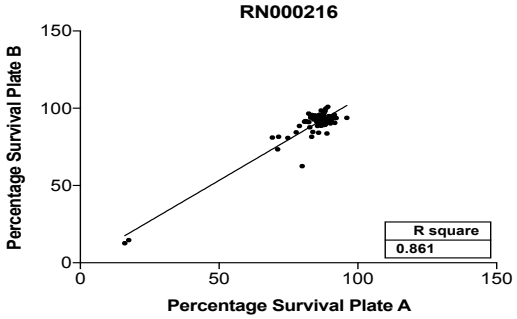
RN000216
Percentage Survival Plate B
Percentage Survival Plate A
R square
0.861

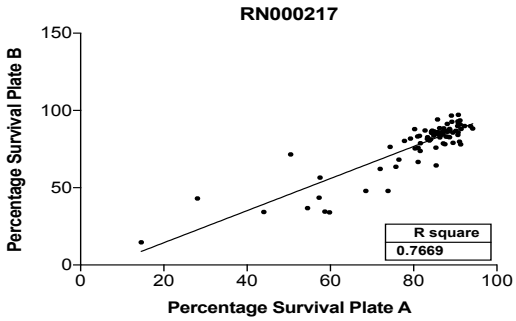
RN000217
Percentage Survival Plate B
Percentage Survival Plate A
R square
0.7669

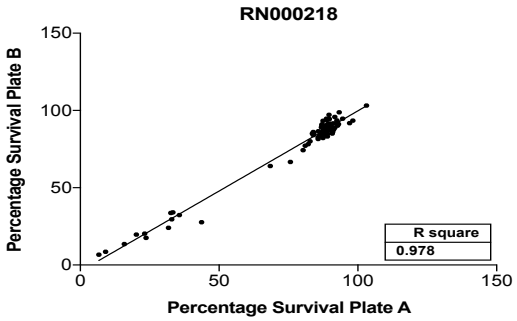
RN000218
Percentage Survival Plate B
Percentage Survival Plate A
R square
0.978

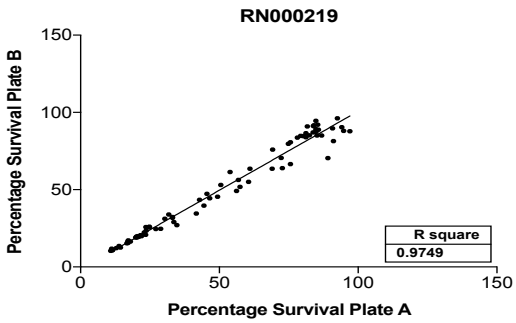
RN000219
Percentage Survival Plate B
Percentage Survival Plate A
R square
0.9749

Appendix 6: A dose response curve to determine the minimum inhibitory concentration for the selected drugs against *M. smegmatis* _pSMT3_eGFP

Tamoxifen citrate

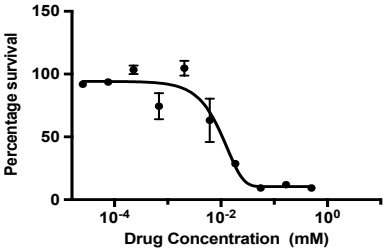

Meclocyline sulfosalicylate

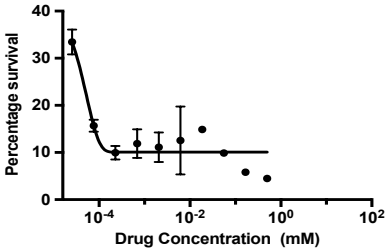

Clomiphene citrate

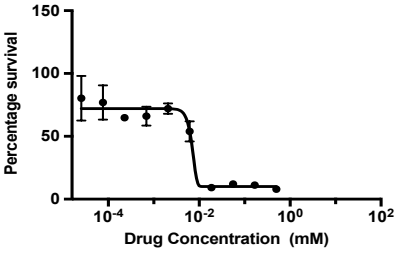

GBR 12909

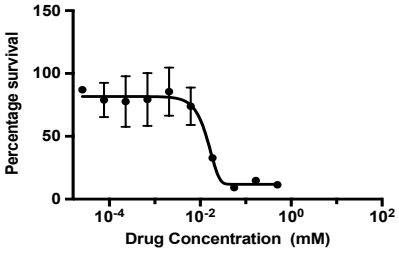

Sulocitidil

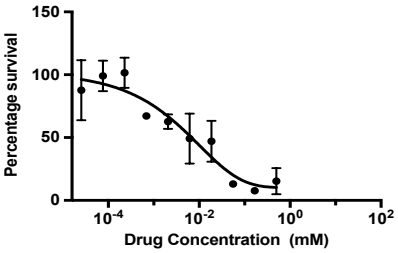

Fendiline hydrochloride

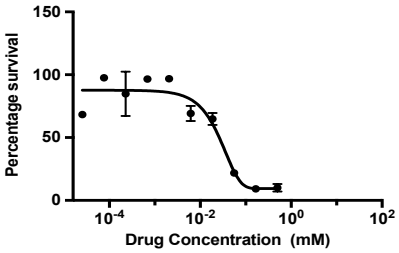

Fendiline hydrochloride

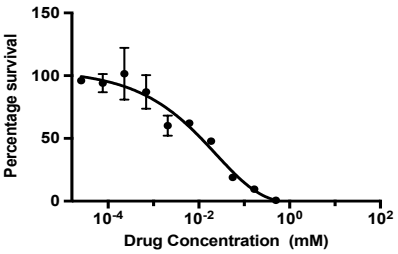

Auranofin

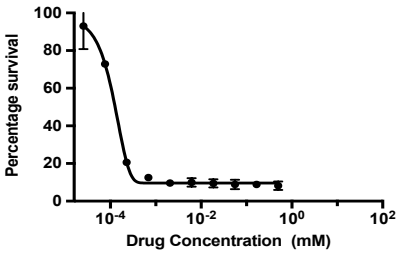

Fluspirelene

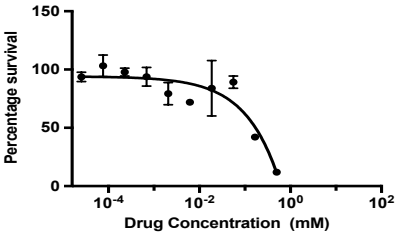

Sertraline

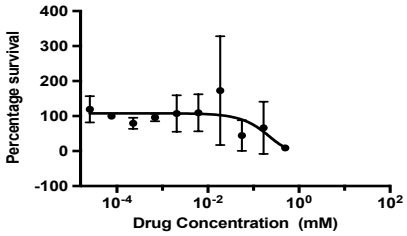

Ebselen

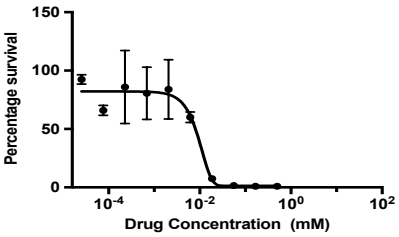

Chlorhexidine

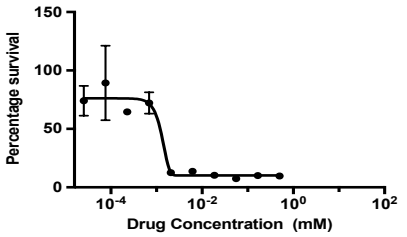

Alexidine

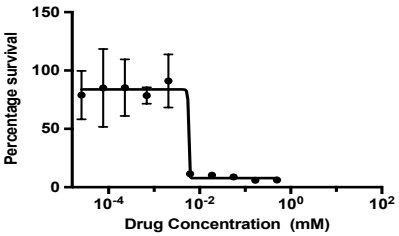

Raloxifene

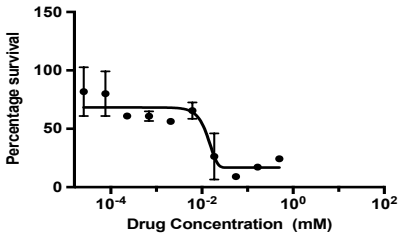

Nisoldipine

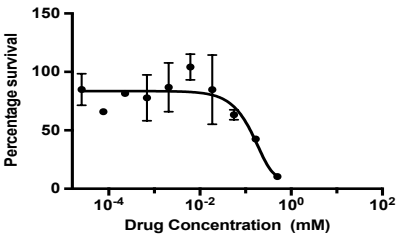

Toremifene

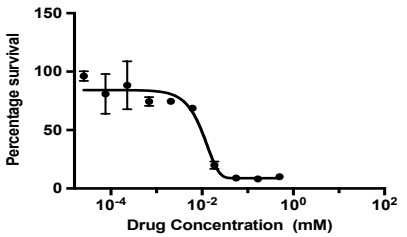

Appendix 7: A dose response curve to determine the minimum inhibitory concentration for the selected drugs against *M. bovis BCG* _pSMT3_eGFP

Josamycin

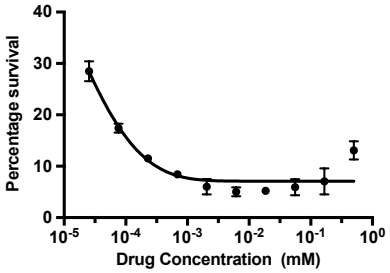

Pentamidine

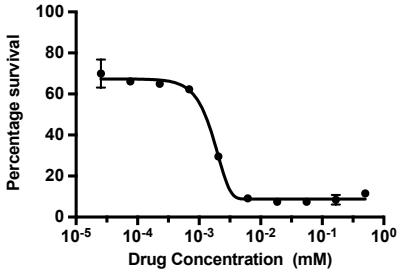

Thonzonium

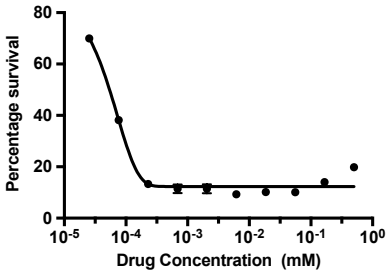

Florfenicol

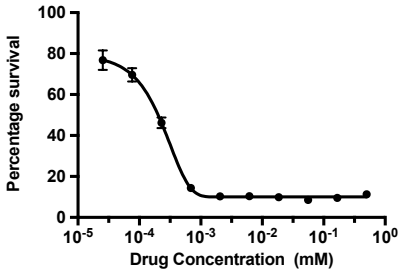

Glipizide

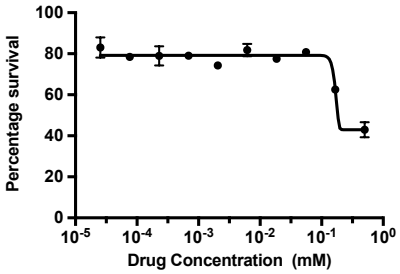

Granisteron

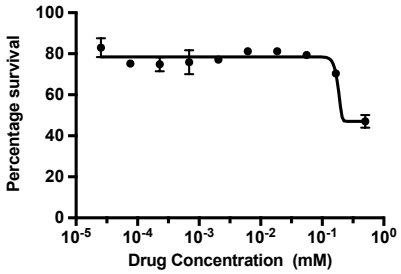

Olopatadine

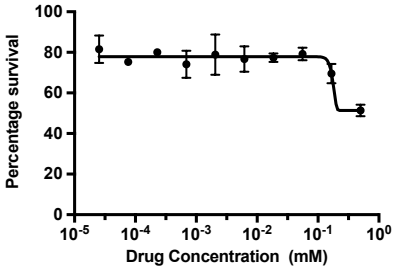

Astemizole

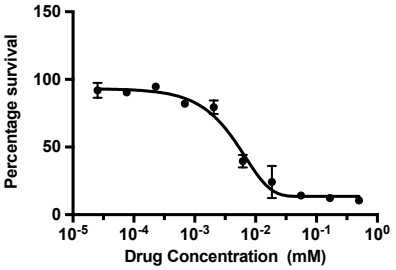

Tripelennamine

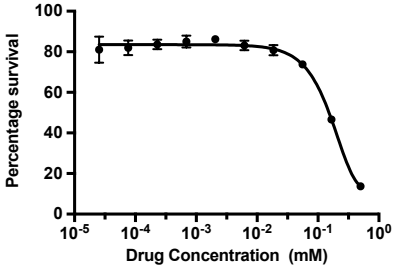

Rosiglitazone

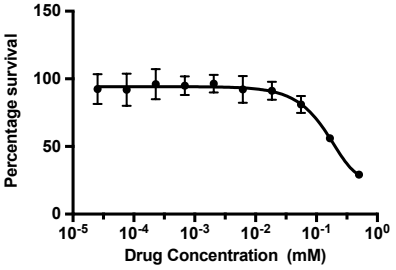

Phenteramine

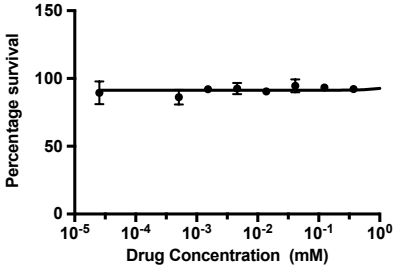

Pinaverium

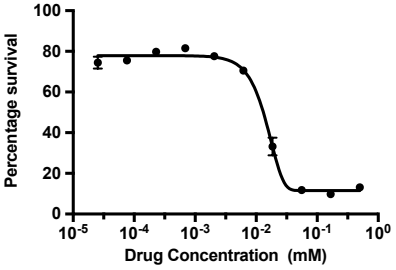

Appendix 8: Solid MIC testing of preliminary hits from the FDA library against *M. smegmatis* mc^{2}155. The solid MIC testing was performed against a. Sulocitidil, b. Auranofin, c. Raloxifen, d. Clomiphene citrate, e. Chlorhexidine, f. Fendiline hydrochloride, g. Tamoxifen citrate, h. Meclocyline sulfosalicylate, i. GBR12909, j. Nisoldipine, k. Sertraline, l. Toremifene, m. Apomorphine in the presence of a negative and positive control.

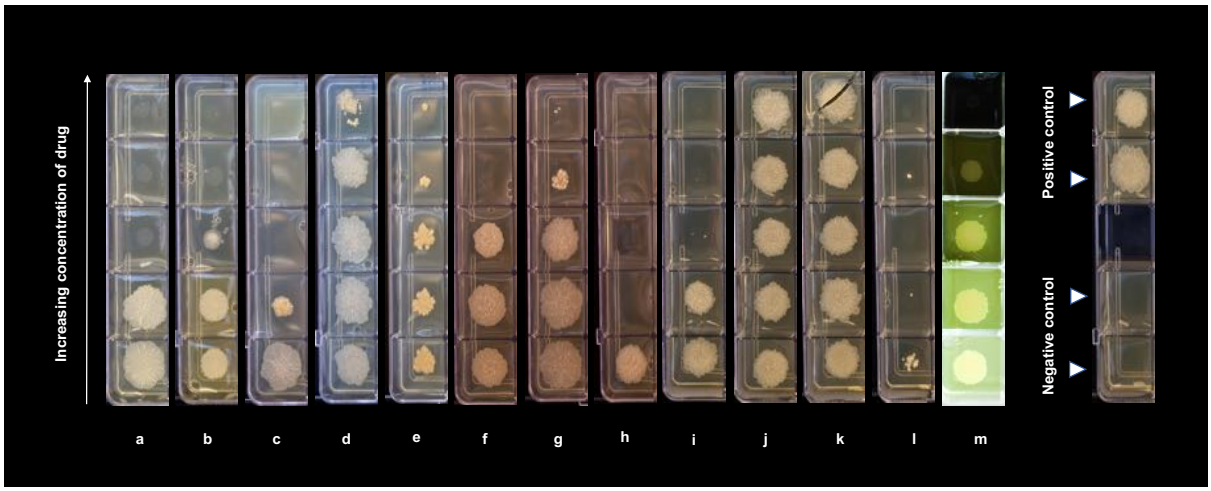

Appendix 9: Solid MIC testing of preliminary hits from the FDA library against *M. bovis* BCG. The solid MIC testing was done against a. Rosiglitazone, b. Pinaverium, c. Astemizole, d. Olopatadine, e. Glipizide, f. Tripelennamine, g. Pentamidine, h. Thonzonium, i. Florfenicol, j. Josamycin in the presence of a negative and positive control

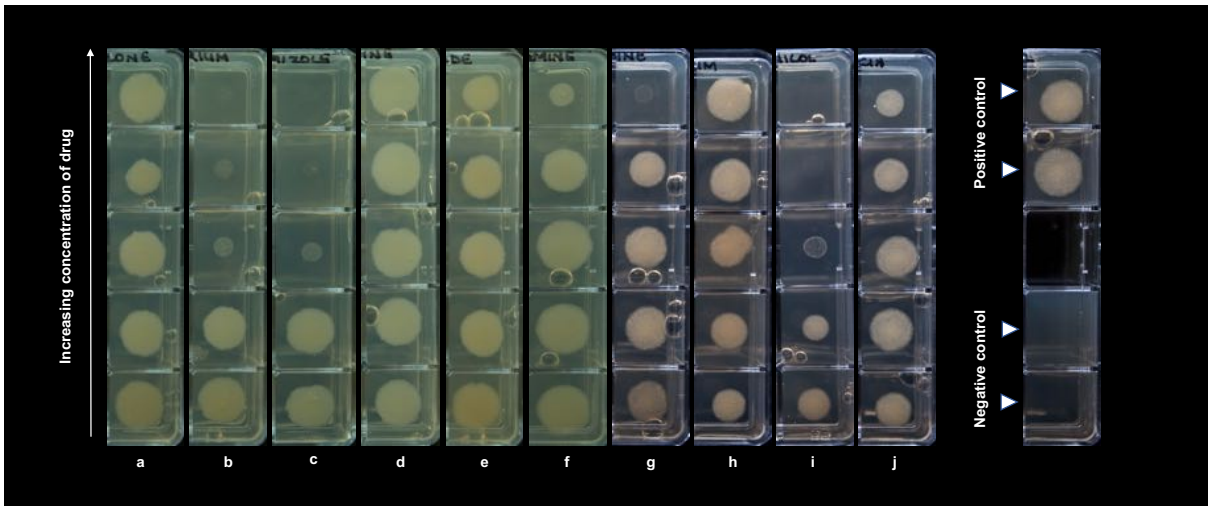

Appendix 10: The Prestwick drug library plate map. The table details the drug name in each assay plate number with the well identification.

Drug name	Plate number	Well ID
Azaguanine-8	RN000205	A02
Allantoin	RN000205	A03
Acetazolamide	RN000205	A04
Metformin hydrochloride	RN000205	A05
Atracurium besylate	RN000205	A06
Isoflupredone acetate	RN000205	A07
Amiloride hydrochloride dihydrate	RN000205	A08
Sulfaguanidine	RN000205	A11
Meticrane	RN000205	B02
Benzonatate	RN000205	B03
Hydroflumethiazide	RN000205	B04
Sulfacetamide sodic hydrate	RN000205	B05
Heptaminol hydrochloride	RN000205	B06
Sulfathiazole	RN000205	B07
Levodopa	RN000205	B08
Idoxuridine	RN000205	B09
Captopril	RN000205	B10
Minoxidil	RN000205	B11
Sulfaphenazole	RN000205	C02
Panthenol (D)	RN000205	C03
Sulfadiazine	RN000205	C04
Norethynodrel	RN000205	C05
Thiamphenicol	RN000205	C06
Cimetidine	RN000205	C07
Doxylamine succinate	RN000205	C08
Ethambutol dihydrochloride	RN000205	C09
Antipyrine	RN000205	C10
Antipyrine, 4-hydroxy	RN000205	C11
Chloramphenicol	RN000205	D02
Epirizole	RN000205	D03
Diprophylline	RN000205	D04
Triamterene	RN000205	D05
Dapsone	RN000205	D06
Troleandomycin	RN000205	D07
Pyrimethamine	RN000205	D08
Hexamethonium dibromide dihydrate	RN000205	D09
Diflunisal	RN000205	D10
Niclosamide	RN000205	D11
Procaine hydrochloride	RN000205	E02
Moxisylyte hydrochoride	RN000205	E03
Betazole hydrochloride	RN000205	E04
Isoxicam	RN000205	E05

Naproxen	RN000205	E06
Naphazoline hydrochloride	RN000205	E07
Ticlopidine hydrochloride	RN000205	E08
Dicyclomine hydrochloride	RN000205	E09
Amyleine hydrochloride	RN000205	E10
Lidocaine hydrochloride	RN000205	E11
Trichlorfon	RN000205	F02
Carbamazepine	RN000205	F03
Triflupromazine hydrochloride	RN000205	F04
Mefenamic acid	RN000205	F05
Acetohexamide	RN000205	F06
Sulpiride	RN000205	F07
Benoxinate hydrochloride	RN000205	F08
Oxethazaine	RN000205	F09
Pheniramine maleate	RN000205	F10
Tolazoline hydrochloride	RN000205	F11
Morantel tartrate	RN000205	G02
Homatropine hydrobromide (R,S)	RN000205	G03
Nifedipine	RN000205	G04
Chlorpromazine hydrochloride	RN000205	G05
Diphenhydramine hydrochloride	RN000205	G06
Minaprine dihydrochloride	RN000205	G07
Miconazole	RN000205	G08
Isoxsuprine hydrochloride	RN000205	G09
Acebutolol hydrochloride	RN000205	G10
Tolnaftate	RN000205	G11
Todralazine hydrochloride	RN000205	H02
Imipramine hydrochloride	RN000205	H03
Sulindac	RN000205	H04
Amitryptiline hydrochloride	RN000205	H05
Fulvestrant	RN000206	A03
Busulfan	RN000206	A10
Nocodazole	RN000206	B11
R(-) Apomorphine hydrochloride hemihydrate	RN000206	C02
Amoxapine	RN000206	C03
Cyproheptadine hydrochloride	RN000206	C04
Famotidine	RN000206	C05
Danazol	RN000206	C06
Nicorandil	RN000206	C07
Pioglitazone	RN000206	C08
Nomifensine maleate	RN000206	C09
Dizocilpine maleate	RN000206	C10
Oxandrolone	RN000206	C11
Naloxone hydrochloride	RN000206	D02
Metolazone	RN000206	D03
Ciprofloxacin hydrochloride monohydrate	RN000206	D04

Ampicillin trihydrate	RN000206	D05
Haloperidol	RN000206	D06
Naltrexone hydrochloride dihydrate	RN000206	D07
Chlorpheniramine maleate	RN000206	D08
Nalbuphine hydrochloride	RN000206	D09
Picotamide monohydrate	RN000206	D10
Triamcinolone	RN000206	D11
Bromocryptine mesylate	RN000206	E02
Amfepramone hydrochloride	RN000206	E03
Dehydrocholic acid	RN000206	E04
Tioconazole	RN000206	E05
Perphenazine	RN000206	E06
Mefloquine hydrochloride	RN000206	E07
Isoconazole	RN000206	E08
Spironolactone	RN000206	E09
Pirenzepine dihydrochloride	RN000206	E10
Dexamethasone acetate	RN000206	E11
Glipizide	RN000206	F02
Loxapine succinate	RN000206	F03
Hydroxyzine dihydrochloride	RN000206	F04
Diltiazem hydrochloride	RN000206	F05
Methotrexate	RN000206	F06
Astemizole	RN000206	F07
Clindamycin hydrochloride	RN000206	F08
Terfenadine	RN000206	F09
Cefotaxime sodium salt	RN000206	F10
Tetracycline hydrochloride	RN000206	F11
Verapamil hydrochloride	RN000206	G02
Dipyridamole	RN000206	G03
Chlorhexidine	RN000206	G04
Loperamide hydrochloride	RN000206	G05
Chlortetracycline hydrochloride	RN000206	G06
Tamoxifen citrate	RN000206	G07
Nicergoline	RN000206	G08
Canrenoic acid potassium salt	RN000206	G09
Thioproperazine dimesylate	RN000206	G10
Dihydroergotamine tartrate	RN000206	G11
Erythromycin	RN000206	H02
Chloroxine	RN000206	H03
Didanosine	RN000206	H04
Josamycin	RN000206	H05
Paclitaxel	RN000206	H06
Ivermectin	RN000206	H07
Gallamine triethiodide	RN000206	H08
Neomycin sulfate	RN000206	H09
Dihydrostreptomycin sulfate	RN000206	H10

Gentamicine sulfate	RN000206	H11
Isoniazid	RN000207	A02
Pentylenetetrazole	RN000207	A03
Chlorzoxazone	RN000207	A04
Ornidazole	RN000207	A05
Ethosuximide	RN000207	A06
Mafenide hydrochloride	RN000207	A07
Riluzole hydrochloride	RN000207	A08
Nitrofurantoin	RN000207	A09
Hydralazine hydrochloride	RN000207	A10
Phenelzine sulfate	RN000207	A11
Tranexamic acid	RN000207	B02
Etofylline	RN000207	B03
Tranylcypromine hydrochloride	RN000207	B04
Alverine citrate salt	RN000207	B05
Aceclofenac	RN000207	B06
Iproniazide phosphate	RN000207	B07
Sulfamethoxazole	RN000207	B08
Mephenesin	RN000207	B09
Phenformin hydrochloride	RN000207	B10
Flutamide	RN000207	B11
Ampyrone	RN000207	C02
Levamisole hydrochloride	RN000207	C03
Pargyline hydrochloride	RN000207	C04
Methocarbamol	RN000207	C05
Aztreonam	RN000207	C06
Cloxacillin sodium salt	RN000207	C07
Catharanthine	RN000207	C08
Pentolinium bitartrate	RN000207	C09
Aminopurine, 6-benzyl	RN000207	C10
Tolbutamide	RN000207	C11
Midodrine hydrochloride	RN000207	D02
Thalidomide	RN000207	D03
Oxolinic acid	RN000207	D04
Nimesulide	RN000207	D05
Asenapine maleate	RN000207	D06
Pentoxifylline	RN000207	D07
Metaraminol bitartrate	RN000207	D08
Salbutamol	RN000207	D09
Prilocaine hydrochloride	RN000207	D10
Camptothecine (S,+)	RN000207	D11
Ranitidine hydrochloride	RN000207	E02
Tiratricol, 3,3',5-triiodothyroacetic acid	RN000207	E03
Flufenamic acid	RN000207	E04
Flumequine	RN000207	E05

Tolfenamic acid	RN000207	E06
Meclofenamic acid sodium salt monohydrate	RN000207	E07
Tibolone	RN000207	E08
Trimethoprim	RN000207	E09
Metoclopramide monohydrochloride	RN000207	E10
Fenbendazole	RN000207	E11
Piroxicam	RN000207	F02
Pyrantel tartrate	RN000207	F03
Fenspiride hydrochloride	RN000207	F04
Gemfibrozil	RN000207	F05
Mefexamide hydrochloride	RN000207	F06
Tiapride hydrochloride	RN000207	F07
Mebendazole	RN000207	F08
Fenbufen	RN000207	F09
Ketoprofen	RN000207	F10
Indapamide	RN000207	F11
Norfloxacin	RN000207	G02
Antimycin A	RN000207	G03
Xylometazoline hydrochloride	RN000207	G04
Oxymetazoline hydrochloride	RN000207	G05
Nifenazone	RN000207	G06
Griseofulvin	RN000207	G07
Clemizole hydrochloride	RN000207	G08
Tropicamide	RN000207	G09
Nefopam hydrochloride	RN000207	G10
Phentolamine hydrochloride	RN000207	G11
Etodolac	RN000207	H02
Scopolamin-N-oxide hydrobromide	RN000207	H03
Hyoscyamine (L)	RN000207	H04
Chlorphensin carbamate	RN000207	H05
Fadrozole hydrochloride	RN000207	H06
Dilazep dihydrochloride	RN000207	H07
Ofloxacin	RN000207	H08
Lomefloxacin hydrochloride	RN000207	H09
Orphenadrine hydrochloride	RN000207	H10
Proglumide	RN000207	H11
Mexiletine hydrochloride	RN000208	A02
Flavoxate hydrochloride	RN000208	A03
Bufexamac	RN000208	A04
Glutethimide, para-amino	RN000208	A05
Dropropizine (R,S)	RN000208	A06
Pinacidil	RN000208	A07
Albendazole	RN000208	A08
Clonidine hydrochloride	RN000208	A09
Bupropion hydrochloride	RN000208	A10
Alprenolol hydrochloride	RN000208	A11

Chlorothiazide	RN000208	B02
Diphenidol hydrochloride	RN000208	B03
Norethindrone	RN000208	B04
Nortriptyline hydrochloride	RN000208	B05
Niflumic acid	RN000208	B06
Isotretinoin	RN000208	B07
Retinoic acid	RN000208	B08
Antazoline hydrochloride	RN000208	B09
Ethacrynic acid	RN000208	B10
Praziquantel	RN000208	B11
Ethisterone	RN000208	C02
Triprolidine hydrochloride	RN000208	C03
Doxepin hydrochloride	RN000208	C04
Dyclonine hydrochloride	RN000208	C05
Dimenhydrinate	RN000208	C06
Disopyramide	RN000208	C07
Clotrimazole	RN000208	C08
Vinpocetine	RN000208	C09
Clomipramine hydrochloride	RN000208	C10
Fendiline hydrochloride	RN000208	C11
Vincamine	RN000208	D02
Indomethacin	RN000208	D03
Cortisone	RN000208	D04
Prednisolone	RN000208	D05
Fenofibrate	RN000208	D06
Bumetanide	RN000208	D07
Labetalol hydrochloride	RN000208	D08
Cinnarizine	RN000208	D09
Methylprednisolone, 6-alpha	RN000208	D10
Quinidine hydrochloride monohydrate	RN000208	D11
Fludrocortisone acetate	RN000208	E02
Fenoterol hydrobromide	RN000208	E03
Homochlorcyclizine dihydrochloride	RN000208	E04
Diethylcarbamazine citrate	RN000208	E05
Chenodiol	RN000208	E06
Perhexiline maleate	RN000208	E07
Oxybutynin chloride	RN000208	E08
Spiperone	RN000208	E09
Pyrilamine maleate	RN000208	E10
Sulfinpyrazone	RN000208	E11
Dantrolene sodium salt	RN000208	F02
Trazodone hydrochloride	RN000208	F03
Glafenine hydrochloride	RN000208	F04
Pimethixene maleate	RN000208	F05
Pergolide mesylate	RN000208	F06
Acemetacin	RN000208	F07

Benzydamine hydrochloride	RN000208	F08
Fipexide hydrochloride	RN000208	F09
Mifepristone	RN000208	F10
Diperodon hydrochloride	RN000208	F11
Lisinopril	RN000208	G02
Lincomycin hydrochloride	RN000208	G03
Telenzepine dihydrochloride	RN000208	G04
Econazole nitrate	RN000208	G05
Bupivacaine hydrochloride	RN000208	G06
Clemastine fumarate	RN000208	G07
Oxytetracycline dihydrate	RN000208	G08
Pimozide	RN000208	G09
Amodiaquin dihydrochloride dihydrate	RN000208	G10
Mebeverine hydrochloride	RN000208	G11
Ifenprodil tartrate	RN000208	H02
Flunarizine dihydrochloride	RN000208	H03
Trifluoperazine dihydrochloride	RN000208	H04
Enalapril maleate	RN000208	H05
Minocycline hydrochloride	RN000208	H06
Glibenclamide	RN000208	H07
Guanethidine sulfate	RN000208	H08
Quinacrine dihydrochloride dihydrate	RN000208	H09
Clofilium tosylate	RN000208	H10
Fluphenazine dihydrochloride	RN000208	H11
Streptomycin sulfate	RN000209	A02
Alfuzosin hydrochloride	RN000209	A03
Chlorpropamide	RN000209	A04
Phenylpropanolamine hydrochloride	RN000209	A05
Ascorbic acid	RN000209	A06
Methyldopa (L,-)	RN000209	A07
Cefoperazone dihydrate	RN000209	A08
Zoxazolamine	RN000209	A09
Tacrine hydrochloride	RN000209	A10
Bisoprolol fumarate	RN000209	A11
Tremorine dihydrochloride	RN000209	B02
Practolol	RN000209	B03
Zidovudine, AZT	RN000209	B04
Sulfisoxazole	RN000209	B05
Zaprinast	RN000209	B06
Chlormezanone	RN000209	B07
Procainamide hydrochloride	RN000209	B08
N6-methyladenosine	RN000209	B09
Guanfacine hydrochloride	RN000209	B10
Domperidone	RN000209	B11
Furosemide	RN000209	C02
Methapyrilene hydrochloride	RN000209	C03

Desipramine hydrochloride	RN000209	C04
Clorgyline hydrochloride	RN000209	C05
Clenbuterol hydrochloride	RN000209	C06
Maprotiline hydrochloride	RN000209	C07
Thioguanosine	RN000209	C08
Chlorprothixene hydrochloride	RN000209	C09
Ritodrine hydrochloride	RN000209	C10
Clozapine	RN000209	C11
Chlorthalidone	RN000209	D02
Dobutamine hydrochloride	RN000209	D03
Moclobemide	RN000209	D04
Clopamide	RN000209	D05
Hycanthone	RN000209	D06
Adenosine 5'-monophosphate monohydrate	RN000209	D07
Amoxicillin	RN000209	D08
Pemirolast potassium	RN000209	D09
Dextromethorphan hydrobromide monohydrate	RN000209	D10
Droperidol	RN000209	D11
Bambuterol hydrochloride	RN000209	E02
Betamethasone	RN000209	E03
Colchicine	RN000209	E04
Metergoline	RN000209	E05
Brinzolamide	RN000209	E06
Ambroxol hydrochloride	RN000209	E07
Benfluorex hydrochloride	RN000209	E08
Bepridil hydrochloride	RN000209	E09
Meloxicam	RN000209	E10
Benzbromarone	RN000209	E11
Ketotifen fumarate	RN000209	F02
Debrisoquin sulfate	RN000209	F03
Amethopterin (R,S)	RN000209	F04
Methylergometrine maleate	RN000209	F05
Methiothepin maleate	RN000209	F06
Clofazimine	RN000209	F07
Nafronyl oxalate	RN000209	F08
Bezafibrate	RN000209	F09
Nefazodone hcl	RN000209	F10
Clebopride maleate	RN000209	F11
Lidoflazine	RN000209	G02
Betaxolol hydrochloride	RN000209	G03
Nicardipine hydrochloride	RN000209	G04
Probucol	RN000209	G05
Mitoxantrone dihydrochloride	RN000209	G06
GBR 12909 dihydrochloride	RN000209	G07
Carbetapentane citrate	RN000209	G08
Dequalinium dichloride	RN000209	G09

Ketoconazole	RN000209	G10
Fusidic acid sodium salt	RN000209	G11
Terbutaline hemisulfate	RN000209	H02
Ketanserin tartrate hydrate	RN000209	H03
Hemicholinium bromide	RN000209	H04
Kanamycin A sulfate	RN000209	H05
Amikacin hydrate	RN000209	H06
Etoposide	RN000209	H07
Clomiphene citrate (Z,E)	RN000209	H08
Oxantel pamoate	RN000209	H09
Prochlorperazine dimaleate	RN000209	H10
Hesperidin	RN000209	H11
Testosterone propionate	RN000210	A02
Haloprogin	RN000210	A03
Thyroxine (L)	RN000210	A04
Idebenone	RN000210	A05
Pepstatin A	RN000210	A06
Morpholinoethylamino-3- benzocyclohepta-(5,6-c)- pyridazine dihydrochloride	RN000210	A07
Adamantamine fumarate	RN000210	A08
Butoconazole nitrate	RN000210	A09
Amiodarone hydrochloride	RN000210	A10
Amphotericin B	RN000210	A11
Androsterone	RN000210	B02
Amifostine	RN000210	B03
Carbarsone	RN000210	B04
Amlodipine	RN000210	B05
Modafinil	RN000210	B06
Bacampicillin hydrochloride	RN000210	B07
Lamivudine	RN000210	B08
Biotin	RN000210	B09
Bisacodyl	RN000210	B10
Erlotinib	RN000210	B11
Suloctidil	RN000210	C02
Zotepine	RN000210	C03
Carisoprodol	RN000210	C04
Cephalosporanic acid, 7-amino	RN000210	C05
Chicago sky blue 6B	RN000210	C06
Buflomedil hydrochloride	RN000210	C07
Dibenzepine hydrochloride	RN000210	C08
Roxatidine Acetate hcl	RN000210	C09
Valacyclovir hydrochloride	RN000210	C10
Cisapride	RN000210	C11
Pefloxacine	RN000210	D02
Corticosterone	RN000210	D03
Cyanocobalamin	RN000210	D04
Cefadroxil	RN000210	D05

Cyclosporin A	RN000210	D06
Digitoxigenin	RN000210	D07
Digoxin	RN000210	D08
Doxorubicin hydrochloride	RN000210	D09
Carbimazole	RN000210	D10
Epiandrosterone	RN000210	D11
Estradiol-17 beta	RN000210	E02
Clobutinol hydrochloride	RN000210	E03
Gabazine bromide	RN000210	E04
Oxcarbazepine	RN000210	E05
Cyclobenzaprine hydrochloride	RN000210	E06
Carteolol hydrochloride	RN000210	E07
Hydrocortisone base	RN000210	E08
Hydroxytacrine maleate (R,S)	RN000210	E09
Pilocarpine nitrate	RN000210	E10
Dicloxacillin sodium salt hydrate	RN000210	E11
Alizapride hcl	RN000210	F02
Stanozolol	RN000210	F03
Calcipotriene	RN000210	F04
Linezolid	RN000210	F05
Mebhydroline 1,5- naphtalenedisulfonate	RN000210	F06
Meclocycline sulfosalicylate	RN000210	F07
Meclozine dihydrochloride	RN000210	F08
Melatonin	RN000210	F09
Butalbital	RN000210	F10
Dinoprost trometamol	RN000210	F11
Tropisetron hcl	RN000210	G02
Cefixime	RN000210	G03
Metrizamide	RN000210	G04
Quetiapine hemifumarate	RN000210	G05
Tosufloxacin hydrochloride	RN000210	G06
Efavirenz	RN000210	G07
Rifapentine	RN000210	G08
Neostigmine bromide	RN000210	G09
Niridazole	RN000210	G10
Ceforanide	RN000210	G11
Vatalanib	RN000210	H02
Itopride	RN000210	H03
Cefotetan	RN000210	H04
Fentiazac	RN000210	H05
Brompheniramine maleate	RN000210	H06
Primaquine diphosphate	RN000210	H07
Progesterone	RN000210	H08
Felodipine	RN000210	H09
Raclopride	RN000210	H10
Closantel	RN000210	H11

Serotonin hydrochloride	RN000211	A02
Cefotiam hydrochloride	RN000211	A03
Rofecoxib	RN000211	A04
Benperidol	RN000211	A05
Cefaclor hydrate	RN000211	A06
Colistin sulfate	RN000211	A07
Daunorubicin hydrochloride	RN000211	A08
Dosulepin hydrochloride	RN000211	A09
Ceftazidime pentahydrate	RN000211	A10
Iobenguane sulfate	RN000211	A11
Metixene hydrochloride	RN000211	B02
Nitrofural	RN000211	B03
Omeprazole	RN000211	B04
Propylthiouracil	RN000211	B05
Terconazole	RN000211	B06
Tiaprofenic acid	RN000211	B07
Vancomycin hydrochloride	RN000211	B08
Artemisinin	RN000211	B09
Propafenone hydrochloride	RN000211	B10
Ethamivan	RN000211	B11
Vigabatrin	RN000211	C02
Biperiden hydrochloride	RN000211	C03
Cetirizine dihydrochloride	RN000211	C04
Etifenin	RN000211	C05
Metaproterenol sulfate, orciprenaline sulfate	RN000211	C06
Sisomicin sulfate	RN000211	C07
Sibutramine hcl	RN000211	C08
Acenocoumarol	RN000211	C09
Bromperidol	RN000211	C10
Cyclizine hydrochloride	RN000211	C11
Fluoxetine hydrochloride	RN000211	D02
Iohexol	RN000211	D03
Norcyclobenzaprine	RN000211	D04
Pyrazinamide	RN000211	D05
Trimethadione	RN000211	D06
Lovastatin	RN000211	D07
Nystatine	RN000211	D08
Budesonide	RN000211	D09
Imipenem	RN000211	D10
Sulfasalazine	RN000211	D11
Lofexidine	RN000211	E02
Thiostrepton	RN000211	E03
Miglitol	RN000211	E04
Tiabendazole	RN000211	E05
Rifampicin	RN000211	E06
Ethionamide	RN000211	E07

Tenoxicam	RN000211	E08
Triflusal	RN000211	E09
Mesoridazine besylate	RN000211	E10
Trolox	RN000211	E11
Pirenperone	RN000211	F02
Isoquinoline, 6,7-dimethoxy-1-methyl-1,2,3,4-tetrahydro, hydrochloride	RN000211	F03
Phenacetin	RN000211	F04
Atovaquone	RN000211	F05
Methoxamine hydrochloride	RN000211	F06
(S)-(-)-Atenolol	RN000211	F07
Piracetam	RN000211	F08
Phenindione	RN000211	F09
Thiocolchicoside	RN000211	F10
Clorsulon	RN000211	F11
Ciclopirox ethanolamine	RN000211	G02
Probenecid	RN000211	G03
Betahistine mesylate	RN000211	G04
Tobramycin	RN000211	G05
Tetramisole hydrochloride	RN000211	G06
Pregnenolone	RN000211	G07
Molsidomine	RN000211	G08
Chloroquine diphosphate	RN000211	G09
Trimetazidine dihydrochloride	RN000211	G10
Parthenolide	RN000211	G11
Hexetidine	RN000211	H02
Selegiline hydrochloride	RN000211	H03
Pentamidine isethionate	RN000211	H04
Tolazamide	RN000211	H05
Nifuroxazide	RN000211	H06
Mirtazapine	RN000211	H07
Dirithromycin	RN000211	H08
Gliclazide	RN000211	H09
DO 897/99	RN000211	H10
Prenylamine lactate	RN000211	H11
Ziprasidone Hydrochloride	RN000212	A02
Mevastatin	RN000212	A03
Pyridostigmine iodide	RN000212	A04
Pentobarbital	RN000212	A05
Atropine sulfate monohydrate	RN000212	A06
Eserine hemisulfate salt	RN000212	A07
Itraconazole	RN000212	A08
Acarbose	RN000212	A09
Entacapone	RN000212	A10
Nicotinamide	RN000212	A11
Tetracaïne hydrochloride	RN000212	B02
Mometasone furoate	RN000212	B03

Troglitazone	RN000212	B04
Dacarbazine	RN000212	B05
Tenatoprazole	RN000212	B06
Acetopromazine maleate salt	RN000212	B07
Escitalopram	RN000212	B08
Ropinirole hcl	RN000212	B09
Lacidipine	RN000212	B10
Argatroban	RN000212	B11
Reboxetine mesylate	RN000212	C02
Camylofine chlorhydrate	RN000212	C03
Papaverine hydrochloride	RN000212	C04
Yohimbine hydrochloride	RN000212	C05
Voriconazole	RN000212	C06
Alfacalcidol	RN000212	C07
Cilostazol	RN000212	C08
Galanthamine hydrobromide	RN000212	C09
Azelastine hcl	RN000212	C10
Etretinate	RN000212	C11
Emedastine	RN000212	D02
Etofenamate	RN000212	D03
Zaleplon	RN000212	D04
Diclofenac sodium	RN000212	D05
Exemestane	RN000212	D06
Fomepizole	RN000212	D07
Temozolomide	RN000212	D08
Xylazine	RN000212	D09
Celiprolol hcl	RN000212	D10
Zopiclone	RN000212	D11
Tranilast	RN000212	E02
Tizanidine hcl	RN000212	E03
Zafirlukast	RN000212	E04
Butenafine Hydrochloride	RN000212	E05
Carbadox	RN000212	E06
Rimantadine Hydrochloride	RN000212	E07
Eburnamonine (-)	RN000212	E08
Oxibendazol	RN000212	E09
Ipsapirone	RN000212	E10
Hydroxychloroquine sulfate	RN000212	E11
Loracarbef	RN000212	F02
Fenipentol	RN000212	F03
Diosmin	RN000212	F04
Carbidopa	RN000212	F05
(-)-Emtricitabine	RN000212	F06
Demecarium bromide	RN000212	F07
Quipazine dimaleate salt	RN000212	F08
Acipimox	RN000212	F09

Diflorasone Diacetate	RN000212	F10
Acamprosate calcium	RN000212	F11
Mizolastine	RN000212	G02
Amisulpride	RN000212	G03
Pyridoxine hydrochloride	RN000212	G04
Mercaptopurine	RN000212	G05
Cytarabine	RN000212	G06
Racecadotril	RN000212	G07
Folic acid	RN000212	G08
Benazepril hcl	RN000212	G09
Aniracetam	RN000212	G10
Dimethisoquin hydrochloride	RN000212	G11
Alendronate sodium	RN000212	H02
Dipivefrin hydrochloride	RN000212	H03
Thiorphan	RN000212	H04
Tomoxetine hydrochloride	RN000212	H05
Aceclidine Hydrochloride	RN000212	H06
Penciclovir	RN000212	H07
Levetiracetam	RN000212	H08
Dexfenfluramine hydrochloride	RN000212	H09
Etoricoxib	RN000212	H10
Sertindole	RN000212	H11
Sulmazole	RN000213	A02
Gefitinib	RN000213	A03
Flunisolide	RN000213	A04
N-Acetyl-DL-homocysteine Thiolactone	RN000213	A05
Flurandrenolide	RN000213	A06
Oxiconazole Nitrate	RN000213	A07
Rebamipide	RN000213	A08
Nilvadipine	RN000213	A09
Etanidazole	RN000213	A10
Pinaverium bromide	RN000213	A11
Glimepiride	RN000213	B02
Picrotoxinin	RN000213	B03
Mepenzolate bromide	RN000213	B04
Benfotiamine	RN000213	B05
Halcinonide	RN000213	B06
Lanatoside C	RN000213	B07
Benzamil hydrochloride	RN000213	B08
Suxibuzone	RN000213	B09
6-Furfurylaminopurine	RN000213	B10
Avermectin B1a	RN000213	B11
Pranlukast	RN000213	C02
Penicillamine	RN000213	C03
Zileuton	RN000213	C04
Loratadine	RN000213	C05

Tetraethylenepentamine pentahydrochloride	RN000213	C06
Nisoldipine	RN000213	C07
Acefylline	RN000213	C08
Acitretin	RN000213	C09
Zonisamide	RN000213	C10
Irsogladine maleate	RN000213	C11
Dydrogesterone	RN000213	D02
Sumatriptan succinate	RN000213	D03
Opipramol dihydrochloride	RN000213	D04
Nalidixic acid sodium salt	RN000213	D05
Oxacillin sodium	RN000213	D06
Beta-Escin	RN000213	D07
Thiamine hydrochloride	RN000213	D08
Tazobactam	RN000213	D09
Ibandronate sodium	RN000213	D10
Warfarin	RN000213	D11
Pranoprofen	RN000213	E02
Secnidazole	RN000213	E03
Pempidine tartrate	RN000213	E04
Clodronate	RN000213	E05
Ibutilide fumarate	RN000213	E06
Thimerosal	RN000213	E07
Tramadol hydrochloride	RN000213	E08
Estropipate	RN000213	E09
Butylscopolammonium (n-) bromide	RN000213	E10
Irinotecan hydrochloride trihydrate	RN000213	E11
Tylosin	RN000213	F02
Citalopram Hydrobromide	RN000213	F03
Promazine hydrochloride	RN000213	F04
Sulfamerazine	RN000213	F05
Venlafaxine	RN000213	F06
Ethotoin	RN000213	F07
3-alpha-Hydroxy-5-beta-androstan-17-one	RN000213	F08
Tetrahydrozoline hydrochloride	RN000213	F09
Hexestrol	RN000213	F10
Cefmetazole sodium salt	RN000213	F11
Trihexyphenidyl-D,L Hydrochloride	RN000213	G02
Succinylsulfathiazole	RN000213	G03
Famprofazone	RN000213	G04
Bromopride	RN000213	G05
Methyl benzethonium chloride	RN000213	G06
Chlorcyclizine hydrochloride	RN000213	G07
Diphenylpyraline hydrochloride	RN000213	G08
Benzethonium chloride	RN000213	G09
Trioxsalen	RN000213	G10
Doxofylline	RN000213	G11

Sulfabenzamide	RN000213	H02
Benzocaine	RN000213	H03
Dipyrone	RN000213	H04
Isosorbide dinitrate	RN000213	H05
Sulfachloropyridazine	RN000213	H06
Pramoxine hydrochloride	RN000213	H07
Finasteride	RN000213	H08
Fluorometholone	RN000213	H09
Cephalothin sodium salt	RN000213	H10
Cefuroxime sodium salt	RN000213	H11
Althiazide	RN000214	A02
Isopyrin hydrochloride	RN000214	A03
Phenethicillin potassium salt	RN000214	A04
Sulfamethoxypyridazine	RN000214	A05
Deferoxamine mesylate	RN000214	A06
Mephentermine hemisulfate	RN000214	A07
Liranaftate	RN000214	A08
Sulfadimethoxine	RN000214	A09
Sulfanilamide	RN000214	A10
Balsalazide Sodium	RN000214	A11
Sulfaquinoxaline sodium salt	RN000214	B02
Streptozotocin	RN000214	B03
Metoprolol-(+,-) (+)-tartrate salt	RN000214	B04
Flumethasone	RN000214	B05
Flecainide acetate	RN000214	B06
Cefazolin sodium salt	RN000214	B07
Atractyloside potassium salt	RN000214	B08
Folinic acid calcium salt	RN000214	B09
Levonordefrin	RN000214	B10
Ebselen	RN000214	B11
Nadide	RN000214	C02
Sulfamethizole	RN000214	C03
Medrysone	RN000214	C04
Flunixin meglumine	RN000214	C05
Glycopyrrolate	RN000214	C07
Aprepitant	RN000214	C08
Monensin sodium salt	RN000214	C09
Isoetharine mesylate salt	RN000214	C10
Mevalonic-D, L acid lactone	RN000214	C11
Terazosin hydrochloride	RN000214	D02
Phenazopyridine hydrochloride	RN000214	D03
Demeclocycline hydrochloride	RN000214	D04
Fenoprofen calcium salt dihydrate	RN000214	D05
Piperacillin sodium salt	RN000214	D06
Diethylstilbestrol	RN000214	D07
Chlorotrianisene	RN000214	D08

Ribostamycin sulfate salt	RN000214	D09
Methacholine chloride	RN000214	D10
Pipenzolate bromide	RN000214	D11
Butamben	RN000214	E02
Sulfapyridine	RN000214	E03
Meclofenoxate hydrochloride	RN000214	E04
Furaltadone hydrochloride	RN000214	E05
Ethoxyquin	RN000214	E06
Tinidazole	RN000214	E07
Guanadrel sulfate	RN000214	E08
Vidarabine	RN000214	E09
Sulfameter	RN000214	E10
Isopropamide iodide	RN000214	E11
Alclometasone dipropionate	RN000214	F02
Leflunomide	RN000214	F03
Norgestrel-(-)-D	RN000214	F04
Fluocinonide	RN000214	F05
Sulfamethazine sodium salt	RN000214	F06
Guaifenesin	RN000214	F07
Alexidine dihydrochloride	RN000214	F08
Proadifen hydrochloride	RN000214	F09
Zomepirac sodium salt	RN000214	F10
Cinoxacin	RN000214	F11
Clobetasol propionate	RN000214	G02
Podophyllotoxin	RN000214	G03
Clofibric acid	RN000214	G04
Bendroflumethiazide	RN000214	G05
Dicumarol	RN000214	G06
Methimazole	RN000214	G07
Merbromin	RN000214	G08
Hexylcaine hydrochloride	RN000214	G09
Drofenine hydrochloride	RN000214	G10
Cycloheximide	RN000214	G11
(R) -Naproxen sodium salt	RN000214	H02
Propidium iodide	RN000214	H03
Cloperastine hydrochloride	RN000214	H04
Eucatropine hydrochloride	RN000214	H05
Isocarboxazid	RN000214	H06
Lithocholic acid	RN000214	H07
Methotrimeprazine maleat salt	RN000214	H08
Dienestrol	RN000214	H09
Pridinol methanesulfonate salt	RN000214	H10
Amrinone	RN000214	H11
Carbinoxamine maleate salt	RN000215	A02
Methazolamide	RN000215	A03
Pyrithyldione	RN000215	A04

Spectinomycin dihydrochloride	RN000215	A05
Piromidic acid	RN000215	A06
Trimipramine maleate salt	RN000215	A07
Chloropyramine hydrochloride	RN000215	A08
Furazolidone	RN000215	A09
Dichlorphenamide	RN000215	A10
Sulconazole nitrate	RN000215	A11
Auranofin	RN000215	B02
Cromolyn disodium salt	RN000215	B03
Bucladesine sodium salt	RN000215	B04
Cefsulodin sodium salt	RN000215	B05
Fosfosal	RN000215	B06
Suprofen	RN000215	B07
Deflazacort	RN000215	B08
Nadolol	RN000215	B09
Moxalactam disodium salt	RN000215	B10
Aminophylline	RN000215	B11
Azlocillin sodium salt	RN000215	C02
Clidinium bromide	RN000215	C03
Sulfamonomethoxine	RN000215	C04
Benzthiazide	RN000215	C05
Trichlormethiazide	RN000215	C06
Oxalamine citrate salt	RN000215	C07
Propantheline bromide	RN000215	C08
Viloxazine hydrochloride	RN000215	C09
Dimethadione	RN000215	C10
Ethaverine hydrochloride	RN000215	C11
Butacaine	RN000215	D02
Cefoxitin sodium salt	RN000215	D03
Ifosfamide	RN000215	D04
Novobiocin sodium salt	RN000215	D05
Tetrahydroxy-1,4-quinone monohydrate	RN000215	D06
Indoprofen	RN000215	D07
Carbenoxolone disodium salt	RN000215	D08
Iocetamic acid	RN000215	D09
Ganciclovir	RN000215	D10
Ethopropazine hydrochloride	RN000215	D11
Olanzapine	RN000215	E02
Trimeprazine tartrate	RN000215	E03
Nafcillin sodium salt monohydrate	RN000215	E04
Procyclidine hydrochloride	RN000215	E05
Amiprilose hydrochloride	RN000215	E06
Ethynylestradiol 3-methyl ether	RN000215	E07
(-) -Levobunolol hydrochloride	RN000215	E08
Iodixanol	RN000215	E09
Clinafloxacin	RN000215	E10

Equilin	RN000215	E11
Paroxetine Hydrochloride	RN000215	F02
Nylidrin	RN000215	F03
Liothyronine	RN000215	F04
Roxithromycin	RN000215	F05
Beclomethasone dipropionate	RN000215	F06
Tolmetin sodium salt dihydrate	RN000215	F07
(+) -Levobunolol hydrochloride	RN000215	F08
Doxazosin mesylate	RN000215	F09
Fluvastatin sodium salt	RN000215	F10
Methylhydantoin-5-(L)	RN000215	F11
Gabapentin	RN000215	G02
Raloxifene hydrochloride	RN000215	G03
Etidronic acid, disodium salt	RN000215	G04
Methylhydantoin-5-(D)	RN000215	G05
Simvastatin	RN000215	G06
Azacytidine-5	RN000215	G07
Paromomycin sulfate	RN000215	G08
Acetaminophen	RN000215	G09
Phthalylsulfathiazole	RN000215	G10
Luteolin	RN000215	G11
Iopamidol	RN000215	H02
Iopromide	RN000215	H03
Theophylline monohydrate	RN000215	H04
Theobromine	RN000215	H05
Reserpine	RN000215	H06
Bicalutamide	RN000215	H07
Scopolamine hydrochloride	RN000215	H08
Ioversol	RN000215	H09
Rabeprazole Sodium salt	RN000215	H10
Carbachol	RN000215	H11
Niacin	RN000216	A02
Bemegride	RN000216	A03
Digoxigenin	RN000216	A04
Meglumine	RN000216	A05
Dolasetron mesilate	RN000216	A06
Clioquinol	RN000216	A07
Oxybenzone	RN000216	A08
Promethazine hydrochloride	RN000216	A09
Diacerein	RN000216	A10
Esmolol hydrochloride	RN000216	A11
Cortisol acetate	RN000216	B02
Flubendazol	RN000216	B03
Felbinac	RN000216	B04
Butylparaben	RN000216	B05
Aminohippuric acid	RN000216	B06

N-Acetyl-L-leucine	RN000216	B07
Pipemidic acid	RN000216	B08
Dioxybenzone	RN000216	B09
Adrenosterone	RN000216	B10
Methylatropine nitrate	RN000216	B11
Hymecromone	RN000216	C02
Abacavir Sulfate	RN000216	C03
Diloxanide furoate	RN000216	C04
Metyrapone	RN000216	C05
Urapidil hydrochloride	RN000216	C06
Fluspirilen	RN000216	C07
S-(+)-ibuprofen	RN000216	C08
Ethynodiol diacetate	RN000216	C09
Nabumetone	RN000216	C10
Nisoxetine hydrochloride	RN000216	C11
(+)-Isoproterenol (+)-bitartrate salt	RN000216	D02
Monobenzone	RN000216	D03
2-Aminobenzenesulfonamide	RN000216	D04
Estrone	RN000216	D05
Lorglumide sodium salt	RN000216	D06
Nitrendipine	RN000216	D07
Flurbiprofen	RN000216	D08
Nimodipine	RN000216	D09
Bacitracin	RN000216	D10
L(-)-vesamicol hydrochloride	RN000216	D11
Nizatidine	RN000216	E02
Thioperamide maleate	RN000216	E03
Xamoterol hemifumarate	RN000216	E04
Rolipram	RN000216	E05
Thonzonium bromide	RN000216	E06
Idazoxan hydrochloride	RN000216	E07
Quinapril HCl	RN000216	E08
Nilutamide	RN000216	E09
Ketorolac tromethamine	RN000216	E10
Protriptyline hydrochloride	RN000216	E11
Propofol	RN000216	F02
S(-)Eticlopride hydrochloride	RN000216	F03
Primidone	RN000216	F04
Flucytosine	RN000216	F05
(-)-MK 801 hydrogen maleate	RN000216	F06
Bephenium hydroxynaphthoate	RN000216	F07
Dehydroisoandosterone 3-acetate	RN000216	F08
Benserazide hydrochloride	RN000216	F09
Iodipamide	RN000216	F10
Allopurinol	RN000216	F11
Pentetic acid	RN000216	G02

Bretylium tosylate	RN000216	G03
Pralidoxime chloride	RN000216	G04
Phenoxybenzamine hydrochloride	RN000216	G05
Salmeterol	RN000216	G06
Altretamine	RN000216	G07
Prazosin hydrochloride	RN000216	G08
Timolol maleate salt	RN000216	G09
(+,-)-Octopamine hydrochloride	RN000216	G10
Stavudine	RN000216	G11
Crotamiton	RN000216	H02
Toremifene	RN000216	H03
(R)-(+)-Atenolol	RN000216	H04
Tyloxapol	RN000216	H05
Florfenicol	RN000216	H06
Megestrol acetate	RN000216	H07
Deoxycorticosterone	RN000216	H08
Urosiol	RN000216	H09
Proparacaine hydrochloride	RN000216	H10
Aminocaproic acid	RN000216	H11
Denatonium benzoate	RN000217	A02
Canrenone	RN000217	A03
Enilconazole	RN000217	A04
Methacycline hydrochloride	RN000217	A05
Floxuridine	RN000217	A06
Sotalol hydrochloride	RN000217	A07
Gestrinone	RN000217	A08
Decamethonium bromide	RN000217	A09
Darifenacin hydrobromide	RN000217	A10
Indatraline hydrochloride	RN000217	A11
Remoxipride Hydrochloride	RN000217	B02
THIP Hydrochloride	RN000217	B03
Pirlindole mesylate	RN000217	B04
Pronethalol hydrochloride	RN000217	B05
Naftopidil dihydrochloride	RN000217	B06
Tracazolate hydrochloride	RN000217	B07
Zardaverine	RN000217	B08
Memantine Hydrochloride	RN000217	B09
Ozagrel hydrochloride	RN000217	B10
Piribedil hydrochloride	RN000217	B11
Nitrocaramiphen hydrochloride	RN000217	C02
Nandrolone	RN000217	C03
Dimaprit dihydrochloride	RN000217	C04
Oxfendazol	RN000217	C05
Guaiacol	RN000217	C06
Proscillaridin A	RN000217	C07
Pramipexole	RN000217	C08

Norgestimate	RN000217	C09
Chlormadinone acetate	RN000217	C10
Phenylbutazone	RN000217	C11
Gliquidone	RN000217	D02
Pizotifen malate	RN000217	D03
Ribavirin	RN000217	D04
Cyclopenthiazide	RN000217	D05
Fluvoxamine maleate	RN000217	D06
Prothionamide	RN000217	D07
Fluticasone propionate	RN000217	D08
Zuclopenthixol dihydrochloride	RN000217	D09
Proguanil hydrochloride	RN000217	D10
Lymecycline	RN000217	D11
Alfadolone acetate	RN000217	E02
Alfaxalone	RN000217	E03
Azapropazone	RN000217	E04
Meptazinol hydrochloride	RN000217	E05
Apramycin	RN000217	E06
Epitiostanol	RN000217	E07
Fursultiamine Hydrochloride	RN000217	E08
Gabexate mesilate	RN000217	E09
Pivampicillin	RN000217	E10
Talampicillin hydrochloride	RN000217	E11
Flucloxacillin sodium	RN000217	F02
Trapidil	RN000217	F03
Deptropine citrate	RN000217	F04
Sertraline	RN000217	F05
Ethamsylate	RN000217	F06
Moxonidine	RN000217	F07
Etilefrine hydrochloride	RN000217	F08
Alprostadil	RN000217	F09
Tribenoside	RN000217	F10
Rimexolone	RN000217	F11
Isradipine	RN000217	G02
Tiletamine hydrochloride	RN000217	G03
Isometheptene mucate	RN000217	G04
Nifurtimox	RN000217	G05
Letrozole	RN000217	G06
Arbutin	RN000217	G07
Tocainide hydrochloride	RN000217	G08
Benzathine benzylpenicillin	RN000217	G09
Risperidone	RN000217	G10
Torsemide	RN000217	G11
Halofantrine hydrochloride	RN000217	H02
Articaine hydrochloride	RN000217	H03
Nomegestrol acetate	RN000217	H04

Pancuronium bromide	RN000217	H05
Molindone hydrochloride	RN000217	H06
Alcuronium chloride	RN000217	H07
Zalcitabine	RN000217	H08
Methyldopate hydrochloride	RN000217	H09
Levocabastine hydrochloride	RN000217	H10
Pyrvinium pamoate	RN000217	H11
Etomidate	RN000218	A02
Tridihexethyl chloride	RN000218	A03
Penbutolol sulfate	RN000218	A04
Prednicarbate	RN000218	A05
Sertaconazole nitrate	RN000218	A06
Repaglinide	RN000218	A07
Piretanide	RN000218	A08
Piperacetazine	RN000218	A09
Oxyphenbutazone	RN000218	A10
Quinethazone	RN000218	A11
Moricizine hydrochloride	RN000218	B02
Iopanoic acid	RN000218	B03
Pivmecillinam hydrochloride	RN000218	B04
Levopropoxyphene napsylate	RN000218	B05
Piperidolate hydrochloride	RN000218	B06
Trifluridine	RN000218	B07
Oxprenolol hydrochloride	RN000218	B08
Ondansetron Hydrochloride	RN000218	B09
Propoxycaine hydrochloride	RN000218	B10
Oxaprozin	RN000218	B11
Phensuximide	RN000218	C02
Ioxaglic acid	RN000218	C03
Naftifine hydrochloride	RN000218	C04
Meprylcaine hydrochloride	RN000218	C05
Milrinone	RN000218	C06
Methantheline bromide	RN000218	C07
Ticarcillin sodium	RN000218	C08
Thiethylperazine dimalate	RN000218	C09
Mesalamine	RN000218	C10
Vorinostat	RN000218	C11
Imidurea	RN000218	D02
Lansoprazole	RN000218	D03
Bethanechol chloride	RN000218	D04
Cyproterone acetate	RN000218	D05
(R)-Propranolol hydrochloride	RN000218	D06
Ciprofibrate	RN000218	D07
Formestane	RN000218	D08
Benzylpenicillin sodium	RN000218	D09
Chlorambucil	RN000218	D10

Methiazole	RN000218	D11
(S)-propranolol hydrochloride	RN000218	E02
(-)-Eseroline fumarate salt	RN000218	E03
Isosorbide mononitrate	RN000218	E04
Levalbuterol hydrochloride	RN000218	E05
Topiramate	RN000218	E06
D-cycloserine	RN000218	E07
2-Chloropyrazine	RN000218	E08
(+,-)-Synephrine	RN000218	E09
(S)-(-)-Cycloserine	RN000218	E10
Homosalate	RN000218	E11
Spaglumic acid	RN000218	F02
Ranolazine	RN000218	F03
Misoprostol	RN000218	F04
Sulfadoxine	RN000218	F05
Cyclopentolate hydrochloride	RN000218	F06
Estriol	RN000218	F07
(-)-Isoproterenol hydrochloride	RN000218	F08
Sarafloxacin	RN000218	F09
Nialamide	RN000218	F10
Toltrazuril	RN000218	F11
Perindopril	RN000218	G02
Fexofenadine HCl	RN000218	G03
4-aminosalicylic acid	RN000218	G04
Clonixin Lysinate	RN000218	G05
Verteporfin	RN000218	G06
Meropenem	RN000218	G07
Ramipril	RN000218	G08
Mephenytoin	RN000218	G09
Rifabutin	RN000218	G10
Parbendazole	RN000218	G11
Mecamylamine hydrochloride	RN000218	H02
Procarbazine hydrochloride	RN000218	H03
Viomycin sulfate	RN000218	H04
Saquinavir mesylate	RN000218	H05
Ronidazole	RN000218	H06
Dorzolamide hydrochloride	RN000218	H07
Azaperone	RN000218	H08
Cefepime hydrochloride	RN000218	H09
Clocortolone pivalate	RN000218	H10
Nadifloxacin	RN000218	H11

Appendix 11: Apolar lipids separated by 2-D TLC on a silica gel plate using Chloroform: Methanol (96:4) in direction one (D1) and Toluene: Acetone (80:20) in direction two (D2). The TLC separation of apolar lipids from four different strains of *M. smegmatis* mc^{2}155 was carried out using two different solvent systems in two directions. The *M. smegmatis* mc^{2}155 strains used are depicted based on the overexpression plasmids they contain: A. mc^{2}155_pVV16, B. mc^{2}155_pVV16_*echA12*_Rv, C. mc^{2}155_pVV16_*echA12*_BCG, D. mc^{2}155_pVV16_G239R_*echA12*. The strains were treated with 0x, 1x, 2x, 5x and 10x MIC of florfenicol..MA, Free Mycolic acids

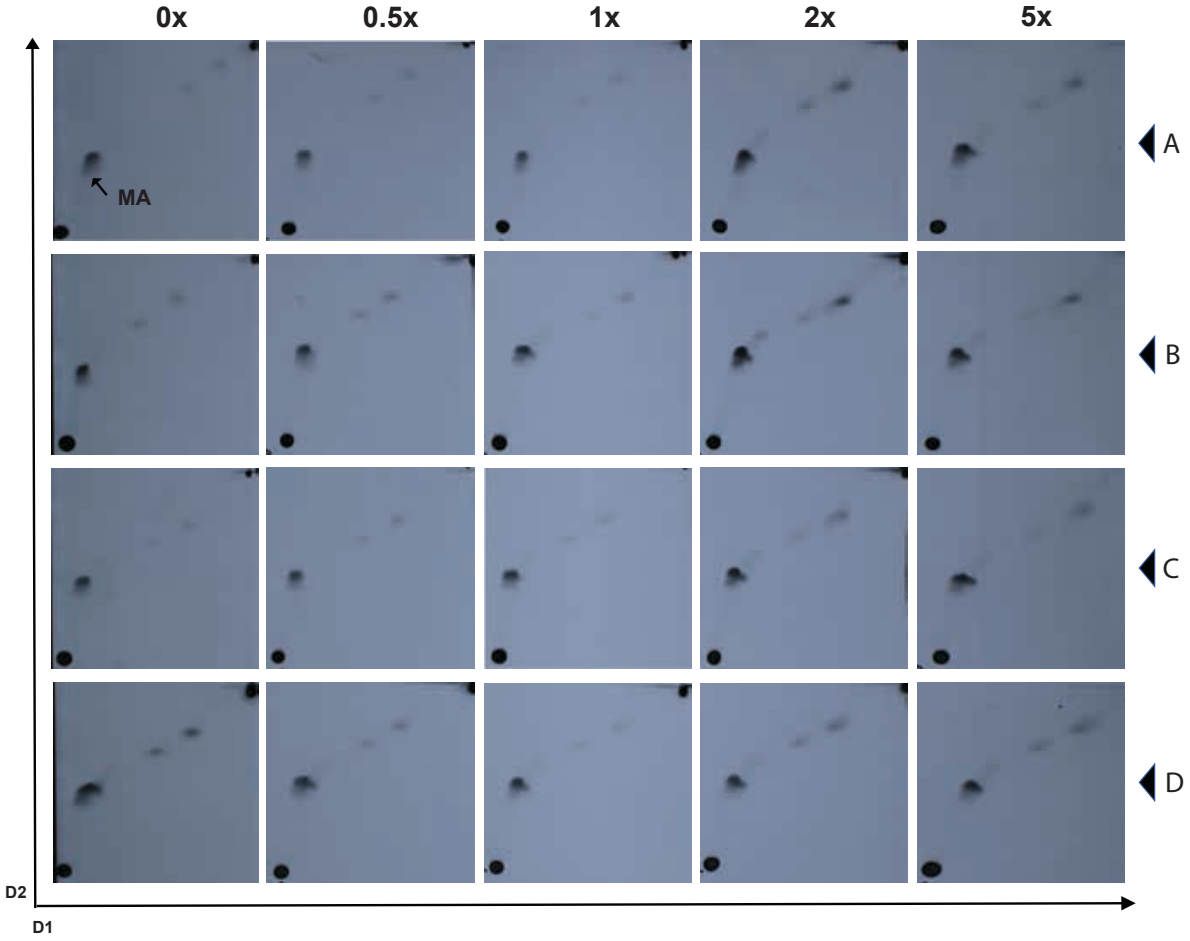

Appendix 12: Apolar lipids separated by 2-D TLC on a silica gel plate using Chloroform: Methanol: Water (100:14:0.8:) in direction one (D1) and Chloroform: Acetone: Methanol: Water (50:60:2.5:3) in direction two (D2). The TLC separation of apolar lipids from four different strains of *M. smegmatis* mc^2155 was carried out using two different solvent systems in two directions. The *M. smegmatis* mc^2155 strains used are depicted based on the overexpression plasmids they contain: A. mc^2155_pVV16, B. mc^2155_pVV16_*echA12*_Rv, C. mc^2155_pVV16_*echA12*_BCG, D. mc^2155_pVV16_G239R_*echA12*. The strains were treated with 0x, 1x, 2x, 5x and 10x MIC of florfenicol.TMM, trehalose monomycolate; TDM, trehalose dimycolate.

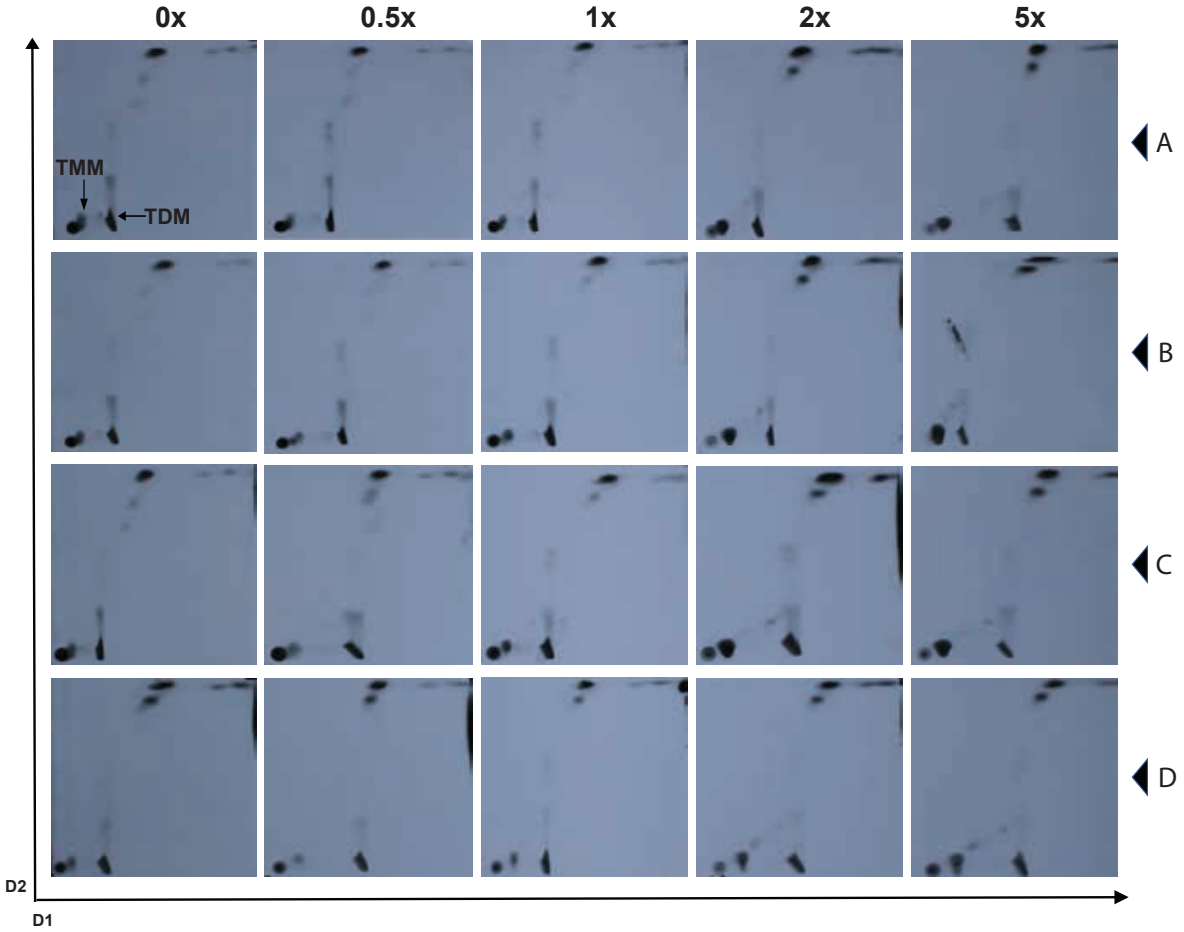

Appendix 13: Apolar lipids separated by 2-D TLC on a silica gel plate using Chloroform: Methanol (96:4) in direction one (D1) and Toluene: Acetone (80:20) in direction two (D2). The TLC separation of apolar lipids from four different strains of M. bovis BCG was carried out using two different solvent systems in two directions. The *M. bovis* BCG strains used are depicted based on the overexpression plasmids they contain; A. *M. bovis* BCG_pVV16, B. *M. bovis* BCG_pVV16_*echA12*_Rv, C. *M. bovis* BCG_pVV16_*echA12*_BCG, D. *M. bovis* BCG_pVV16_G239_*echA12*. The strains were treated with 0x, 1x, 2x, 5x and 10x MIC of florfenicol. DAG, Diacyl Glycerol.

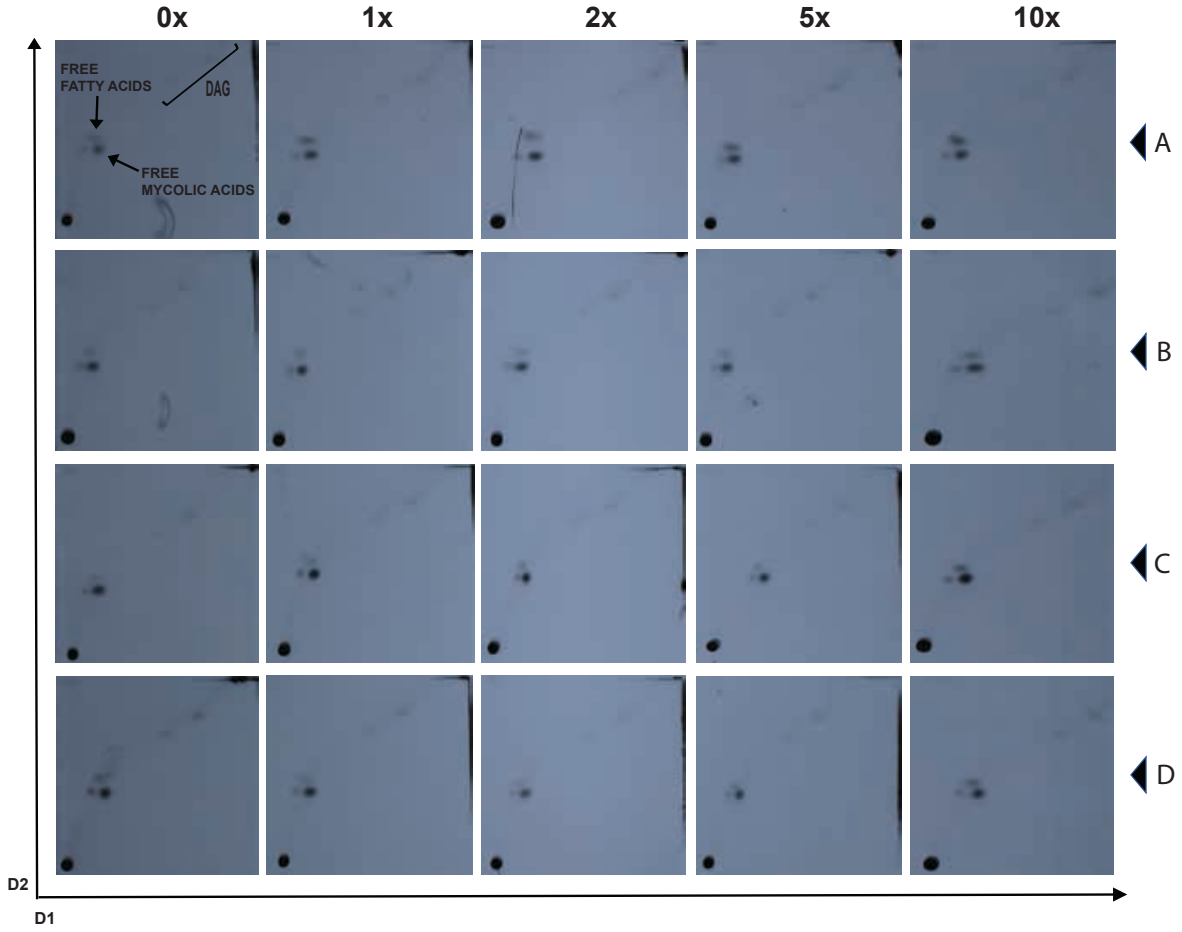

Appendix 14: Apolar lipids separated by 2-D TLC on a silica gel plate using Chloroform: Methanol: Water (100:14:0.8:) in direction one (D1) and Chloroform: Acetone: Methanol: Water (50:60:2.5:3) in direction two (D2). The TLC separation of apolar lipids from four different strains of M. bovis BCG was carried out using two different solvent systems in two directions. The *M. bovis* BCG strains used are depicted based on the overexpression plasmids they contain; A. *M. bovis* BCG_pVV16, B. *M. bovis* BCG_pVV16_*echA12*_Rv, C. *M. bovis* BCG_pVV16_*echA12*_BCG, D. *M. bovis* BCG_pVV16_G239_*echA12*. The strains were treated with 0x, 1x, 2x, 5x and 10x MIC of florfenicol.GMM, Glucose monomycolate; TDM, Trehalose dimycolate; DAT, Diacylated trehalose; SL, Sulpholipid.

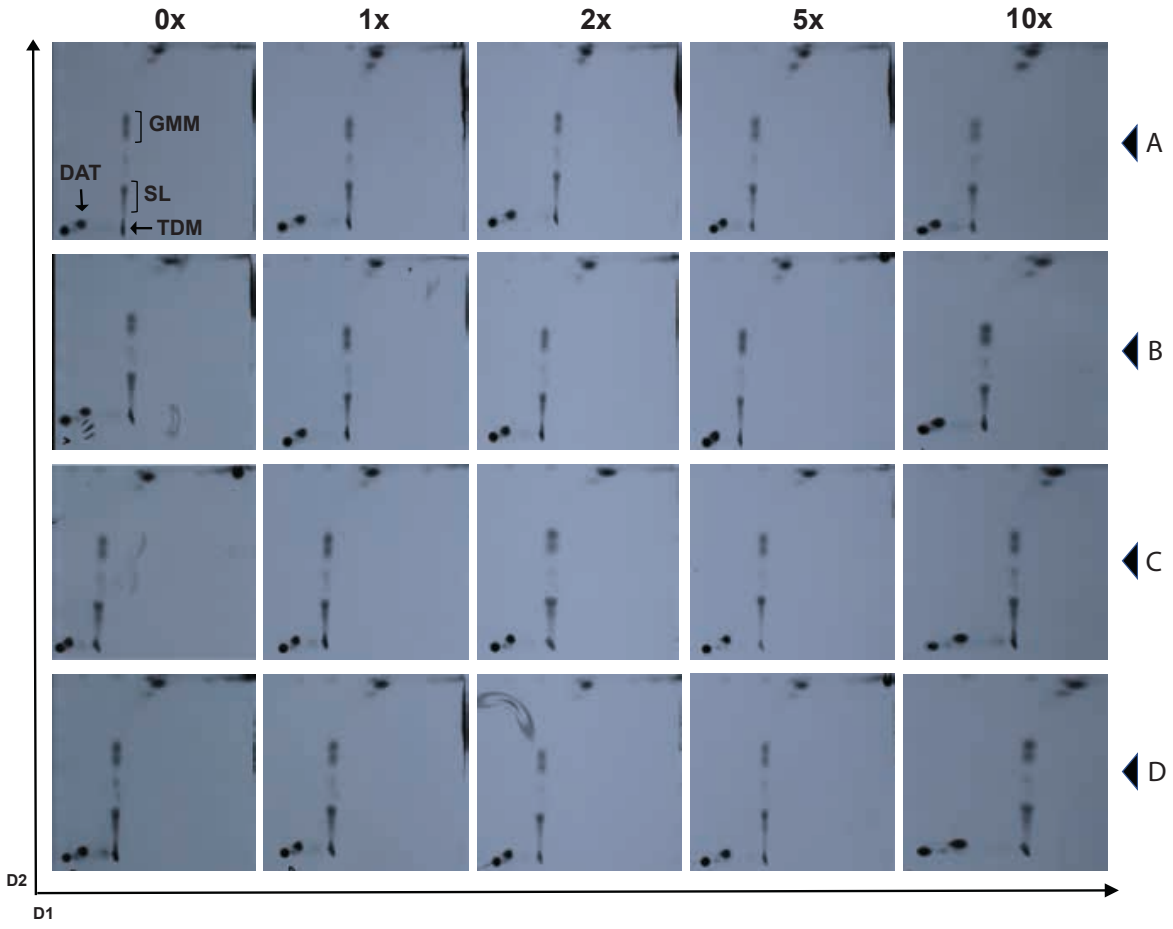

Appendix 15: Fold change values for the overexpression screen against the extended GSK177 library.

Plate 1				
Sample number	Fold change	Plate bar code	Compound Identification	Well ID
X1	0.737827534	G214G8D	GSK1859936A	A2
X2	0.728844663	G214G8D	GSK991960A	A3
X3	0.975761609	G214G8D	GW339685X	A4
X4	0.927707416	G214G8D	GI103688B	A5
X5	0.674843954	G214G8D	SB-204804-A	A6
X6	0.686566918	G214G8D	GSK1788487A	A7
X7	1.210016841	G214G8D	GSK1832831A	A8
X8	0.973956806	G214G8D	GSK1589673A	A9
X9	0.774270411	G214G8D	GSK347301A	A10
X10	1.561607378	G214G8D	GSK353071A	A11
X11	1.687240787	G214G8D	GSK1857145A	B2
X12	1.182563541	G214G8D	GSK1955236A	B3
X13	0.689766052	G214G8D	GSK2260003B	B4
X14	1.113060903	G214G8D	GW369335X	B5
X15	0.902096101	G214G8D	GSK829969A	B6
X16	0.853294757	G214G8D	GSK1742694A	B7
X17	0.528381779	G214G8D	GSK1990858A	B8
X18	0.911632334	G214G8D	GSK749336A	B9
X19	1.758904866	G214G8D	GSK921295A	B10
X20	1.171862757	G214G8D	GSK920703A	B11
X21	0.793860766	G214G8D	GSK1863309A	C2
X22	1.973013763	G214G8D	GSK2059310A	C3
X23	1.58547645	G214G8D	GSK1329151A	C4
X24	1.131015477	G214G8D	BRL-51093AM	C5
X25	1.006854046	G214G8D	GSK847913A	C6
X26	1.746275598	G214G8D	GSK1783710A	C7
X27	1.164603028	G214G8D	GSK468214A	C8
X28	1.935942344	Empty		C9
X29	2.201886684	G214G8D	GSK1051703A	C10
X30	0.522310065	G214G8D	GSK426032A	C11
X31	1.336947359	G214G8D	GSK1733953A	D2
X32	1.463835533	G214G8D	GSK1996236A	D3
X33	1.079096075	G214G8D	GSK353069A	D4
X34	1.770412504	G214G8D	GSK1985270A	D5
X35	0.787866504	G214G8D	GSK754716A	D6

X36	0.700768591	G214G8D	GSK1759150A	D7
X37	0.720431195	G214G8D	GSK1829816A	D8
X38	1.762582588	G214G8D	GSK2379464A	D9
X39	0.94785988	G214G8D	GSK146660A	D10
X40	1.120800284	G214G8D	GSK731389A	D11
X41	1.553098075	G214G8D	GSK1925843A	E2
X42	1.861113789	G214G8D	GSK2215855A	E3
X43	0.967715341	G214G8D	GSK2200150A	E4
X44	1.106090893	G214G8D	GSK2437987A	E5
X45	1.142144075	G214G8D	GSK437009A	E6
X46	1.170384852	G214G8D	GSK1941290A	E7
X47	1.165443323	G214G8D	GSK1982256A	E8
X48	1.572040771	G214G8D	GR153167X	E9
X49	2.1521069	G214G8D	GR135487X	E10
X50	0.535425083	G214G8D	GW857165X	E11
X51	1.292782118	G214G8D	GSK1829676A	F2
X52	1.532106617	G214G8D	GSK735816A	F3
X53	0.904429114	G214G8D	GSK1589671A	F4
X54	1.228417282	G214G8D	GV187303X	F5
X55	1.073408697	G214G8D	SB-829405	F6
X56	0.948336708	G214G8D	GSK1829819A	F7
X57	1.856661181	G214G8D	GSK2247256A	F8
X58	1.062911648	G214G8D	CCI7967	F9
X59	0.942499114	G214G8D	GSK124576A	F10
X60	0.388100255	G214G8D	SB-811137-V	F11
X61	1.583842997	G214G8D	GSK1829729A	G2
X62	1.102690927	G214G8D	AH24761A	G3
X63	1.258342587	G214G8D	GSK270670A	G4
X64	0.755355436	G214G8D	GSK888636A	G5
X65	0.971884702	Empty		G6
X66	0.715454842	G214G8D	GSK1829736A	G7
X67	0.893209171	G214G8D	GSK1873486A	G8
X68	0.660854727	G214G8D	GSK345724A	G9
X69	0.885001787	G214G8D	GSK798463A	G10
X70	0.749617641	G214G8D	GW369808A	G11
X71	0.973376203	G214G8D	GSK2043267A	H2
X72	1.026310168	G214G8D	GR135490X	H3
X73	1.166808055	G214G8D	BRL-8903SA	H4
X74	0.90714021	G214G8D	GSK276001A	H5
X75	1.242465651	G214G8D	SB-811796-V	H6

X76	0.556586056	G214G8D	GSK1829674A	H7
X77	1.087724533	G214G8D	CCI14012	H8
X78	1.058415814	G214G8D	GSK479031A	H9
X79	0.730840216	G214G8D	GSK892651A	H10
X80	0.800935537	G214G8D	SB-746177	H11

Plate 2				
Sample number	Fold change	Plate bar code	Compound Identification	Well ID
X1	0.848123619	Empty		A2
X2	0.5376698	G214G8E	GSK1812410A	A3
X3	0.480460907	G214G8E	GSK1829732A	A4
X4	0.623746545	G214G8E	SKF-98621-A	A5
X5	0.532093892	G214G8E	GW859039X	A6
X6	1.036425265	G214G8E	GSK498315A	A7
X7	0.53178537	G214G8E	SB-650816	A8
X8	1.167167867	G214G8E	GSK1310678A	A9
X9	0.345019537	G214G8E	GW288013X	A10
X10	1.031923669	G214G8E	GSK237561A	A11
X11	1.141507972	G214G8E	GSK937733A	B2
X12	0.565513925	G214G8E	GSK1691553A	B3
X13	2.004920259	G214G8E	GSK1829728A	B4
X14	0.450953358	G214G8E	GW508363A	B5
X15	1.982787313	G214G8E	GSK810016A	B6
X16	1.144895769	G214G8E	GSK937213A	B7
X17	0.641206488	G214G8E	GSK275628A	B8
X18	0.487951391	G214G8E	GSK1372568A	B9
X19	0.830407331	G214G8E	GSK445886A	B10
X20	0.650308827	G214G8E	GR135486X	B11
X21	1.035464732	G214G8E	GSK622400A	C2
X22	1.164921621	G214G8E	GSK1750922A	C3
X23	0.65594806	G214G8E	GSK1829820A	C4
X24	0.752029391	G214G8E	GSK2423307A	C5
X25	1.368678028	G214G8E	GSK352635A	C6
X26	0.478002986	G214G8E	GSK275984A	C7
X27	0.43952968	G214G8E	GSK262906A	C8
X28	0.996946661	G214G8E	GSK1570606A	C9
X29	1.409252758	G214G8E	GSK735826A	C10
X30	0.601981902	G214G8E	GW664700A	C11
X31	0.984865239	G214G8E	GSK1434490A	D2
X32	0.768965226	G214G8E	GSK1731114A	D3

X33	0.774186685	G214G8E	GSK1829733A	D4
X34	1.594065384	G214G8E	GSK2200160A	D5
X35	0.977097565	G214G8E	GSK153890A	D6
X36	0.743145125	G214G8E	GSK385518A	D7
X37	0.716694688	G214G8E	GSK358607A	D8
X38	0.85837146	G214G8E	GSK1402290A	D9
X39	0.73895632	G214G8E	BRL-51091AM	D10
X40	0.572440257	G214G8E	GSK2457140A	D11
X41	1.291889288	G214G8E	GSK1668869A	E2
X42	0.743925011	G214G8E	GSK1758774A	E3
X43	0.862108435	G214G8E	GSK2266306A	E4
X44	0.814701363	G214G8E	GSK2623870A	E5
X45	0.459987911	G214G8E	GSK1107112A	E6
X46	0.286467339	G214G8E	GW623128X	E7
X47	0.730942067	G214G8E	GSK547481A	E8
X48	0.665443747	G214G8E	GSK1611550A	E9
X49	0.531499718	G214G8E	BRL-8088SA	E10
X50	0.46891923	G214G8E	GSK1905227A	E11
X51	0.944150369	G214G8E	GSK3011724A	F2
X52	0.853172007	G214G8E	GSK1829671A	F3
X53	0.547677079	G214G8E	GSK1793659A	F4
X54	0.879536026	G214G8E	GSK1744926A	F5
X55	0.758542214	G214G8E	GSK463114A	F6
X56	0.361607421	G214G8E	GSK921190A	F7
X57	0.617218802	G214G8E	GSK695914A	F8
X58	0.530175256	G214G8E	GSK1385423A	F9
X59	0.695748336	G214G8E	GSK1072678A	F10
X60	0.715107256	G214G8E	GSK762874A	F11
X61	0.998873757	G214G8E	GSK1826247A	G2
X62	0.768345846	G214G8E	GSK1829727A	G3
X63	1.19958166	G214G8E	GSK2225703A	G4
X64	0.791600793	G214G8E	GSK316438A	G5
X65	0.659855135	G214G8E	GSK636544A	G6
X66	0.375661494	G214G8E	GSK2352192A	G7
X67	0.811234766	G214G8E	GSK1180781A	G8
X68	0.961572149	G214G8E	GSK1055950A	G9
X69	0.402298956	G214G8E	SB-435634	G10
X70	0.551086703	G214G8E	GSK1174628A	G11
X71	0.908952114	G214G8E	GSK1826089A	H2
X72	0.846006443	G214G8E	GSK1829660A	H3

X73	0.836245128	G214G8E	GSK2119567A	H4
X74	0.496008641	G214G8E	GSK847920A	H5
X75	0.552142575	G214G8E	GSK810037A	H6
X76	0.687767244	G214G8E	BRL-10143SA	H7
X77	0.535235908	G214G8E	GSK1302651A	H8
X78	0.839294143	G214G8E	GSK2032710A	H9
X79	0.384108407	G214G8E	GSK889423A	H10
X80	0.447366159	G214G8E	GI207342A	H11

Plate 3				
Sample number	Fold change	Plate bar code	Compound Identification	Well ID
X1	0.508800209	G214FNZ	GSK920684A	A2
X2	0.466476112	G214FNZ	GR232543X	A3
X3	0.86007699	G214FNZ	GSK1650514A	A4
X4	0.78645034	G214FNZ	GSK353496A	A5
X5	0.902319687	G214FNZ	GW356807A	A6
X6	0.627513394	G214FNZ	SB-516933	A7
X7	1.159225301	Empty		A8
X8	0.923235025	Empty		A9
X9	0.81582318	Empty		A10
X10	0.492296339	Empty		A11
X11	1.097739074	G214FNZ	BRL-7940SA	B2
X12	0.827571596	G214FNZ	GI247341A	B3
X13	0.489584148	G214FNZ	GW713556X	B4
X14	0.786629139	G214FNZ	GSK2584213A	B5
X15	1.071513683	G214FNZ	GSK547543A	B6
X16	0.707021793	G214FNZ	GSK1148219A	B7
X17	1.039419778	Empty		B8
X18	0.89810849	Empty		B9
X19	1.184698107	Empty		B10
X20	1.097591833	Empty		B11
X21	0.623283561	G214FNZ	GSK2595326A	C2
X22	0.611213861	G214FNZ	GSK2523007A	C3
X23	1.623751314	G214FNZ	GSK2595882A	C4
X24	0.851936041	G214FNZ	GSK2428832A	C5
X25	0.900129304	G214FNZ	GSK2425105A	C6
X26	0.46730337	G214FNZ	GSK1518999A	C7
X27	1.10149435	Empty		C8
X28	0.922671964	Empty		C9
X29	1.168033723	Empty		C10

X30	1.125935455	Empty		C11
X31	0.984992896	G214FNZ	BRL-10988SA	D2
X32	0.872510082	G214FNZ	GSK2479712A	D3
X33	0.817370575	G214FNZ	GSK848336A	D4
X34	0.982308523	G214FNZ	GW861072X	D5
X35	0.894285139	G214FNZ	GSK957094A	D6
X36	1.296573563	G214FNZ	GSK2157753A	D7
X37	1.172754629	Empty		D8
X38	0.958679834	Empty		D9
X39	0.960562085	Empty		D10
X40	1.20715095	Empty		D11
X41	0.612980823	G214FNZ	GW360240X	E2
X42	0.644288512	G214FNZ	GSK1826825A	E3
X43	0.804675041	G214FNZ	GSK2582297A	E4
X44	1.033219599	G214FNZ	GSK2240645A	E5
X45	0.810316851	G214FNZ	GSK994258A	E6
X46	1.149546938	Empty		E7
X47	0.59539256	Empty		E8
X48	0.952383668	Empty		E9
X49	0.947813341	Empty		E10
X50	0.902709803	Empty		E11
X51	1.016774601	G214FNZ	SB-626246	F2
X52	0.835323203	G214FNZ	GSK381407A	F3
X53	1.38908045	G214FNZ	GSK2429242A	F4
X54	0.797350014	G214FNZ	GSK861337A	F5
X55	0.811708914	G214FNZ	SB-354364	F6
X56	1.01985396	Empty		F7
X57	0.621879808	Empty		F8
X58	0.802226909	Empty		F9
X59	0.938894162	Empty		F10
X60	0.873138069	Empty		F11
X61	0.61912727	G214FNZ	GSK1066288A	G2
X62	0.923348088	G214FNZ	SB-712970	G3
X63	0.626430762	G214FNZ	GSK2527753A	G4
X64	0.740728268	G214FNZ	GSK2548665A	G5
X65	0.618136736	G214FNZ	GSK831784A	G6
X66	0.970841479	Empty		G7
X67	0.95959454	Empty		G8
X68	0.887397185	Empty		G9
X69	0.907243823	Empty		G10

X70	0.638752465	Empty		G11
X71	1.329512644	G214FNZ	GSK2423650A	H2
X72	0.637212599	G214FNZ	GSK163574A	H3
X73	0.56542354	G214FNZ	GSK2440337A	H4
X74	0.789970624	G214FNZ	GSK560927A	H5
X75	0.99354367	G214FNZ	GSK1121877A	H6
X76	0.967352396	Empty		H7
X77	0.893127627	Empty		H8
X78	1.039508433	Empty		H9
X79	0.806904112	Empty		H10
X80	0.61637511	Empty		H11

Appendix 16: GSK177 extended library plate map

Plate 1					
Barcode	Reg number	OI	MolWt	Original Well ID	Well ID (Intermediate plate)
G214G8D	GSK1859936A	ST/1348528	410.489	A1	A2
G214G8D	GSK1857145A	ST/1346270	377.459	B1	B2
G214G8D	GSK1863309A	ST/1342494	352.45	C1	C2
G214G8D	GSK1733953A	ST/1264695	385.816	D1	D2
G214G8D	GSK1925843A	ST/1388681	392.926	E1	E2
G214G8D	GSK1829676A	ST/1325472	411.387	F1	F2
G214G8D	GSK1829729A	ST/1325525	339.341	G1	G2
G214G8D	GSK2043267A	ST/1473690	433.432	H1	H2
G214G8D	GSK991960A	ST/796668	412.871	A2	A3
G214G8D	GSK1955236A	ST/1414819	349.826	B2	B3
G214G8D	GSK2059310A	ST/1488738	450.557	C2	C3
G214G8D	GSK1996236A	ST/1439630	368.38	D2	D3
G214G8D	GSK2215855A	N6398-41-1	489.563	E2	E3
G214G8D	GSK735816A	ST/642098	328.387	F2	F3
G214G8D	AH24761A	420/150	345.272	G2	G3
G214G8D	GR135490X	C1789/8/1	215.257	H2	H3
G214G8D	GW339685X	0037U 73***	324.356	A3	A4
G214G8D	GSK2260003B	N8444-19-4	513.419	B3	B4
G214G8D	GSK1329151A	VMPA/7572/91/A2	396.49	C3	C4
G214G8D	GSK353069A	SC/104322	205.279	D3	D4
G214G8D	GSK2200150A	JM108692-131D2	357.467	E3	E4
G214G8D	GSK1589671A	ST/1140264	434.478	F3	F4
G214G8D	GSK270670A	U20764/121/2	373.426	G3	G4
G214G8D	BRL-8903SA	IM100406-132E8	386.287	H3	H4
G214G8D	GI103688B	0013X 55U*B	466.925	A4	A5

G214G8D	GW369335X	1747U 88U*A	318.396	B4	B5
G214G8D	BRL-51093AM	IM100406-198N6	400.314	C4	C5
G214G8D	GSK1985270A	N5160-40-3	383.835	D4	D5
G214G8D	GSK2437987A	N21274-25-1	356.803	E4	E5
G214G8D	GV187303X	VMEG/1774/72/2	290.359	F4	F5
G214G8D	GSK888636A	N15309-56-2	345.398	G4	G5
G214G8D	GSK276001A	SC/90411	349.405	H4	H5
G214G8D	SB-204804-A	EXSB/LNB14457-77	388.934	A5	A6
G214G8D	GSK829969A	ST/704868	319.402	B5	B6
G214G8D	GSK847913A	SC/121801	347.357	C5	C6
G214G8D	GSK754716A	SC/118156	318.126	D5	D6
G214G8D	GSK437009A	ST/510821	320.392	E5	E6
G214G8D	SB-829405	DF202930-012A4B7C7	385.884	F5	F6
					G6
G214G8D	SB-811796-V	YW200769-143A22B12C5	655.649	H5	H6
G214G8D	GSK1788487A	ST/1288745	423.316	A6	A7
G214G8D	GSK1742694A	ST/1251778	332.444	B6	B7
G214G8D	GSK1783710A	ST/1284842	383.467	C6	C7
G214G8D	GSK1759150A	ST/1239788	446.492	D6	D7
G214G8D	GSK1941290A	ST/1393958	475.606	E6	E7
G214G8D	GSK1829819A	ST/1325613	269.306	F6	F7
G214G8D	GSK1829736A	ST/1325532	402.206	G6	G7
G214G8D	GSK1829674A	ST/1325470	388.179	H6	H7
G214G8D	GSK1832831A	ST/1327779	359.467	A7	A8
G214G8D	GSK1990858A	JM108964-082A2F8	475.518	B7	B8
G214G8D	GSK468214A	ST/541154	389.455	C7	C8
G214G8D	GSK1829816A	ST/1325610	245.327	D7	D8
G214G8D	GSK1982256A	N3440-21-A2	310.443	E7	E8
G214G8D	GSK2247256A	N8628-22-A3	399.946	F7	F8
G214G8D	GSK1873486A	JA209270-002A2	479.624	G7	G8
G214G8D	CCI14012	PWS/700/1	246.249	H7	H8
G214G8D	GSK1589673A	ST/1140266	458.476	A8	A9
G214G8D	GSK749336A	ST/651380	350.411	B8	B9
					C9
G214G8D	GSK2379464A	N26258-34-A1	330.83	D8	D9
G214G8D	GR153167X	GDD/40216	357.427	E8	E9
G214G8D	CCI7967	GDD/636	380.874	F8	F9
G214G8D	GSK345724A	SC/96881	256.224	G8	G9
G214G8D	GSK479031A	ST/551212	302.822	H8	H9
G214G8D	GSK347301A	N22583-50-5	325.276	A9	A10

G214G8D	GSK921295A	ST/759089	327.424	B9	B10
G214G8D	GSK1051703A	ST/816262	335.357	C9	C10
G214G8D	GSK146660A	ST/415658	368.38	D9	D10
G214G8D	GR135487X	C1789/11/1	253.223	E9	E10
G214G8D	GSK124576A	ST/397469	385.254	F9	F10
G214G8D	GSK798463A	ST/688668	335.357	G9	G10
G214G8D	GSK892651A	ST/754412	271.343	H9	H10
G214G8D	GSK353071A	SC/104324	231.317	A10	A11
G214G8D	GSK920703A	ST/758791	375.896	B10	B11
G214G8D	GSK426032A	ST/501405	425.392	C10	C11
G214G8D	GSK731389A	ST/644172	335.444	D10	D11
G214G8D	GW857165X	ST/366979	371.228	E10	E11
G214G8D	SB-811137-V	YW200769-143A17B11C3	671.691	F10	F11
G214G8D	GW369808A	9145W 95C*A	322.323	G10	G11
G214G8D	SB-746177	GA200759-052A5B6	305.374	H10	H11

Plate 2					
Barcode	Regno	OI	MolWt	Original Well ID	Well ID (Intermediate plate)
					A2
G214G8E	GSK937733A	ST/784417	458.444	B1	B2
G214G8E	GSK622400A	U21612/131/1	301.383	C1	C2
G214G8E	GSK1434490A	ST/1057085	382.388	D1	D2
G214G8E	GSK1668869A	ST/1198663	344.772	E1	E2
G214G8E	GSK3011724A	MV103783-173A4B1	267.347	F1	F2
G214G8E	GSK1826247A	DJ107586-048A5B4	465.543	G1	G2
G214G8E	GSK1826089A	DJ107586-046A6B9	494.629	H1	H2
G214G8E	GSK1812410A	ST/1317324	301.339	A2	A3
G214G8E	GSK1691553A	ST/1224178	347.394	B2	B3
G214G8E	GSK1750922A	ST/1256539	364.365	C2	C3
G214G8E	GSK1731114A	ST/1262042	370.465	D2	D3
G214G8E	GSK1758774A	ST/1239379	412.32	E2	E3
G214G8E	GSK1829671A	ST/1325467	363.299	F2	F3
G214G8E	GSK1829727A	ST/1325523	323.277	G2	G3
G214G8E	GSK1829660A	ST/1325456	307.389	H2	H3
G214G8E	GSK1829732A	ST/1325528	377.326	A3	A4
G214G8E	GSK1829728A	ST/1325524	337.304	B3	B4
G214G8E	GSK1829820A	ST/1325614	285.364	C3	C4

G214G8E	GSK1829733A	ST/1325529	391.396	D3	D4
G214G8E	GSK2266306A	ST/1702103	351.389	E3	E4
G214G8E	GSK1793659A	JA207862-149A3	502.417	F3	F4
G214G8E	GSK2225703A	N7713-10-1	699.557	G3	G4
G214G8E	GSK2119567A	N4136-29-D1	382.507	H3	H4
G214G8E	SKF-98621-A	EXSB/154/4665/C	397.93	A4	A5
G214G8E	GW508363A	R4670/61/3	395.925	B4	B5
G214G8E	GSK2423307A	ST/2078881	280.173	C4	C5
G214G8E	GSK2200160A	N17110-20-2	333.511	D4	D5
G214G8E	GSK2623870A	N21285-13-1	329.397	E4	E5
G214G8E	GSK1744926A	N22583-50-6	397.353	F4	F5
G214G8E	GSK316438A	ST/459399	346.212	G4	G5
G214G8E	GSK847920A	SC/121808	302.382	H4	H5
G214G8E	GW859039X	ST/365235	374.497	A5	A6
G214G8E	GSK810016A	ST/691898	379.482	B5	B6
G214G8E	GSK352635A	N21275-55-3	222.555	C5	C6
G214G8E	GSK153890A	FNDO/U1016/10/1	320.372	D5	D6
G214G8E	GSK1107112A	ST/838662	314.786	E5	E6
G214G8E	GSK463114A	ST/536298	336.384	F5	F6
G214G8E	GSK636544A	ST/619924	345.866	G5	G6
G214G8E	GSK810037A	ST/691920	328.415	H5	H6
G214G8E	GSK498315A	ST/564849	309.327	A6	A7
G214G8E	GSK937213A	ST/783889	365.426	B6	B7
G214G8E	GSK275984A	SC/90390	331.414	C6	C7
G214G8E	GSK385518A	ST/471267	240.3	D6	D7
G214G8E	GW623128X	N15054-12-1	328.836	E6	E7
G214G8E	GSK921190A	ST/2357076	327.424	F6	F7
G214G8E	GSK2352192A	ST/2279683	321.395	G6	G7
G214G8E	BRL-10143SA	IM100406-152B1	400.314	H6	H7
G214G8E	SB-650816	MV49014-067A33B21	348.398	A7	A8
G214G8E	GSK275628A	SC/89993	435.32	B7	B8
G214G8E	GSK262906A	ST/436268	345.433	C7	C8
G214G8E	GSK358607A	ST/464156	352.384	D7	D8
G214G8E	GSK547481A	GA203953-122A11B1C11	549.714	E7	E8
G214G8E	GSK695914A	AS104968-001A1B12	397.466	F7	F8
G214G8E	GSK1180781A	ST/894921	410.471	G7	G8
G214G8E	GSK1302651A	ST/982060	283.755	H7	H8
G214G8E	GSK1310678A	ST/986476	300.241	A8	A9
G214G8E	GSK1372568A	ST/1013805	301.387	B8	B9
G214G8E	GSK1570606A	ST/1129554	313.349	C8	C9

G214G8E	GSK1402290A	ST/1032424	315.372	D8	D9
G214G8E	GSK1611550A	ST/1170223	325.385	E8	E9
G214G8E	GSK1385423A	ST/1023242	430.456	F8	F9
G214G8E	GSK1055950A	ST/1259151	435.539	G8	G9
G214G8E	GSK2032710A	ST/1469817	435.585	H8	H9
G214G8E	GW288013X	6010W 95C*A	301.199	A9	A10
G214G8E	GSK445886A	N21275-66-1	288.755	B9	B10
G214G8E	GSK735826A	ST/642108	354.406	C9	C10
G214G8E	BRL-51091AM	IM100406-198N7	441.151	D9	D10
G214G8E	BRL-8088SA	IM100406-130H1	392.294	E9	E10
G214G8E	GSK1072678A	ST/817840	327.424	F9	F10
G214G8E	SB-435634	JH99186-039A1	228.247	G9	G10
G214G8E	GSK889423A	ST/751070	344.835	H9	H10
G214G8E	GSK237561A	FCBS/U1038/66/1	336.368	A10	A11
G214G8E	GR135486X	C1789/10/1	219.67	B10	B11
G214G8E	GW664700A	R4564/113/1	485.519	C10	C11
G214G8E	GSK2457140A	ST/2400260	343.427	D10	D11
G214G8E	GSK1905227A	N31856-90-A2	291.39	E10	E11
G214G8E	GSK762874A	ST/2357078	309.362	F10	F11
G214G8E	GSK1174628A	ST/2357077	259.305	G10	G11
G214G8E	GI207342A	0277C 76***	255.143	H10	H11

Plate 3					
Barcode	Regno	OI	MolWt	Original Well ID	Well ID (Intermediate plate)
G214FNZ	GSK920684A	ST/762581	329.349	A1	A2
G214FNZ	BRL-7940SA	IM100406-081J4	428.367	B1	B2
G214FNZ	GSK2595326A	ST/2298269	328.412	C1	C2
G214FNZ	BRL-10988SA	IM100406-082R2	456.377	D1	D2
G214FNZ	GW360240X	0358U 83UA	324.38	E1	E2
G214FNZ	SB-626246	N26788-35-A2	219.193	F1	F2
G214FNZ	GSK1066288A	M476/72/1	424.934	G1	G2
G214FNZ	GSK2423650A	ST/2400259	354.267	H1	H2
G214FNZ	GR232543X	M179/15/4	314.362	A2	A3
G214FNZ	GI247341A	U4907/144/1	732.566	B2	B3
G214FNZ	GSK2523007A	ST/2400218	339.84	C2	C3
G214FNZ	GSK2479712A	ST/2400217	341.404	D2	D3
G214FNZ	GSK1826825A	ST/1332234	427.641	E2	E3
G214FNZ	GSK381407A	ST/476208	358.824	F2	F3
G214FNZ	SB-712970	ST/958820	368.43	G2	G3
G214FNZ	GSK163574A	FFJG/252/176/1	370.859	H2	H3

G214FNZ	GSK1650514A	ST/1195396	351.831	A3	A4
G214FNZ	GW713556X	ST/276160	340.373	B3	B4
G214FNZ	GSK2595882A	ST/2400266	343.377	C3	C4
G214FNZ	GSK848336A	SC/122269	294.394	D3	D4
G214FNZ	GSK2582297A	ST/2400270	312.363	E3	E4
G214FNZ	GSK2429242A	ST/2400268	233.697	F3	F4
G214FNZ	GSK2527753A	ST/2400271	305.395	G3	G4
G214FNZ	GSK2440337A	N32690-7-1	348.392	H3	H4
G214FNZ	GSK353496A	SC/104897	211.307	A4	A5
G214FNZ	GSK2584213A	ST/1925584	357.478	B4	B5
G214FNZ	GSK2428832A	ST/1768863	306.363	C4	C5
G214FNZ	GW861072X	ST/371072	356.439	D4	D5
G214FNZ	GSK2240645A	N5936-27-A9B6	379.528	E4	E5
G214FNZ	GSK861337A	ST/717997	364.395	F4	F5
G214FNZ	GSK2548665A	ST/1880136	350.399	G4	G5
G214FNZ	GSK560927A	U21540/77/1	425.343	H4	H5
G214FNZ	GW356807A	0039Y64	555.459	A5	A6
G214FNZ	GSK547543A	GA203953-122A11B7C11	544.674	B5	B6
G214FNZ	GSK2425105A	ST/1763945	229.281	C5	C6
G214FNZ	GSK957094A	ST/767164	265.317	D5	D6
G214FNZ	GSK994258A	ST/798779	336.427	E5	E6
G214FNZ	SB-354364	ST97588-129J2	349.423	F5	F6
G214FNZ	GSK831784A	DY103972-187A22B13	406.478	G5	G6
G214FNZ	GSK1121877A	SC/131398	467.562	H5	H6
G214FNZ	SB-516933	ST97588-166E0	350.411	A6	A7
G214FNZ	GSK1148219A	VBEJ/7059/132/1	425.863	B6	B7
G214FNZ	GSK1518999A	RW105197-087A63B12	540.536	C6	C7
G214FNZ	GSK2157753A	ST/1546914	320.43	D6	D7

Appendix 17: GSK177 plate map

Plate 1					
Barcode	**Regno**	OI	MolWt	Original Well ID	Well ID (Intermediate plate)
G2140M1	GW859039X	ST/365235	374.497	A1	A2
G2140M1	GSK276001A	SC/90411	349.414	B1	B2
G2140M1	GSK124945A	ST/398039	307.33	C1	C2
G2140M1	GW713556X	ST/276160	340.373	D1	D2
G2140M1	GSK889423A	ST/751070	344.835	E1	E2
G2140M1	GSK957094A	ST/767164	265.317	F1	F2
G2140M1	GSK1072678A	ST/817840	327.424	G1	G2
G2140M1	GSK1826089A	DJ107586-046A6B9	494.639	H1	H2
G2140M1	GSK1783710A	ST/1284842	383.467	A2	A3
G2140M1	GSK1731114A	ST/1262042	370.474	B2	B3
G2140M1	GSK1758774A	ST/1239379	412.327	C2	C3
G2140M1	GSK1829728A	ST/1325524	337.304	D2	D3
G2140M1	GSK1829819A	ST/1325613	269.306	E2	E3
G2140M1	GSK1829733A	ST/1325529	391.396	F2	F3
G2140M1	GSK2200157A	JM108692-133D4	317.453	G2	G3
G2140M1	SB-650816	MV49014-067A33B21	348.408	H2	H3
G2140M1	SB-204804-A	EXSB/LNB14457-77	388.934	A3	A4
G2140M1	GSK754716A	SC/118156	318.126	B3	B4
G2140M1	GSK810016A	ST/691898	379.482	C3	C4
G2140M1	GSK829969A	ST/704868	319.402	D3	D4
G2140M1	GSK1650514A	ST/1195396	351.831	E3	E4
G2140M1	GSK1859936A	ST/1348528	410.498	F3	F4
G2140M1	GSK1733953A	ST/1264695	385.826	G3	G4
G2140M1	GSK1925843A	ST/1388681	392.932	H3	H4
G2140M1	GSK1829660A	ST/1325456	307.399	A4	A5
G2140M1	GSK1832831A	ST/1327779	359.478	B4	B5
G2140M1	GSK1829816A	ST/1325610	245.327	C4	C5
G2140M1	GW857165X	ST/397470	371.236	D4	D5
G2140M1	GSK547543A	GA203953-122A11B7C11	544.686	E4	E5
G2140M1	GSK498315A	ST/564849	309.327	F4	F5
G2140M1	GSK463114A	ST/536298	336.394	G4	G5
G2140M1	GSK762874A	ST/658375	309.371	H4	H5
G2140M1	GSK798463A	ST/688668	335.357	A5	A6
G2140M1	GSK810037A	ST/691920	328.415	B5	B6
G2140M1	GSK847913A	SC/121801	347.357	C5	C6
G2140M1	GSK1829732A	ST/1325528	377.326	D5	D6

G2140M1	GSK1829736A	ST/1325532	402.206	E5	E6
G2140M1	GSK731389A	ST/644172	335.45	F5	F6
G2140M1	BRL-7940SA	IM100406-081J4	428.367	G5	G6
G2140M1	SB-516933	ST97588-166E0	350.411	H5	H6
G2140M1	SB-811137-V	YW200769-143A17B11C3	671.705	A6	A7
G2140M1	GSK124576A	ST/397469	385.263	B6	B7
G2140M1	GSK353071A	SC/104324	231.322	C6	C7
G2140M1	GSK636544A	ST/619924	345.876	D6	D7
G2140M1	GSK892651A	ST/754412	271.343	E6	E7
G2140M1	GSK937213A	ST/783889	365.426	F6	F7
G2140M1	GSK921295A	ST/759089	327.429	G6	G7
G2140M1	GSK1180781A	ST/894921	410.471	H6	H7
G2140M1	GSK1107112A	ST/838662	314.786	A7	A8
G2140M1	GSK1402290A	ST/1032424	315.372	B7	B8
G2140M1	GSK1826247A	DJ107586-048A5B4	465.553	C7	C8
G2140M1	GSK1691553A	ST/1224178	347.401	D7	D8
G2140M1	GSK1750922A	ST/1256539	364.365	E7	E8
G2140M1	GSK1863309A	ST/1342494	352.458	F7	F8
G2140M1	GSK1829727A	ST/1325523	323.277	G7	G8
G2140M1	GR135487X	C1789/11/1	253.223	H7	H8
G2140M1	SB-435634	JH99186-039A1	228.253	A8	A9
G2140M1	GSK275984A	SC/90390	331.424	B8	B9
G2140M1	GSK437009A	ST/510821	320.4	C8	C9
G2140M1	GSK695914A	AS104968-001A1B12	397.478	D8	D9
G2140M1	GSK831784A	DY103972-187A22B13	406.489	E8	E9
G2140M1	GSK994258A	ST/798779	336.427	F8	F9
G2140M1	GSK1051703A	ST/816262	335.357	G8	G9
G2140M1	GSK1310678A	ST/986476	300.241	H8	H9
G2140M1	GSK1519001A	RW105197-087A65B12	526.523	A9	A10
G2140M1	GSK1434490A	ST/1057085	382.388	B9	B10
G2140M1	GSK1611550A	ST/1170223	325.385	C9	C10
G2140M1	GSK920684A	ST/762581	329.349	D9	D10
G2140M1	GSK1788487A	ST/1288745	423.316	E9	E10
G2140M1	GSK1759150A	ST/1239788	446.501	F9	F10
G2140M1	GSK2059310A	ST/1488738	450.566	G9	G10
G2140M1	GSK2157753A	ST/1546914	320.43	H9	H10
G2140M1	GSK1742694A	ST/1251778	332.444	A10	A11
G2140M1	GSK1826825A	ST/1332234	427.649	B10	B11
G2140M1	GSK1744926A	ST/1252505	397.353	C10	C11
G2140M1	GSK847920A	SC/121808	302.382	D10	D11

G2140M1	GSK921190A	ST/759036	327.429	E10	E11
G2140M1	GSK888636A	ST/750242	345.398	F10	F11
G2140M1	GSK1385423A	ST/1023242	430.456	G10	G11
G2140M1	SB-712970	ST/958820	368.43	H10	H11

Plate 2					
Barcode	**Regno**	OI	MolWt	Original Well ID	Well ID (Intermediate plate)
G2140M1	GSK861337A	ST/717997	364.395	A11	A2
G2140M1	GSK1729177A	N5160-41-1	435.539	B11	B2
G2140M1	GSK445886A	N21275-66-1	288.755	C11	C2
G2140M1	GSK254610A	AP103231-016A1B176	441.522	D11	D2
G2140M1	GSK385518A	ST/471267	240.308	E11	E2
G2140M1	GSK547511A	GA203953-122A10B4C11	543.699	F11	F2
G2140M1	GSK547481A	GA203953-122A11B1C11	549.724	G11	G2
G2140M1	GSK479031A	ST/551212	302.822	H11	H2
G2140LL	GV187303X	VMEG/1774/72/2	290.359	A1	A3
G2140LL	GSK1174628A	ST/876385	259.305	B1	B3
G2140LL	GSK1372568A	ST/1013805	301.387	C1	C3
G2140LL	GSK1518999A	RW105197-087A63B12	540.55	D1	D3
G2140LL	GSK1570606A	ST/1129554	313.349	E1	E3
G2140LL	GSK1829676A	ST/1325472	411.387	F1	F3
G2140LL	GSK1829674A	ST/1325470	388.179	G1	G3
G2140LL	GSK1955236A	ST/1414819	349.826	H1	H3
G2140LL	GSK1985270A	N5160-40-3	383.835	A2	A4
G2140LL	GSK2200150A	JM108692-131D2	357.475	B2	B4
G2140LL	GSK735816A	ST/642098	328.392	C2	C4
G2140LL	GI247341A	U4907/144/1	732.566	D2	D4
G2140LL	GSK1905227A	ST/1367355	291.399	E2	E4
G2140LL	GSK749336A	ST/651380	350.411	F2	F4
G2140LL	GSK1598164A	R14229/126/205	416.549	G2	G4
G2140LL	CCI7967	GDD/636	380.874	H2	H4
G2140LL	GW664700A	R4564/113/1	485.519	A3	A5
G2140LL	GSK735826A	ST/642108	354.406	B3	B5
G2140LL	GI103688B	0013X 55U*B	466.925	C3	C5
G2140LL	GSK275628A	SC/89993	435.33	D3	D5
G2140LL	BRL-51093AM	IM100406-198N6	400.314	E3	E5
G2140LL	GSK316438A	ST/459399	346.215	F3	F5

G2140LL	GSK130506A	SC/84383	367.717	G3	G5
G2140LL	GSK1829820A	ST/1325614	285.37	H3	H5
G2140LL	SB-354364	ST97588-129J2	349.423	A4	A6
G2140LL	GSK690382A	ST/638013	340.428	B4	B6
G2140LL	GSK1857145A	ST/1346270	377.468	C4	C6
G2140LL	GSK163574A	FFJG/252/176/1	370.859	D4	D6
G2140LL	SB-811796-V	YW200769-143A22B12C5	655.662	E4	E6
G2140LL	GSK347301A	SC/98355	325.276	F4	F6
G2140LL	GSK426032A	ST/501405	425.401	G4	G6
G2140LL	GW360240X	0358U 83U*A	324.38	H4	H6
G2140LL	BRL-10143SA	IM100406-152B1	400.314	A5	A7
G2140LL	GSK270670A	U20764/121/2	373.434	B5	B7
G2140LL	BRL-8903SA	IM100406-132E8	386.287	C5	C7
G2140LL	BRL-51091AM	IM100406-198N7	441.151	D5	D7
G2140LL	GSK381407A	ST/476208	358.833	E5	E7
G2140LL	GSK146660A	ST/415658	368.39	F5	F7
G2140LL	GR135486X	C1789/10/1	219.67	G5	G7
G2140LL	GSK848336A	SC/122269	294.394	H5	H7
G2140LL	GW369335X	1747U 88U*A	318.396	A6	A8
G2140LL	GSK262906A	ST/436268	345.442	B6	B8
G2140LL	GSK352635A	SC/103704	222.555	C6	C8
G2140LL	GSK2043267A	ST/1473690	433.432	D6	D8
G2140LL	GW356807A	0039Y 64***	555.471	E6	E8
G2140LL	GSK1365028A	ST/1009933	339.408	F6	F8
G2140LL	GSK1941290A	ST/1393958	475.606	G6	G8
G2140LL	GSK2032710A	ST/1469817	435.585	H6	H8
G2140LL	SB-829405	DF202930-012A4B7C7	385.894	A7	A9
G2140LL	GW623128X	N15054-12-1	328.836	B7	B9
G2140LL	GSK345724A	SC/96881	256.229	C7	C9
G2140LL	GSK1829671A	ST/1325467	363.299	D7	D9
G2140LL	GSK1829729A	ST/1325525	339.341	E7	E9
G2140LL	GSK358607A	ST/464156	352.393	F7	F9
G2140LL	GSK1589671A	ST/1140264	434.478	G7	G9
G2140LL	GSK133167A	JT101283-005A8B13C12	491.506	H7	H9
G2140LL	GSK1812410A	ST/1317324	301.339	A8	A10
G2140LL	GSK2111534A	ST/1535805	299.762	B8	B10
G2140LL	GSK1996236A	ST/1439630	368.38	C8	C10
G2140LL	GSK237561A	FCBS/U1038/66/1	336.375	D8	D10
G2140LL	GR223839X	GDD/58841	324.423	E8	E10
G2140LL	GR153167X	GDD/40216	357.427	F8	F10

G2140LL	GSK353496A	SC/104897	211.309	G8	G10
G2140LL	GSK1635139A	NS107584-055A93B10	380.513	H8	H10
G2140LL	GW861072X	ST/371072	356.447	A9	A11
G2140LL	GSK468214A	ST/541154	389.46	B9	B11
G2140LL	GSK991960A	ST/796668	412.876	C9	C11
G2140LL	SB-746177	GA200759-052A5B6	305.383	D9	D11
G2140LL	GSK353069A	SC/104322	205.283	E9	E11
G2140LL	BRL-10988SA	IM100406-082R2	456.377	F9	F11
G2140LL	BRL-8088SA	IM100406-130H1	392.294	G9	G11
G2140LL	GSK2200160A	JM108692-134C3	333.518	H9	H11